

A THERMODYNAMIC STUDY OF
TRANSITION METAL OXIME
COMPLEXES

A thesis
submitted in partial fulfilment
of the requirements for the Degree
of
Doctor of Philosophy in Chemistry
in the
University of Canterbury

by

J. M. Russell

University of Canterbury

1977

ABSTRACT

This thesis reports the preparation of the O-methyldioxime and bis(O-methyloxime) derivatives of the diamine 4,4,9,9-tetramethyl-5,8-diazadodecane-2,11-dione, and the preparation of the oxime and O-methyloxime derivatives of the diamine 2,6,6-trimethyl-2,5-diazanonan-8-one. The chelating reactions of the diamine dioximes (tetradentate ligands) and the diamine oximes (tridentate ligands) towards divalent transition metal ions have been studied.

The E,Z configurations of these ligands were determined by p.m.r. spectroscopy. The rates of acid catalysed E-Z isomerization of the oxime and O-methyloxime groups, as determined by p.m.r. spectroscopy, are reported. The observed rates of isomerization are oxime > O-methyloxime.

Thermodynamic data are reported for the stepwise amino protonation of the tetradentate diamine dioxime ligands (log K (potentiometric), ΔH (calorimetric) and ΔS) and of the tridentate diamine oxime ligands (log K) at 25.0°C and I = 0.10M NaCl.

Log K (potentiometric) data are reported for (1) the formation of complexes between the diamine dioxime ligand and the divalent metal ions Fe, Ni and Zn and are compared with the known values for Co and Cu, (2) the formation of complexes between the diamine O-methyldioxime and the divalent metal ions Co, Ni, Cu and Zn, and (3) the formation of the copper(II) complex of the diamine bis(O-methyldioxime) at 25.0°C and I = 0.10M NaCl. ΔH (calorimetric) at ΔS data are also reported for the formation of copper(II) complexes of the tetradentate ligands and these are interpreted in terms of the known structural data. Log K data are reported for the formation of the copper(II) complexes of the tridentate diamine oxime ligands.

The order of donor strengths observed is oximato >> oxime > O-methyloxime. Deprotonation from a complexed oxime group involves the

formation of either an intramolecular hydrogen bond or hydrogen bonds with the solvent. Intramolecular oxime-oximato hydrogen bonding is favoured by a positive entropy change.

CONTENTS

	Page
CHAPTER 1	
INTRODUCTION	1
1.1 SOME ASPECTS OF OXIME CHEMISTRY	3
1.1.1 Preparation and Structure of Oximes	3
1.1.2 Isomerism of Oximes	5
1.1.3 <u>E-Z</u> Isomerization of Oximes	8
1.1.4 Catalysed <u>E-Z</u> -Isomerization	10
1.1.5 Methods of Determining the Isomers of Oximes	11
1.1.6 Acid-Base Properties of Oximes	14
1.2 METAL-OXIME COMPLEXES	15
1.2.1 Structures of Metal Oxime Complexes	16
1.2.2 Thermodynamic Data for Oxime Complexes	20
1.2.3 Proton Dissociation from Co-ordinated Oximes	25
1.2.4 Hydrogen Bonding in Oxime Complexes	26
1.2.5 π Bonding in Metal Oxime Complexes	27
1.2.6 Metal-Metal Bonding in Oxime Complexes	30
1.3 ANALYTICAL APPLICATIONS OF OXIMES	35
1.3.1 The Stability of Oxime Complexes	35
1.3.2 Solubility Factors	36
1.3.3 Solvent Extraction Techniques	38
1.4 THIS WORK	39
CHAPTER 2	
THERMODYNAMIC CONSIDERATIONS	42
2.1 DETERMINATION OF ΔG° , ΔH° AND ΔS°	42
2.1.1 Determination of the Thermodynamic Equilibrium Constant	42
2.1.2 Enthalpy and Entropy Changes	44
2.2 EFFECT OF AN INERT ELECTROLYTE ON THE THERMODYNAMIC PARAMETERS	46
2.3 FACTORS DETERMINING THE MAGNITUDE OF THE THERMODYNAMIC PARAMETERS	48

2.3.1	Free Energy Changes	48
2.3.2	Enthalpy Changes	49
2.3.3	Entropy Changes	50
2.4	DETERMINATION OF HYDROGEN ION CONCENTRATION	54
CHAPTER 3	EXPERIMENTAL	
A.	PHYSICAL MEASUREMENTS	
3.1	pH MEASUREMENTS	57
3.1.1	Equipment	57
3.1.2	pH Calibration against Standard Buffers	59
3.1.3	The Glass Electrode as a Hydrogen Ion Probe	60
3.1.4	Titration Procedure	62
3.2	CALORIMETRIC MEASUREMENTS	64
3.2.1	The Calorimeter	64
3.2.2	Temperature Measurement	65
3.2.3	Thermal Calibration of the Calorimeter	70
3.2.4	The Accuracy of a Calorimetric Measurement	70
3.2.5	Procedure for a Calorimetric Titration	73
3.3	OXYGEN-FREE AND OXYGENATION STUDIES	75
3.3.1	Equipment	76
3.3.2	Oxygen Measurement	76
3.3.3	Preparation of Oxygen-free Nitrogen Gas	78
3.3.4	Procedure for an O ₂ -free Titration	79
3.3.5	Procedure for the Oxygenation of a Cobalt(II) Complex	79
3.4	SPECTROPHOTOMETRIC MEASUREMENTS	80
3.5	MICROANALYSES	80
B.	SYNTHESIS OF LIGANDS AND COMPLEXES	
3.6	PREPARATION OF LIGANDS	80
3.7	PREPARATION OF METAL COMPLEXES	85

C.	PREPARATION OF STANDARD SOLUTIONS	
3.8.1	Glassware	87
3.8.2	Carbonate-free Distilled Water	87
3.8.3	Sodium Hydroxide (1M)	88
3.8.4	Hydrochloric Acid (1M)	88
3.8.5	Metal(II) chloride Solutions	88
3.8.6	Iron(II) sulphate Solution	89
3.8.7	Adjustment to Constant Ionic Strength	90
CHAPTER 4	CALCULATIONS	91
4.1	DETERMINATION OF EQUILIBRIUM CONSTANTS	91
4.1.1	Protonation Constants of the Ligands	91
4.1.2	Equilibrium Constants for Metal Complexes	94
4.2	DETERMINATION OF ENTHALPY CHANGES	99
4.2.1	Calculation of Enthalpy Changes for Protonation of the Ligands	100
4.2.2	Calculation of Enthalpy Changes for Metal Complex Equilibria	102
4.3	SELECTION OF A MODEL EQUILIBRIUM SYSTEM	105
4.4	METHODS OF SOLVING THE MASS BALANCE EQUATIONS	106
4.5	THE LEAST SQUARES METHOD	108
4.6	STATISTICAL METHODS	110
4.6.1	"Goodness of Fit" of Experimental and Calculated Data	111
4.6.2	Limitations in the Use of Statistical Parameters	113
4.7	COMPUTER PROGRAMS	114
CHAPTER 5	LIGAND SYNTHESIS AND PHYSICAL PROPERTIES	115
5.1	LIGAND SYNTHESIS	115
5.1.1	Reaction Mechanism	115
5.1.2	Determination of Experimental Conditions	116

5.2	LIGAND ISOMERISM	118
5.2.1	Configurational Assignment	119
5.2.2	Ligand Isomerization	124
5.3	INFRARED STUDIES	128
CHAPTER 6	PROTONATION OF THE LIGANDS	131
6.1	PROTONATION OF METHOXYAMINE	131
6.1.1	Results	131
6.1.2	Discussion	132
6.2	PROTONATION OF THE TETRADENTATE DIAMINE DIOXIME LIGANDS	135
6.2.1	Results	135
6.2.2	Discussion	146
6.3	PROTONATION OF THE TRIDENTATE DIAMINE OXIME LIGANDS	152
6.3.1	Results	152
6.3.2	Discussion	157
6.4	PROTONATION OF THE OXIME NITROGEN	158
CHAPTER 7	COPPER(II) COMPLEXES OF THE DIAMINE OXIME LIGANDS	159
7.1	RESULTS	159
7.2	DISCUSSION	166
7.2.1	The Complexes $\text{Cu}(\text{Hdno})^{2+}$ and $\text{Cu}(\text{dnm})^{2+}$	166
7.2.2	The Complex $\text{Cu}(\text{dno})^+$	168
7.2.3	Hydroxy Complex Species	169
CHAPTER 8	METAL COMPLEXES OF THE DIAMINE DIOXIME LIGANDS	172
8.1	COPPER(II) COMPLEXES OF THE TETRADENTATE LIGANDS	172
8.1.1	Results	172
8.1.2	The Molecular Structure of $\text{Cu}(\text{dddm})-(\text{ClO}_4)^+$	185
8.1.3	Formation of the Complexes $\text{Cu}(\text{H}_2\text{dddo})^{2+}$, $\text{Cu}(\text{Hddmo})^{2+}$ and $\text{Cu}(\text{dddm})^{2+}$	189

8.1.4	The Complexes $\text{Cu}(\text{Hdddo})^+$ and $\text{Cu}(\text{ddmo})^+$	195
8.2	THE METAL COMPLEXES OF H_2dddo	200
8.2.1	Results	200
8.2.2	Discussion	206
8.2.3	The Complexes $\text{Ni}(\text{Hdddo})(\text{ClO}_4) \cdot \text{H}_2\text{O}$ and $\text{Zn}(\text{Hdddo})(\text{ClO}_4)$	211
8.3	THE METAL COMPLEXES OF Hddmo	214
8.3.1	Results	214
8.3.2	Discussion	226
8.4	THE METAL COMPLEXES OF dddm	231
8.4.1	Results	231
8.4.2	Discussion	231
8.5	THE INFLUENCE OF 0.1M NaCl ON THE METAL-LIGAND EQUILIBRIA	233
	APPENDIX	234
	REFERENCES	246

ABBREVIATIONS

dien	1,5-diamino-3-azapentane
edta	ethylenediaminetetraacetic acid
en	ethylenediamine
H ₂ dmg	dimethylglyoxime
M	mol dm ⁻³
NiB(ClO ₄) ₂	5,7,7,12,12,14-hexamethyl-1,4,8,11-tetraazacyclo- tetradecane-4,14-diene nickel(II) perchlorate
Nioxime	cyclohexane-1,2-dione dioxime
Tris	amino-tri-(hydroxymethyl)methane

CHAPTER 1

INTRODUCTION

Oximes are widely used as selective reagents in qualitative and quantitative inorganic analysis of metal ions.^{1,2} The reagents have been used since Tschugauff discovered in 1905 that nickel(II) gives a specific reaction with dimethylglyoxime in ammonia solution.³ Since that time the number of oxime reagents used in inorganic analysis and the number of metal ions for which they are utilized has rapidly increased.

The oxime reagents generally used in inorganic analysis fall into three major classes (see fig. 1.1):

- (1) the vicinal α -dioximes such as dimethylglyoxime, α -furyl dioxime, cyclohexan-1,2-dione dioxime (nioxime) etc.
- (2) the ortho-hydroxybenzaldoxime and ortho-hydroxybenzketoxime reagents such as salicylaldoxime, and
- (3) the α -acyloinoximes such as α -benzoinoxime.

These reagents form metal complexes with most transition metal ions and have been used in the determinations of cobalt(II), copper(II), iron(II), iron(III), lead(II), manganese(II), nickel(II), molybdate ion, bismuth(III), palladium(II), rhenium(VII) and platinum(II).^{1,2,4} The analytical techniques employed in these determinations include gravimetric, volumetric, amperometric and spectrophotometric. The utility of oxime reagents in the determination of metal ions is related to two major factors:

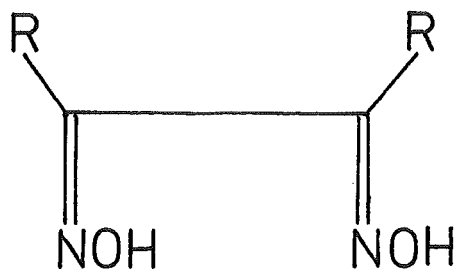
- (1) the high stability of the metal complexes, and
- (2) the solubility of the complexes in various solvents.

This chapter reviews some aspects of oxime group chemistry (as relevant to this work), and factors which affect the stability and

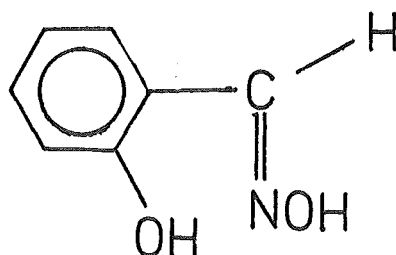
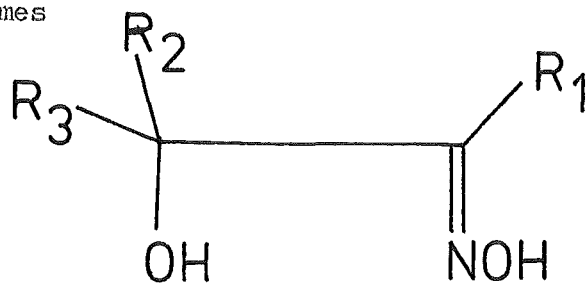
Fig. 1.1

Classes of Oxime Reagents Used in Inorganic Analysis

(1) Vicinal dioximes



(2) o-Hydroxyaldoximes

(3) α acyloinoximes

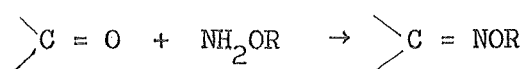
solubility of metal-oxime complexes. The application of oxime reagents to inorganic analysis will be discussed, followed by an outline of the metal oxime chemistry studied in this work.

1.1 SOME ASPECTS OF OXIME CHEMISTRY

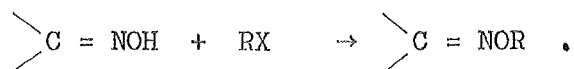
1.1.1 Preparation and Structure of Oximes

Oximes are derivatives of aldehydes and ketones and they are prepared from the parent carbonyl by reaction with hydroxylamine under neutral or basic conditions.⁵

O-alkyl oximes can be prepared by the reaction of the parent ketone with the corresponding O-alkyl hydroxylamine derivative;^{6,7}



or by alkylation of the parent oxime under basic conditions with the appropriate alkyl sulphate or alkyl halide:^{7,8,9}

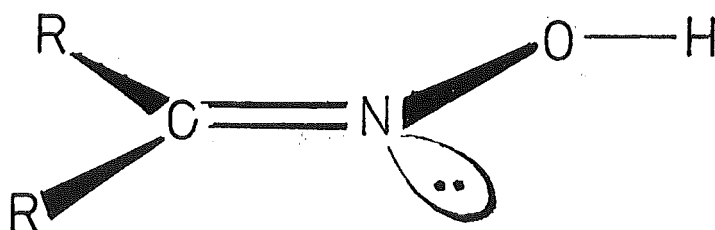


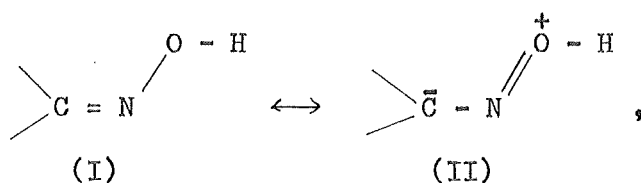
N-alkylation is a side reaction⁸ when the alkyl sulphate or halide reaction is employed.

The hybridization of the oxime carbon and nitrogen atomic orbitals is sp^2 . Bonding between the carbon and nitrogen atoms consists of a σ C-N bond and the overlap of the singly occupied unhybridized p orbitals to give a π C-N bond. The lone pair of electrons on the nitrogen atom occupies one of the sp^2 hybrid orbitals (see fig. 1.2).¹⁰ As a consequence of the sp^2 hybridization and of π bond formation, the atoms R_1 , R_2 , C, N and O all lie in a plane and the C-N-O angle is approximately 120° . Resonance is possible in the oxime group,¹¹ the contributing structures being:

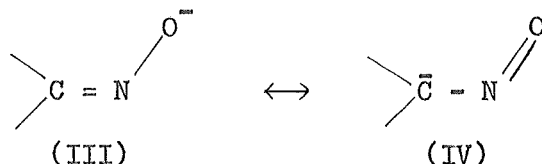
Fig. 1.2

Bonding in the Oxime Functional Group





and in the oximate group:



Typical bond lengths observed for the C-N double bond, N-O bond and O-H bond are 1.27 Å, 1.44 Å and 1.02 Å respectively.³ Similar bond lengths are calculated from the sums of covalent radii and the electronegativity of the constituent atoms.¹² It is inferred that structure (II) makes a minor contribution to the electronic structure of oximes. However with electron withdrawing groups attached to the imino carbon, structures (II) (and (IV)) may become more important.¹¹

Oximes contain electronegative nitrogen and oxygen atoms, and an hydrogen atom which is electropositive in character. Hydrogen bonding is therefore possible between these atoms. In the solid state hydrogen bonding does occur as evidenced by infrared measurements on a variety of oximes,^{13,14,15} and crystal structure analyses on monoximes^{16,17} and dioximes.^{18,19,20} In the solid state dimethylglyoxime hydrogen bonds to form long chains throughout the crystal^{18,19} as does (Z)-p-chlorobenzaldoxime,¹⁷ whereas (E)-p-chlorobenzaldoxime forms hydrogen bonded dimers.¹⁶ Infrared measurements on a series of aldoximes showed $\nu(\text{O-H})$ at 3250 cm^{-1} in solution¹⁵ (a free O-H stretches at $3500 - 3600 \text{ cm}^{-1}$) indicating that oximes also have a tendency to associate in aprotic solvent.

1.1.2 Isomerism of Oximes

The hybridization of the atomic orbitals about the carbon and

nitrogen atoms of oximes imposes a strict stereochemistry on the oxime group. Analogous to the alkenes, oximes can exist in E and Z forms (see fig. 1.3(a)) depending on whether the hydroxyl group is trans or cis to the priority selected group (R_1) in the oxime $R_1R_2C=NOH$.²¹ If the OH and R_1 groups are on opposite sides of a reference plane passing through the C-N double bond (and perpendicular to the plane containing these atoms and those directly attached to them) then the configuration is termed E (previously termed anti) and if on the same side of the reference plane then termed Z (previously syn).

With symmetric dioximes there exist three different configurations for the hydroxyl groups with respect to the C-N double bonds (see fig. 1.3(b)). These are designated as (E,E), (Z,Z) and (E,Z). (The E,Z isomer was previously known as the amphi isomer.) The fact that more than one isomer may exist for oximes and dioximes has been known for over 100 years and in 1890 Werner and Hantzsch correctly accounted for this isomerism in terms of restricted rotation about the C-N double bond.^{22,23}

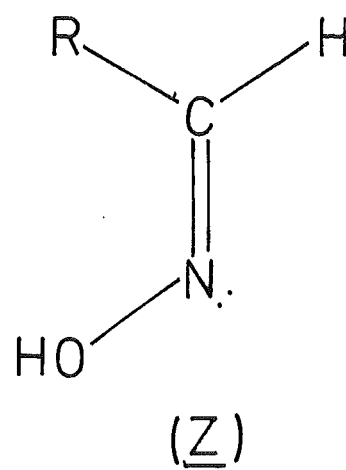
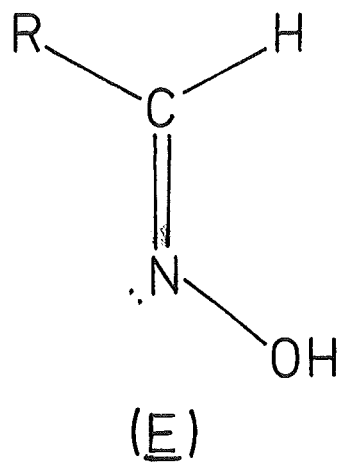
The preferred configuration about the C-N double bond is determined by both steric and electronic factors. In the more stable isomer the hydroxyl group is usually trans to the most bulky substituent on the oxime carbon²⁴ (the group R in aldoximes). With ketoximes a mixture of isomers may result and the most stable form is often difficult to predict.²⁵ Electronic factors may play a part in determining the preferred configuration; for example where a particular configuration may be stabilized by hydrogen bonding to a group adjacent to the oxime hydroxyl.²⁶

Theoretical molecular orbital calculations predict approximately 20% double bond character between the two carbons in dimethylglyoxime.²⁷ There is therefore a (small) barrier to rotation about the

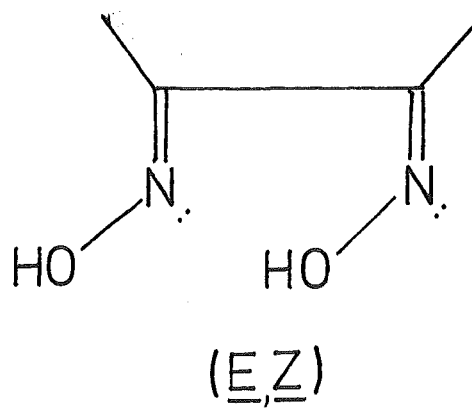
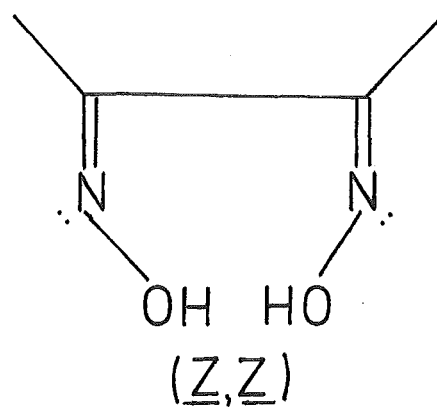
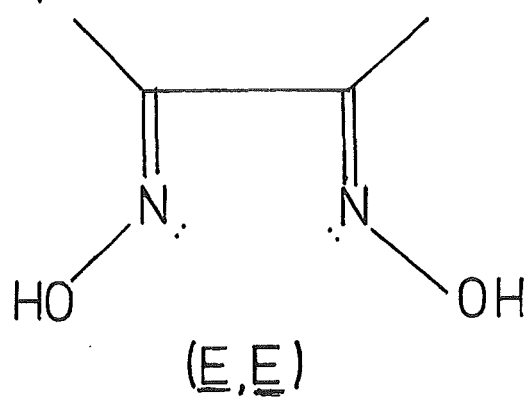
Fig. 1.3

Possible Configurations for (a) Aldoximines and (b) Vic-dioximes

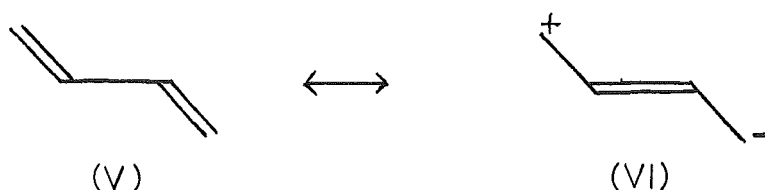
a)



b)



C-C "single" bond such that a further form of isomerism is possible in vic-dioximes viz. cis-trans isomerism. In the solid state dimethylglyoxime has a planar trans configuration.^{18,19} For the trans dioxime form the structure (V) will be the predominant canonical form contributing to the resonance structure:



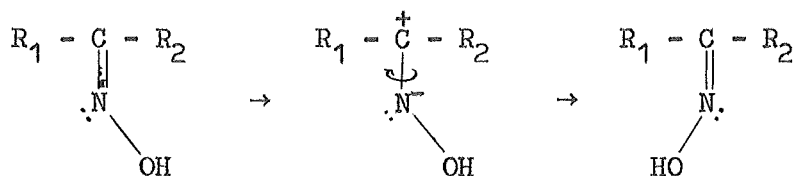
There is some doubt as to which configuration is important in solution.⁴

Theoretical calculations, and dipole moment measurements,²⁷ indicate that the cis form is probably the predominant form in dioxane solution although solvent effects may play a large role in other solvents.

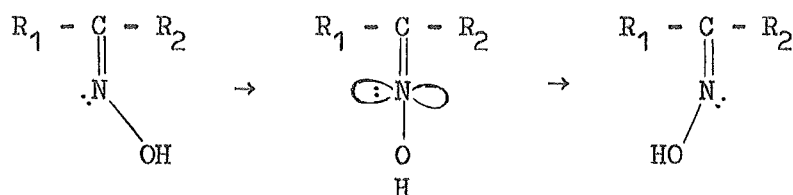
1.1.3 E-Z Isomerization of Oximes

The interconversion of the E and Z configurations of an oxime has been postulated to occur by 3 different mechanisms. These are:^{28,29}

(1) A rotation mechanism where isomerization is effected by torsion about the C-N double bond. The hybridization about the nitrogen atom does not change during isomerization.



(2) An inversion mechanism involving a planar inversion of the oxime hydroxyl group. The hybridization of the oxime nitrogen changes from sp^2 to sp in the transition state



(3) A combination of mechanisms (1) and (2).

The rate of isomerization of oximes has been contrasted with the rate of isomerization of alkenes.³⁰ Typical activation energies for E-Z isomerization of oximes and alkenes are 54 - 105 kJ mol⁻¹ and 150 - 250 kJ mol⁻¹ respectively. The markedly lower activation energies and higher rates of isomerization of oximes and oxime derivatives indicates that there is a mechanism available to oximes which is not available to alkenes. This mechanism is considered to be the planar inversion mechanism (2).

Evidence in support of the inversion mechanism comes from studies involving changes in the substituents on both the imino carbon and nitrogen atoms. Substituents on a phenyl group attached to the imino carbon have little effect on the rate of E-Z isomerization.^{29,31} Assuming a heterolytic breaking of the C=N double bond, the rotation mechanism involves a transition state in which the carbon develops a charge and the absence of a substituent effect suggests that rotation about the C-N bond is not the correct mechanism. Studies on N-(2,6-dialkylphenyl) imines²⁹ show that the activation energy for isomerization is lowered on increasing the size of the alkyl substituents. This observation was interpreted as being in support of a linear inversion transition state which would have lower steric hindrance. However the effect of an heteroatom containing a lone pair of electrons and bonded to the imino carbon is to lower the barrier to E-Z isomerization;²⁸ this observation supports a mechanism involving breaking the C-N double bond (viz. a rotation mechanism). However molecular orbital calculations on the ground state and transition states involved in the two mechanisms under consideration indicate that the heteroatom would also have an effect on the activation energy in the inversion mechanism.²⁸ Perhaps the greatest support for the inversion mechanism comes from theoretical molecular orbital-energy calculations

performed on the imines.^{28,32} The calculated activation energies for a rotation mechanism generally lie between 252 and 336 kJ mol⁻¹ whereas the calculated activation energy for an inversion mechanism is lower by about 84 to 126 kJ mol⁻¹. Although the relative activation energies are useful in assessing the likely mechanism, the absolute values are not easily compared with experimentally determined values (because of the approximations involved in the calculations). Similar theoretical calculations on the ethane molecule overestimate the C-C rotational barrier by a factor of 2 (experimental 272 kJ mol⁻¹, calculated 577 kJ mol⁻¹).³² In summary, however, the inversion mechanism is the favoured mechanism at this time.

An unusual feature of the rate of E-Z isomerization of imines is the extreme configurational stabilities of some classes of imine. Two of these are the N-haloimines and the O-alkyloximes (compared to oximes).³⁰ The high configurational stability of O-alkyloximes has been known since early in the 20th century.³³

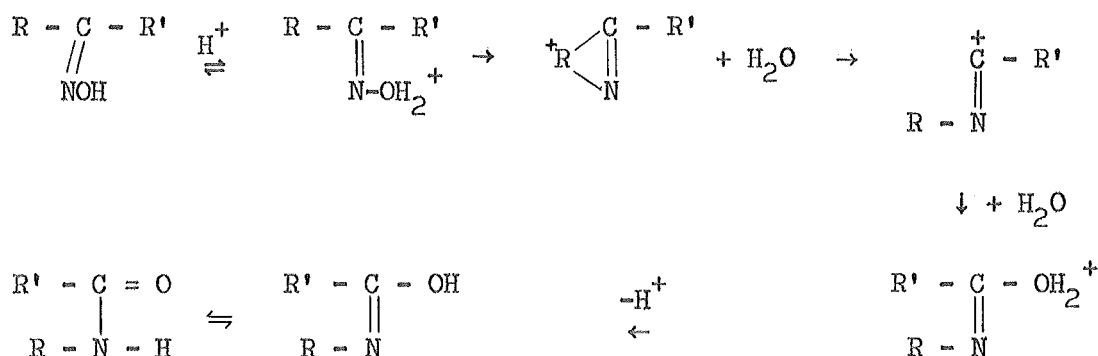
1.1.4 Catalysed E-Z Isomerization

The rate of E-Z isomerization is observed to be increased by the presence of acids,³⁴ bases^{35,36,37} and metal ions³⁸ although few quantitative studies have been reported on catalysed E-Z isomerization. The rate of isomerization of phenyl-2-pyridyl ketoxime is slow in 1M hydrochloric acid³⁸ whereas the rates of isomerization of 1,4-benzoquinone monoxime derivatives are enhanced in 3M hydrochloric acid.³⁴ It is well known that the formation of hydrochloride salts of oximes is often accompanied by E-Z isomerization.³⁹ It has been reported that trace amounts (10⁻⁵M) of Fe(II), Ni(II) and Cu(II) ions increase the rate of isomerization of oximes approximately 100 fold.³⁸ This observation is consistent with the observation of Frazer et al⁴⁰

that the E,E and Z,Z dioximes used in this study yield the same metal complexes with Ni(II) and Cu(II). Oximes are also isomerized by bases in ionizing solvents.³⁶ Qualitative observations on O-alkyloximes also suggest that E-Z isomerization can be effected by acids.⁴¹

1.1.5 Methods of Determining the Isomers of Oximes

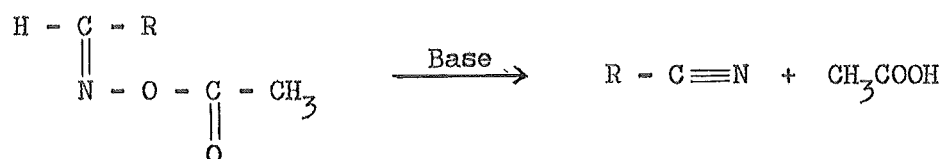
Before the advent of modern instrumental methods the most commonly used method for determining E and Z configurations of oximes was the Beckmann rearrangement.^{42,43} This rearrangement is an acid catalysed transformation of a ketoxime to an amide. The postulated mechanism for the rearrangement is



The alkyl group that migrates is the group anti to the hydroxyl group. The reaction is therefore useful in determining the orientation of the hydroxyl group relative to the substituents R and R'. A disadvantage of using the Beckmann rearrangement is that acids have been observed to isomerize oxime groups.^{34,43} If acid catalysed isomerization occurs then a mixture of amides (or the amide indicating the opposite configuration) may result. Cases of a non-stereospecific reaction have been reported in the literature.⁴⁴

The Beckmann rearrangement cannot be used for aldoximes because the hydrogen seldom migrates.⁴³ The reaction most commonly used to determine the configuration of aldoximes was the trans elimination of

water from the oxime (or the trans elimination of acetic acid from the O-acetyl derivative of the oxime) under basic conditions.⁴²



The elimination is stereospecific: the action of base on the E isomer results in the oxime being unchanged (or the O-acetyl derivative producing the oxime). A problem with the use of this reaction is that the Z isomer may isomerize under basic conditions to the more stable E isomer.³⁷ As a result a mixture of products may form.

The Beckmann rearrangement for ketoximes and the elimination of water for aldoximes have been used extensively to determine the configurations of oximes. However the mechanisms of these reactions, as presented in the earlier literature, were not fully understood; the Beckmann rearrangement was believed to involve a cis migration of the alkyl group and formation of nitriles with the cis elimination of acetic acid (or water). In 1921 Meisenheimer showed,⁴² by examining an oxime derived from a cyclic compound (and therefore having a fixed configuration), that a trans (with respect to the OH group) migration was involved in the Beckmann rearrangement. The configurational assignments made before 1921 were therefore wrong and because Meisenheimer's work was not immediately accepted some configurations assigned after 1921 were also in error. Published assignments must therefore be assessed carefully. Similar confusion exists in the literature concerning the formation of nitriles from aldoximes.

More recently physical methods have been used to determine the configurations of oximes. The dipole moments of the E and Z isomers of oximes are expected to be different. However oximes are generally associated via hydrogen bonds in aprotic solution. In order

to measure the dipole moment this association is eliminated by formation of the N-methyl derivatives of the parent oximes. Dipole moment measurements have been used successfully to determine the configuration of 4-nitrobenzophenone oximes⁴⁵ and to characterise the E and Z configurations of O-methyl derivatives of aldoximes (the formation of the O-alkyloxime eliminates hydrogen bonding).⁴⁶ This method of determining configuration is most applicable to oximes which have a large dipole moment, and has been used most successfully in aryl molecules containing a p-nitro group.

Infrared measurements have also been used to determine the E,Z configurations of aldoximes. In the solid state the two configurations form intermolecular hydrogen bonds and the O-H stretching frequency is different for each isomer.^{13,14,15} For aldoximes known to have the E configuration $\nu(\text{O-H})$ generally lies between 3280 cm^{-1} and 3320 cm^{-1} while for Z isomers $\nu(\text{O-H})$ generally lies between 3130 and 3170 cm^{-1} . In contrast the O-H stretching frequency for both E and Z isomers in solution is generally about 3250 cm^{-1} . This difference in frequency of the O-H stretching vibration in the solid state has been attributed to different crystal structures.¹⁴ E oximes tend to form hydrogen bonded dimers¹⁶ while Z oximes tend to form "chains".¹⁷ Although this pattern of O-H stretching frequencies is observed for a large variety of aldoximes, some exceptions exist. For example (E)-pyridine-2-aldoxime and (E)-pyridine-4-aldoxime have O-H stretching frequencies between 2700 and 2880 cm^{-1} (however this may be a result of hydrogen bond formation between the oxime proton and the pyridine nitrogen).

The third commonly used method of determining E,Z configurations of ketoximes and aldoximes is by nuclear magnetic resonance spectroscopy. The protons α to the oxime function resonate at different frequencies

when cis or trans to the oxime hydroxyl group.^{47,48,49} The difference in frequencies is observed to be solvent dependent. A mixture of (E)- and (Z)-ethylmethylketoxime shows a difference in the resonance frequencies for the α -methyl and α -methylene protons of 0.05 ppm and 0.25 ppm respectively in C_6D_6 and a difference of 0.04 ppm and 0.12 ppm in CF_3COOH .⁴⁹ In both solvents the resonance is at lower field when the α -methyl and α -methylene protons are cis to the OH group. This same dependence on configuration is also observed for propionaldoxime, where both the aldehydic proton and the α -methylene protons resonate at lower field when cis to the oxime OH. Similar results have also been obtained for a wide range of oximes and oxime ethers.^{48,50}

In contrast, recent studies have shown that for some oximes in solvent D_2O the α -methyl resonance peak shifts to lower field when the methyl group is trans to the OH and the α -methylene resonance shifts to lower field when the methylene group is cis to the OH group⁵¹ (see section 5.2.1).

The cause of this anisotropic deshielding has been attributed both to the nitrogen lone pair of electrons,⁵⁰ and to the proximity of the hydroxyl group.⁵²

1.1.6 Acid-Base Properties of Oximes

The oxime functional group is amphiprotic, the hydroxyl proton being slightly acidic while the nitrogen and oxygen atoms may show weak basicity.

The hydroxyl proton in hydroxylamine is slightly acidic with a pK_a of 13.74.⁵³ The effect of the π -electron system in oximes is to slightly increase the acidity of this proton. Typical pK_a values for oximes lie in the range 10 to 13⁴³ (c.f. typical pK_a value for an alcohol ca. 18).⁵⁴ Electron withdrawing groups (such as C=O or C=NOH)

α to the oxime group further enhance the acidity. The contribution of the resonance form (II) to the structure of oximes has been correlated with their acidities.¹¹ Factors which favour this resonance form (by stabilizing the negative charge on the oxime carbon through inductive or resonance effects) also increase the acidity of the oxime function. A correlation exists between the experimental pK_a 's of some oximes and the calculated "positive" charges on their oxygen atoms.¹¹

In nitrogen-containing compounds the basicity is a consequence of the lone pair of electrons on the nitrogen atom. On changing the hybridization of the nitrogen atomic orbitals from sp^3 to sp^2 , the s(lower energy) contribution to the hybrid orbital increases, the result being that the lone pair of electrons is of lower energy.⁵⁵ The pK_a of the conjugate acid will also be lowered⁵⁵ (compare $R_3C-OH_2^+$, $pK_a \sim -2$, and $R_2C=OH^+$, $pK_a \sim -7$ ⁵⁴ where the hybridization of the oxygen atomic orbitals changes from sp^3 to sp^2). The presence of an electronegative atom adjacent to the nitrogen atom will also lower the basicity (compare $CH_3NH_3^+$, pK_a 10.64, and $HONH_3^+$, pK_a 5.95).⁵⁶ There is little information available on the basicity of oximes. The pK_a of the conjugate acid of dimethylglyoxime has been determined as -0.94⁵⁷ and -0.77,⁴ values which may be compared with the pK_a for the conjugate acid of acetoxime, 1.75⁵⁸ and 1.92.⁵⁹

As a consequence of their basicity, oximes form hydrochloride salts. Infrared measurements on these show the presence of an $N-H^+$ stretching frequency at 2645 cm^{-1} and a $C=N^+$ stretching frequency at 1696 cm^{-1} .^{50,60,61} These measurements were interpreted in terms of protonation on the nitrogen atom. Protonation on the oxygen atom has also been suggested.⁶²

1.2 METAL-OXIME COMPLEXES

Direct correlations between the stability of metal ion complexes

and the basicity of the co-ordinating group have been established.² The pK_a of a protonated oxime group is approximately -1 and consequently an oxime is expected to co-ordinate very weakly to metal ions. The oxime hydroxyl proton is very weakly acidic and co-ordination through the oximato oxygen is expected to occur at high pH. However oxime groups are known to co-ordinate strongly to metal ions in slightly acidic or acidic solution.² Metal oxime complexes are generally low spin² (e.g. $Ni(Hdmg)_2$ and $Fe^{II}(Hdmg)_2$) but high spin complexes are also known.^{63,64}

1.2.1 Structure of Metal Oxime Complexes

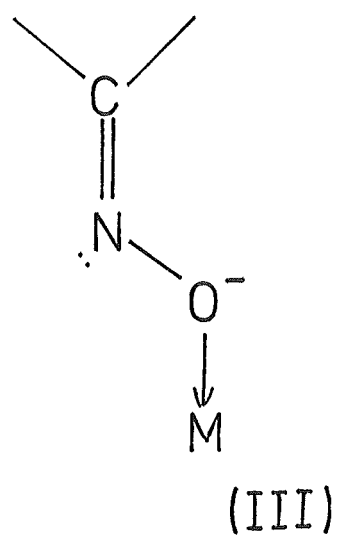
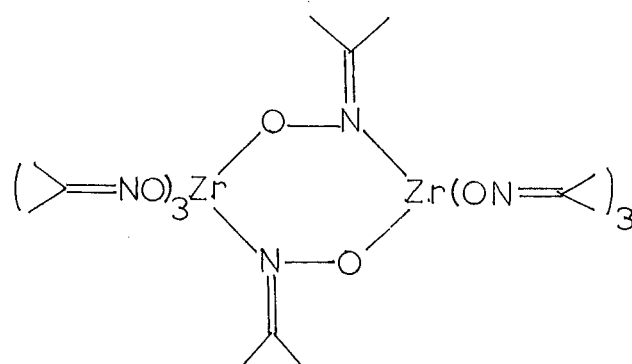
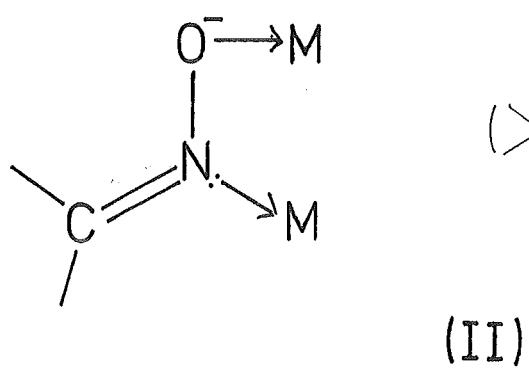
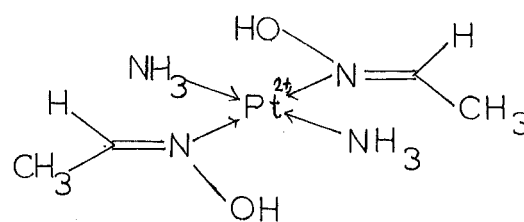
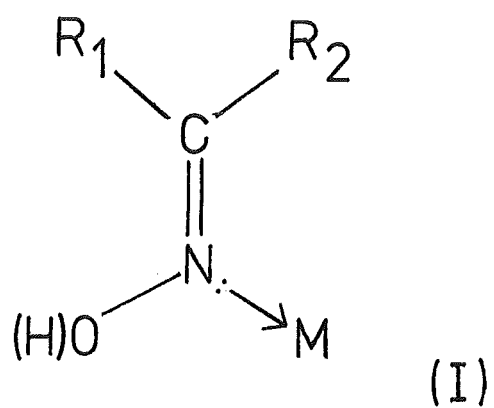
The oxime group offers two possible sites for co-ordination to metal ions. These are the nitrogen atom and the oximato oxygen atom. Co-ordination through both sites is known and there are three different classes of co-ordination commonly encountered³ (see fig 1.4). These are:

(I) Co-ordination through the nitrogen atom. This type of co-ordination is known both where the oxime group is intact and deprotonated (oximato). In the former the oxime proton may hydrogen bond with adjacent groups or ligands. A typical example is the trans(bis-(E)-acetaldoxime) and trans bis-(acetoxime) complexes of platinum(II)^{65,66} shown in fig. 1.4 (I). These complexes also form with the oxime groups successively deprotonated. The cis complexes have also been characterised. Nickel(II) bis-(dimethylglyoxime) complexes are known where the oxime groups co-ordinate in the protic form,⁶⁷ and a dichloro-dimethylglyoxime copper(II) complex has been isolated from non-aqueous solution.⁶⁸ In the solid state the oxime groups hydrogen bond to chlorine atoms in adjacent molecules.⁶⁹

(II) The deprotonated oxime group (oximato) co-ordinates to two metal

Fig. 1.4

Classes of Co-ordination of Oximes to Metal Ions



ions: both the nitrogen and the oxygen atoms are utilized. An example of this type of co-ordination is a zirconium acetoxime complex⁷⁰ (see fig 1.4 (II)), and copper(II) bis-(dimethylglyoximate) in the solid state where the complex is dimeric and one oximate oxygen co-ordinates to the fifth co-ordination site on each copper atom.⁷¹

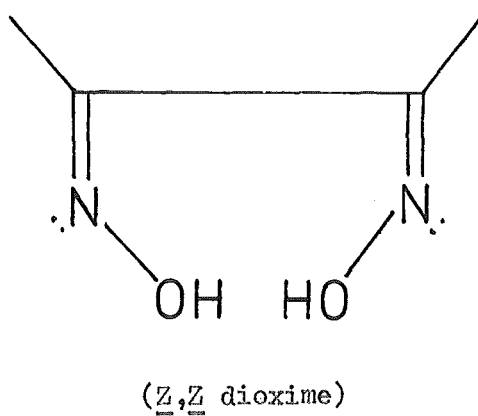
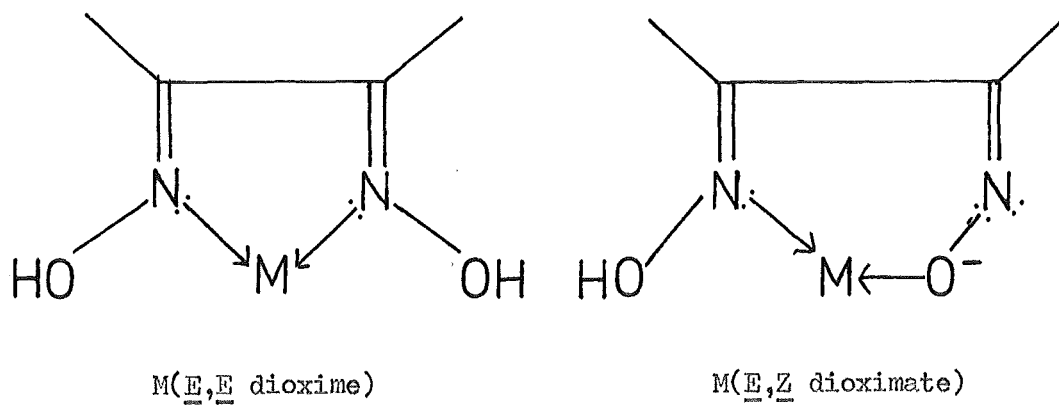
(III) Co-ordination through only the oximate oxygen. Only a few examples of this class of oxime co-ordination are known (e.g. a bis(α -benzoinoxime) titanium(IV) complex)⁷² (see fig 1.4 (III)).

Dioximes have three possible configurations (see fig 1.3 (b)). Co-ordination of oximes having the E,E configuration (through two oxime nitrogens) and the E,Z configuration (through one oxime nitrogen and one oximate oxygen) are known⁷³ but co-ordination of the Z,Z dioxime is unknown (see fig 1.5).

Single crystal X-ray structure determinations have been completed for many oxime complexes.³ Most structures have been determined for oximes that are of analytical importance. The important features observed are that the length of the C-N double bond is generally unaffected by co-ordination and the N-O bond is generally shortened. Typical C-N bond distances are 1.25 - 1.30 Å, and N-O bond distances are 1.30 - 1.44 Å.^{74,75,76,77,78}

Divalent iron, cobalt, nickel, platinum, palladium, rhodium and copper generally co-ordinate two vic-dioxime molecules in a square planar arrangement.^{3,78} In the case of iron(II), cobalt(II) and copper(II) the fifth (and sixth) octahedral co-ordination sites may be occupied by other ligands. The bis-(dimethylglyoximate) copper(II) complex has a crystal structure which shows that one axial co-ordination site of each copper atom is occupied by an oximate oxygen from the adjacent complex unit.⁷¹ The complex therefore exists as dimers in the solid state.

Fig. 1.5

Co-ordination of Vic-dioximes to Metal Ions

1.2.2 Thermodynamic Data for Oxime Complexes

Stability constants have been measured for many analytically important metal oxime complexes,⁷⁹ but few measurements of enthalpy and entropy change data have been reported.⁸⁰

Stability constant data have been reported for the analytical reagents dimethylglyoxime,^{81,82,83,84} salicylaldoxime,⁸⁵ cyclohexane-1,2-dione dioxime,⁸³ cycloheptane-1,2-dione dioxime,⁸³ and α -furylglyoxime⁶⁴ in their reactions with copper(II) and nickel(II) ions. Stability constant measurements have been reported on other structurally related dioximes, such as diphenylglyoxime,⁸⁴ ethylmethylglyoxime,⁸³ diethylglyoxime,⁸³ and alkyl substituted cyclohexane-1,2-dione dioximes.⁸³ Numerous measurements of stability constants have been reported for ligands containing only a single oxime group;⁷⁹ these include furil-2-aldoxime,⁸⁶ pyridine-2-aldoxime,^{87,88} and derivatives of salicylaldoxime substituted in the 5 position.⁸⁵ The stability constants for the tridentate ligand 1-amino-4,4-dimethyl-3-azahexan-5-one oxime with nickel(II) and copper(II) ions have been reported⁸⁹ and for the mixed ammine acetoxime complexes of platinum(II).⁶⁵

Some data for dioxime complexes of nickel(II) and copper(II) are presented in table 1.1. These data show that in general $\log K_1 - \log K_2 \leq 0.9$ for dioxime complexes. The predicted ratio of stability constants calculated from statistical considerations for bidentate ligands forming square planar complexes is $K_1/K_2 = 8$,⁹⁰ and for most complexes other factors contribute to make $K_1/K_2 \gg 8$ (i.e. $\log K_1 - \log K_2 \gg 0.9$). The second factor to emerge from the stability constant data is the high stability of oxime complexes. Vic-dioximes generally form complexes of lower stability than ethylenediamine but of higher stability than 2,2'-dipyridyl in solvent water. This illustrates the anomalous behaviour of the stabilities of

TABLE 1.1

Stability Constant Data for Some Oximes, Dioximes and Amines.

Oxime	Metal Ion	$\log K_1^a$	$\log K_2^b$	Solvent, T(°C)
Dimethylglyoxime ^c	Cu ²⁺	11.9	11.2	50% dioxane, 25°C
Dimethylglyoxime ^c	Ni ²⁺	11.6	10.5	" "
Dimethylglyoxime ^c	Zn ²⁺	7.7	6.2	" "
α -furilaldoxime ^d	Cu ²⁺	8.5	8.1	75% dioxane, 25°C
α -furilaldoxime ^d	Ni ²⁺	6.9	5.8	" "
Salicylaldoxime ^e	Cu ²⁺	(K ₂ >K ₁ ; $\log \beta_2=21.5$)		" "
Salicylaldoxime ^e	Ni ²⁺	6.9	7.4	" "
Dimethylglyoxime ^f	Ni ²⁺	7.9	9.1	H ₂ O , 25°C
Ethylmethylglyoxime ^f	Ni ²⁺	7.3	10.0	H ₂ O , 25°C
Nioxime ^f	Ni ²⁺	8.5	8.8	H ₂ O , 25°C
Ethylenediamine ^g	Cu ²⁺	10.2	8.8	H ₂ O , 25°C
2,2'-dipyridyl ^g	Cu ²⁺	8.1	5.0	H ₂ O , 25°C

^aFor the reaction $M^{2+} + LH^- \rightleftharpoons MLH^+$ (LH₂ = oxime or dioxime).^bFor the reaction $MLH^+ + LH^- \rightleftharpoons M(LH)_2$.^cFrom ref. 81.^dFrom ref. 86.^eFrom ref. 85.^fFrom ref. 83.^gFrom ref. 79, $\log K_1 (M^{2+} + L \rightleftharpoons ML^{2+})$ and $\log K_2 (ML^{2+} + L \rightleftharpoons ML_2^{2+})$.

dioximes as predicted from their basicities. The overall basicity ($\sum pK_a$'s) of dimethylglyoxime is < -1 whereas those of ethylenediamine and 2,2'-dipyridyl are 17.0^{91} and ca. 4.0^{92} respectively.

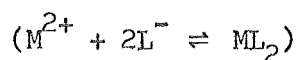
Enthalpy and entropy change data for the co-ordination of oximes is sparse. The enthalpy changes for complexation of dimethylglyoxime to nickel(II) and copper(II) ions have been determined⁸² by the temperature variation method. These data are shown in table 1.2. The enthalpy change for formation of the bis-(dimethylglyoximate) complex of copper(II) is approximately half that for the bis-(ethylenediamine) complex. The data suggest that the driving force for the formation of the dimethylglyoxime complexes is derived largely from the increase in entropy. This has been related to the desolvation of the oximate group and the metal ion in forming the neutral complex.

The enthalpy and entropy changes for the formation of the nickel(II) and copper(II) bis complexes of 2-amino-2-methylbutan-3-one oxime and its N-methyl, N-ethyl and N-propyl derivatives have been determined^{89,93} and the relative strengths of the intramolecular hydrogen bonds in these complexes determined. The data have been interpreted in terms of a decrease in solvation on increasing the size of the N-alkyl substituent, and suggest that the strengths of the hydrogen bonds in the nickel complexes are greater than those in the copper complexes. The enthalpy and entropy changes for the reaction of phenylpyridine-2-ketoxime with nickel(II) and zinc(II) ions have been reported.⁹⁴

Thermodynamic data are published for only one O-methyloxime ligand. The stability constants for the formation of the manganese(II), cobalt(II), nickel(II), copper(II) and zinc(II) complexes of the O-methyl ether of dimethylglyoxime have been determined^{81,82} (table 1.3). No enthalpy or entropy data were reported. These data show that the dimethylglyoxime O-methyloxime complexes of the metals studied have a

TABLE 1.2

Thermodynamic Data for the Reaction of Dimethylglyoxime (HL)
with Nickel(II) and Copper(II) Ions.^a



Metal Ion	ΔH (kJ mol ⁻¹)	ΔS (J mol ⁻¹ K ⁻¹)
Ni ²⁺	8.8	445
Cu ²⁺	-58.1	253

^aFrom ref. 82; solvent 50% dioxane

TABLE 1.3

Stability Constant Data for the O-methyloxime of Dimethylglyoxime.

Metal Ion	$\log K_1^a$	$\log K_2^b$	$\log \beta_2$
Mn ²⁺ ^c	6.18	5.42	11.60
Co ²⁺ ^d	9.80	6.25	16.05
Ni ²⁺ ^c	6.38	5.69	12.07
Cu ²⁺ ^c	9.5	6.6	16.1
Zn ²⁺ ^c	7.47	6.89	14.36

^aFor the reaction $M^{2+} + L^{-} \rightleftharpoons ML^{+}$ (HL = dimethylglyoxime
O-methylether)

^bFor the reaction $ML^{+} + L^{-} \rightleftharpoons ML_2$

^cFrom ref. 82; solvent 50% dioxane

^dFrom ref. 81; solvent 50% dioxane

greatly lowered stability compared to the corresponding dimethylglyoxime complexes. This lowered stability was rationalized in terms of loss of hydrogen bonding in the O-methyloxime complexes, and steric hindrance associated with the O-CH₃ groups.^{81,82} However these workers overlooked the possibility of the different co-ordinating power of the C=NOH and C=NOCH₃ groups. The data obtained for the O-methyloxime complexes show that the ligand only co-ordinates after the loss of an oxime proton.

Much of the thermodynamic data available on oximes and oxime complexes result from measurements in non-aqueous solvents;⁷⁹ this is because of the low solubility of the oxime ligands or complexes in water. The solubility products of the nickel(II) complexes of dimethyl-, ethylmethyl-, diethyl- and dipropyl- derivatives of glyoxime, of cyclohexane-1,2-dione dioxime, and its 3-methyl, 4-methyl and 4-propyl derivatives, and of cycloheptane-1,2-dione dioxime have been determined.⁹⁵ The heats of solution of nickel(II) and copper(II) dimethylglyoxime complexes,^{96,97} and the nickel(II) complex of ethylmethylglyoxime⁹⁷ have been reported for a variety of solvents. In nickel(II) bis-(dimethylglyoximate) metal-metal bonding occurs in the solid state whereas no such bonding occurs for α -nickel(II) bis-(ethylmethylglyoximate) or in copper(II) bis-(dimethylglyoximate). Comparison of the heats of solution of these complexes suggested that the metal-metal bond stabilizes the complex by ca. 42 kJ mol⁻¹ but measurement for the dimethylglyoximate complex of copper(II) suggests that solvation may be important.

For dⁿ transition metal ions the crystal field stabilization energy is a contributing factor to the overall enthalpy change for a complexation reaction.^{98,99} However the position of dimethylglyoximate in the spectrochemical series is not listed in the extensive tabulations

of the series by Jorgensen¹⁰⁰ or by Cotton and Wilkinson.¹⁰¹

The spectroscopic data reported for nickel(II) bis-(dimethylglyoximate)¹⁰² suggest that the ligand generates a crystal field splitting slightly greater than ethylenediamine.¹⁰⁰

1.2.3 Proton Dissociation from Co-ordinated Oximes

On co-ordination of a metal ion to ligands such as amines, oximes,^{88,103} water¹⁰⁴ and hydroxylamine,^{105,106} which contain an acidic proton adjacent to the donor atom, the acidity of that proton is observed to increase. For the ligand pyridine-2-aldoxime the pK_a of the oxime proton is 10.22. On co-ordination to iron(II) to form a tris complex the second and third pK_a values were measured as 3.36 and 7.13 respectively.⁸⁸ The first pK_a was too low to measure. For the copper(II) bis complex the first and second proton dissociation constants (pK_a) were measured as 2.77 and 6.70 respectively.⁸⁷ The increase in the acidity of the oxime proton by up to 7.4 pK units was rationalized in terms of stabilization of the oximato group by conjugation with the pyridine ring, the metal ion stabilizing one of the canonical forms. A smaller increase in the acidity of an oxime proton is observed in the trans-diammine bis-(acetoxime)-platinum(II) complex^{65,66} where the first and second pK_a values are 5.66 and 7.40 respectively. This increase in acidity can only result from an inductive interaction between the metal ion and the oxime O-H bond. This contrasts with copper(II) bis-(pyridine-2-aldoxime) where conjugative as well as inductive effects may be important.

The formation of intramolecular hydrogen bonds also enhances the formation of oximato complexes. This accounts for the lower pK_a for the first deprotonation from the copper(II) bis-(pyridine-2-aldoxime) complex.

The effect of proton dissociation from the oxime group is to enhance its donor strength. Dimethylglyoxime O-methyloxime will only co-ordinate to metal ions in the oximate form.^{81,82} The increased donor strength of the oximate group compared to the oxime group is illustrated by the copper(II) complexes of 1-amino-4,4-dimethyl-3-azahexan-5-one oxime.⁸⁹ With the ligand in the oxime form $\lambda_{\max} = 587 \text{ nm}$ but on deprotonation (oximate form) the ligand field strength increases to give $\lambda_{\max} = 518 \text{ nm}$.

1.2.4 Hydrogen Bonding in Oxime Complexes

Metal oxime complexes often involve strong intramolecular hydrogen bonds.^{2,3} Hydrogen bonding may occur where an oxime group (containing an electropositive hydrogen atom) and an oximate or phenoxide group (affording a negatively charged oxygen atom) are in the same co-ordination sphere. This type of hydrogen bonding occurs in vic-dioxime complexes, and in other metal complexes where two oxime ligands are adjacent to each other e.g. the cis diammine bis-(acetoxime) platinum(II) complex⁶⁵ and in salicylaldoxime complexes of manganese(II), iron(II), cobalt(II) and zinc(II).² The common feature is two oxime groups occupying adjacent co-ordination sites on the metal ion. The most widely studied complexes containing strong intramolecular hydrogen bonds are the transition metal vic-dioxime complexes, and numerous single crystal X-ray structure determinations have been performed on this type of complex.^{78,107,108,109,110,111,112} The structure determinations show an O-O distance of between 2.33 and 3.03 Å in dioxime complexes. For O-O distances of between 2.33 and 2.50 Å the hydrogen bond is expected to be symmetrical.³ This situation occurs in many complexes (e.g. $\text{Ni}(\text{Hdmg})_2$,⁷⁸ $\text{Pd}(\text{Hdmg})_2$ ¹¹³ and various cobalt(III) complexes^{74,75}). On increasing the O-O distance the hydrogen bond becomes non-symmetric.

This situation is observed in the crystalline bis-(dimethylglyoximate)-copper(II) dimer where there are two different O-O distances (2.70 \AA and 2.53 \AA ^{71,108}). The weaker (longer) hydrogen bonds involve the oximate oxygens which are also bonded to the fifth co-ordination site on a copper atom. In solution these metal-oxygen bonds are broken and symmetric hydrogen bonds are thought to result.

Apart from X-ray structure analysis the strongest evidence for hydrogen bonding in oxime complexes comes from their infrared spectra. Infrared investigations^{113,114} have shown that the stretching mode of the O-H---O group has a frequency between 2200 and 2700 cm^{-1} , and the bending mode a frequency near 1700 cm^{-1} . Burger *et al.*¹¹⁴ have estimated the strength of the hydrogen bond from the observed O-H---O stretching frequency. In dimethylglyoxime complexes the order of hydrogen bond strengths for a range of metal ions is $\text{Ni(II)} \sim \text{Pd(II)} \sim \text{Pt(II)} \sim \text{Cu(II)} \gg \text{Fe(II)} \sim \text{Co(II)}$.

In dimethylglyoxime complexes the formation of hydrogen bonds between adjacent ligands stabilizes the bis-(dimethylglyoximate). As a result the stability constant for the bis complex is often greater than that for the mono complex^{64,84,85} which contrasts with the situation for most bidentate ligands where the second formation constant $K_2(\text{ML} + \text{L} \xrightleftharpoons{K_2} \text{ML}_2)$ is less than the first formation constant $K_1(\text{M} + \text{L} \xrightleftharpoons{K_1} \text{ML})$.^{2,98} The ratio K_2/K_1 shows that the hydrogen bond strength decreases in the order $\text{Cu(II)} > \text{Ni(II)} > \text{Co(II)} > \text{Fe(II)}$.

1.2.5 π Bonding in Metal Oxime Complexes

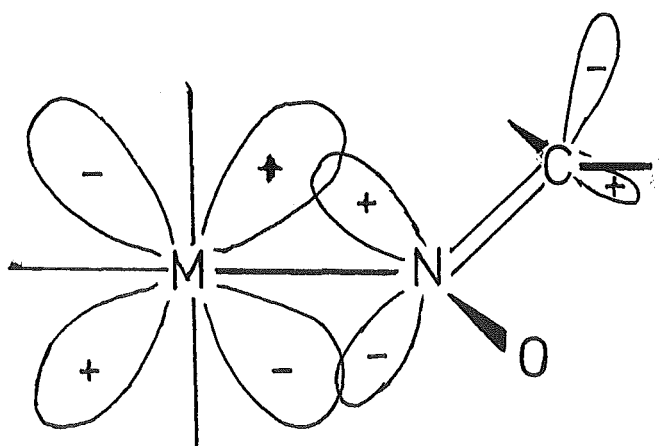
On co-ordination of an oxime to a metal ion a co-ordinate bond develops between the lone pair of electrons in the nitrogen sp^2 orbital and the available orbitals (s, p, d) on the metal. If the metal t_{2g} orbitals are occupied it is possible for back co-ordination

to occur from these orbitals to the oxime ligand π^* orbital (see fig 1.6). The strength of the π back bond relates to the relative energies of the t_{2g} and π^* orbitals. The stability of the t_{2g} orbitals is given by the third ionization potential of the metal ion. The third ionization potential increases from iron to zinc in the first row transition metals and iron(II) complexes are expected to form the strongest π co-ordinate bonds (assuming that the energy of the ligand π^* orbital is greater than that of the metal t_{2g} orbitals). The strength of π back bonding is also related to the degree of overlap of the π^* and t_{2g} orbitals. The geometry of the co-ordinated oxime group in relation to the metal orbitals will decrease the efficiency of this overlap.

π bonding in metal oxime complexes was first postulated by Williams¹¹⁵ on the basis of spectrophotometric measurements. Further experimental evidence for π back bonding comes from infrared,¹¹⁴ e.p.r.¹¹⁶ and stability constant data.⁸⁴ π back bonding places electron density in the C-N π^* molecular orbital, and a decrease in the strength of the C-N double bond is therefore expected. The C=N stretching frequency of iron(II), cobalt(II), nickel(II) and copper(II) bis-(dimethylglyoximate) complexes show¹¹⁴ that the strength of the π back donation increases in the order Cu(II) < Ni(II) < Co(II) < Fe(II). E.p.r. measurements on various copper(II) α - and β -dioximates support the postulate of π donation from the metal to the ligand in these complexes.¹¹⁶ The stability constants of the dimethylglyoxime complexes of the transition metals manganese(II) to zinc(II) indicate that the iron(II) mono complex has a greater stability (Mn < Fe ~ Co < Ni > Cu > Zn) than that predicted from the Irving-Williams series (Mn < Fe < Co < Ni < Cu > Zn).⁸⁴ A similar result is obtained for diphenylglyoxime.⁸⁴ It can be inferred that

Fig. 1.6

Showing the (minimal) Overlap Between Oxime π^*
and Metal t_{2g} Orbitals



this extra stability results from the ability of Fe(II) to form stable π bonds.

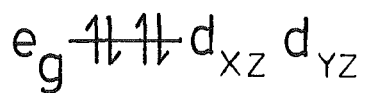
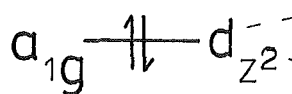
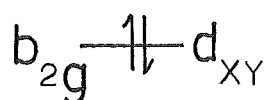
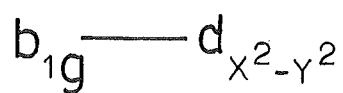
Other forms of π delocalization have been postulated to contribute to the high thermodynamic stability of the vic-dioxime complexes. Delocalization has been postulated for the π -electrons in the 5-membered chelate ring of dimethylglyoxime complexes. This delocalization would use the partially filled unhybridized p orbitals of the ligand carbon and nitrogen atoms and the t_{2g} orbitals of the metal.¹⁰⁷ The single crystal X-ray structure analysis indicates however, that little cyclic delocalization occurs in the bis-(dimethylglyoximate) copper(II) complex. Cyclic delocalization has also been suggested in the hydrogen bridge ring of dimethylglyoximate complexes, this delocalization utilizing the metal t_{2g} orbitals and the nitrogen and oxygen p orbitals.¹¹⁷

1.2.6 Metal-Metal Bonding in Oxime Complexes

The X-ray crystal structure of bis-(dimethylglyoximate)-nickel(II)⁷⁸ shows the square planar units to be stacked one above the other throughout the crystal lattice. Alternate complex molecules are staggered at 90° to each other and the nickel atoms, which are separated by 3.23 \AA , form long chains throughout the crystal. Isomorphous structures are observed for the palladium(II)¹¹² and platinum(II)¹¹⁰ bis-(dimethylglyoximate) complexes, as well as for the β form of bis-(ethylmethylglyoximate) nickel(II).¹¹⁸ Because of the short metal-metal distances in these crystal structures metal-metal bonding has been postulated.¹¹⁹

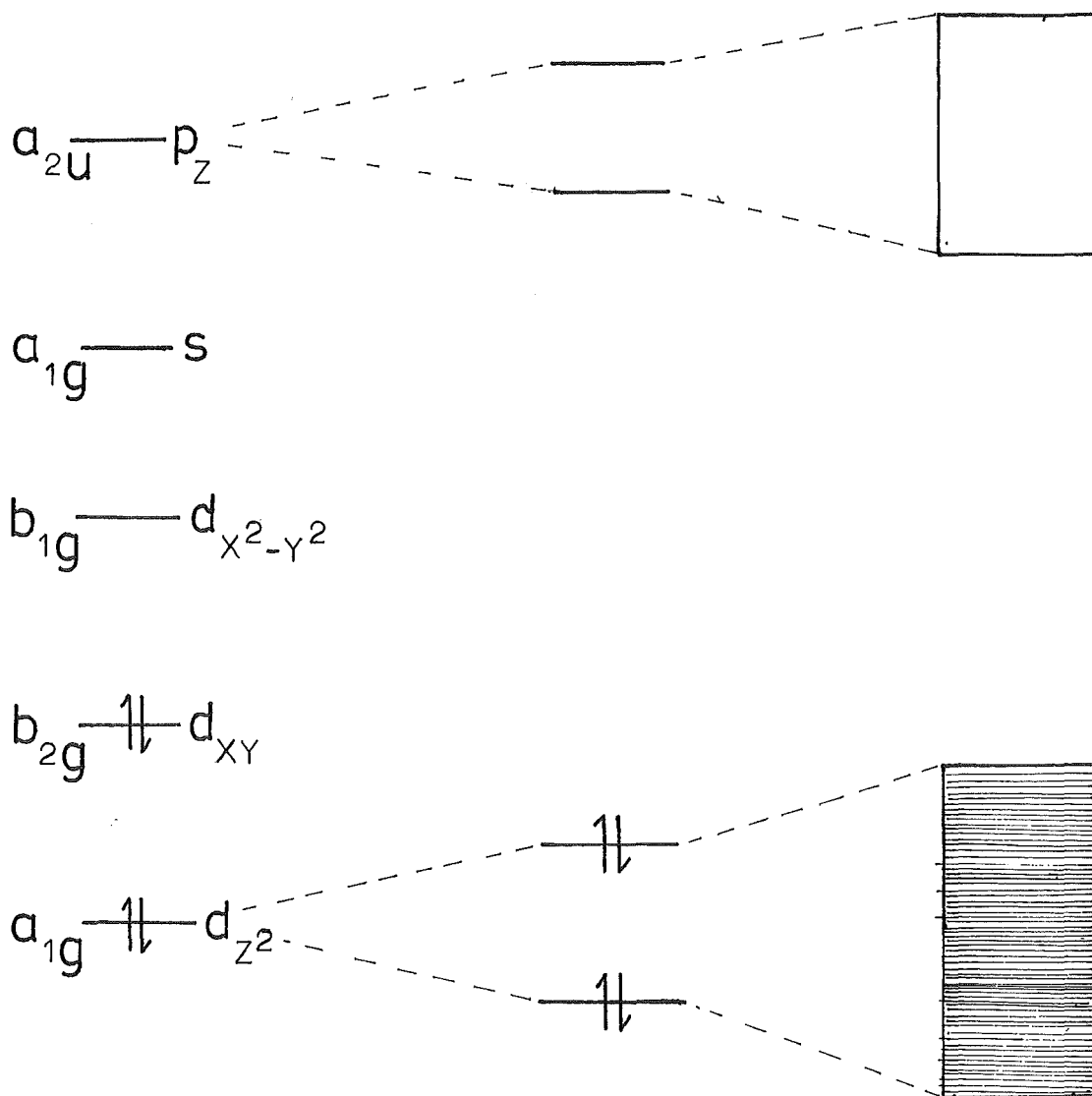
The metal-metal bonding may be described in terms of molecular orbital theory.^{119,120,121} The order of metal energy levels in a square planar complex molecule is as shown in fig 1.7.

Fig. 1.7

Metal-Metal Bonding in $M(\text{Hdmg})_2$ Isolated $M(\text{Hdmg})_2$

Effect of d_{z^2} and p_z
on the approach of a
second $M(\text{Hdmg})_2$

Effect of bonding
between $M(\text{Hdmg})_2$
units in a chain



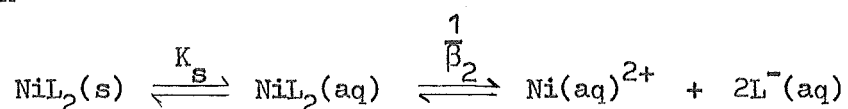
On approach of a second metal complex unit along the z-axis of the molecule the d_{z^2} atomic orbitals overlap to form a bonding and antibonding molecular orbital. A similar bonding and antibonding orbital is formed from the two p_z orbitals. The bonding and antibonding orbitals from the d_{z^2} orbitals are both filled and no net bonding interaction takes place. If a large number of orbitals overlap in this way then an orbital band is formed. The d_{z^2} band is completely occupied while the p_z band is empty. One criticism of this description for the bonding in metal chain compounds is that no bonding takes place in the ground state; the number of antibonding electrons is equal to the number of bonding electrons. However if some electrons are promoted from the d_{z^2} band to the p_z band, or if the complex is partially oxidised, an overall bonding interaction results. The gold(I)-gold(III) bis-(dimethylglyoximate) complex consists of gold(I) and gold(III) units alternating in a chain structure in the solid state.¹²² An overall bonding interaction also results if some mixing of the d_{z^2} and p_z orbitals occurs.

A theoretical molecular orbital calculation¹²³ on the metal-metal bonding in bis-(dimethylglyoximate) nickel(II) indicates that some mixing of energy levels must occur for a bonding interaction to result in the ground state of the molecule. These calculations indicate that the stabilization of the metal-metal bond is only ca. 67 J mol^{-1} .

The earliest evidence for metal-metal bonding in dimethylglyoxime complexes came from solubility measurements. The extremely low solubility of nickel(II) bis-(dimethylglyoximate) was thought to result from the stabilization of the solid state by the formation of metal-metal bonds. It has been inferred from solubility data that

the strength of the metal-metal bond in crystalline nickel(II) bis-(dimethylglyoximate) is ca. 41.8 kJ mol^{-1} ⁹⁷ (see section 1.2.2).

Comparison of solubility products for complexes with their metal-metal bond lengths suggests only a partial correlation exists. The solubility product decreases with a decrease in metal-metal bond length only for ligands which are structurally related⁹⁵ e.g. the structurally related ligands cyclohexane-1,2-dione dioxime (nioxime), 3-methyl nioxime and cycloheptan-1,2-dione dioxime (see table 1.4). The solubility product refers to the composite reaction



where HL is a dioxime ligand, K_s is the solubility of the complex NiL_2 and β_2 is the overall formation constant for the complex NiL_2 . However nickel(II) bis-(dimethylglyoximate) has a higher solubility (K_s) than that predicted from the crystalline nickel-nickel bond distance.⁸³ Varying solvation of the complexes may explain these results. Structural variations in the ligands have also been correlated with solubility.¹²⁴

The presence of a metal-metal interaction may also be inferred from absorption spectra. Crystalline bis-(dimethylglyoximate)-nickel(II) shows bands at 500 nm and 190 nm which are polarized parallel to the crystallographic c axis (axis of metal-metal bonds) and are absent in solution spectra.¹⁰² However, interpretation of these bands does not require metal-metal bonding but only requires an electrostatic interaction between neighbouring complex units.¹²⁵

Conductivity measurements on solid bis-(dimethylglyoximate)-nickel(II) have indicated that the conductivity along the c axis is 10^5 times as great as in compressed powder discs.¹²⁶ The conduction was increased by an increase in temperature, suggesting that electron

TABLE 1.4

Solubility Products and Nickel-Nickel Bond Distances

for Some bis(dioximato)nickel(II) Complexes.^a

Dioxime	Ni-Ni in Solid State ($\overset{\circ}{\text{A}}$)	$K_{\text{sp}} (\text{M}^3)$
Dimethylglyoxime	3.233	2.2×10^{-24}
Nioxime	3.237	4.1×10^{-29}
3-methylnioxime	3.470	2.4×10^{-28}
Cycloheptane-1,2-dioxime	3.596	2.3×10^{-27}

^aFrom ref. 95.

promotion from the d_{z^2} band to the p_z band increases conductivity. The crystal therefore acts as a semiconductor.

1.3 ANALYTICAL APPLICATIONS OF OXIMES

The analytical application of oximes for the determination of metal ions is a consequence of the high stability and low solubility of the complexes. Stability is enhanced by:

- (1) the formation of metal to ligand π bonds, and
- (2) the formation of strong intramolecular hydrogen bonds in the complexes. The low solubility of the metal oxime complexes in water, which has been attributed to the formation of metal-metal bonds, facilitates their application in gravimetric analysis and in solvent extraction.

1.3.1 The Stability of Oxime Complexes

The stability of oxime complexes is much higher than that predicted from the basicity of the oxime nitrogen; this has been attributed to metal to ligand π bonding.¹¹⁴ The result of hydrogen bond formation between adjacent oxime groups is to increase the stability of the bis complex. Measurements of the stability constants of dimethylglyoxime complexes of cobalt(II), nickel(II), copper(II) and zinc(II)⁸⁴ show the ratio K_1/K_2 to be less than expected on the basis of statistical considerations (see section 1.2.2). For the bis complexes of iron(II), nickel(II), copper(II) and zinc(II) with α -furylglyoxime⁶⁴ and for the cobalt(II), nickel(II), copper(II) and zinc(II) complexes of salicylaldoxime $K_1/K_2 < 1.0$.⁸⁵ The overall stabilities of the bis-(salicylaldoxime) complexes with nickel(II) and copper(II) ions are given by $\log \beta_2$ 14.3 and 21.5 respectively.⁸⁵ No mono-(salicylaldoxime) copper(II) complex was detected. The effect of the high stability is that a lower excess

quantity of ligand (or a lower pH) is required to effect complete formation of the bis complex (compare fig 1.8(a), (c) and (d)).

A further consequence of the high stability of the bis complex is to reduce the relative concentration of the mono complex in solution. When $K_1 = K_2$ the maximum concentration of the mono ligand species is only 33% of the total metal present whereas when $K_1 = 10^4 K_2$ 98% of the total metal ion may be present as the mono complex (see fig 1.8(b) and (c)). If $K_2 > K_1$ then the mono ligand complex is of only minor importance (never the major metal species in solution) at any time in the analytical determination of the metal ion.

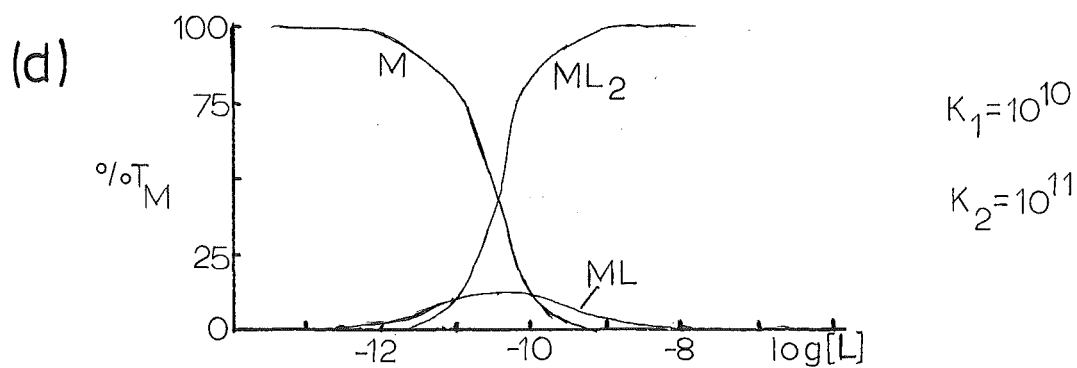
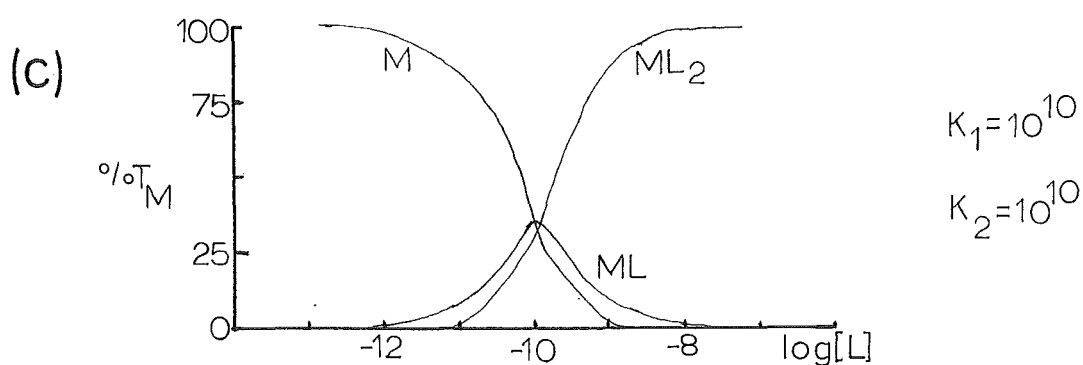
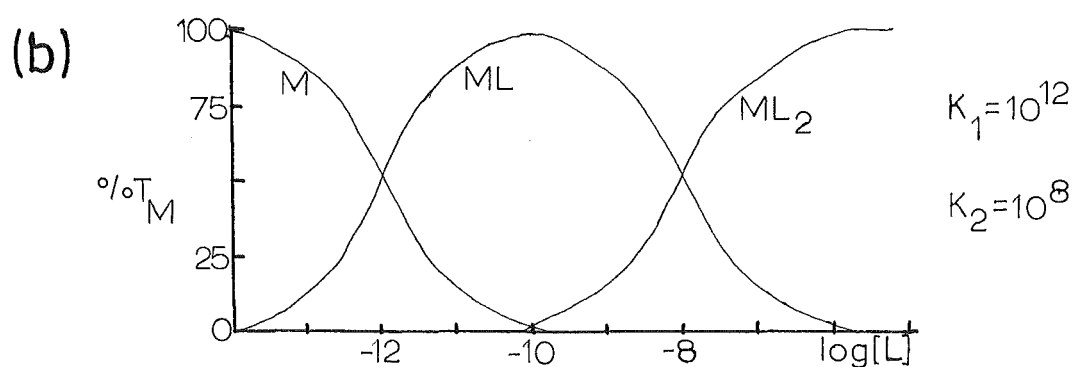
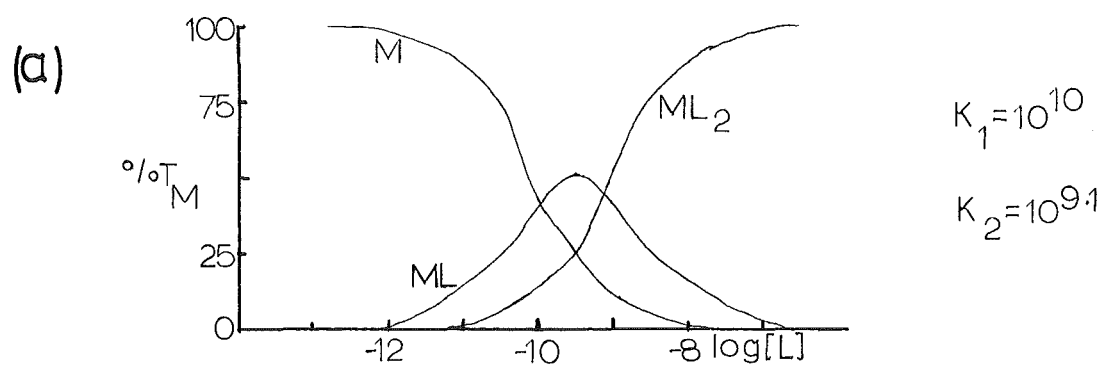
Most oxime and dioxime reagents commonly used in gravimetric analysis have a low solubility in water. In order to prevent precipitation of the organic reagent along with the metal complex an excess of the organic reagent must not be added. The high stability of dioxime complexes ensures that the amount of organic reagent added is kept to a minimum.

1.3.2 Solubility Factors

Gravimetric determinations of metal ions requires a complex to have a low solubility to facilitate its collection and weighing. Many dioxime complexes have this property and the low solubility can be attributed to:

- (i) the presence of a large hydrophobic group in the complexes (salicylaldoxime, dimethylglyoxime ligands),
- (ii) the zero charge on the complexes (resulting from loss of protons from the ligands), and
- (iii) the stabilization of the crystal lattice of the complexes through metal-metal bonding.

Fig. 1.8

Distribution Curves for the Formation of Species ML and ML_2 

Dimethylglyoxime forms a more stable complex with palladium(II) than with nickel(II). Palladium(II) can therefore be determined in the presence of nickel(II) ions at low pH (where the nickel(II) complex will not form).² On increasing the pH the nickel(II) complex forms but the palladium complex does not interfere because of the tendency of the metal-metal bonded palladium(II) complex to form a monomeric hydroxy species $[\text{Pd}(\text{Hdmg})_2\text{OH}]^-$ with an OH^- co-ordinated in the trans octahedral position.²

1.3.3 Solvent Extraction Techniques

Many oxime complexes are observed to have a higher solubility in organic solvents than in water.¹²⁴ Utilization of this allows water insoluble metal oxime complexes to be extracted into an organic phase and the concentration to be determined colorimetrically.¹²⁷ For example this process is used to determine nickel by extracting the red dimethylglyoximate complex into chloroform at pH 7 - 12.¹²⁷ The amount of complex extracted into the organic phase will depend upon a number of factors.^{4,127} These include the pH, the ionization constants for the ligand in aqueous solution, the formation constants for the complex and the distribution constants for the complex and ligand between the organic and aqueous phases. Optimum pH and concentration conditions can be determined to maximise the amount of complex extracted into the organic phase or to maximise the separation of different metals.

Similar solvent extraction techniques with oxime reagents have been used in the commercial extraction of metals from leachates.¹²⁸ Salicylaldoxime analogues have been found to selectively extract copper(II) ions from iron(III) ion solutions. The extraction reagents often contain a long alkyl chain para to the phenolic hydroxyl group to reduce solubility in the aqueous phase. To further reduce solubility

the aldehydic proton is replaced by a second phenyl group i.e. the extraction reagent is an alkyl substituted α -hydroxybenzophenone oxime.

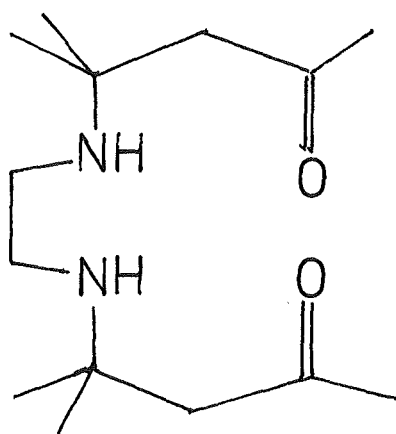
1.4 THIS WORK

Oxime complexes are stabilized by (1) deprotonation of the oxime and (2) hydrogen bonding. In most cases these two processes occur simultaneously and the aim of this work has been to prepare ligands for which these two important processes can be studied separately in the formation of their metal complexes. The ligands chosen were H_2dddo , $Hddmo$ and $dddm$ (see fig 1.9). These ligands generally form 1 : 1 complexes with metal ions. Within this series of ligands the formation of $Cu(H_2dddo)^{2+}$ can be compared with $Cu(Hdddo)^+$ to determine the increase in the stability of oxime complexes associated with the simultaneous oxime deprotonation and intramolecular hydrogen bond formation. Comparison of the thermodynamic data for the 1 : 1 complexes of $Hddmo$ and $ddmo^-$ yields information on the effect of deprotonation (in the absence of intramolecular hydrogen bond formation) on complex stability. Comparison of the stability of $Cu(dddm)^{2+}$ with the corresponding 1 : 1 copper(II) complexes of H_2dddo and $Hddmo$ gives information on the relative donor strengths of the $=NOCH_3$ and $=NOH$ functional groups.

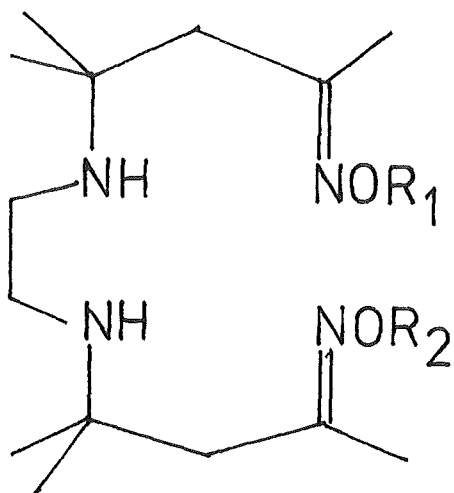
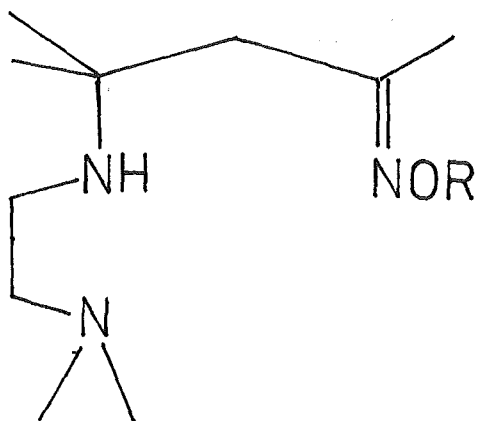
Log K (potentiometric), ΔH (calorimetric) and ΔS values for the formation and deprotonation reactions of the ligands $Hddmo$ and $dddm$ with copper(II) ions have been determined and the data compared with that for the diamine dioxime H_2dddo as determined by Hedwig.¹²⁹

Fig. 1.9

Ligands: Structures and Abbreviations



dddk

 $R_1=R_2=H$; H₂dddo. $R_1=H, R_2=CH_3$;
Hddmo. $R_1=R_2=CH_3$; dddm. $R=H$; Hdno. $R=CH_3$; dnm.

The relative donor strengths of the oxime and O-methyloxime functional groups was assessed from log K data for the reaction of Hdno and dnm with copper(II) ions. Models of the complexes $\text{Cu}(\text{Hdno})^{2+}$ and $\text{Cu}(\text{dnm})^{2+}$ do not indicate any steric hindrance associated with the oxime OR group whereas in the corresponding complexes of H_2dddo , Hddmo and dddm models indicate that steric effects may contribute to the magnitude of log K.

The effect which change of metal ion has on the tendency of the co-ordinated oxime group to deprotonate (and hydrogen bond) was determined for the divalent metal ions iron, cobalt, nickel, copper and zinc by measurement of the stabilities of the complexes of these metal ions with H_2dddo and Hddmo.

The protonation constants (amino) for the ligands Hddmo, dddm, Hdno and dnm have been determined and the corresponding ΔH (calorimetric) and ΔS data determined for Hddmo and dddm.

The relative tendencies of the oxime and O-methyloxime functional groups to undergo E-Z isomerization in acid solution has been investigated.

CHAPTER 2

THERMODYNAMIC CONSIDERATIONS

The determination of the free energy change ΔG° for an equilibrium reaction requires a knowledge of the activity quotient for the equilibrium K° (thermodynamic equilibrium constant). After determination of the enthalpy change ΔH° , the entropy change ΔS° is determined from

$$\Delta G^\circ = \Delta H^\circ - T\Delta S^\circ \quad 2.1$$

This chapter outlines methods of determining ΔG° and ΔH° and some of the factors which determine the magnitude of the thermodynamic functions. The determination of hydrogen ion concentration is also discussed.

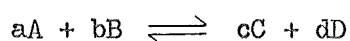
2.1 DETERMINATION OF ΔG° , ΔH° AND ΔS°

2.1.1 Determination of the Thermodynamic Equilibrium Constant

The determination of an equilibrium activity quotient requires a knowledge of the activities of all species taking part in the equilibrium reaction. The activity a_x of a species X is defined as

$$a_x = [X]\gamma_x \quad 2.2$$

where $[X]$ is the concentration of X in solution and γ_x is the single ion activity coefficient of X. The activity coefficient is a function of the ionic strength of the solution. For a general equilibrium



the thermodynamic equilibrium constant is defined as

$$K^O = \frac{[C]^c [D]^d \gamma_C^c \gamma_D^d}{[A]^a [B]^b \gamma_A^a \gamma_B^b} = \frac{a_C^c a_D^d}{a_A^a a_B^b} \quad 2.3$$

In order to determine K^O the activity coefficients γ_i need to be known. Experimental values of the activity coefficients can only be obtained for pairs of ions in solution,¹³⁰ and only limited data are available. Empirical equations for γ_i generally apply to single electrolytes in dilute solution. The usual method of determining K^O is to consider it as a function of the concentration quotient K_c , where

$$K_c = \frac{[C]^c [D]^d}{[A]^a [B]^b}, \quad 2.4$$

and of the ionic strength (I); i.e.

$$K^O = K_c \cdot f(I) \quad 2.5$$

The extended form of the Debye-Huckel equation can be used to calculate values for mean activity coefficients;

$$\log \gamma_{\pm} = \frac{-A |Z_+ Z_-| \sqrt{I}}{1 + B \sqrt{I}} + CI \quad 2.6$$

where γ_{\pm} is the mean activity coefficient for the positive and negative ions taking part in the reaction; A, B and C are constants dependent on the nature of the ions in solution, the solvent and the temperature; and Z_+ and Z_- are the charges of the positive and negative ions respectively. Substitution of equations 2.4 and 2.6 into equation 2.3 gives an equation for the thermodynamic equilibrium constant in terms of the concentration quotient and the ionic strength. In practise the value of K_c may be determined at a variety of ionic

strengths and $\log K_c$ is plotted against a function of the ionic strength such that the plot is linear. At zero ionic strength (where all activity coefficients are unity) $\log K_c = \log K^0$.

2.1.2 Free Energy Changes

The chemical potential of a species i is defined relative to a standard state as

$$\mu_i = \mu_i^0 + RT \ln a_i \quad 2.7$$

where μ_i^0 is the chemical potential of the species i in the standard state and a_i is the activity of the species i . The free energy change for a reaction at constant temperature and pressure is defined as the chemical potential of the products less that of the reactants. Thus for reaction I

$$\Delta G = d\mu_D + c\mu_C - a\mu_A - b\mu_B \quad 2.8$$

Substitution of equation 2.7 into equation 2.8 gives

$$\begin{aligned} \Delta G &= (d\mu_D^0 + c\mu_C^0 - a\mu_A^0 - b\mu_B^0) + RT \ln \frac{a_C^c a_D^d}{a_A^a a_B^b} \\ &= \Delta G^0 + RT \ln K^0 \end{aligned} \quad 2.9$$

For a reaction at equilibrium $\Delta G = 0$ and hence

$$\Delta G^0 = -RT \ln K^0 \quad 2.10$$

If K^0 can be determined at a constant temperature the free energy change ΔG^0 can also be determined.

2.1.3 Enthalpy and Entropy Changes

Two methods exist for determining the enthalpy change for a reaction. These are (1) the temperature variation method and (2) the

direct calorimetric measurement method.

Temperature Variation Method The free energy change for a reaction is composed of the enthalpy change and the entropy change according to equation 2.1 or

$$\ln K^{\circ} = \frac{-\Delta H^{\circ}}{RT} + \frac{\Delta S^{\circ}}{R}$$

At constant pressure

$$\frac{\partial(\ln K^{\circ})}{\partial T} = \frac{\Delta H^{\circ}}{RT^2} \quad 2.11$$

The enthalpy change can therefore be determined from the change in $\ln K^{\circ}$ with temperature. This approach requires that the equilibrium constants are known very accurately and that a wide temperature range is used. However, if there is a large variation of ΔH° with temperature, the relation

$$\log K^{\circ} = a + bT + cT^2 \quad 2.12$$

must be solved for the parameters a, b, and c. Equations 2.11 and 2.12 then yield

$$\Delta H^{\circ} = 2.303 RT^2(b + cT) \quad 2.13$$

and ΔH° may be determined from equation 2.13.

Direct Calorimetric Measurement The direct measurement of the enthalpy change for a reaction in a calorimeter is a superior method for determining the enthalpy change for a reaction.⁹⁸ This method was used in this work.

Once the free energy change (ΔG°) and the enthalpy change (ΔH°) are known the entropy change for a reaction can be derived from equation 2.1.

Under certain circumstances both $\log K^\circ$ and ΔH° may be determined in the same experiment. Such an experiment is known as an "entropy titration".^{131,132} The condition for the technique to be applicable to an equilibrium system is that the formation of the products of the equilibrium must be appreciable but incomplete under the reaction conditions (i.e. $2 < \log K < 4$).¹³³ There exist unique values of ΔH° and $\log K^\circ$ which satisfy the equations relating the concentration of the species in solution and the observed heat changes for all stoichiometries of the reactant species. The "best" values of $\log K$ and ΔH have been found by graphical and least squares processes.^{131,132} The technique has been used to determine thermodynamic data for the proton ionization from HSO_4^- ¹³¹ and for the reaction between metal ions (zinc(II), magnesium(II) and calcium(II)) and sulphate ions,¹³⁴ though some critical analyses have been offered.¹³²

2.2 EFFECT OF AN INERT ELECTROLYTE ON THE THERMODYNAMIC PARAMETERS

Most measurements made on metal-ligand equilibrium systems have involved solutions with a relatively high concentration (0.1 - 3.0M) of an "inert" electrolyte. The assumptions made are that the "inert" electrolyte does not have specific ionic interactions with the species under study and that the activity coefficients of the reacting species do not change with different concentrations of reactants, i.e. the activity coefficients of the reacting species are determined only by the ionic strength of the solution. Equations 2.3 and 2.10 give

$$\Delta G^\circ = -RT \ln K_c - RT \ln \frac{\gamma_D^d \gamma_C^c}{\gamma_A^a \gamma_B^b} \quad 2.14$$

A "free energy" term can be defined for an ionic strength other than 0.0M as

$$\Delta G^1 = -RT \ln K_c$$

and equation 2.14 becomes

$$\Delta G^0 = \Delta G^1 - RT \ln \left(\frac{\gamma_D^d \gamma_C^c}{\gamma_A^a \gamma_B^b} \right) \quad 2.15$$

For the purpose of comparing free energy changes it is assumed

that the term $RT \ln \left(\frac{\gamma_D^d \gamma_C^c}{\gamma_A^a \gamma_B^b} \right)$

has the same magnitude in the systems under comparison.

A similar expression for the effect of ionic strength on enthalpy changes can be derived from equations 2.3 and 2.11 as

$$\begin{aligned} \Delta H^1 &= RT^2 \frac{\partial(\ln K_c)}{\partial T} \\ &= \Delta H^0 - RT^2 \frac{\partial}{\partial T} \ln \left(\frac{\gamma_D^d \gamma_C^c}{\gamma_A^a \gamma_B^b} \right) \end{aligned} \quad 2.16$$

The relation

$$\frac{\partial(n_i \log \gamma_i)}{\partial T} = n_i \cdot 2 \times 10^{-3} \log \gamma_i \quad 2.17$$

where the terms n_i are the exponents of the activity coefficients in equation 2.3, has been found to hold approximately at ambient temperatures,⁹⁸ and substitution of equation 2.6 and 2.17 into equation 2.16 yields

$$\Delta H^1 = \Delta H^0 + RT^2 \cdot 2 \times 10^{-3} \frac{AI^{\frac{1}{2}}}{1 + BI^{\frac{1}{2}}} \sum_i n_i Z_i^2 \quad 2.18$$

where n_i is positive for product species and negative for reactants.¹³⁵ Thus for a reaction where $\sum n_i Z_i^2 = 0$, $\Delta H^0 \simeq \Delta H^1$ (e.g. for the reaction $H^+ + L \rightleftharpoons HL^+$). For a reaction where $\sum n_i Z_i^2 = 2$ (e.g. $HL^+ + H^+ \rightleftharpoons H_2L^{2+}$) $\Delta H^0 = \Delta H^1 - 0.82 \text{ kJ mol}^{-1}$ for ΔH^1 measured at $I = 0.1M$ and $\Delta H^0 = \Delta H^1 - 1.41 \text{ kJ mol}^{-1}$ for ΔH^1 measured at $I = 0.5M$.

By substitution of equations 2.15 and 2.18 into equation 2.10 the entropy change at an ionic strength different from zero can be derived as

$$\Delta S^1 = \Delta S^0 - R \left(T \frac{\partial}{\partial T} \ln \left(\frac{\gamma_D^d \gamma_C^c}{\gamma_A^a \gamma_B^b} \right) + \ln \left(\frac{\gamma_D^d \gamma_C^c}{\gamma_A^a \gamma_B^b} \right) \right) \quad 2.19$$

A secondary standard state is usually defined (e.g. $I = 0.1M$) where the activity coefficients are equated to unity. This procedure is valid so long as similar metal-ligand systems are compared at the same ionic strength. Under these circumstances the activity coefficients of the equilibrium species being compared are assumed to be identical at the same ionic strength.

2.3 FACTORS DETERMINING THE MAGNITUDE OF THE THERMODYNAMIC PARAMETERS

The free energy change for a reaction is dependent on the magnitude and sign of the enthalpy and entropy change for that reaction at a given temperature according to equation 2.1.

2.3.1 Free Energy Changes

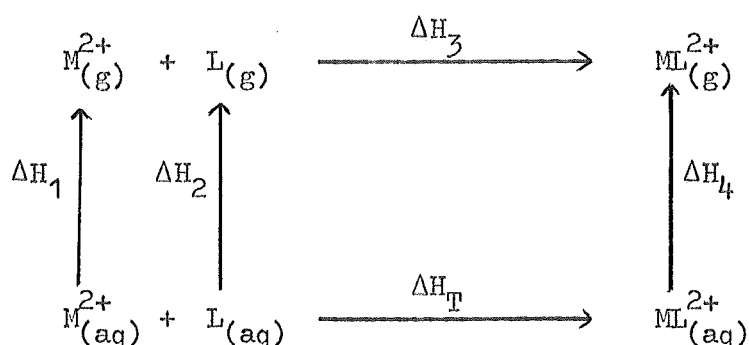
In the absence of enthalpy and entropy change data for a reaction, free energy changes can only be compared for reactions containing similar ligands (and metal ions). If the reactant ligands and metal ions, and product metal-ligand species are of similar structure

then entropy changes for the systems under study are assumed to be of similar magnitude and the free energy change is a measure of the enthalpy change.

The magnitudes of free energy changes for metal complexation reactions have been correlated with⁹⁸ (1) the ionic charge and radius of the metal ion, (2) the metal ionization potential, (3) the crystal-field stabilization energy for the metal complex ion, (4) the donor atom or groups, and (5) the basicity of the ligand.

2.3.2 Enthalpy Changes

For a metal complexation reaction with a ligand L, the enthalpy change is contributed to by (1) an endothermic heat change associated with the breaking of metal-water bonds, (2) an exothermic heat change associated with the formation of metal-ligand bonds and (3) a heat change associated with different secondary sphere solvation of the complex compared to the free metal ion and the free ligand molecule. These contributing factors to the overall enthalpy change can be considered in terms of an enthalpy cycle:



The total enthalpy change in solution (ΔH_T) is given by Hess's Law as

$$\Delta H_T = \Delta H_3 + \Delta H_1 + \Delta H_2 - \Delta H_4.$$

The heat change associated with the formation of metal-ligand bonds is denoted by ΔH_3 and the heat change involving desolvation of the metal

ion and ligand, and solvation of the complex species (factors (1) and (3) above) is given by $\Delta H_1 + \Delta H_2 - \Delta H_4$.

The importance of these solvation terms is illustrated by reference to the reaction between aluminium ions and fluoride ions. For the reaction $\text{Al}^{3+} + 6\text{F}^- \longrightarrow \text{AlF}_6^{3-}$ in the gas phase $\Delta H = -975 \text{ kJ mol}^{-1}$ ¹³⁶ whereas in aqueous solution the observed enthalpy change is 0.42 kJ mol^{-1} ¹³⁷. The difference is attributable to the solvation terms ΔH_1 , ΔH_2 and ΔH_4 .

2.3.3 Entropy Changes

The solvent largely determines the entropy change for a reaction. Consider a metal complexation reaction



Ions and molecules in solution order the solvent molecules because of the charge or polarity of the metal ion or ligand species. The ordering of solvent molecules about a metal ion can be considered to result from two separate phenomena: (1) the formation of a primary co-ordination sphere in which the metal ion forms co-ordinate bonds with the neighbouring water molecules (e.g. $\text{Co}(\text{H}_2\text{O})_6^{2+}$), and, (2) the formation of a secondary hydration sphere which consists of solvent molecules ordered about the metal ion by dipole-dipole and dipole-charge interactions. On co-ordination of the ligand L the release of a water molecule from the co-ordination sphere of the metal ion will contribute a positive entropy change. Changes in the solvent ordering ability of the metal aqua and metal complex ions will contribute to the entropy change. If (as is generally the case) the ligand is to some extent hydrophobic in character (e.g. an ethylenic chain linking donor atoms) the complex will order the solvent less than does the free metal ion and a positive

entropy change will result. Similarly water molecules released from the ligand on co-ordination will contribute a small positive entropy change.

Contributions to the overall entropy change arise from changes in the number of degrees of freedom (rotational, vibrational and translational) of the ligand on co-ordination to a metal ion. There is a decrease in the translational degrees of freedom and changes in the vibrational and rotational modes of the ligand molecule. These changes make a negative contribution to the overall entropy change.

The Chelate Effect Metal chelate complexes are generally more stable than the corresponding complexes containing the same number of donor atoms formed from monodentate ligands. For example the overall stability of $\text{Cu}(\text{NH}_3)_2^{2+}$ is less than that for $\text{Cu}(\text{en})^{2+}$ (where en represents ethylenediamine) (see table 2.1). The chelate effect is considered to be largely an entropy effect. However the thermodynamic parameters can be converted to a dimensionless unitary function by using a mole fraction scale for concentrations instead of mol litre^{-1} :⁹⁸

$$\Delta G^u = \Delta G + \Delta n RT \ln 55.5$$

$$\Delta H^u = \Delta H$$

$$\Delta S^u = \Delta S - \Delta n R \ln 55.5$$

where ΔG^u , ΔH^u and ΔS^u are the unitary free energy, enthalpy and entropy changes respectively and Δn is the number of moles of products less the moles of reactants. When the entropy change is converted to the unitary entropy change the magnitude of the effect is substantially reduced (see fig. 2.1).

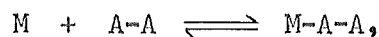
TABLE 2.1

Thermodynamic Data for the Formation of $\text{Cu}(\text{NH}_3)_2^{2+}$ and $\text{Cu}(\text{en})^{2+}$ at 25°C .^a

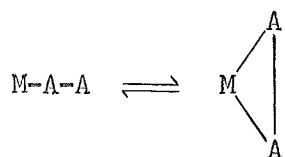
Reaction	ΔG (kJ mol ⁻¹)	ΔH (kJ mol ⁻¹)	ΔS (J mol ⁻¹ K ⁻¹)	ΔS^u (J mol ⁻¹ K ⁻¹)
$\text{Cu}^{2+} + 2\text{NH}_3 \rightleftharpoons \text{Cu}(\text{NH}_3)_2^{2+}$	-43.4	-41.8	5.4	71.9
$\text{Cu}^{2+} + \text{en} \rightleftharpoons \text{Cu}(\text{en})^{2+}$	-61.1	-54.4	22.6	55.6

^aData from Poulsen, I., and Bjerrum, J., Acta Chem. Scand. (1955), 9, 1407.

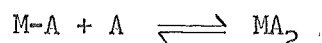
An explanation of the chelate effect is that formation of the chelate complex proceeds in distinct steps.^{138,139} In the first step the ligand occupies one co-ordination site only i.e.



and in the second step the ring is formed,



In the second step the effective "activity" of the second donor atom is high because of its close proximity to the metal ion. Ring closure therefore occurs with greater probability than the co-ordination of a second monodentate ligand in the equilibrium



The favourable enthalpy of chelation has been attributed to the reduction in donor group repulsive forces in a chelate compound compared with two complexed monodentate ligands¹³⁸ and to the larger crystal field stabilization energy associated with a chelate ligand.¹⁴⁰

Statistical Effects Statistical factors contribute to the entropy change under some circumstances. These are best considered in terms of an example. For the co-ordination of a monodentate ligand to a tetrahedral metal aquo ion there are four possible sites for co-ordination of the first donor and only one possible site for loss of a ligand molecule. ΔS_1 therefore has a statistical contribution of $+R \ln \frac{4}{1}$. For the co-ordination of a second ligand molecule only three sites remain but dissociation of the resultant complex can occur in two different ways. ΔS_2 therefore has a contribution of

$+R \ln \frac{3}{2}$. By similar considerations ΔS_3 and ΔS_4 have contributions of $+R \ln \frac{2}{3}$ and $+R \ln \frac{1}{4}$ respectively.⁹⁰ The order $\Delta S_1 > \Delta S_2 > \Delta S_3 > \Delta S_4$ contributes to the order $K_1 > K_2 > K_3 > K_4$. Similar analyses are used to determine the statistical contributions to octahedral and square planar complexes of mono and polydentate ligands,⁹⁰ and to the protonation of bases.¹⁴¹

2.4 DETERMINATION OF HYDROGEN ION CONCENTRATION

The method employed in the present study to determine the equilibrium concentration quotients and enthalpy changes was to solve a series of mass balance equations to find the equilibrium concentrations of all species in solution as outlined in chapter 4. Once one concentration is known the concentration of all other species in equilibrium with it can be determined. The approach used in the present work was to determine the hydrogen ion concentration, $[H^+]$, and all other required concentrations were calculated from this and the mass balance equations.

For a cell

glass electrode//test solution/KCl(sat.), $Hg_2Cl_2(s)$, $Hg(l)$

the e.m.f. is given by

$$E = E^O + E_{as} + E_{LJ} - \frac{RT}{F} \ln a_{H^+}$$

where E^O is the standard e.m.f. for the cell, E_{as} is the asymmetry potential of the glass membrane, E_{LJ} is the liquid junction potential for the cell and a_{H^+} is the activity of hydrogen ions in the test solution.

The e.m.f. of a standard buffer solution is related to the defined pH(S) as

$$E_s = E^O + E_{as} + E_{LJ}^s + 2.303 \frac{RT}{F} \text{pH}(S) \quad 2.21$$

and for a solution of unknown pH as

$$E_x = E^O + E_{as} + E_{LJ}^x + 2.303 \frac{RT}{F} pH^x. \quad 2.22$$

From equations 2.21 and 2.22 the unknown pH^x for the test solution is given by

$$pH^x = pH(S) - \frac{(E_{LJ}^x - E_{LJ}^S) + (E_s - E_x)}{2.303 \frac{RT}{F}} \quad 2.23$$

$pH(S)$ values for a set of standard solutions have been determined in a cell without liquid junction using Pt/H₂ and Ag/AgCl electrodes.¹⁴² These standard buffer solutions set up a conventional activity scale. Measurements of pH will only approach this conventional activity scale if the residual liquid junction potential ($E_{LJ}^x - E_{LJ}^S$) is small. This situation occurs if the ionic strength of the standard and test solutions are the same. This is seldom the case. The ionic strength of the test solutions used in this work is 0.1M whereas the ionic strength of the potassium hydrogen phthalate buffer, for example, is 0.053M.

To convert the measured pH^x from the conventional activity scale to the hydrogen ion concentration $[H^+]$ the relation

$$pH^x = p[H^+] - \log \gamma_{H^+}$$

is required where γ_{H^+} is the activity coefficient of the hydrogen ion. In practice it is assumed that a simple equation (e.g. equation 2.5) accurately defines γ_{H^+} for a given ionic strength.

These assumptions concerning the residual liquid junction potential and activity coefficients can be avoided by calibration of the cell against solutions of known $[H^+]$ and with the same ionic strength (and background) as the test solutions. This calibration requires a knowledge of accurate concentration quotients for buffer

systems so as the response of the electrode system to known $[H^+]$ may be determined. Accurate concentration quotients are known for the acetate-acetic acid buffer system¹⁴³ and the ethylenediamine-ethylenediammonium buffer system.¹⁴¹ The concentration quotients for the acetic acid system were determined in a cell without liquid junction and the ethylenediamine concentration quotients in a cell with liquid junction in such a way that the residual liquid junction potential was eliminated by extrapolation of data to zero concentration of buffer.

This method of calibration can establish a correlation curve between $[H^+]$ and the measured pH at a fixed ionic strength. The correlation is relative to a response of the electrodes to the standard buffers and as a result only the response of the cell to the standard buffers need be redetermined before use.

This method of calibration of the cell against solutions of known ionic strength and hydrogen ion concentration was used in this work (see section 3.1.3).

CHAPTER 3

EXPERIMENTAL

A. PHYSICAL MEASUREMENTS

3.1 pH MEASUREMENTS

All pH measurements used in the determination of protonation constants for the ligands, and stability constants for the metal-ligand complexes, were made using a cell with liquid junction: glass electrode//test solution/KCl(sat.), $\text{Hg}_2\text{Cl}_{2(s)}$, $\text{Hg}_{(l)}$.

The potential of this cell is given by

$$E^x = E^0 + E_{as} + E_{LJ}^x - \frac{RT}{F} \ln a_{H^+}$$

where E_{as} is the asymmetry potential of the glass membrane and E_{LJ}^x is the e.m.f. of the reference electrode with KCl(sat) chosen as the standard state. The pH for an unknown solution is related to that for a standard buffer by

$$p a_{H^+} = pH(s) - \frac{(E_s - E^x) + (E_{LJ}^x - E_{LJ})}{2.303 RT/F}$$

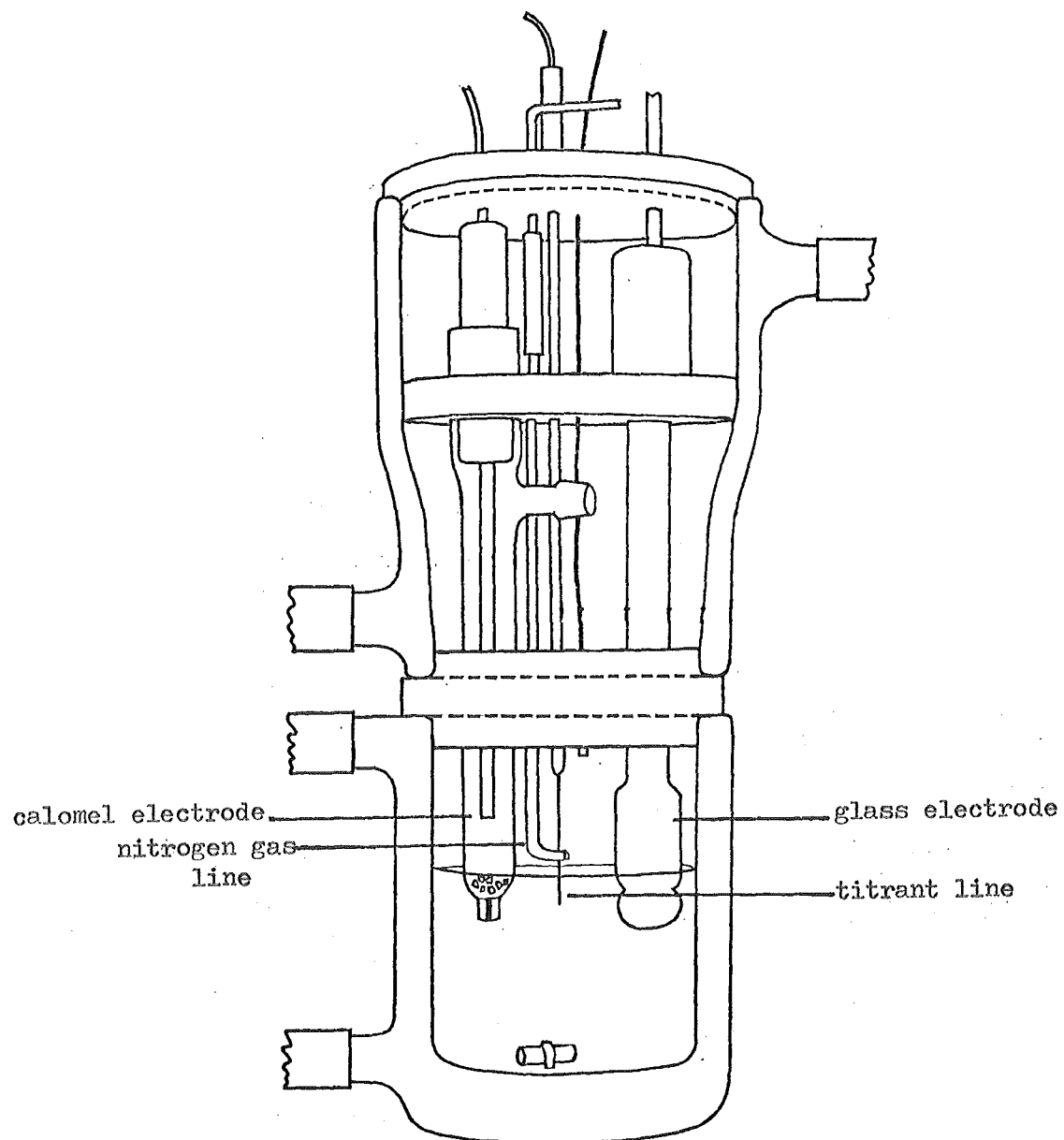
where $pH(s)$, E_s and E_{LJ} refer to values determined for a defined (conventional) standard buffer (see section 2.4).

3.1.1 Equipment

pH was recorded using a Beckman research pH meter with a Beckman E2 glass electrode (type 39004) and a Beckman frit junction calomel reference electrode (type 39071, saturated KCl). The thermostatted titration cell and electrode housing have been described¹²⁹ and are shown diagrammatically in fig 3.1. For oxygenation studies on cobalt complexes and stability constant determinations on the oxygen

Fig. 3.1

Thermostatted Titration Cell and Electrode Housing



sensitive cobalt and iron complexes (which required a titration cell of limited capacity and no air space) a JEN^{AR} glass/calomel combination electrode was used (see section 3.3).

3.1.2 pH Calibration against Standard Buffers

Calibration of the electrodes was effected against the (conventional) primary standard buffers defined by the National Bureau of Standards (N.B.S.) (viz. 1 : 1 phosphate, pH(S) 6.865; borax (0.01m), pH(S) 9.183; and potassium hydrogen phthalate (0.05m), pH(S) 4.008).¹⁴² Standard borax, 1 : 1 phosphate and phthalate buffers were prepared according to Bates,¹⁴² using AnalaR chemicals dissolved in carbonate-free distilled water. Hedwig¹²⁹ has shown that buffers prepared in this way have pH values identical with those buffers prepared from N.B.S. certified chemicals. Fresh buffer solutions were prepared regularly.

The electrode system was standardized against these buffers before and after each set of titrations. The linearity of response to these buffers in a cell with liquid junction was determined by measuring the response of the electrodes to the borax and phthalate buffers relative to the 1 : 1 phosphate buffer as a primary standard. With the Beckman electrodes the pH measured (pH_m) for the standard buffers relative to the 1 : 1 phosphate buffer were within ± 0.004 of the defined pH(S) values. However for the potassium hydrogen phthalate buffer the response of the electrode system was not consistent with the N.B.S. scale (pH_m 4.032, pH(S) 4.008) as described by Hedwig¹²⁹ and confirmed by Taylor.¹⁴⁴ Hedwig also observed pH_m values of 1.679 ± 0.003 for tetroxalate buffer (pH(S) 1.679) and 3.570 for potassium hydrogen tartrate buffer (pH(S) 3.557) in cells with liquid junction. On the basis of these data a correction curve was established and this curve was used to correct data for the pH range 1.7 - 5.6.

By use of both Ag/AgCl and calomel reference electrodes Taylor¹⁴⁴ has shown that the discrepancies between pH_m and $pH(S)$ at $pH_m < 5.6$ arises from the combined effects of (1) a non-Nernstian response of the electrodes and (2) the effect of pH on E_{LJ} at $pH < 3$.

3.1.3 The Glass Electrode as a Hydrogen Ion Concentration Probe

To obtain protonation quotients and stability quotients from pH measurements it is necessary to know the equilibrium concentration of hydrogen ion $[H^+]$ in solution. The glass electrode measures pH (pa_H) and it is necessary to convert pH_m to $p[H^+]$. This was done by calibrating the electrode system against buffer systems of known $[H^+]$ and at a fixed ionic strength as described in section 2.4. This avoids assumptions that otherwise have to be made concerning activity coefficients and liquid junction potentials.

The Beckman glass electrode and Beckman calomel electrode pair were previously calibrated by Hedwig between pH 2 and 10 by titration of standard sodium hydroxide against (1) dilute HCl solutions, (2) acetic acid solutions and (3) ethylenediammonium chloride solutions at constant ionic strength.¹⁴⁵ The electrode pair was found to obey the linear relationship

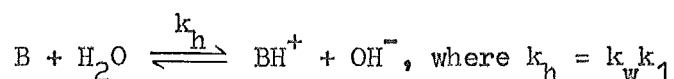
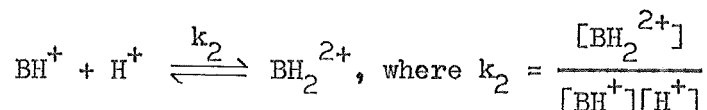
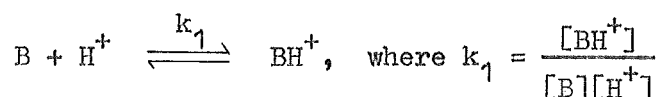
$$pH_m = (0.9951 \pm 0.0003) p[H^+] + (0.088 \pm 0.002)$$

The JEN^{AR} glass/calomel combination electrode was calibrated as a hydrogen ion concentration probe in the range pH 6 - 10 by titration of standard sodium hydroxide (0.283M) against solutions of ethylenediamine dihydrochloride (ca. $2 \times 10^{-3}M$) at constant ionic strength (0.10M NaCl).

The response of the JEN^{AR} electrode to the standard borax buffer was found to be pH_m 9.152 ($pH(S)$ 9.183) with respect to the phosphate buffer. The concentration quotients for protonation of

ethylenediamine at 25.0°C and $I = 0.10M$ were interpolated as $\log k_1 = 9.960$ and $\log k_2 = 7.105$.¹⁴¹

For each point on the titration curve the equilibrium concentrations of the species OH^- , B , BH^+ , BH_2^{2+} and H^+ (where B represents deprotonated ethylenediamine), are related by the following equations



The equilibrium concentrations of these species and the analytical (stoichiometric) concentrations of base (ethylenediamine) T_B , and of titratable protons T_H , are related by

$$\begin{aligned} T_B &= [B] + [BH] + [BH_2] \\ &= [B] + k_1[B][H] + k_1k_2[B][H]^2 \end{aligned} \quad 3.1$$

and

$$\begin{aligned} T_H &= [H] + [BH] + 2[BH_2] - [OH] \\ &= [H] + k_1[B][H] + 2k_1k_2[B][H]^2 - [OH] \end{aligned} \quad 3.2$$

where charges have been omitted for clarity.

T_H is found experimentally as the total analytical concentration of ionizable hydrogen ions in the initial solution less that removed by reaction with the added alkali;

$$T_H = 2 \times T_B - \frac{v \times A}{v + V} \quad 3.3$$

where v is the volume of A molar alkali added to the initial volume V of ethylenediamine dihydrochloride solution. A term C can be derived where

$$\begin{aligned} C &= [\text{BH}] + 2[\text{BH}_2] \\ &= T_H + [\text{OH}] - [\text{H}] \end{aligned} \quad 3.4$$

From equations 3.1 and 3.4

$$\begin{aligned} C - T_B &= [\text{BH}_2] - [\text{B}] \\ &= [\text{B}](k_1 k_2 [\text{H}]^2 - 1) \end{aligned} \quad 3.5$$

By substituting the expression for $[\text{B}]$ obtained from equation 3.1 into equation 3.5 the quadratic equation 3.6 is obtained:

$$[\text{H}]^2(k_1 k_2 C - 2k_1 k_2 T_B) + [\text{H}](k_1 C - k_1 T_B) + C = 0 \quad 3.6$$

An initial estimate of C was found from the experimental pH_m , assuming $[\text{H}^+] = 10^{-\text{pH}}$, and the volume of alkali added. Equation 3.6 was solved to obtain a better estimate of $[\text{H}^+]$. An iterative procedure was used to obtain the best value of $[\text{H}^+]$ and $\text{p}[\text{H}^+]$.

The values obtained for pH_m and $\text{p}[\text{H}^+]$ are given in table 3.1. In contrast to the results for the Beckman E2 glass electrode a graph of $\text{p}[\text{H}^+]$ versus pH_m was non-linear with increasing slope at higher pH . This non-linearity can be ascribed to sodium ion errors at $\text{pH} > 9$. Measured pH values were corrected from this curve.

This calibration is made relative to standardization against the standard N.B.S. buffers and is valid when the electrodes give an internally consistent response to these buffers.

3.1.4 Titration Procedure

For titrations involving ligand-proton equilibria or ligand-

TABLE 3.1

pH_m and $\text{p}[\text{H}^+]$ Data for ethylenediamine-ethylenediammonium Buffers at
 $I = 0.10\text{M NaCl}, 25.0^\circ\text{C}.$

Initial Solution Composition: $[\text{en}, 2\text{HCl}] = 2.009 \times 10^{-3}\text{M}$

Vol^a	pH_m^b	$\text{p}[\text{H}^+]^c$	Vol^a	pH_m^b	$\text{p}[\text{H}^+]^c$
0.06	6.482	6.414	0.25	7.531	7.477
0.07	6.564	6.496	0.26	7.592	7.536
0.08	6.634	6.659	0.27	7.656	7.599
0.09	6.700	6.637	0.28	7.723	7.667
0.10	6.759	6.699	0.39	9.050	9.041
0.11	6.818	6.758	0.40	9.144	9.144
0.12	6.872	6.813	0.41	9.226	9.233
0.13	6.924	6.867	0.42	9.304	9.313
0.14	6.978	6.919	0.43	9.370	9.384
0.15	7.028	6.969	0.44	9.430	9.450
0.16	7.078	7.019	0.45	9.490	9.511
0.17	7.127	7.068	0.46	9.544	9.568
0.18	7.175	7.116	0.47	9.592	9.623
0.19	7.224	7.165	0.48	9.640	9.674
0.20	7.271	7.214	0.49	9.684	9.724
0.21	7.318	7.264	0.50	9.724	9.772
0.22	7.367	7.315	0.52	9.804	9.864
0.23	7.418	7.367	0.54	9.881	9.953
0.24	7.474	7.421	0.56	9.954	10.040

^aVolume (ml) of 0.2829M NaOH added to 49.93 ml of en,2HCl solution

^b pH_m = measured pH

^c $\text{p}[\text{H}^+]$ = negative logarithm of hydrogen ion concentration

metal ion equilibria the following procedures were used:

Method (a) A 50 ml aliquot of a previously prepared stock solution of the ligand or ligand and metal ion, of known concentration and adjusted to constant ionic strength ($I = 0.10M$ NaCl), was transferred to the titration cell. Standard NaOH solution was added incrementally from a Gilmont or Agla micrometer syringe. The volume of standard alkali and the measured pH were recorded.

Method (b) This method for performing a titration was used when conservation of ligand was essential. A weighed sample of the ligand was placed in the titration cell and 50 ml of carbonate-free distilled water was added. The calculated volume of standard metal ion solution was added from a micrometer syringe and the resultant solution was adjusted to constant ionic strength by addition of solid NaCl to $I = 0.10M$. Titrant was added as above.

3.2 CALORIMETRIC MEASUREMENTS

Enthalpy measurements were made by measuring the heat evolved (Q_{obs}) on the incremental addition of HCl ($\sim 1M$) to basic solutions of the ligands or metal-complex solutions in a titration calorimeter. The composition of the calorimeter solution was determined from iterative calculations based on a parallel titration. ΔH values were calculated from

$$Q_{obs} = a_1\Delta H_1 + a_2\Delta H_2 + \dots + a_n\Delta H_n$$

where a_1, a_2, \dots, a_n are the amounts of each species formed and $\Delta H_1, \Delta H_2, \dots, \Delta H_n$ are the associated enthalpy changes.

3.2.1 The Calorimeter

The titration calorimeter consisted of a thin walled glass titration cell enclosing a 10,000 Ω thermister (one arm of an a-c

wheatstone bridge), a stirrer driven by a synchronous motor, an evaporation cooler (a small bulb containing ca. 0.25 ml of water which was partially evaporated under a stream of air to cool the test solution), a capillary tube connected to an Agla micrometer syringe for delivery of titrant and a wire wound heater for heating the solution. The titration cell was covered with aluminium foil and this cell was suspended in an air cavity in a water tight brass can. This outer can was immersed in a well-stirred water bath thermostatted to $25.00 \pm 0.01^{\circ}\text{C}$ as determined by a calibrated calorimetric thermometer (calibrated in 100ths of a degree). The temperature of the water bath was controlled to better than $\pm 0.001^{\circ}\text{C}$ during a titration as determined by thermister measurements. (See fig 3.2.) Full descriptions of the calorimeter construction and of the a-c wheatstone bridge and heating circuits have been given.¹²⁹

3.2.2 Temperature Measurement

The temperature measuring device in the calorimeter is a thermister, a thermally sensitive resistor. The resistance R of a thermister at a temperature T is represented by the equation

$$\log R = \frac{a}{T} + b$$

where a and b are constants characteristic of the thermister.

Over small temperature ranges (as used in this study) it has been determined¹²⁹ that an equation of the type

$$R = d - cT$$

applies where d and c are constants. The absolute temperature inside the calorimeter could be estimated from the value of R_3 (see fig 3.3) when the wheatstone bridge is at balance. Temperature

Fig. 3.2

Titration Calorimeter

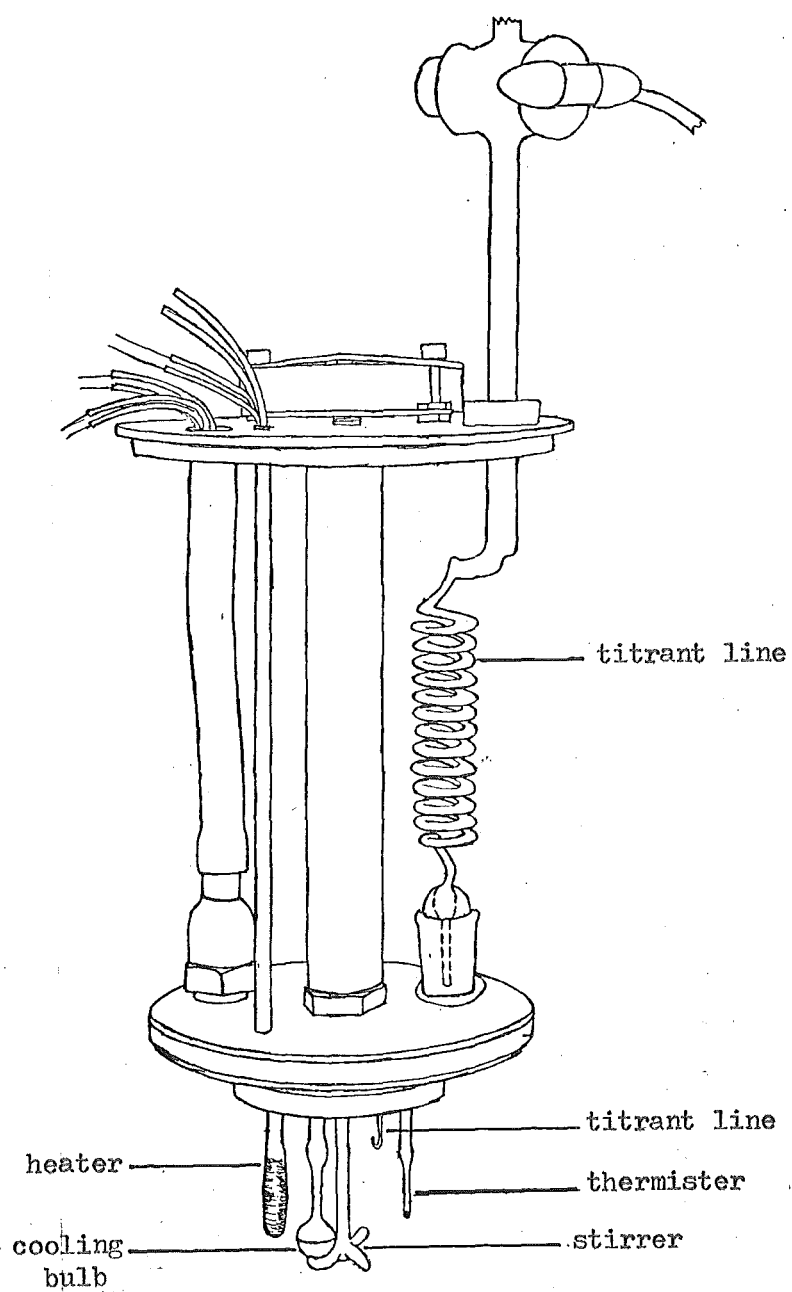
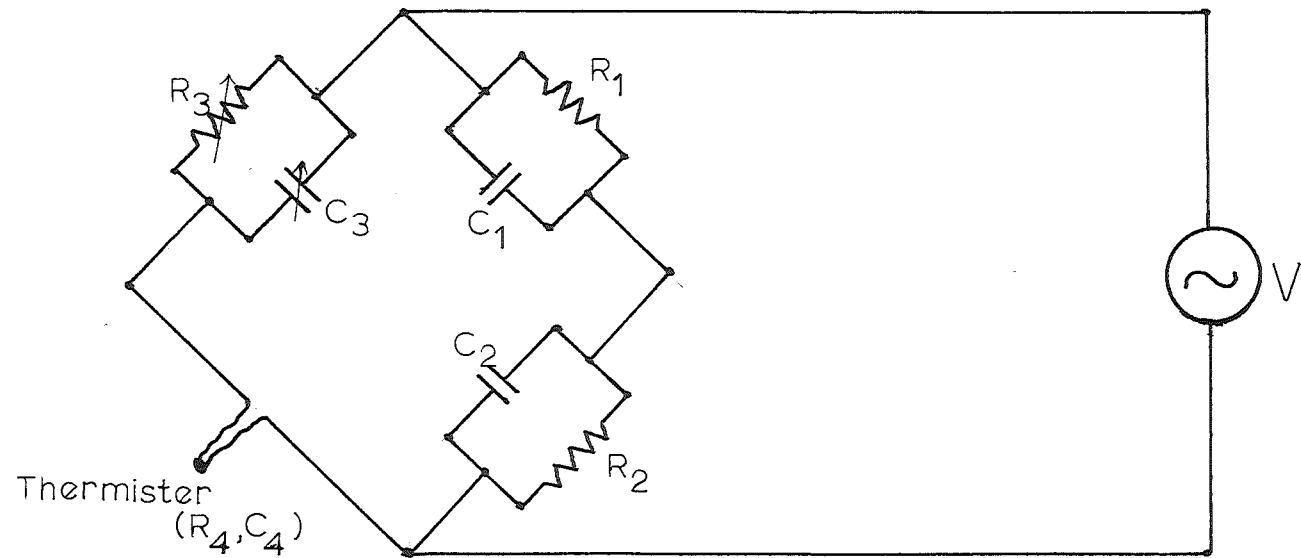


Fig. 3.3

A.C. Bridge Circuit Incorporating a Thermister



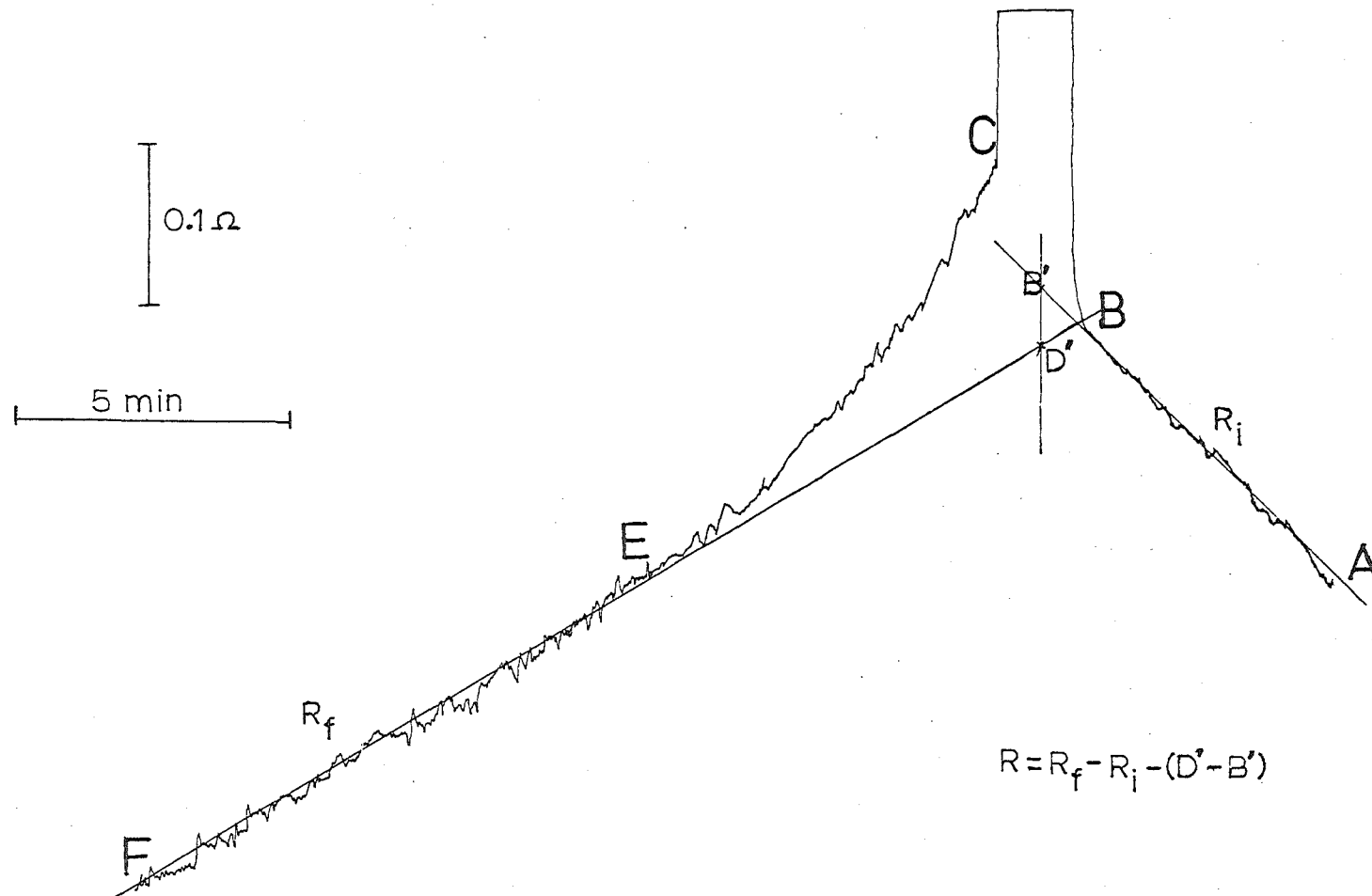
$$R_4 = \frac{R_2}{R_1} R_3$$

variations in the calorimeter (due to heat transfer or chemical reactions) were determined by recording the out of balance current of the bridge on a Honeywell Elektronik 194 lab/test recorder.

A typical recorder trace is shown in fig 3.4. The calorimeter solution will be at its equilibrium temperature when energy supplied to the solution (in the form of stirring, heat transfer, etc.) is equal to the energy lost to its surroundings. At point A the solution has been cooled to a temperature lower than its equilibrium temperature and as heat is transferred from the surroundings the solution warms (line AB). The initial temperature at A was adjusted so that the rate of warming was ca. $0.03 \Omega \text{ min}^{-1}$ i.e. $1 \times 10^{-4} \text{ } ^\circ\text{C min}^{-1}$. At point A the a-c wheatstone bridge was balanced (both capacitance and resistance) and the balance resistance (R_i) recorded. When the warming curve (AB) was near linear (point B) either titrant was added to effect a chemical change or the heater circuit was switched on to effect a thermal calibration. The addition of titrant was complete (or the heater circuit was opened) at point C and the wheatstone bridge was again balanced (capacitance and resistance). The balance resistance (R_f) was recorded and the solution allowed to cool (CF). The cooling curve followed Newton's Law of cooling (in region EF) and became approximately linear after 10 to 15 minutes. The trace was followed for a further 10 - 15 minutes. Non-Newton cooling (CE) was observed initially because of localized heating of regions of the calorimeter. The warming curve (AB) and the linear region of the cooling curve (EF) were extrapolated to the mid-point of the heating period (or point where half the titrant increment had been added). The change in R_z , which is proportional to the change in temperature of the calorimeter, is given by $R_f - R_i$ plus a correction for the non-coincidence of points B' and D'. This correction was calculated

Fig. 3.4

Typical Calorimetric Recorder Trace



from the measured effect of a change of 0.1Ω in R_3 on the recorder trace (ca. 12 chart divisions).

3.2.3 Thermal Calibration of the Calorimeter

Energy changes in the calorimeter were detected by comparing ΔR_3 for a chemical reaction with the change in R_3 when a known amount of electrical energy had been discharged in the calorimeter ($\Delta R_3'$). By varying the current to the heater and the heating time it was possible to have $\Delta R_3' \sim \Delta R_3$ and

$$Q_{\text{chemical}} \text{ (J.)} = \frac{R_3 \times Q_{\text{electrical}} \text{ (J.)}}{\Delta R_3'}$$

The thermal (electrical) calibration of the calorimeter contributes to the precision and accuracy of the value obtained for Q_{chemical} . The precision of this calibration was checked by repeated heating cycles when the calorimeter contained either 100 ml of distilled water or a test solution ($I = 0.10M \text{ NaCl}$). The heating period was varied (140 - 260 sec.) and the heating current varied (12 - 36 mA). Values of $Q_{\text{electrical}}/\Delta R_3'$ are given in table 3.2. In a calorimetric titration the total volume of solution inside the calorimeter increases as titrant is added. Therefore the heat capacity of the calorimeter varies and $Q_{\text{electrical}}/\Delta R_3'$ should increase linearly with small increases in titrant volume. A plot of $Q_{\text{electrical}}/\Delta R_3'$ against volume was constructed (see fig 3.5); such plots were used to interpolate values of $Q_{\text{electrical}}/\Delta R_3'$ during subsequent titrations.

3.2.4 The Accuracy of a Calorimetric Measurement

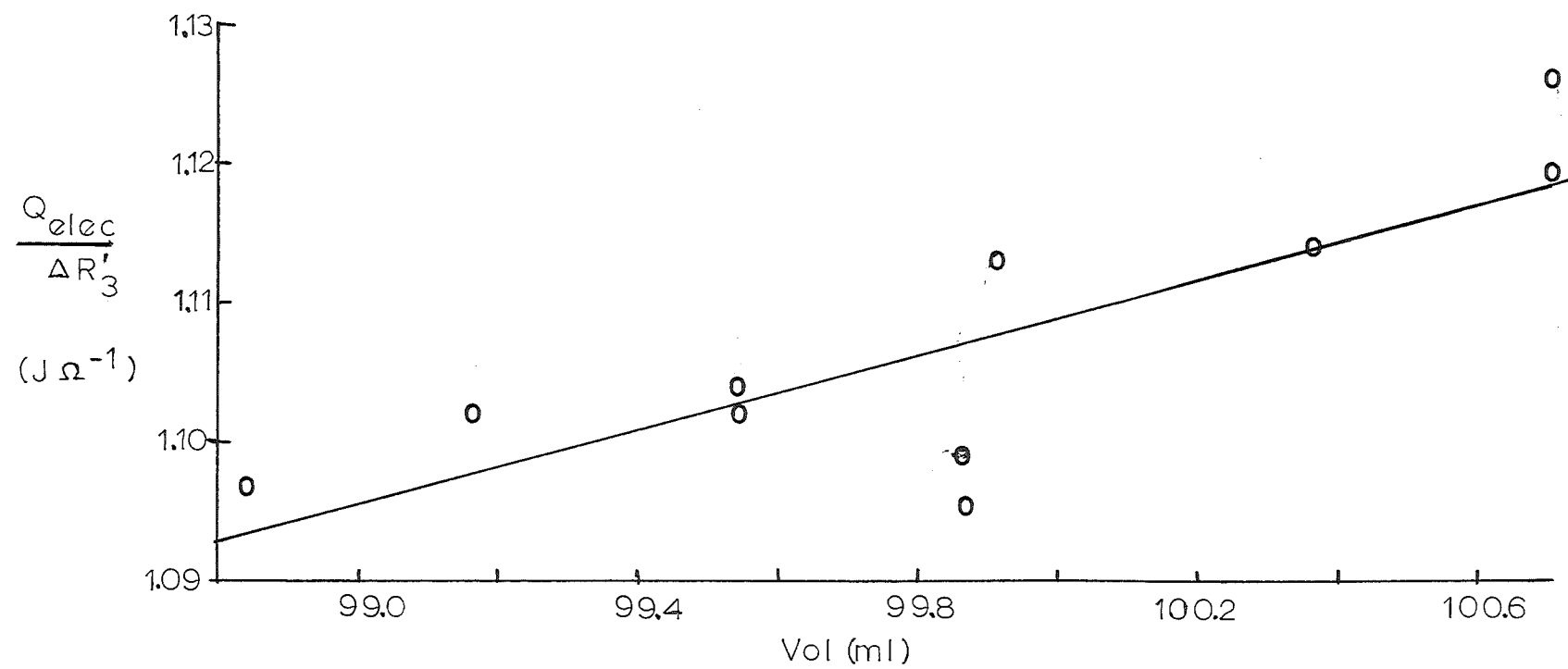
The accuracy of a calorimetric measurement was determined by measuring the enthalpy change for a "standard reaction" viz. the

TABLE 3.2Calibration Constants for the Calorimeter at $25.0 \pm 0.01^{\circ}\text{C}$

Total Volume (ml.)	Q_{elec} (J)	ΔR (Ω)	$Q_{\text{elec}}/\Delta R$ (J Ω^{-1})
98.84	6.9233	6.312	1.097
99.16	6.9342	6.294	1.102
99.54	6.0510	5.492	1.102
99.54	3.4290	3.106	1.104
99.86	6.0809	5.566	1.093
99.86	6.0897	5.556	1.096
99.91	6.0691	5.454	1.113
100.36	3.1615	2.838	1.114
100.70	6.0885	5.440	1.119
100.70	6.0902	5.409	1.126

Fig. 3.5

Plot of $Q_{elec}/\Delta R_3'$ vs. Volume of Calorimeter Solution



protonation of an aqueous solution of aminotri-(hydroxymethyl) methane (Tris), a monobasic compound.

A buffered solution of Tris in the calorimeter was titrated incrementally with HCl (0.984M) and the heat changes noted. A Tris solution with composition 0.008M TrisH and 0.007M Tris allowed 4 titration increments each with a heat change of ca. 7.7 J. The mean and standard deviation of 8 measurements was $\Delta H = -47.43 \pm 0.29 \text{ kJ mol}^{-1}$ (literature values^{146,147} -47.48 and -47.44 kJ mol⁻¹). Calorimetric results are given in table 3.3.

3.2.5 Procedure for a Calorimetric Titration

Calorimetric titrations were performed in two different ways.

Method (a) A 100 ml aliquot of a previously prepared thermostatted stock solution of known ligand and metal ion concentrations, and adjusted to constant ionic strength ($I = 0.10\text{M NaCl}$) was transferred to the calorimeter cell. The assembled calorimeter was then immersed in the thermostatted water bath. The temperature of the test solution was adjusted to the equilibrium temperature of the calorimeter (ca. 0.010 - 0.015°C above the bath temperature) by means of the calorimeter heater on the cooling bulb. The calorimeter was left in this condition for at least one hour to allow the test solution to reach true thermal equilibrium with its surroundings. Attainment of the equilibrium was inferred from the value of R_z when the bridge was at balance or from a recorder trace with slope zero. The solution was then cooled by ca. 0.005 - 0.010°C and the solution allowed to warm by the transfer of heat from the titration cell surroundings into the test solution (fig 3.4, region AB). When a plot of thermister resistance versus time was near linear, a known volume of standard HCl was added (fig 3.4, region BC) to effect the chemical reaction and then

TABLE 3.3

Representative Calorimetric Data from the Protonation of
Aminotri(hydroxymethyl)methane (Tris) at 25.00°C.

<u>Vol</u> ^a	<u>10⁴Δ(Tris)</u> ^b	<u>ΔR</u>	<u>Q_{react}</u> ^c	<u>Q_m</u> ^d	<u>-ΔH</u>
(ml)	(mol)	(Ω)	(J)	(J)	(kJ mol ⁻¹)
0.16	1.574	6.792	7.641	7.389	46.932
0.16	1.574	6.890	7.772	7.520	47.764
0.16	1.574	6.745	7.629	7.377	46.856
0.16	1.574	6.830	7.745	7.493	47.592
0.16	1.574	6.850	7.775	7.523	47.781
0.16	1.574	6.804	7.729	7.477	47.491
0.16	1.574	6.780	7.729	7.477	47.491

^aVolume (ml) of 0.984M HCl added to solution

^bMoles of Tris converted to HTris

^cMeasured heat change

^dQ_{react} corrected for heat of dilution of HCl

the solution was allowed to cool (region CEF). Temperature changes and heat changes were determined as in sections 3.2.2 and 3.2.3. When a measurement was completed the calorimeter solution was then cooled and the procedure repeated for further titrant increments or thermal calibrations.

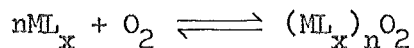
Method (b) This method of performing a calorimetric titration was used when it was necessary to conserve ligand. Weighed samples of ligand and of NaCl (to attain constant ionic strength) were added to the calorimeter cell. A 100 ml aliquot of thermostatted distilled water was added. This process was most efficient when the distilled water was 2 - 3°C above the equilibrium temperature of the calorimeter as the solution cooled during the process of transfer to the calorimeter cell. As required metal ion solution was added from a micrometer syringe. The procedure was then as for method (a).

Due to the low solubility of the ligands, and the tendency of the ligands to float on water rather than dissolve, the most efficient method found to dissolve the ligand (especially in method (b) where excessive shaking was not possible) was to store the weighed sample of ligand in the calorimeter cell in a humid atmosphere for 24 hours before dissolution, and to slowly add the distilled water so that the solid ligand was thoroughly wetted before the bulk of the water was added.

3.3 OXYGEN-FREE STUDIES AND OXYGENATION STUDIES

Many cobalt(II) amine complexes are susceptible to oxidation to cobalt(III) complexes by atmospheric oxygen. Iron(II) ions are readily oxidised by O₂ to iron(III) ions in neutral or alkaline solution. In order to obtain reliable stability constants for these metal ion systems it is necessary

to carry out the measurements under oxygen-free conditions. The oxygenation reactions shown by other cobalt(II) complexes;



can be studied from knowledge of the stability constants for the complexes and measurements of the change in oxygen concentration of the metal complex solution. The measurement and control of the oxygen concentration is therefore essential in studies on complexes of cobalt(II) and iron(II).

3.3.1 Equipment

The oxygen-sensitive systems (Co(II) and Fe(II)) and the oxygenation reactions (Co(II)) were studied in the titration cell shown in fig 3.6. All pH measurements were recorded on a Beckman Research pH meter using a JEN^{AR} glass/calomel combination electrode (see sections 3.1.1 and 3.1.3). The concentration of dissolved oxygen was determined with a Beckman 100802 Fieldlab oxygen analyser and a Beckman 39550 polarographic oxygen electrode.

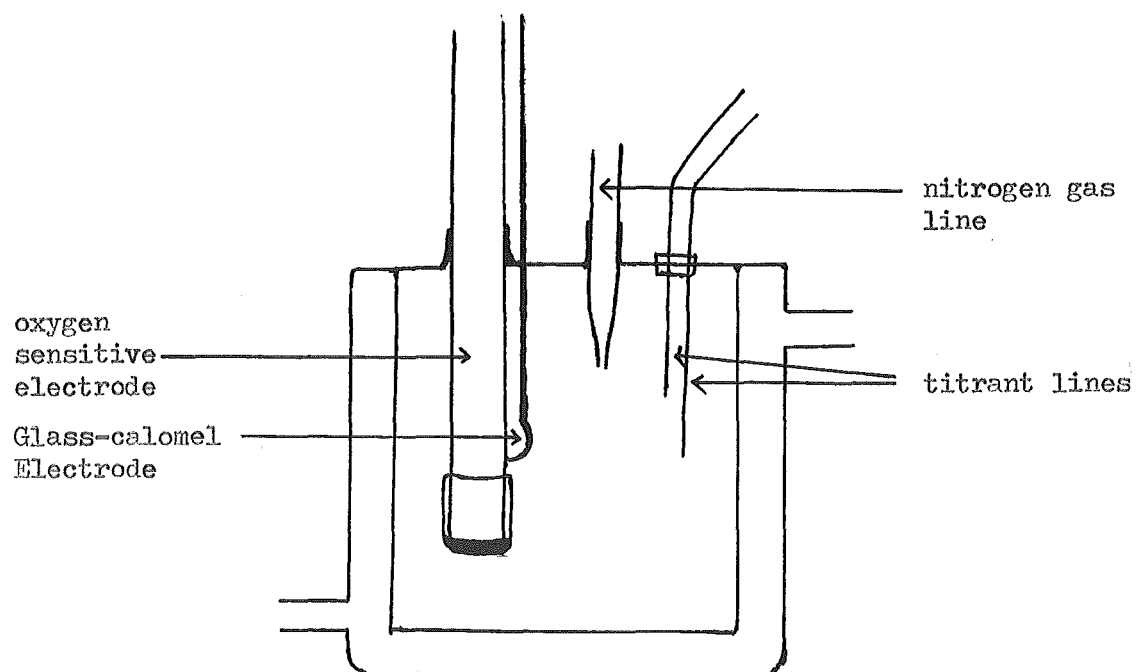
The thermostatted titration cell of total volume 64 ml was air tight. The glass/calomel combination electrode, oxygen sensitive electrode, syringe needles and a nitrogen gas line passed into the solution through entry ports through the top of the cell. When the cell was sealed from the atmosphere it was necessary to have a capillary venting tube as the oxygen-sensitive electrode was sensitive to small pressure changes caused by the addition of titrant. This titration cell has been described in more detail elsewhere.¹⁴⁸

3.3.2 Oxygen Measurement

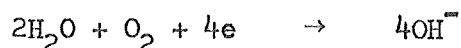
The oxygen-sensitive electrode detects the partial pressure

Fig. 3.6

The Oxygenation Cell



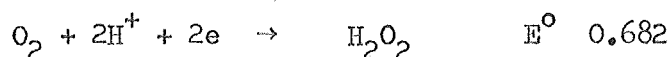
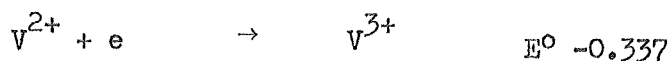
of dissolved oxygen by a polarographic method. Oxygen dissolved in the test solution diffuses through a gas-permeable teflon membrane to the electrode assembly (a rhodium cathode and Ag/AgCl anode). A potential of 0.53 V is applied between the electrodes. The oxygen is reduced at the cathode



and a current flows which is proportional to the partial pressure of oxygen in the bulk solution. Kee¹⁴⁸ has determined that the response of the oxygen sensor is linear with the concentration of dissolved oxygen. The sensor was restandardized before use by reference to air-saturated distilled water ($[\text{O}_2] = 8.48$ ppm at 25°C)¹⁴⁹ and to oxygen-free distilled water. An empirical adjustment for the varying oxygen solubility with changing ionic strength was made according to the manufacturers manual.

3.3.3 Preparation of Oxygen-free Nitrogen Gas

Oxygen-free nitrogen gas was prepared by bubbling commercial nitrogen gas through an acidic vanadium(II) solution which was prepared by the reduction of vanadyl sulphate solution by zinc amalgam. Traces of oxygen in the commercial nitrogen were removed by the following reactions:



Preparation of Zinc Amalgam The zinc amalgam was prepared by stirring a 2% mercuric chloride solution with zinc pellets for 10 minutes. The resultant zinc amalgam was washed three times with distilled water.

Stock Vanadyl Sulphate Solution A stock VOSO_4 solution was prepared by dissolving $\text{VOSO}_4 \cdot 2\text{H}_2\text{O}$ (2.5 g) in water. Concentrated H_2SO_4 (7 ml) was added and the resulting mixture diluted to 250 ml.

Preparation of Vanadium(II) Solution The acidic VOSO_4 solution was added to the zinc amalgam in a gas bottle until the zinc amalgam was covered. On bubbling nitrogen gas through the zinc amalgam/ VOSO_4 the colour changed from blue (VO^{2+}) to green (V^{3+}) to violet (V^{2+}).

3.3.4 Procedure for an O_2 -free Titration

Weighed samples of the ligand and NaCl (to attain constant ionic strength) were added to the titration cell and the cell filled with thermostatted carbon dioxide-free water. Oxygen-free nitrogen gas was bubbled through the ligand solution until the oxygen sensor registered an oxygen concentration of zero. The calculated volume of metal ion solution was added from a micrometer syringe and the total volume adjusted so that there was no air space in the titration cell. Nitrogen gas was bubbled through the solution until the $[\text{O}_2]$ was again zero. When this condition was achieved the titration cell was sealed (except for the capillary to equalize pressures), or a flow of oxygen-free nitrogen was kept flowing over the exposed surface of the solution. Standard NaOH was added incrementally and pH data collected.

3.3.5 Procedure for the Oxygenation of a Cobalt(II) Complex

When the oxygenation of a cobalt(II) complex was studied the titration cell described in section 3.3.1 was adjusted such that two syringes entered the test solution. Weighed samples of ligand and NaCl were added to the titration cell and the cell was filled with air-saturated water. The titration cell was sealed (except for

the capillary to maintain equality of pressures) and the solution pH adjusted to the pH range under study by addition of standard NaOH from one of the micrometer syringes. The pH was recorded and an aliquot of cobalt(II) in solution added from the second micrometer syringe. The pH and $[O_2]$ were recorded. The pH was readjusted to the initial pH value and the procedure repeated.

3.4 SPECTROPHOTOMETRIC MEASUREMENTS

All p.m.r. spectra were run at 60 MHz and at ca. 30°C on a Varian T-60 instrument. Infrared spectra were recorded for nujol or halocarbon mulls on a Shimadzu IR-27G spectrophotometer. Ultra-violet and visible absorption spectra were recorded on a Shimadzu MPS-50L spectrophotometer or a Varian Techtron 635 spectrophotometer. Atomic absorption spectroscopy measurements for nickel and copper analyses were made on a Varian Techtron A.A.5 spectrophotometer.

3.5 MICROANALYSES

Microanalysis of the ligands and complexes for C, H and N were performed by Dr A. Campbell at the Microanalytical Laboratory, University of Otago, Dunedin.

B. SYNTHESIS OF LIGANDS AND COMPLEXES

3.6 PREPARATION OF LIGANDS

The β -aminoketoxime or O-methyloxime ligands were synthesised by the formation of the β -aminoketone (by reaction of the protonated parent diamine with acetone) followed by reaction with hydroxylamine ($HONH_2$) or methoxyamine (CH_3ONH_2). An alternative method for the preparation of O-methyloxime derivatives of ketones involves the reaction of methyl sulphate (or halide) with the parent oxime. This

reaction could not be used to prepare the ligands used in this study because alkyl sulphate (or halide) reacts with secondary (tertiary) amines to produce tertiary amines (quaternary ammonium salts).

3.6.1 Methoxyamine hydrochloride, $\text{CH}_3\text{ONH}_2\cdot\text{HCl}$

Methoxyamine was prepared by the methods of Hjeds¹⁵⁰ and of Scherer et al¹⁵¹ and was distilled from the strongly alkaline reaction mixture at 55 - 70°C. The product was converted to the hydrochloride salt by addition of concentrated hydrochloric acid to a solution in propan-2-ol. The product was not normally further purified for preparative work. A pure sample was obtained by recrystallisation from propan-2-ol (Found: C, 14.5; H, 7.1; N, 17.2. Calc. for CH_6ClNO : C, 14.4; H, 7.2; N, 16.8%).

3.6.2 4,4,9,9-Tetramethyl-5,8-diazadodecane-2,11-dione dihydroperchlorate, $\text{dddk}\cdot 2\text{HClO}_4$

Method (a) Tris(ethylenediamine) nickel(II) perchlorate was reacted with acetone to form the macrocyclic complex 5,7,7,12,12,14-hexamethyl-1,4,8,11-tetraazacyclo-tetradecane-4,14-diene nickel(II) perchlorate ($\text{NiB}(\text{ClO}_4)_2$). The macrocyclic ligand (which is stable only in non-aqueous solution) was isolated by stirring the nickel complex (5 g) with KCN (2 g) in dry methanol (70 ml) for 10 minutes.¹⁵² Ether (50 ml) was added to precipitate KClO_4 and $\text{K}_2\text{Ni}(\text{CN})_4$ and the mixture filtered under suction. The ether was evaporated at room temperature in a stream of air; addition of dilute perchloric acid, with stirring, gave the dione dihydroperchlorate $\text{dddk}\cdot 2\text{HClO}_4$. Stirring is essential as the dione has a tendency to form as an oil on the surface of the aqueous solvent. Yield 80%.

Method (b) Mesityl oxide (4 ml) was added to ethylenediamine (1 ml) and the reaction mixture left for 5 minutes. The solution was

then poured into a mixture of 70% perchloric acid (4 ml) and crushed ice (6 g).¹⁵³ The product crystallised on stirring. Yield 4 - 10%.

Method (c) Ethylenediamine dihydroperchlorate (40 g, 0.15 mol), acetone (200 ml) and ethylenediamine (0.5 ml) were mixed in a stoppered flask. After 24 hours a precipitate formed (di-N-isopropylidene) which slowly redissolved over a period of 4 weeks and yielded a precipitate of the product. The product was filtered by suction and washed with ethanol.¹⁵⁴ Yield 70%.

3.6.3 4,4,9,9-Tetramethyl-5,8-diazadodecane-2,11-dione bis-(O-methyloxime) dihydroperchlorate, dddm, 2HClO₄

Method (a) The dione dihydroperchlorate (dddk, 2HClO₄) (10 g, 0.022 mol) and methoxyamine hydrochloride (5 g, 0.060 mol) were stirred in methanol (100 ml) and the pH adjusted to ca. 9 with NaOH (2M). The product was isolated after 4 days by addition of 70% HClO₄ to pH < 3. The dihydroperchlorate salt dddm, 2HClO₄, crystallised rapidly and was recrystallised from methanol. Yield 4.9 g, 43%. (Found: C, 37.4; H, 7.0; N, 10.9. Calc. for C₁₆H₃₆Cl₂N₄O₁₀: C, 37.3; H, 7.0; N, 10.9%).

Method (b) The dione dihydroperchlorate (1.0 g, 0.0022 mol) and Cu(ClO₄)₂·6H₂O (0.365 g, 0.0044 mol) were slurried in methanol (15 ml) and the pH was adjusted to 7.5 - 8 with NaOH (2M). The deep blue solution turned green after 24 hours and purple crystals of Cu(dddm)(ClO₄)₂ formed; yield after 3 days 0.45 g, 40%. dddm, 2HClO₄ precipitated immediately on addition of HClO₄ (70%) to an aqueous solution of Cu(dddm)(ClO₄)₂. Addition of HClO₄ (70%) to the green solution yielded dddm, 2HClO₄ only slowly.

3.6.4 4,4,9,9-Tetramethyl-5,8-diazadodecane-2,11-dione O-methyldioxime dihydroperchlorate, Hddmo, 2HClO₄

The dione dihydroperchlorate (10 g, 0.022 mol) and hydroxylamine

hydrochloride (1.56 g, 0.022 mol) were dissolved in methanol (100 ml) and the pH adjusted to ca. 9 with NaOH (2M). The resultant solution was set aside at 4°C for 12 hours. Methoxyamine hydrochloride (4.0 g, 0.048 mol) was added and the pH again adjusted to 9. The solution was set aside for 24 hours at 4°C and a further 24 hours at room temperature before evaporating to small volume under a stream of nitrogen. The dihydroperchlorate salt, $\text{Hddmo}, 2\text{HClO}_4$, slowly crystallised on addition of 70% HClO_4 . Infrared and p.m.r. spectra run on the crude product indicated the presence of variable (small) amounts of $\text{H}_2\text{dddo}, 2\text{HClO}_4$, $\text{dddm}, 2\text{HClO}_4$ and $\text{dddk}, 2\text{HClO}_4$. The product was dissolved in water at pH 9; the dione impurity decomposed by hydrolysis and any dioxime present precipitated as H_2dddo . The solution was acidified with HClO_4 to give the product. Further recrystallisation from methanol removed the sparingly soluble $\text{dddm}, 2\text{HClO}_4$. Yield 2.25 g, 20%. (Found: C, 35.9; H, 6.7; N, 11.1. Calc. for $\text{C}_{15}\text{H}_{34}\text{Cl}_2\text{N}_4\text{O}_{10}$: C, 35.9; H, 6.8; N, 11.2%).

3.6.5 4,4,9,9-Tetramethyl-5,8-diazadodecane-2,11-dione dioxime dihydroperchlorate, $\text{H}_2\text{dddo}, 2\text{HClO}_4$

Method (a) $\text{NiB}(\text{ClO}_4)_2$ (see section 3.6.2) (5 g) was treated with KCN (2 g) and the methanolic solution of the diamine dione, dddk , was prepared as in section 3.6.2 (method (a)). Following the method of Frazer et al.⁴⁰ hydroxylamine hydrochloride (3.4 g, 0.049 mol) in 30% aqueous methanol (30 ml) was added to the solution of dddk , and the pH adjusted to ca. 9 with NaOH (2M). After 4 days the solution was evaporated in a stream of nitrogen and the white crystalline H_2dddo separated. The dihydroperchlorate salt was formed by dissolving the dioxime in dilute NaOH (0.1M) and precipitating the product $\text{H}_2\text{dddo}, 2\text{HClO}_4$ by addition of perchloric acid (60%) to pH < 3. Yield 1.45 g, 43%.

Method (b) The dione dihydroperchlorate (5 g, 0.011 mol) and hydroxylamine hydrochloride (3.1 g, 0.044 mol) were dissolved in methanol (50 ml) by the addition of NaOH (2M) to pH ca. 9. After 4 days the dioxime could be filtered from the alkaline reaction mixture or the dihydroperchlorate salt $H_2dddo, 2HClO_4$ could be formed by addition of $HClO_4$ (70%) to the mother liquor. Yield of dihydroperchlorate salt 3.23 g, 60%. The dihydroperchlorate salt was purified by the methods of Hedwig¹²⁹ and Kee¹⁴⁸ by dissolving the salt in water, adjusting the pH to ca. 9 and allowing the dioxime to crystallise. The dioxime isolated in this way was converted to the dihydroperchlorate salt by addition of perchloric acid (60%) to pH <3. (Found: C, 34.7; H, 6.6; N, 11.9. Calc. for $C_{14}H_{32}Cl_2N_4O_{10}$: C, 34.5; H, 6.6; N, 11.5%)

3.6.6 2,6,6-Trimethyl-2,5-diazanonan-8-one O-methyloxime dihydroperchlorate, dnm, $2HClO_4$

To a solution of N,N-dimethylethylenediamine (10 ml, ca. 0.11 mol) in acetone (10 ml), 70% $HClO_4$ (9.7 ml, ca. 0.11 mol) was added dropwise. Acetone (50 ml) was added and the flask was stoppered and set aside for 5 days at room temperature. The excess acetone was then removed by evaporation in a stream of air. The residue, containing 2,6,6-trimethyl-2,5-diazanonan-8-one was dissolved in methanol (30 ml); methoxyamine hydrochloride (19.3 g, 0.23 mol) was added, the solution adjusted to pH 9 with NaOH (2M) and set aside in a stoppered flask for 4 days. The unreacted methoxyamine and organic solvents were removed by evaporation in a stream of air. The residue was extracted 3 times with ether (20 ml) to obtain the diamine O-methyloxime. After evaporation of the ether extract, propan-2-ol (20 ml) was added and the solution acidified with $HClO_4$ (70%) until the pH was <3. On addition of an excess of ether an oil formed from which the product crystallised

slowly at 4°C . The product was recrystallised from the minimum volume of dry propan-2-ol until p.m.r. and infrared spectra showed no trace of the parent amine or ketoamine. Yield 2g, 4.5%.

3.6.7 2,6,6-Trimethyl-2,5-diazanonan-8-one oxime dihydroperchlorate,
Hdno, 2HClO_4

This ligand was prepared as for dnm, 2HClO_4 except hydroxylamine hydrochloride (20 g, 0.286 mol) was used instead of methoxyamine hydrochloride. After evaporation of the ether extract (obtained as described in section 3.4.6) two volumes of dry ethanol were added to the residue followed by 70% HClO_4 until the pH was < 3 . The solution was dried over Na_2SO_4 . On addition of dry ether an oil formed; this oil was twice slurried with an equal volume of cold, dry propan-2-ol to remove excess acid and water. The oil was dissolved in warm propan-2-ol (20 ml) and the product crystallised over 24 hours. The product was recrystallised as for dnm, 2HClO_4 . Yield 0.53 g, 1.2%. (Found C, 30.1; H, 6.2; N, 10.3. Calc. for $\text{C}_{10}\text{H}_{25}\text{Cl}_2\text{N}_3\text{O}_9$: C, 29.9; H, 6.2; N, 10.5%).

3.7 PREPARATION OF METAL COMPLEXES

3.7.1 (4,4,9,9-Tetramethyl-5,8-diazadodecane-2,11-dione bis(O-methyloxime)) copper(II) Perchlorate, $\text{Cu}(\text{dddm})(\text{ClO}_4)_2$

Method (a) See section 3.6.3

Method (b) The ligand dddm, 2HClO_4 (1.2 g, 0.0023 mol) was dissolved in methanol (15 ml) by the dropwise addition of NaOH (2M). A solution of $\text{Cu}(\text{ClO}_4)_2 \cdot 6\text{H}_2\text{O}$ (0.810 g, 0.0022 mol) in methanol (10 ml) was added to the ligand solution. Purple crystals of $\text{Cu}(\text{dddm})(\text{ClO}_4)_2$ appeared immediately from the blue-purple solution. Yield 0.98 g, 77%.

(Found: C, 33.2; H, 6.0; N, 10.2. Calc. for $[\text{C}_{16}\text{H}_{34}\text{CuN}_4\text{O}_2](\text{ClO}_4)_2$: C, 33.3; H, 5.9; N, 9.7%).

3.7.2 (4,4,9,9-Tetramethyl-5,8-diazadodecane-2,11-dione oxime oximate) nickel(II) Perchlorate monohydrate, $\text{Ni}(\text{Hdddo})(\text{ClO}_4)\cdot\text{H}_2\text{O}$

$\text{H}_2\text{dddo}, 2\text{HClO}_4$ (0.500 g, 0.0011 mol) was added to a solution of $\text{Ni}(\text{ClO}_4)_2\cdot 6\text{H}_2\text{O}$ (0.375 g, 0.0010 mol) in water (10 ml) and NaOH (2M) was added dropwise and with stirring until the ligand had dissolved. The amorphous product precipitated immediately and was redissolved by heating the solution. On cooling the red crystalline product appeared after 3 - 4 hours, and was recrystallised from hot water containing 1 - 2 drops of NaOH (2M). Yield 0.228 g, 50%. (Found: C, 36.3; H, 6.6; N, 12.2. Calc. for $[\text{C}_{14}\text{H}_{29}\text{N}_4\text{NiO}_2](\text{ClO}_4)\cdot\text{H}_2\text{O}$: C, 36.4; H, 6.7; N, 12.1%).

3.7.3 (4,4,9,9-Tetramethyl-5,8-diazadodecane-2,11-dione oxime oximate) zinc(II) Perchlorate, $\text{Zn}(\text{Hdddo})(\text{ClO}_4)$.

$\text{H}_2\text{dddo}, 2\text{HClO}_4$ (0.500 g, 0.0011 mol) was added to a solution of $\text{ZnSO}_4\cdot 7\text{H}_2\text{O}$ (0.295 g, 0.0010 mol) in water (10 ml). NaOH (2M) was added dropwise with stirring until the pH was between 7 and 8 (see titration curve, section 8.3.1). A white precipitate formed immediately. This sparingly soluble product ($\text{Zn}(\text{Hdddo})(\text{ClO}_4)$) was purified by digestion in water for 30 minutes. Yield 0.315 g, 70%. (Found C, 36.2; H, 6.2. Calc. for $[\text{C}_{14}\text{H}_{29}\text{N}_4\text{O}_2\text{Zn}](\text{ClO}_4)_2$: C, 37.3; H, 6.5%).

3.7.4 (4,4,9,9-Tetramethyl-5,8-diazadodecane-2,11-dione bis(O-methyloxime)) nickel(II) Perchlorate, $\text{Ni}(\text{dddm})(\text{ClO}_4)_2$.

$\text{dddm}, 2\text{HClO}_4$ (0.515 g, 0.0010 mol) was dissolved in dry ethanol (5 ml) by the addition of NaOH (0.080 g, 0.002 mol) and a

solution of $\text{Ni}(\text{ClO}_4)_2 \cdot 6\text{H}_2\text{O}$ (0.354 g, 0.00097 mol) dissolved in dry ethanol (5 ml) was added slowly with stirring. A finely divided orange product formed immediately from the resultant solution. The product, which was insoluble in ethanol, methanol and acetone, and decomposed in acetonitrile and water, could not be recrystallised. The nickel content was determined by atomic absorption analysis on a sample dissolved in dilute HCl (instrumental parameters: air/acetylene oxidising flame, 352.4 nm). Infrared absorptions recorded at 3590, 3200 and 1635 cm^{-1} were assigned to $\nu(\text{O-H})$, $\nu(\text{N-H}^+)$ and $\nu(\text{C=N})$ respectively. Absorptions also occurred at 1000-1100 and at 625 cm^{-1} and were assigned to stretching modes of the perchlorate ion.¹⁵⁵ Infrared and nickel analysis data suggested that the product is a basic complex of stoichiometry $\text{Ni}(\text{dddm})(\text{ClO}_4)_2\text{Ni}(\text{OH})_2 \cdot \text{H}_2\text{O}$. (Found: Ni, 17.2. Calc. for $\text{Ni}(\text{dddm})(\text{ClO}_4)_2\text{Ni}(\text{OH})_2 \cdot \text{H}_2\text{O}$: Ni, 17.2%).

C. PREPARATION OF STANDARD SOLUTIONS

3.8.1 Glassware

All pipettes used in quantitative work were calibrated by weighing the volume of water delivered at 20°C . Titrations were carried out using a Gilmont micrometer syringe (capacity 2.5 ml) or an Agla glass micrometer syringe (capacity 0.5 ml). A calibration by Hedwig¹²⁹ showed the volume delivered by these syringes to be within 0.06% of the indicated volume.

3.8.2 Carbonate-free Distilled Water

Carbonate-free distilled water was prepared by boiling distilled water for 5 minutes to remove all dissolved carbon dioxide. While cooling to room temperature the water was flushed with N_2 .

3.8.3 Sodium Hydroxide (1M)

AnalaR NaOH pellets (5 g) were placed in a beaker and a small volume of carbonate-free distilled water was added to form a slurry. The pellets were washed and the water discarded. This washing procedure, which removes sodium carbonate from the pellets, was repeated. The NaOH was then dissolved in carbonate-free distilled water and the solution made up to approximately 100 ml.

The NaOH solution was standardized by potentiometric (pH) titration against potassium hydrogen phthalate, the end point titre being determined from a plot of ΔpH versus titre. Repeated measurements established a precision of $\geq 99.7\%$.

3.8.4 Hydrochloric Acid (1M)

AnalaR concentrated hydrochloric acid (44 ml) was diluted to 500 ml with carbonate-free water. The acid solution was standardized by four methods: (1) against B.D.H. AnalaR disodium tetraborate decahydrate (borax), (2) against borax which had been recrystallised from distilled water, (3) against sodium carbonate (dried at 260°C) and (4) against previously standardized sodium hydroxide. The last three methods gave consistent results to within $\pm 0.2\%$ whereas the first gave a value which was ca. 2% too low. This established the need to use freshly recrystallised borax as a primary standard for the determination of acid concentrations.

3.8.5 Metal(II) chloride Solutions

A weighed sample of B.D.H. AnalaR metal(II) chloride (cobalt, nickel, copper and zinc) was dissolved in carbonate-free water. To suppress hydrolysis of the metal-aquo ions standard HCl solution was accurately added to give an acid concentration of ca. $1 \times 10^{-3}\text{M}$.

The metal ion concentration was accurately determined by titimetric or gravimetric analysis. Cobalt(II) was determined gravimetrically as cobalt(II) tetrapyridine dithiocyanate.¹⁵⁶ Nickel(II) was determined gravimetrically as bis(dimethylglyoximate) nickel(II).¹⁵⁷ Zinc(II) was determined by complexometric titration against EDTA using eriochrome black T indicator.¹⁵⁸

Copper(II) was determined gravimetrically as (benzoinoximate) copper(II) but with some modification to the procedure given by Vogel.¹⁵⁹ Ammonia solution (2M) was added to the copper(II) solution until the solution was a deep blue colour. A 2% alcoholic benzoinoxime solution was added dropwise to the copper tetrammine solution until precipitation of (benzoinoximate) copper(II) was complete. The solution was then heated to near boiling and digested for $1\frac{1}{2}$ hours. A small volume of benzoinoxime reagent was then added to ensure complete complexation. This method gave an easily filtered product and also suppressed the formation of copper(II) oxide which was observed during the heating of the copper-ammine solution (prior to the addition of the benzoinoxime reagent) in the method outlined by Vogel. Copper(II) ion was also determined gravimetrically as bis(salicylaldoximate) copper(II)¹⁵⁹ and by complexometric titration against EDTA, using murexide indicator.¹⁶⁰

3.8.6 Iron(II) sulphate Solution

B.D.H. AnalaR $\text{FeSO}_4 \cdot 7\text{H}_2\text{O}$ was dissolved in carbonate-free distilled water. A known volume of standard HCl was added until the acid concentration was ca. $1 \times 10^{-2}\text{M}$. Acid suppresses the atmospheric oxidation of Fe(II) to Fe(III) which is rapid in neutral or alkaline solution. The acidic iron(II) solution was sufficiently stable ($\text{Fe}^{3+}/\text{Fe}^{2+} < 0.03$) for approximately 2 weeks. Slow oxidation of Fe(II) to Fe(III) was evident by a developing yellow colour in the stock solution.

The total iron concentration ($\text{Fe(II)} + \text{Fe(III)}$) was determined gravimetrically as Fe_2O_3 ¹⁶¹ as outlined in Vogel.¹⁶² The Fe(III) concentration was quantitatively determined by spectrophotometric measurement using the $\text{Fe(NCS)(H}_2\text{O)}_5^{2+}$ complex.

3.8.7 Adjustment to Constant Ionic Strength

Constant ionic strength of test solutions was maintained by adding the calculated weight of NaCl (B.D.H. AnalaR).

CHAPTER 4

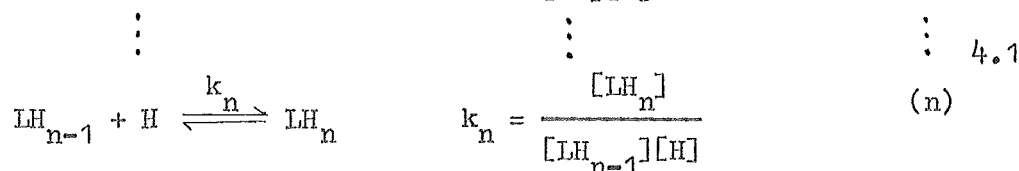
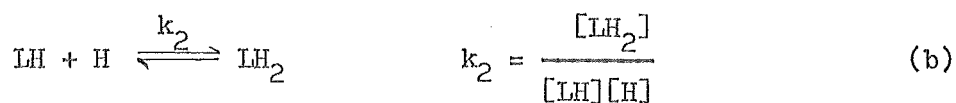
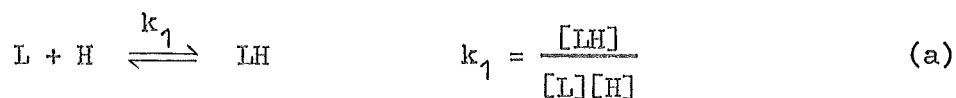
CALCULATIONS

Equilibrium constants and enthalpy changes have been calculated from the volume -pH data and the volume-heat change data obtained from potentiometric (pH) titrations and calorimetric titrations respectively, by solving the series of mass balance equations which describe the system under study. General methods of deriving the mass balance equations, a description of the equilibria which were considered in this study, and the methods of solving the mass balance equations are described in this chapter.

4.1 DETERMINATION OF EQUILIBRIUM CONSTANTS

4.1.1 Protonation Constants of the Ligands

Consider a ligand L which is capable of forming a conjugate acid containing n ionizable protons (LH_n^{n+}). The concentrations of the species H^+ , L, LH^+ , ... LH_n^{n+} at any point throughout a titration are related by the following equilibria and equilibrium (protonation) constants:



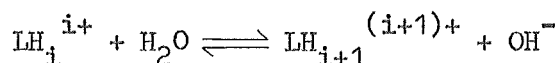
4.1

where the charges have been omitted for clarity. The mass balance equations describing the total (stoichiometric) concentration of ligand (T_L) and the total concentration of ionizable protons (T_H) are related to the equilibrium concentrations by

$$T_L = [L] + [LH] + [LH_2] + \dots + [LH_n] \quad 4.2$$

$$\text{and } T_H = [H] + [LH] + 2[LH_2] + \dots + n[LH_n] - [OH] \quad 4.3$$

The term $[OH]$, the concentration of hydroxide ion, arises from hydrolysis reactions of the type



and is determined from the ionic product of water ($[OH] = K_W/[H]$ where K_W is defined as $[H][OH]/(\gamma_H\gamma_{OH^-}/a_{H_2O})^{163}$). The value of T_H for each titration point ($T_H(\text{obs})$) is given by the total stoichiometric concentration of hydrogen ions initially associated with the ligand ($n \times T_L$) plus the concentration of added acid (A) less that which has reacted with the added alkali

$$\text{i.e. } T_H(\text{obs}) = n \times T_L + A - \frac{[NaOH] \times v}{V + v} \quad 4.4$$

where v is the volume (ml) of added NaOH and V is the total initial volume of test solution.

A secondary concentration variable \bar{n}_H ^{98,164} defined as the average number of protons bound per ligand molecule, is given by

$$\bar{n}_H = \frac{[LH] + 2[LH_2] + \dots + n[LH_n]}{T_L} \quad 4.5$$

From equation 4.3, \bar{n}_H can be rewritten as

$$\bar{n}_H = \frac{T_H - [H] + [OH]}{T_L} \quad 4.6$$

By use of the equilibrium constants defining the system (equations 4.1), and equations 4.2 and 4.5, \bar{n}_H can be defined as

$$\bar{n}_H = \frac{[L](k_1[H] + 2k_1k_2[H]^2 + \dots + nk_1k_2 \dots k_n[H]^n)}{[L](1 + k_1[H] + k_1k_2[H]^2 + \dots + k_1k_2 \dots k_n[H]^n)} \quad 4.7$$

or, by defining a cumulative protonation constant β_i by $\beta_i = \prod_{j=1}^i k_j$, a general expression

$$\bar{n}_H = \frac{\sum_{i=1}^n i \beta_i [H]^i}{1 + \sum_{i=1}^n \beta_i [H]^i} \quad 4.8$$

can be obtained. Thus \bar{n}_H can also be defined as a function of the protonation constants (k_i) and the hydrogen ion concentration. From the known total ionizable acid concentration ($T_H(\text{obs})$), known total ligand concentration and known hydrogen ion concentration (derived from the measured pH, as outlined in section 3.1.3) an experimental value of \bar{n}_H ($\bar{n}_H(\text{obs})$) can be derived for each point throughout the titration (equation 4.6). From trial values of the equilibrium constants (k_i) and the measured hydrogen ion concentration at each point during a titration, a calculated value of \bar{n}_H ($\bar{n}_H(\text{calc})$) can also be determined (equation 4.7). The function

$$\bar{n}_H = f(k_1, k_2, \dots k_n, [H^+]),$$

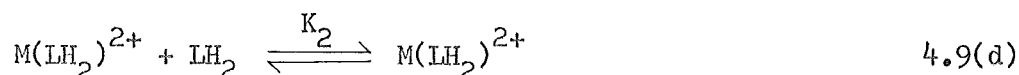
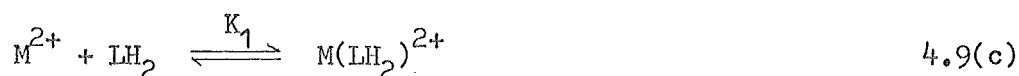
a function containing n unknown parameters ($k_1, k_2, \dots k_n$), can be solved by the method of least squares for the parameters $k_1, k_2, \dots k_n$ (see section 4.6). In summary this involves varying initial trial parameters $k_1^1, k_2^1, \dots k_n^1$ such that the sum of the squares of the residuals over all data points, $\sum (\bar{n}_H(\text{obs}) - \bar{n}_H(\text{calc}))^2$, is minimised.

In the present study of diamine oxime ligands only three ligand species were detected in solution between pH 2 and 10. These

species were the free oxime LH_2 and the protonated (ammonium) species LH_3^+ and LH_4^{2+} . The oxime hydroxyl protons do not significantly deprotonate throughout the pH range studied as the oxime hydroxyl proton is only weakly acidic; $\log K(\text{C}=\text{NO}^- + \text{H}^+ \rightleftharpoons \text{C}=\text{NOH}) = 12.3$ ¹⁶⁵ (i.e. at pH 10 the concentrations of LH^- and L^{2-} would be less than 1% of total ligand present). The oxime nitrogen was not observed to protonate significantly in the pH range studied. The oxime nitrogen is only weakly basic, $\log K(\text{C}=\text{NOH} + \text{H}^+ \rightleftharpoons \text{C}=\text{N}^+\text{HOH}) \sim -1$,⁴ and its protonation is negligible at $\text{pH} > 2$.

4.1.2 Equilibrium Constants for Metal Complexes

Equilibrium constants for metal-ligand equilibria were determined from experiments in which alkali was added incrementally to a solution containing protonated ligand and metal ions. In such systems the metal ion competes with hydrogen ions for co-ordination to the ligand molecules.¹⁶⁴ This process is best illustrated by reference to an example. Consider a diamine dioxime ligand LH_2 which may protonate on the amino nitrogens to form the species LH_3^+ and LH_4^{2+} . The ligand LH_2 may also form mono and possibly bis complexes with metal ions ($\text{M}(\text{LH}_2)^{2+}$ and $\text{M}(\text{LH}_2)_2^{2+}$). The species H^+ , M^{2+} , LH_2 , LH_3^+ , LH_4^{2+} , $\text{M}(\text{LH}_2)^{2+}$ and $\text{M}(\text{LH}_2)_2^{2+}$ are related in solution by the following equilibria

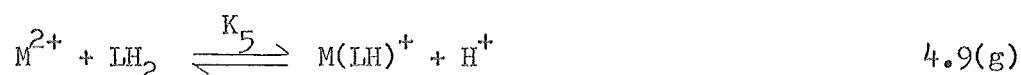


If the co-ordinated oxime can also deprotonate (to form LH^- and L^{2-}) then the following equilibria are also possible:



The protonation constants k_1 and k_2 would be determined from a separate experiment as described in section 4.1.1. In the determination of equilibrium constants several distinct cases arise.

(1) The simple case in which only one metal-ligand equilibrium process is important in a given buffer region (e.g. only the species $\text{M}(\text{LH}_2)^{2+}$ or $\text{M}(\text{LH})^+$ is formed, not both). In this case a value for the unknown equilibrium constant can conveniently be obtained for each individual data point. For example, if the reaction is one in which the oxime ligand LH_2 co-ordinates and deprotonates in a concerted step,



then the mass balance equations describing the total concentrations of ligand (T_L), metal (T_M) and ionizable protons (T_H) are

$$T_L = [\text{M}(\text{LH})] + [\text{LH}_2] + [\text{LH}_3] + [\text{LH}_4] \quad 4.10$$

$$T_M = [\text{M}] + [\text{M}(\text{LH})] \quad 4.11$$

$$T_H = [\text{H}] + [\text{M}(\text{LH})] + 2[\text{LH}_2] + 3[\text{LH}_3] + 4[\text{LH}_4] - [\text{OH}] \quad 4.12$$

By subtracting T_H from T_L equation 4.13 is obtained

$$\begin{aligned} T_H - T_L &= [\text{H}] + [\text{LH}_2] + 2[\text{LH}_3] + 3[\text{LH}_4] - [\text{OH}] \\ &= [\text{H}] + [\text{LH}_2](1 + 2k_1[\text{H}] + 3k_1k_2[\text{H}]^2) - [\text{OH}] \end{aligned} \quad 4.13$$

which can be solved to determine $[\text{LH}_2]$. The value of $[\text{LH}_2]$ can then be substituted into equation 4.10 to give $[\text{M}(\text{LH})]$ and equation 4.11 yields $[\text{M}]$. K_5 as defined by equation 4.9(g) can be calculated for each data point from the experimental values of T_H , T_L , T_M and $[\text{H}^+]$.

(2) The case where two metal-ligand species are formed ($\text{M}(\text{LH}_2)^{2+}$ and $\text{M}(\text{LH}_2)_2^{2+}$) but no deprotonated metal complex species are formed. In this case the ligand can be considered to contain only two ionizable protons (the oxime protons are "fixed" and do not contribute to T_H). The mass balance equations in this case are

$$T_L = [\text{LH}_2] + [\text{LH}_3] + [\text{LH}_4] + [\text{M}(\text{LH}_2)] + 2[\text{M}(\text{LH}_2)_2] \quad 4.14$$

$$T_M = [\text{M}] + [\text{M}(\text{LH}_2)] + [\text{M}(\text{LH}_2)_2] \quad 4.15$$

$$T_H = [\text{H}] + [\text{LH}_3] + 2[\text{LH}_4] - [\text{OH}] \quad 4.16$$

By substitution of expressions for $[\text{LH}_3]$ and $[\text{LH}_4]$, derived from equations 4.9(a) and (b), equation 4.16 can be solved for each data point to determine $[\text{LH}_2]$. Rearrangement of the equilibrium equations 4.9(c) and (d) gives expressions for $[\text{M}(\text{LH}_2)]$ and $[\text{M}(\text{LH}_2)_2]$, in terms of $[\text{M}]$, $[\text{LH}_2]$ and K_i , and by substitution of these into expression 4.15 an expression for the free metal ion concentration $[\text{M}]$ can be found:

$$[\text{M}] = \frac{T_M}{1 + K_1[\text{LH}_2] + K_1K_2[\text{LH}_2]^2} \quad 4.17$$

One approach to determine K_1 and K_2 is to calculate $[\text{M}]$ from equation 4.17 using trial values of K_1 and K_2 . A least squares procedure is then applied to equation 4.14 ($T_L = f([\text{H}], [\text{M}], [\text{LH}_2], K_1, K_2, k_i)$) to obtain "better" values of K_1 and K_2 such that the sum of squares of residuals over all data points is minimised (i.e. $\sum (T_L(\text{obs}) - T_L(\text{calc}))^2$).

where $T_L(\text{obs})$ is the measured stoichiometric concentration of ligand and $T_L(\text{calc})$ is the total ligand concentration calculated from the right hand side of equation 4.14). The procedure is repeated with the new trial values of K_1 and K_2 until the "best" values of K_1 and K_2 are obtained (see section 4.6).

Alternatively a secondary concentration variable, \bar{n}_L , defined as the average number of ligand molecules bound per metal ion, can be used

$$\begin{aligned}\bar{n}_L &= [M(LH_2)] + 2[M(LH_2)_2] \\ &= \frac{K_1[M][LH_2] + 2K_1K_2[M][LH_2]^2}{T_M}\end{aligned}\quad 4.18$$

A value of $[LH_2]$ is obtained for each data point and a value of $[M]$ is determined from trial values of K_1 and K_2 as described above. An observed value of \bar{n}_L is obtained in terms of the known quantities $[LH_2]$, $[H^+]$, T_L and T_M as

$$\bar{n}_L(\text{obs}) = \frac{T_L - [LH_2](1 + k_1[H] + k_1k_2[H]^2)}{T_M}$$

where the numerator equals the concentration of co-ordinated ligand which equals the total concentration of ligand minus un-coordinated ligand, and $\bar{n}_L(\text{calc})$ is obtained from the right hand side of equation 4.18. A least squares procedure is used to obtain the "best" values of K_1 and K_2 .

(3) The case where more than one metal-ligand species is formed and at least one of the metal-ligand species contains the ligand in the deprotonated (or protonated) form. Consider the example where three metal-ligand species are formed $M(LH_2)^{2+}$, $M(LH)^+$ and $M(L)$ (equations 4.9(c), (e) and (f)). In this case the least squares analysis

must minimise a function of T_H as the number of titratable protons is different in the species $M(LH_2)^{2+}$, $M(LH)^+$ and $M(L)$. The function \bar{n}_L cannot be used as the three metal-ligand species each contain one metal ion and one ligand molecule per complex. The mass balance equations in this example are

$$T_L = [LH_2] + [LH_3] + [LH_4] + [M(LH_2)] + [M(LH)] + [M(L)] \quad 4.19$$

$$T_M = [M] + [M(LH_2)] + [M(LH)] + [M(L)] \quad 4.20$$

$$T_H = 2[LH_2] + 3[LH_3] + 4[LH_4] + 2[M(LH_2)] + [M(LH)] - [OH] \quad 4.21$$

As equation 4.21 contains terms for ligand and metal species it cannot be solved directly to obtain $[LH_2]$. By use of the equilibrium expressions 4.9(a), (b), (c), (e) and (f), expression 4.20 can be rearranged to give

$$[M] = \frac{T_M}{1 + K_1[LH_2] + \frac{K_1K_3[LH_2]}{[H]} + \frac{K_1K_3K_4[LH_2]}{[H]^2}} \quad 4.22$$

Substitution of this into equation 4.19 yields

$$T_L = [LH_2] \left(1 + k_1[H] + k_1k_2[H]^2 + \frac{T_M(K_1 + K_1K_3 + K_1K_3K_4)}{1 + K_1[LH_2] + \frac{K_1K_3[LH_2]}{[H]} + \frac{K_1K_3K_4[LH_2]}{[H]^2}} \right) \quad 4.23$$

Multiplying equation 4.23 through by the denominator of equation 4.22 gives the quadratic equation

$$[LH_2]^2 \left(K_1 + \frac{K_1K_3}{[H]} + \frac{K_1K_3K_4}{[H]^2} + K_1k_1[H] + K_1K_3k_1 + \frac{K_1K_3K_4k_1}{[H]} \right. \\ \left. + K_1k_1k_2[H]^2 + K_1K_3k_1k_2[H] + K_1K_3K_4k_1k_2 \right)$$

$$\begin{aligned}
& + [\text{LH}_2] \left(1 + k_1[\text{H}] + k_1k_2[\text{H}]^2 + K_1T_M + \frac{K_1K_3T_M}{[\text{H}]} + \frac{K_1K_3K_4T_M}{[\text{H}]^2} \right. \\
& \left. - K_1T_L - \frac{K_1K_3T_L}{[\text{H}]} - \frac{K_1K_3K_4T_L}{[\text{H}]^2} \right) \\
& - T_L = 0
\end{aligned}
\tag{4.24}$$

which contains only the unknown quantities $[\text{LH}_2]$, K_1 , K_3 and K_4 . Trial values of K_1 , K_3 and K_4 can be assumed, a trial value of $[\text{LH}_2]$ is derived from equation 4.24 and $T_H(\text{calc})$ is found from the right hand side of equation 4.21 and the equilibrium expressions 4.9(c), (e) and (f). A least squares procedure is used to obtain "better" values of K_1 , K_3 and K_4 by minimising the sum of the squares of the residuals over all data points, i.e. minimising $\sum (T_H(\text{obs}) - T_H(\text{calc}))^2$ where $T_H(\text{obs})$ is defined as in equation 4.4.

In the present study generally the only metal-ligand species detected were $\text{M}(\text{LH}_2)^{2+}$, $\text{M}(\text{LH})^+$ and $\text{M}(\text{LH})(\text{OH})$ (an exception is the species $\text{Zn}(\text{Hddmo})_2^{2+}$, see section 8.3). As the hydroxy species $\text{M}(\text{LH})(\text{OH})$ and the species ML contain the same number of titratable protons (equal to zero) and the same number of ligand molecules, the type of analysis described above for the deprotonation of $\text{M}(\text{LH})^+$ is equally valid for the deprotonation of a co-ordinated water molecule in $\text{M}(\text{LH})_{(\text{aq})}$ to produce the species $\text{M}(\text{LH})(\text{OH})$.

4.2 DETERMINATION OF ENTHALPY CHANGES

The calculation of ΔH from measured heat changes upon the incremental addition of acid to the calorimeter solution, requires a knowledge of the composition of the calorimeter solution before and after each acid addition. For a single reaction that goes to completion the extent of reaction for a titrant addition is determined by the number of moles of the titrant species added to the calorimeter, so

long as the titrant is not added in excess. For an equilibrium reaction that does not go to completion however, the extent of reaction following titrant addition must be calculated from the known equilibrium constants and the $[H^+]$ of the calorimeter solution. As the pH of the calorimeter solution is not conveniently determined during a calorimetric titration (a glass electrode affords a large heat capacity and heat pathway from the calorimeter and therefore lowers sensitivity) the $p[H^+]$ must be calculated independently from the known stoichiometry of the calorimeter solution and the volume of titrant added (section 4.2.1). An initial estimate of the pH can be obtained by reference to a formation or titration curve. An alternative procedure is to back titrate the calorimeter solution after completion of the calorimetric titration and determine the $p[H^+]$ at each calorimetric titration point from the pH- volume data. The initial estimates of the pH are used in an iterative calculation to obtain the $p[H^+]$.

4.2.1 Calculation of Enthalpy Changes for Protonation of the Ligands

Calculation of Solution Composition For a general base L which forms a conjugate acid containing n ionizable protons (LH_n^{n+}), equations 4.2 and 4.3 can be rearranged to give

$$[L] = \frac{T_L}{1 + k_1[H] + k_1k_2[H]^2 + \dots + k_1k_2 \dots k_n[H]^n} \quad 4.25$$

and

$$T_H - [H] + [OH] = [L](1 + k_1[H] + 2k_1k_2[H]^2 + \dots + nk_1k_2 \dots k_n[H]^n) \quad 4.26$$

Substitution of equation 4.25 into equation 4.26 yields:

$$T_H = [H] - [OH] + \frac{T_L(k_1[H] + 2k_1k_2[H]^2 + \dots + nk_1 \dots k_n[H]^n)}{1 + k_1[H] + k_1k_2[H]^2 + \dots + k_1k_2 \dots k_n[H]^n} \quad 4.27$$

Multiplication of equation 4.27 by the denominator of equation 4.25 gives a general equation of the form

$$\begin{aligned} f([H]^+) &= a[H]^{n+1} + b[H]^n + \dots + m[H] - [OH] - T_H \\ &= 0 \end{aligned} \quad 4.28$$

The coefficients a, b, c, ... m are readily calculated from the known values of $k_1, k_2 \dots k_n, T_L, T_H$ and $[OH] (= \frac{K_w}{[H]})$.

The $[H^+]$ in solutions formed by addition of acid to a ligand solution in the calorimeter was determined by solution of equation 4.28 by the Newton-Raphson method.¹⁶⁶ An initial estimate for $[H^+]$ was obtained from examination of the \bar{n}_H -pH curve determined from titration of the protonated ligand with hydroxide ion or from an approximate pH obtained from a back titration of the calorimeter solution after the completion of the heat change measurements. Generally less than 4 cycles of the Newton-Raphson process were required to obtain a convergent solution for $p[H^+]$. The condition used to determine convergence was that two $p[H^+]$ values calculated in successive cycles did not differ by more than 0.0005. The $p[H^+]$ values thus obtained were used to calculate (1) the concentration of free ligand from equation 4.25, and (2) the concentration of the species LH_i ($i = 1, 2, \dots n$), from the equilibrium expressions 4.1 (a)-(n), for each point throughout the titration.

Calculation of Enthalpy Changes

For the ligand L the stepwise enthalpy change for the equilibrium $LH_{i-1}^{(i-1)+} + H^+ \rightleftharpoons LH_i^{i+}$ is ΔH_i . On addition of the acid titrant to the calorimeter the overall measured heat change Q_m (corrected for the secondary reactions of (1) dilution of the acid¹⁶⁷ and (2) reaction with hydroxide ($H^+ + OH^- \rightarrow H_2O$))

168 can be expressed in terms of the stepwise enthalpy changes:

$$Q_m = a_1 \Delta H_1 + a_2 \Delta H_2 + \dots + a_n \Delta H_n \quad 4.29$$

The terms a_i are the number of moles of the species LH_i formed during each titrant increment. The terms a_i were calculated as follows. On addition of the acid titrant some of the species LH_{i-1} is converted to the species LH_i . a_1 is the amount of L that is converted to LH (i.e. $a_1 = (L)_{\text{initial}} - (L)_{\text{final}}$). a_2 is the amount of LH that is converted to LH_2 . a_2 is therefore given by the initial number of moles of $LH((LH)_i)$ plus the number of moles of LH formed from L (which equals a_1) less the final number of moles of $LH((LH)_f)$, i.e.

$$a_2 = (LH)_i - (LH)_f + a_1$$

In general a_i is given by

$$a_i = (LH_{i-1})_i - (LH_{i-1})_f + a_{i-1} \quad 4.30$$

except that the term a_n for the fully protonated species is given by

$$a_n = (LH_n)_f - (LH_n)_i \quad 4.31$$

The terms a_i in equation 4.29 can therefore be calculated from knowledge of the solution composition before and after each titrant increment. Equation 4.29, an equation with n variables (ΔH_i), can be solved from n or more experimental measurements of Q_m .

4.2.2. Calculation of Enthalpy Changes for Metal Complex Equilibria

The procedure was similar to that described above, viz. the ΔH_i values were determined from solution of an equation analogous to equation 4.29 but including terms for both the formation of metal-ligand species and the deprotonation of ligand-proton species.

calculate the solution composition was an iterative process starting with an initial estimate of the solution composition and the mass balance equations describing the system. An initial estimate of the $p[H^+]$ of the solution was obtained from a parallel pH titration performed on a solution of similar composition to the solution used in the calorimeter. Using the estimated $[H^+]$ an estimated value for the free ligand concentration $[LH_2]$ was obtained from the known equilibrium constants and stoichiometry describing the system; this involved substitution of the estimated $[H^+]$ into equation 4.13, 4.16 or 4.24 (cases (1), (2) and (3) respectively in section 4.1.2). Substitution of the derived value of $[LH_2]$ into equation 4.11, 4.17 or 4.22 gave an estimate of the free metal ion concentration $[M]$. These estimated values of $[M]$ and $[LH_2]$ were used in the expression for T_L (equation 4.10, 4.14 or 4.19) which is a polynomial in $[H^+]$ with coefficients which are readily calculated from the known values of T_L , T_M , T_H , k_1 , k_2 , $K_1 - K_5$ and $[OH]$. This polynomial was solved for $[H^+]$ by the Newton-Raphson method to obtain a "better" estimate of $[H^+]$. The process was repeated until the difference between successive $p[H^+]$ estimates differed by less than 0.0005 pH units.

Calculation of Enthalpy Changes

The heat change Q_m , measured from the calorimetric titration was corrected for dilution of the acid titrant and for the heat change resulting from neutralization of the titrant with hydroxide ions. It can be expressed as a sum of enthalpy changes resulting from (1) the endothermic decomposition of the metal-ligand complexes, and (2) the exothermic protonation of the resultant ligand i.e.

$$Q_M = -b_1 \Delta H_{M1} - b_2 \Delta H_{M2} - \dots - b_m \Delta H_{Mm} + a_1 \Delta H_1 + a_2 \Delta H_2 + \dots + a_n \Delta H_n \quad 4.32$$

where the terms b_i and ΔH_{Mi} refer to the amount of complex $M(L)_i$ dissociated into $M(L)_{i-1}$ and the unknown enthalpy change for this equilibrium respectively. The terms a_i and ΔH_i refer to the amount of the species LH_i formed and the enthalpy change for the i th protonation of the ligand respectively. As an example consider a ligand which forms a bis complex $(M(L)_2)$ and a mono complex $(M(L))$. The number of moles of bis complex decomposing to the mono complex is denoted by b_2 and is given by the difference in the number of moles of ML_2 present before $((M(L)_2)_i)$ and after $((M(L)_2)_f)$ the addition of titrant, i.e.

$$b_2 = (M(L)_2)_i - (M(L)_2)_f \quad 4.33$$

The term b_1 is given by the initial number of moles of the mono complex $((M(L))_i)$ plus the number of moles of $M(L)$ formed from $M(L)_2$ (equal to b_2) less the final number of moles of the mono complex $((M(L))_f)$

$$b_1 = (M(L))_i - (M(L))_f + b_2 \quad 4.34$$

The terms a_i for the protonation of the ligand produced throughout the titration can be derived as

$$a_n = (LH_n)_f - (LH_n)_i$$

$$a_{n-1} = a_n + (LH_{n-1})_f - (LH_{n-1})_i$$

Once the terms $a_1, a_2 \dots a_n$ and $b_1, b_2, \dots b_m$ have been determined from the solution composition, equation 4.32 can be solved so long as the number of data points equals or exceeds the number of unknown enthalpy changes. Equation 4.32 was set up for x data points ($x > m$) and ΔH_{Mi} was then obtained from a linear least squares calculation.

4.3 SELECTION OF A MODEL EQUILIBRIUM SYSTEM

In order to obtain values for the unknown equilibrium constants it is helpful to firstly determine the most likely ligand and metal species and equilibria occurring in solution. These species and equilibria determine the form of the mass balance equations. The species and equilibria occurring in solution may be determined in a variety of ways.

(1) Some information on the species occurring in solution can be gained by reference to analogous chemical systems. For example a buffer region in a titration curve may be thought to result from the formation of a metal-hydroxy species ($ML(OH)$). Comparison with data from other systems which contain a similar ligand and metal ion may answer this question. As an example, $\log K (ML + OH \rightleftharpoons ML(OH))$ is ~ 4.5 for copper-ligand species. This type of reaction is therefore expected to occur at a pH centred on 9.5.

(2) The form of the titration curve may afford useful guidelines. If well defined end-points occur then these will correspond to the quantitative formation of a species in solution. By determining the number of protons lost from the ligand in titrating to the end-points, and comparing this with the metal/ligand ratio and with the pH range where deprotonation of excess ligand would occur, the nature of the species in solution may often be inferred.

(3) Electronic absorption spectra run throughout a titration may also yield useful information on the number and stoichiometry of the species present in solution. If solid samples of the complexes can be obtained and characterized then their spectral parameters may further support a postulated equilibrium system.

In general a combination of these methods is used to select the model system which best explains the experimental results.

Once a model has been established for an equilibrium system and the equilibrium constants determined, the correctness of the model can be estimated from the closeness of the fit of the experimental data to the data calculated from the derived equilibrium constants. If this fit is "good" then the model system can be assumed to adequately explain the system under study, but if the fit is "poor" then additional or alternative equilibria may need to be considered (see section 4.6, Statistical Methods). As a cross check on the model system a second electrode or other sensing device (if these exist) may be incorporated in the titration system¹⁶⁹ in order that the concentration of two or more species may be determined independently. The derived (calculated) concentration of the second species may then be compared with the measured value; large discrepancies would indicate that the system was inadequately explained by the model.

4.4 METHODS OF SOLVING THE MASS BALANCE EQUATIONS

Once the appropriate model equilibrium system has been chosen, the derived equation containing the known and unknown equilibrium constants (or enthalpy changes), the known stoichiometric parameters and $[H^+]$ must be solved to obtain best values of the unknown parameters. Various successive approximation,^{90,170} graphical,^{171,172} and computer methods^{173,174} exist for obtaining solutions of these equations.

In the present study ligand protonation constants were determined from $\bar{n}_H - [H^+]$ data using a non-linear least squares procedure; the term $\sum_{i=1}^m ((\bar{n}_H(\text{obs}))_i - (\bar{n}_H(\text{calc}))_i)^2$ (the sum of the squares of the residuals) was minimised, where m is the number of data points. All observations were weighted equally, as suggested by Hedwig.¹²⁹

In the determination of metal-ligand equilibrium constants the technique used for solving the mass balance equations depended

on the nature of the titration curve, and the number of parameters being determined. If in any buffer region only one equilibrium involving metal ions was important (as inferred from both absorption spectra and a well defined end-point) then the mass balance equations contained only one unknown parameter and the value of K could be obtained independently for each point throughout the titration. The standard deviation of the equilibrium constants derived in this way was an indication as to whether the equilibrium under study was independent of other equilibria in the system. A systematic trend in the derived equilibrium constants would indicate that more than one metal-ligand equilibrium contributed measurably to a given buffer region, thus requiring an alternative approach. The condition adopted in the present study that the metal-ligand equilibrium in a given buffer region was independent of reactions in preceding or following buffer regions was that the mid-points of two adjacent buffer regions were more than two pH units apart. In general the criterion used to establish that only one metal ion equilibrium is predominant in a particular buffer region depends on the number of protons lost from the ligand to form the complex, or the proton change associated with the metal equilibrium. For example if two protons are lost in forming a complex (e.g. two amino protons in the diamine oxime ligands, $M + H_2L \longrightarrow ML + 2H^+$) then an increase of 0.5 pH units from the middle of the buffer region increases the extent of reaction from 50 to ca. 90%. A further 0.5 pH unit change increases the extent of complexation to ca. 99%. A second buffer region starting at >1 pH unit from the middle of this complexation buffer region will not significantly be affected by the complexation equilibrium. Data points close to an end-point ($\bar{n} > 0.9$, or < 0.1) were routinely eliminated from calculations.

If for a given buffer region more than one equilibrium is

important then the mass balance equations must contain more than one unknown parameter; a least squares procedure was used to determine these parameters. For equilibrium measurements the function normally minimised was $\sum_{i=1}^N ((T_H - [H^+])_{\text{obs},i} - (T_H - [H^+])_{\text{calc},i})^2$ where

$(T_H - [H^+])_{\text{obs},i}$ and $(T_H - [H^+])_{\text{calc},i}$ are the observed and calculated

values of $T_H - [H^+]$ respectively for the i th titration point. With enthalpy change measurements the function minimised was $\sum_{i=1}^N w_i (Q_{\text{obs},i} - Q_{\text{calc},i})^2$ where Q_{obs} was the measured heat change (corrected for secondary reactions not represented in equation 4.32) and Q_{calc} was obtained from the right hand side of equation 4.32. The term w_i is a weighting factor given to each observation. The major source of uncertainty in a measurement of Q arises from (1) the uncertainty in the measurement of the resistance change of the thermister, and (2) the uncertainty in the calorimeter calibration constant (see section 3.2.3). The weighting factor used for each value of Q was $w_i = \frac{1}{\sigma_i^2}$ where σ_i was the estimated uncertainty on the i th observation (generally 0.05 J).

4.5 THE LEAST SQUARES METHOD¹⁷⁵

Consider a function f containing n measurable variables x_1, x_2, \dots, x_n and n unknown parameters p_1, p_2, \dots, p_n such that

$$f = p_1 x_1 + p_2 x_2 + \dots + p_n x_n \quad 4.35$$

The function f may be measured at m different points ($m > n$) to yield observed values of f (f_o) for known values of the variables x_1, x_2, \dots, x_n . Similarly for the known values of x_i an expression for f can be derived from equation 4.35 (f_c). The best values of the parameters p_1, p_2, \dots, p_n (in the least-squares sense), are those values

which minimise the sum of the squares of the residual terms $(f_o - f_c)$ over the m observations, i.e. minimise the function

$$R = \sum_{r=1}^m w_r ((f_o)_r - (f_c)_r)^2 \quad 4.36$$

where w_r is a weighting factor for the i th observation. The minimum value of the function R is found by differentiating the function R with respect to each parameter in turn and setting the derivatives equal to zero. The procedure gives

$$\frac{\partial R}{\partial p_j} = \sum_{r=1}^m w_r ((f_o)_r - (f_c)_r) \frac{\partial (f_c)_r}{\partial p_j} = 0 \quad 4.37$$

for the j th parameter. By considering the n parameters in turn, n equations of the type 4.37 are obtained. The partial derivative of f_c with respect to p_j is determined and this partial derivative is substituted into equation 4.37. This procedure gives a set of n equations 4.38.

$$\begin{aligned} \sum_{r=1}^m w_r ((f_o)_r - (x_1)_r p_1 - (x_2)_r p_2 - \dots - (x_n)_r p_n) (x_1)_r &= 0 \\ \sum_{r=1}^m w_r ((f_o)_r - (x_1)_r p_1 - (x_2)_r p_2 - \dots - (x_n)_r p_n) (x_2)_r &= 0 \\ &\vdots \\ &\vdots \\ \sum_{r=1}^m w_r ((f_o)_r - (x_1)_r p_1 - (x_2)_r p_2 - \dots - (x_n)_r p_n) (x_n)_r &= 0 \end{aligned} \quad 4.38$$

A set of m equations is therefore contracted into a set of n equations containing n unknowns $(p_1, p_2 \dots p_n)$ and the solution of these n equations gives the best values of the parameters $p_1, p_2 \dots p_n$ in the least-squares sense. The set of n equations is solved with the aid of a computer using matrix techniques.

If the function f is not linear in the parameters p_i ,

$$\text{e.g. } f = p_1 x_1 + p_1 p_2 x_2 + p_1 p_2 p_3 x_3 + \dots$$

as is frequently the case for multiple equilibrium systems then it can be approximated to a linear function by using a Taylor series i.e.

$$f(p_1, p_2, \dots, p_n) = f(a_1, a_2, \dots, a_n) + \frac{\partial f}{\partial p_1} (p_1 - a_1) + \dots + \frac{\partial f}{\partial p_n} (p_n - a_n) \quad 4.39$$

where the terms a_i are initial approximations of the parameters p_i and the terms of order greater than one in the Taylor series

$\frac{\partial^2 f}{\partial p_i^2}$ are ignored. Equation 4.39 can be rewritten as

$$f(p_1 \dots p_n) = f(a_1 \dots a_n) + \frac{\partial f}{\partial p_1} \Delta p_1 + \dots + \frac{\partial f}{\partial p_n} \Delta p_n \quad 4.40$$

where $\Delta p_i = p_i - a_i$. This process leads to m linear equations to which the least squares procedure can be applied. If the a_i terms are sufficiently good approximations of the p_i terms then the least squares process will yield values of Δp_i such that a "better" approximation (a_i^1) of the p_i terms is obtained

$$a_i^1 = a_i + \Delta p_i \quad 4.41$$

Successive cycles of this procedure will yield "better" values for the terms a_i . Several cycles are required because equation 4.39 is only an approximate expression for the function f . The number of cycles is determined by a test condition on the change between two successive values of a_i^1 .

4.6 STATISTICAL METHODS

Statistical parameters are generally used to determine how well a postulated model explains the experimental results. These statistical

parameters are used to ultimately determine if a model system will be accepted or rejected.

4.6.1 "Goodness of Fit" of Experimental and Calculated Data

After values for equilibrium constants (or enthalpy changes) have been obtained it must be determined whether or not the calculated results can adequately account for the experimental data. If they do not then further equilibria, or a different model system may be implicated.

Methods of determining goodness of fit usually involve an examination of the residual terms ($f_o - f_c$). A systematic trend in these residual terms indicates the possible influence of further equilibria. A systematic trend in the residual terms is possible with the least squares technique as the method only leads to values of the residuals such that their mean is zero.

Another method of examining the residual terms is to examine the standard deviation of the residuals. Ideally the residual terms should have a normal distribution¹⁷⁶ of mean zero and standard deviation σ . The estimated standard deviation of the residuals is given by the statistic s

$$s = \frac{\sum w_i (f_o - f_c)^2}{NO - NV} \quad 4.42$$

where NO is the number of observations and NV is the number of variables being determined. The estimate of the standard deviation of the residuals (s) can therefore be used as a test of "goodness of fit" (where a value of s as low as possible is desirable). The parameter s can also be used as a test of convergence in the least squares process where convergence to a satisfactory level is said to have occurred when a change in the unknown parameters results in a change in s within a certain tolerance.

Another parameter often calculated to determine the "goodness of fit" of the calculated results to the experimental data is the "crystallographic" R factor¹⁷⁷ defined as

$$R = \frac{\sum_i w_i ((f_o)_i - (f_c)_i)^2}{\sum_i w_i (f_o)_i^2} \quad 4.43$$

The lower the value of R the better the fit of the experimental data to the calculated data.

Tests can be performed¹⁷³ to determine how closely the residual terms follow a normal distribution of mean zero and standard deviation estimated by s . The usual method used is the χ^2 test.¹⁷⁸ The residual terms are divided up into ranges in which the number of residuals occurring in each range is compared with the number of residuals expected to occur in each range if the distribution was in fact normal. For example if the residual terms are divided up into the 8 ranges $(-\infty\sigma$ to $-1.15\sigma)$, $(-1.15\sigma$ to $-0.675\sigma)$, $(-0.675\sigma$ to $-0.312\sigma)$, $(-0.312\sigma$ to $0.0\sigma)$, $(0.0\sigma$ to $0.312\sigma)$, $(0.312\sigma$ to $0.675\sigma)$, $(0.675\sigma$ to $1.15\sigma)$ and $(1.15\sigma$ to $\infty\sigma)$ for which the expected percentage of residual terms (for a normal distribution) falling in each range is 12.5%, the statistic χ^2 is calculated as $\chi^2 = \sum_{i=1}^8 \frac{(O_i - E_i)^2}{E_i}$ where O_i is the observed frequency of residuals occurring in the i th range and E_i is the expected number (12.5%). The value of χ^2 obtained for a particular model can be compared with those obtained for other model systems, or the value of χ^2 can be compared with the expected value of χ^2 at a fixed level of significance using appropriate tables.

The χ^2 statistic and R factor are also used to determine whether or not the addition of another parameter (another equilibrium constant) results in a significant improvement in the fit of the experimental data to the calculated results. The Hamilton test^{177,179} is used to determine if, on adding further parameters to the least-squares

equation, the reduction in the R factor is significant or in fact could have arisen by chance. Similarly if the fit of the calculated results to the experimental data is improved by adding further parameters then the residual terms should more closely follow a normal distribution. A reduction in the value of χ^2 calculated from the residual terms may indicate a better fit of the data. If the calculated χ^2 statistic increases in magnitude this may indicate a substantially poorer fit of the data.

4.6.2 Limitations in the Use of Statistical Parameters

The uses of the R factor and the χ^2 parameter have various limitations when applied experimental data. The first of these involves the type of function used in the least-squares determination.

The R factor is a variable of the residual terms and of $(f_o)^2$. If the transformation $f^1 = f + h$ is performed on f where h is a constant (or variable) then the R factor as defined by equation 4.43 becomes

$$\begin{aligned}
 R &= \frac{\sum_i w_i ((f_o + h)_i - (f_c + h)_i)^2}{\sum_i w_i (f_o + h)_i^2} \\
 &= \frac{\sum_i w_i ((f_o)_i - (f_c)_i)^2}{\sum_i w_i (f_o + h)_i^2}
 \end{aligned}
 \tag{4.44}$$

which differs from equation 4.43. A criterion of "closeness of fit" may be an allowed maximum value of R (predetermined from previous experience) calculated from the residuals. If however the function minimised is changed from say \bar{n} to $T_H - [H^+]$ then the value of R obtained for \bar{n} will in fact be different from that for the function $T_H - [H^+]$, and the maximum value of the R factor must be adjusted to compensate for this effect.

The use of the χ^2 statistic to determine how accurately the residual terms follow a normal distribution is also not without limitations. With the limited number of sample points in a single titration (generally <40) an accurately defined distribution is not possible. Coupled with any bias in a titration (e.g. error in weighing ligand, in alkali concentration, etc.) the probability of the limited number of residual terms closely following a normal distribution may in fact be small. The only method of avoiding this problem is to increase the number of data points (increase the number of samplings of the residual terms) and to combine the residual terms from several titrations to minimise the effect of experimental error.

The statistical measures of goodness of fit are useful indicators of goodness of fit between experimental and calculated data but the limitations of using small sample sizes and the influence of experimental error must always be considered.

4.7 COMPUTER PROGRAMS

Programs and subroutines used in this study to calculate $\bar{n}_H(\text{obs})$ and $\bar{n}_H(\text{calc})$ for the protonation of the diamine oxime ligands, equilibrium quotients for the formation of metal-ligand complexes, calorimetric solution compositions and enthalpy changes are given in the appendix (page 234). A listing of the general least-squares program used in this study has been given by Hedwig.¹²⁹

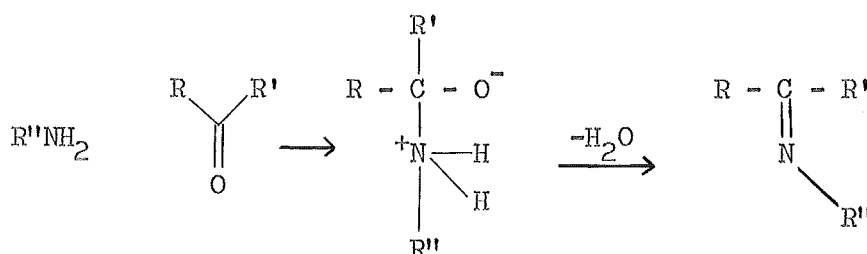
CHAPTER 5

LIGAND SYNTHESIS AND PHYSICAL PROPERTIES

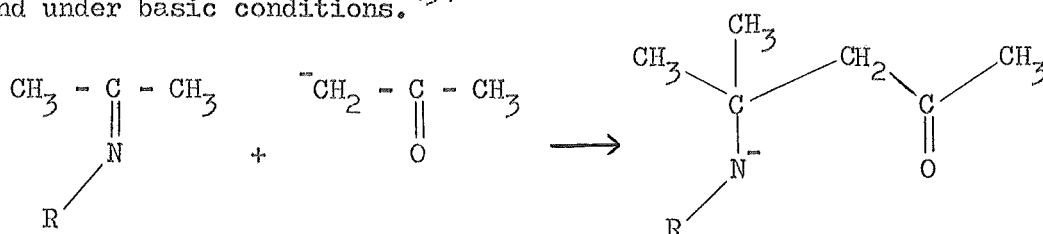
The appropriate experimental conditions for the synthesis of Hddmo and dddm were established by a p.m.r. study of the rate of reaction of the diamine dione dddk with methoxyamine. The ligands were characterized by infrared and p.m.r. spectroscopy, and spectroscopic data for the ligands are reported in this chapter. The ligands H₂dddo and dddm were observed to isomerize (E-Z) under acid conditions, and isomerization data, as determined by p.m.r. spectroscopy are reported.

5.1 LIGAND SYNTHESIS5.1.1 Reaction Mechanism

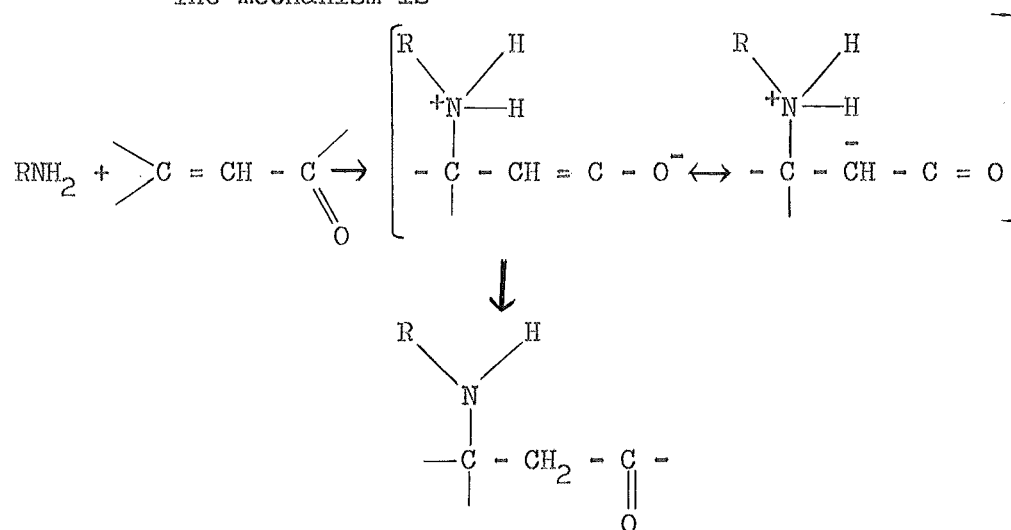
The diamine oxime ligands were prepared by the reaction of the parent diamine with acetone to yield the diamine ketone^{154,180} followed by reaction with either hydroxylamine or methoxyamine as outlined in section 3.4. The reaction of the parent diamine with acetone can be considered to be an addition of the amine to the C-O double bond of acetone^{154,180,181} to yield an imine;



This reaction is followed by the addition of acetone to the C-N double bond under basic conditions.¹⁵⁴



Alternatively, the diamine ketone can be prepared by a Michael addition of the amine to the C-C double bond of mesityl oxide.^{180,182,183} The mechanism is¹⁸²



The Michael reaction is reversible and the product may be decomposed by bases.¹⁸³ Hedwig¹⁸⁴ has observed that the diamine dione dddk decomposes in alkaline solution (pH 8 - 10).

5.1.2 Determination of Experimental Conditions

To determine appropriate experimental conditions for the synthesis of Hddmo, a p.m.r. study of the rate of reaction of CH_3ONH_2 with the diamine dione (dddk) in alkaline D_2O was undertaken. The diamine dione dihydroperchlorate (4×10^{-5} moles) and methoxyamine (12×10^{-5} moles) were placed in a p.m.r. sample tube and D_2O (ca. 0.3 ml) was added. Solid NaOH was added until all solids had dissolved. The p.m.r. spectrum was recorded after intervals of time at 25°C and the extent of reaction was determined from the ratio of the resonance integral for the O-methyloxime protons (increasing with time) to the resonance integral for the gem-dimethyl protons. The results are summarized in table 5.1. Starting with a 3 : 1 mole ratio of reactants, 50% of the ketone groups were converted to an O-methyloxime derivative after 4.5 hours at 25°C . This rate experiment also established that an excess of the methoxyamine reactant

TABLE 5.1Extent of Reaction of dddk with CH_3ONH_2 at 25°C

<u>Time</u> (hrs)	<u>Extent (%) of Reaction</u> ^a
0.25	18
3.0	45
6.0	53
25.0	67

^aExtent of reaction (%) determined from p.m.r. spectrum as the ratio of twice the integral for the O-methyloxime proton resonance to the integral for the gem-dimethyl protons.

would be required to convert all carbonyl groups to the O-methyloxime derivative. This may have resulted from the volatility of methoxyamine (b. pt. 49°C).¹⁸⁵ Because the diamine dione slowly decomposes to give mesityl oxide and diamine in alkaline solution¹⁸⁴ the synthesis was carried out at 0°C . Details of this preparation are given in section 3.4.4. In working up the reaction mixture unreacted dione, and the byproducts $\text{H}_2\text{dddo}, 2\text{HClO}_4$ and $\text{dddm}, 2\text{HClO}_4$ were removed as described in section 3.4.4. Under alkaline conditions the unreacted dione was hydrolysed to ethylenediamine and mesityl oxide, while H_2dddo precipitated as the free dioxime.⁴⁰ The ligand $\text{dddm}, 2\text{HClO}_4$ was separated from $\text{Hddmo}, 2\text{HClO}_4$ by repeated recrystallization from aqueous solution.

The oxime and O-methyloxime functional groups are slowly hydrolysed in acid solution.^{4,7} Acidic ($\text{pH} < 2$) aqueous solutions of H_2dddo , Hddmo and dddm were observed to yield varying amounts (0 - 10%) of the dione dddk over 3 - 4 hours. The ligands Hdno and dnm were also observed to decompose in aqueous acid solution; therefore these ligands were isolated as the dihydroperchlorate salts from aqueous/organic solvent at $\text{pH} \sim 3$.

5.2 LIGAND ISOMERISM

Two isomers of the diamine dioxime (H_2dddo) have been isolated and characterized, viz. an E,E form (anti-methylene) and a Z,Z form (syn-methylene).⁴⁰ It was observed that these geometric configurations are "frozen" in solvent CF_3COOH but, as observed by Norris and Sternhill,³⁴ oxime isomerization occurs rapidly in $\text{CF}_3\text{COOH}/\text{D}_2\text{O}$. The salt (Z,Z) $\text{H}_2\text{dddo}, 2\text{HCl}$ did not isomerise in D_2O and the addition of small amounts of sodium chloride, sodium hydroxide and hydrochloric acid did not affect the p.m.r. spectrum. Hedwig et al reported¹⁶⁵ that both the E,E and Z,Z isomers of H_2dddo react spontaneously in aqueous solution to give the same complex with

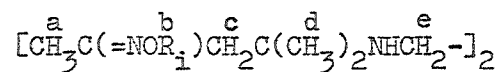
copper(II) ions, indicating a rapid isomerization of the ligand in the presence of metal ions ($>5 \times 10^{-4} \text{ M}$).

5.2.1 Configurational Assignment

The p.m.r. spectroscopic assignments for the ligands H_2dddd , Hddmo , dddm , Hdno and dnm in CF_3COOH and $\text{D}_2\text{O}/\text{CF}_3\text{COOH}$ (50 : 50) are given in tables 5.2 and 5.3. In contrast to H_2dddd , the ligands Hddmo and dddm were isolated in only one isomeric form as determined by p.m.r.; acid salts (ClO_4^- , Cl^- , Br^-) of the other isomer appear to be too soluble to permit isolation. In contrast to H_2dddd the ligands Hddmo and dddm would not crystallise under alkaline conditions. The ligand dddm formed an oil on evaporation of alkaline aqueous solutions.

The dddm isomer isolated from the diamine dione dddk by direct synthesis (section 3.4.3, method (a)), and the isomer isolated from the metal template synthesis (section 3.4.3, method (b)) are identical as determined by p.m.r. and infrared spectroscopy. The ligand isolated on acidification of the complex $\text{Cu}(\text{dddm})(\text{ClO}_4)_2$ reacts with copper(II) ions to spontaneously reform the 1 : 1 complex. The X-ray crystal structure determination¹⁸⁶ and the visible absorption spectrum of the complex $\text{Cu}(\text{dddm})(\text{ClO}_4)_2$ establish that the ligand is co-ordinated to the metal ion through two amino nitrogens and two oxime nitrogens i.e. the ligand is co-ordinated in the $\underline{\text{E}}, \underline{\text{E}}$ form (see section 8.1.3). It is inferred that the dihydroperchlorate salt of dddm is also the $\underline{\text{E}}, \underline{\text{E}}$ isomer. The green mother liquor left from the metal template synthesis (section 3.4.3, method (b)) gave the $\underline{\text{E}}, \underline{\text{E}}$ isomeric form of $\text{dddm}, 2\text{HClO}_4$ very slowly on acidification. The green solution possibly contains the $\underline{\text{Z}}, \underline{\text{Z}}$ isomer of dddm co-ordinated to the copper(II) ion through two amino nitrogens and two oxime oxygens. On acidification the green colour is discharged, but before the ligand can be isolated as the dihydroperchlorate salt it must first isomerise.

TABLE 5.2

P.m.r. Spectral Assignments for the Ligands $H_2dddo, 2HClO_4$, $Hddmo, 2HClO_4$ and $dddm, 2HClO_4$ 

Compound	R_1	Solvent [†]	$\delta(p.p.m.)$ [†]				
			a	b	c	d	e
(<u>E</u> , <u>E</u>)-dddm, $2HClO_4$	$R_1 = R_2 = CH_3$	TFA	2.16	4.08	2.90	1.66	3.73
(<u>E</u> , <u>E</u>)-dddm, $2HClO_4$	$R_1 = R_2 = CH_3$	TFA/ D_2O	1.96	3.92	2.66	1.55	3.55
(<u>Z</u> , <u>Z</u>)-dddm, $2HClO_4$	$R_1 = R_2 = CH_3$	TFA/ D_2O	2.30	3.98	3.03	1.58	3.56
(<u>E</u> , <u>E</u>)- $H_2dddo, 2HClO_4$	$R_1 = R_2 = H$	TFA	2.40	-	3.15	1.70	3.85
(<u>Z</u> , <u>Z</u>)- $H_2dddo, 2HCl$	$R_1 = R_2 = H$	TFA	2.53	-	3.55	1.75	3.92
(E,E)-Hddmo, $2HClO_4$	$R_1 = H; R_2 = CH_3$	TFA	2.18*	4.13	2.93 ⁺	1.68	3.82
			2.42**		3.20 ⁺⁺		
Hddmo, $2HClO_4$	$R_1 = H; R_2 = CH_3$	TFA/ D_2O	1.98*	3.94	3.03*	1.53	3.52
			2.32 ⁺		2.67 ⁺		
			2.07**		3.03**		
			2.32 ⁺⁺		2.72 ⁺⁺		

TABLE 5.2 Continued

[†] CF₃COOH (TFA) or 50% CF₃COOH/D₂O

[†] Relative to TMS as reference

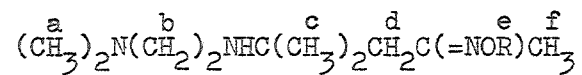
* cis-OCH₃

** cis-OH

[†]trans-OCH₃

⁺⁺trans-OH

TABLE 5.3

P.m.r. Spectral Assignments for the Ligands Hdno, 2HClO₄ and dnm, 2HClO₄

Compound	Solvent ⁺	<u>R</u>	<u>δ(p.p.m.)⁺⁺</u>					
			a	b	c	d	e	f
(E)-Hdno, 2HClO ₄	TFA	H	3.18	3.86	1.73	3.18	-	2.46
			3.27					
(E)-dnm, 2HClO ₄	TFA	CH ₃	3.30	3.97	1.83	3.15	4.26	2.38
			3.40					
Hdno, 2HClO ₄	TFA/D ₂ O	H	3.03	3.58	1.48	2.68*	-	2.03*
						3.03**	-	2.28**
dnm, 2HClO ₄	TFA/D ₂ O	CH ₃	3.08	3.67	1.51**	2.66*	3.95*	1.98*
					1.55*	3.08**	3.98**	2.33**

TABLE 5.3 Continued

⁺CF₃COOH(TFA) or 50% CF₃COOH/D₂O

⁺⁺Relative to TMS as reference

* For (E)-configuration

** For (Z)-configuration

From the assigned configuration for the dddm isomer the nuclear magnetic resonances for cis (OCH_3) α -methyl and trans (OCH_3) α -methylene groups are determined. From isomerization studies ($\underline{\text{E}}, \underline{\text{E}} \rightleftharpoons \underline{\text{Z}}, \underline{\text{Z}}$ in 50% $\text{D}_2\text{O}/\text{CF}_3\text{COOH}$) assignments were also made for the respective trans and cis configurations. By analogy, assignments were made for the α -methyl and α -methylene groups in the $\underline{\text{E}}, \underline{\text{E}}$ and $\underline{\text{Z}}, \underline{\text{Z}}$ forms of H_2dddo and Hddmo . These are reported in table 5.2. Assignments for the ligands Hdno and dnm were made by analogy to dddm and from isomerization studies in 50% $\text{D}_2\text{O}/\text{CF}_3\text{COOH}$. These assignments are shown in table 5.3.

From the configurational assignments for the ligands used in this study two facts emerge. Firstly the resonance for both the α -methylene and α -methyl protons are at higher field for the $\underline{\text{E}}, \underline{\text{E}}$ isomer than for the $\underline{\text{Z}}, \underline{\text{Z}}$ isomer when p.m.r. spectra are recorded in CF_3COOH and $\text{D}_2\text{O}/\text{CF}_3\text{COOH}$. This observation contrasts with those reported for several oximes^{40,187} and oxime ethers²⁵ in other solvents which indicated that α -methyl and α -methylene protons resonate at higher field when trans to the $-\text{OR}$ group. However a similar result has been observed for ethyl 3-(hydroxyimino)butanoate (in solvent D_2O) for which the α -methylene and α -methyl protons resonate at higher field when trans and cis respectively to the $-\text{OR}$ group.⁵¹ The second fact to emerge from the present assignments is that the assignments made previously for H_2dddo (on the basis of infrared spectra) were in error and the correct assignments are given in table 5.2.

5.2.2 Ligand Isomerization

The $\underline{\text{E}}-\underline{\text{Z}}$ isomerization of the diamine oxime ligands was studied in CF_3COOH , D_2O and 50% $\text{D}_2\text{O}/\text{CF}_3\text{COOH}$ by p.m.r. spectroscopy. A ligand sample was dissolved in the appropriate solvent and the p.m.r.

spectrum run after specified intervals of time. The extent of isomerization was determined from the relative ratios of both the α -CH₃ and α -CH₂ resonances in the two isomeric forms. In fig 5.1 the results are summarized as the extent of E-Z isomerization with time for the ligands H₂dddo,2HClO₄ and dddm,2HClO₄ in 50% D₂O/CF₃COOH. The ligand dddm,2HClO₄ isomerized 17 times more slowly than did the dioxime ligand H₂dddo,2HClO₄ in D₂O/CF₃COOH solution (assuming no E,Z isomer was formed).

The rates of E-Z isomerization of Hdno and dnm were examined as described for the dioxime ligands. The results are summarized in fig 5.2. In contrast to the results obtained for H₂dddo,2HClO₄ and dddm,2HClO₄ the rate of E-Z isomerization of dnm,2HClO₄ in 50/50 D₂O/CF₃COOH is only 4 times slower than that for Hdno. The observed rate of isomerization of the O-alkyloximes compared to the oximes in acid solution parallels the known rates of uncatalysed isomerization of oximes and O-alkyloximes (oxime > O-alkyloxime).³⁰

None of the ligands examined isomerized measurably (over 24 hours) in the solvents CF₃COOH or D₂O. Isomerization was however observed on the addition of concentrated HCl to D₂O solutions of Hdno and dnm. Isomerization occurred at an appreciable rate when the concentration of HCl exceeded ca. 0.5M. A similar result has been obtained for the isomerization of 1,4-benzoquinone monoxime derivatives where the rates of isomerization are enhanced in 3M HCl,³⁴ although, in contrast, the isomerization of phenyl-2-pyridine ketoxime is slow in 1M HCl.³⁸

The calculated [H⁺] in CF₃COOH ($pK_a \sim -0.8$)¹⁸⁸/D₂O (50 : 50) is ca. 4M. If the oxime has a pK_a of ca. -0.9⁴ then in 50/50 CF₃COOH/D₂O the extent of protonation will be approximately 50% and in 0.5M HCl ca. 5%. This suggests that acid catalysed E-Z isomerization of oximes proceeds by a mechanism involving protonation of the oxime

Fig. 5.1

Isomer Ratios for the Acid Catalysed Isomerization of
the E,E isomer of the Diamine Dioxime Ligands

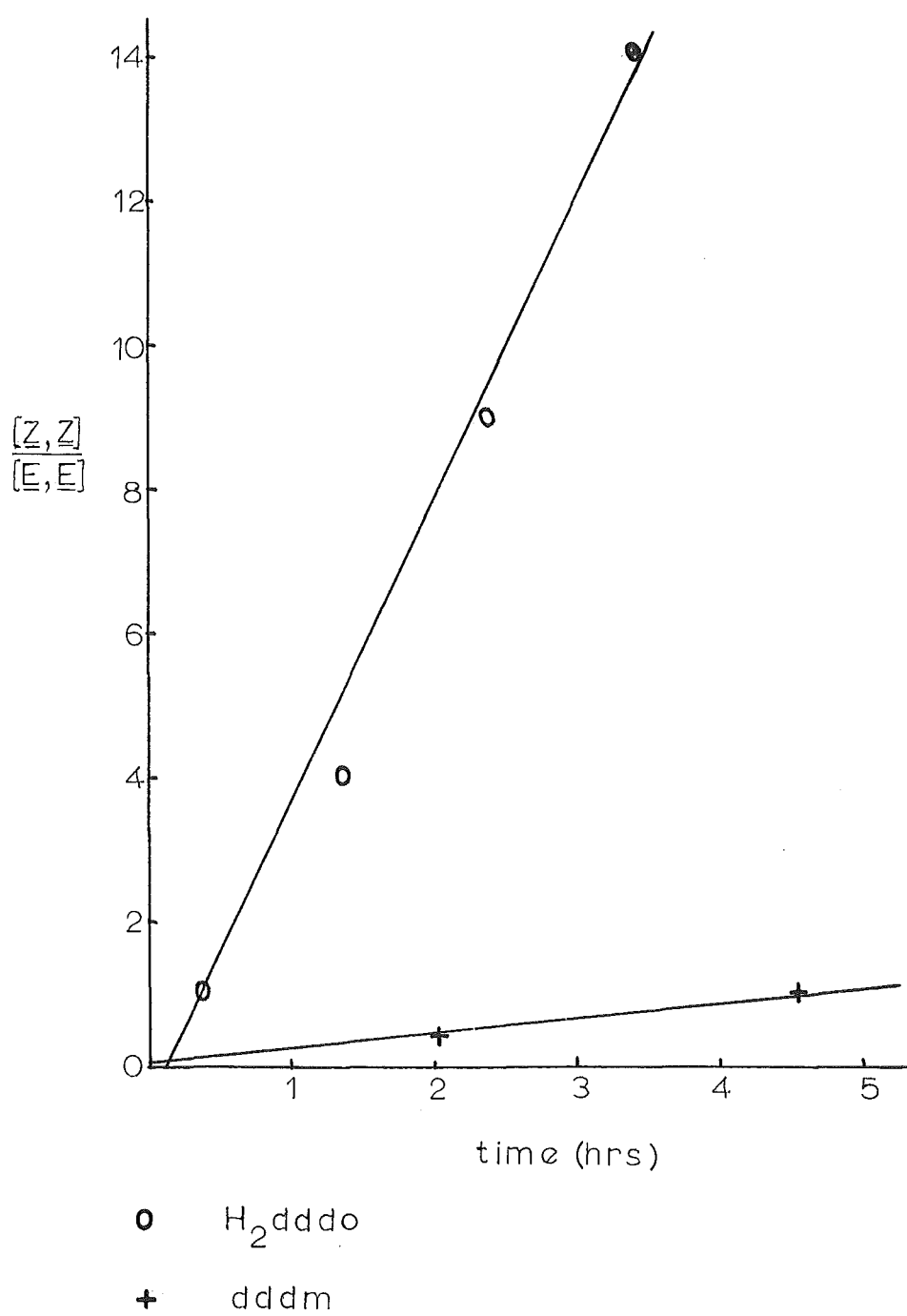
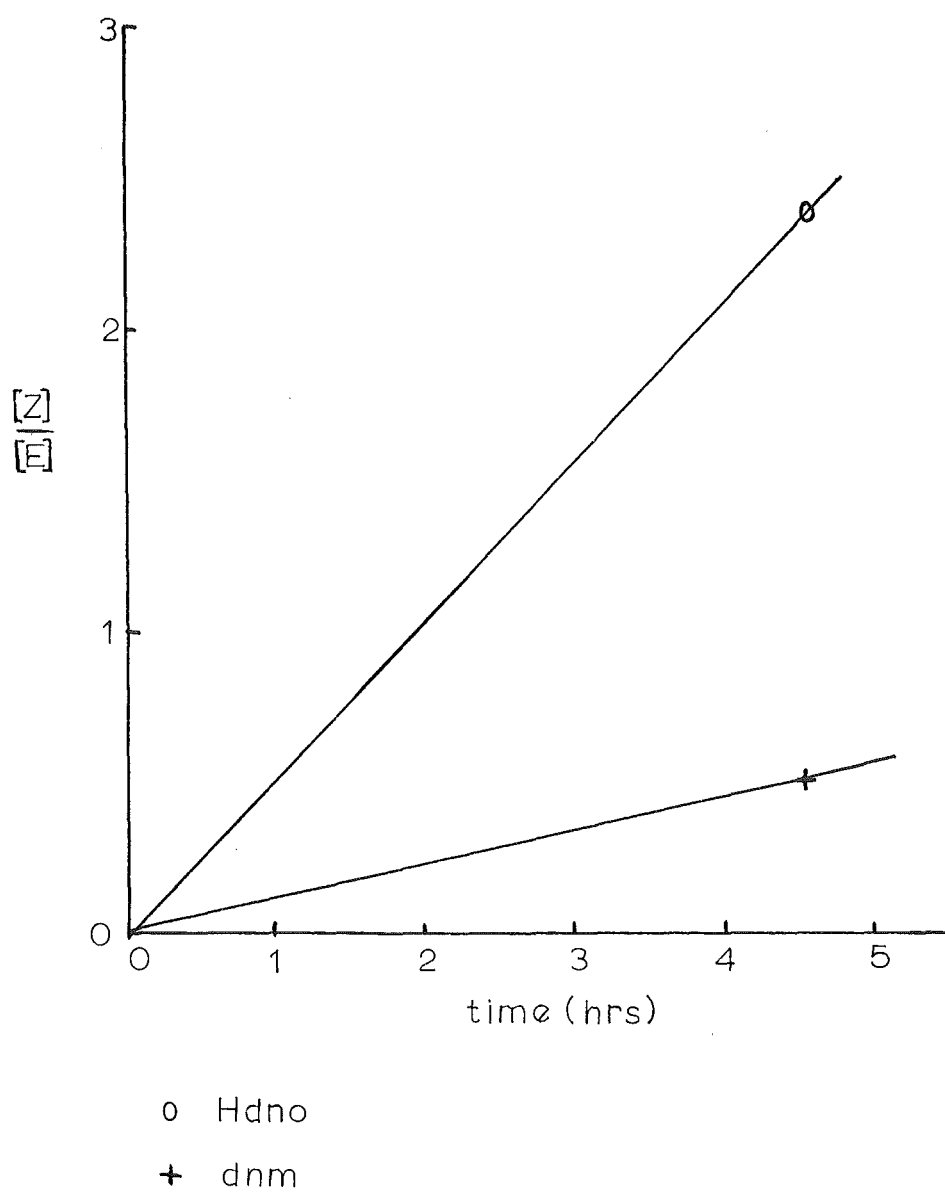
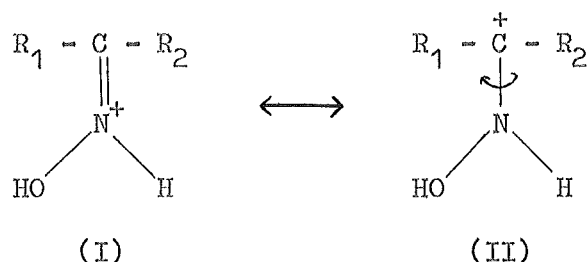


Fig. 5.2

Isomer Ratios for the Acid Catalysed Isomerization of
the E isomer of the Diamine Oxime Ligands



nitrogen i.e. via the intermediate;



An inversion mechanism for acid-catalysed E-Z isomerization is blocked by the protonation of the oxime nitrogen. The contribution of the canonical form (II) to the structure of the protonated oxime lowers the C-N double bond character. The most likely mechanism for acid catalysed isomerization is via the protonated oxime, with rotation about the C-N bond.

In pure solvent CF_3COOH no isomerization is observed. The acid dissociation quotient is lower in the pure solvent (and concentrated solutions) than in dilute aqueous solution.¹⁸⁸ The extent of protonation of the oxime nitrogen is therefore expected to be lower. Further, in pure solvent CF_3COOH the structures (I) and (II) may not be sufficiently stabilized by the solvent because of its low dielectric constant ($\epsilon_{20^\circ C} = 8.24$).^{189,190}

5.3 INFRARED STUDIES

The infrared spectrum of $H_2dddo, 2HClO_4$ in the region 3700-1500 cm^{-1} has been reported.⁴⁰ The infrared spectra and band assignments for the ligands $Hddmo, 2HClO_4$, $dddm, 2HClO_4$, $Hdno, 2HClO_4$ and $dnm, 2HClO_4$ are reported in table 5.4 along with the band assignments made for $H_2dddo, 2HClO_4$. As well as the bands assigned in table 5.4 all diamine oxime dihydroperchlorate salts showed perchlorate stretching modes at 1120 - 1050 cm^{-1} and at 615 cm^{-1} .¹⁵⁵ The oxime ligands $H_2dddo, 2HClO_4$, $Hddmo, 2HClO_4$ and $Hdno, 2HClO_4$ all show an absorption band near 3500 cm^{-1} characteristic of a free O-H group.¹⁹¹ There appears

TABLE 5.4

Infrared Spectral data (cm^{-1}) for the Diamine oxime dihydroperchlorate Ligands^a

<u>Ligand</u>	<u>$\nu(\text{O-H})$</u>	<u>$\nu(\text{NH}_2^+)$</u>	<u>$\nu(\text{C=NOH})$</u>	<u>$\nu(\text{C=NOCH}_3)$</u>	<u>$\delta(\text{NH}_2^+)$</u>	<u>$\nu(\text{N-OH})$</u>	<u>$\nu(\text{N-OCH}_3)$</u>	<u>$\delta(\text{N-OH})^b$</u>
$\text{H}_2\text{dddo}, 2\text{HClO}_4$	3512(s) ^c	3110(m) ^c	1680(w) ^c	-	1564(m) ^c	965(w) 838(w)	-	675(m)
$\text{Hddmo}, 2\text{HClO}_4$	3500(s)	3100(s)	1675(w)	1650(w)	1565(m)	965(w) 838(w)	858(m)	675(m)
$\text{dddmm}, 2\text{HClO}_4$	-	3100(s)	-	1650(w)	1570(m)	-	858(m)	-
$\text{Hdno}, 2\text{HClO}_4$	3500(s)	3140(m)	1675(w)	-	1568(m)	968(w) 840(w)	-	675(w)
$\text{dnm}, 2\text{HClO}_4$	-	3150(m)	-	1650(w)	1580(m)	-	850(m)	-

^as = strong; m = medium; w = weak^bOut of plane deformation mode^cData from ref. 40

to be no appreciable hydrogen bonding of the oxime hydroxyl group in the solid state in the dihydroperchlorate salts. The stretching mode of the N-O bond was assigned by reference to other oxime molecules.^{15,192,193} It is generally regarded that this absorption is not a pure mode. The band at 675 cm^{-1} is characteristic of these oxime molecules and is assigned to an out-of-plane bending mode of the oxime OH group.¹⁹¹

The $\nu(\text{N-OH})$, $\nu(\text{N-OCH}_3)$ and the out-of-plane bending mode of the OH group, which show characteristic absorptions in the oxime ligands, were useful in determining the nature of the products produced in the synthesis of the ligands.

CHAPTER 6

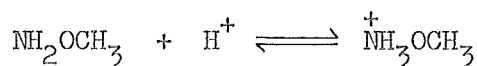
PROTONATION OF THE LIGANDS

The diamine oxime ligands examined in this study contain 2 amine groups for which protonation data have been obtained. Log K, ΔH and ΔS data (at 25.0°C and I = 0.10M NaCl) are reported for the protonation of the ligands H₂dddo, Hddmo and dddm, and log K data (at 25.0°C and I = 0.10M NaCl) for the protonation of the ligands Hdno, and dnm. The ligands also contain an oxime group which affords a weakly basic nitrogen ($pK_a \sim -0.9$)⁴ and a weakly acidic hydroxyl proton. An attempt to measure the protonation constant of the oxime nitrogen was unsuccessful (section 6.4). The dissociation constant for the oxime hydroxyl proton has previously been determined for the ligand H₂dddo (pK_a 12.3 \pm 0.2),¹⁶⁵ and no attempt was made to measure this constant for the ligands Hddmo and Hdno. It was assumed that the pK_a for oxime hydroxyl deprotonation was 12.3. The amine protonation data (log k) (25.0°C, I = 0.10M NaCl and I = 0.002M NaCl) for methoxyamine are reported.

6.1 PROTONATION OF METHOXYAMINE

6.1.1 Results

The protonation constant for the equilibrium



was determined by titration of NaOH (0.242M) into solutions of methoxyamine hydrochloride (ca. $2 \times 10^{-3}M$). The ionic strength was maintained at either 0.10M or 0.002M by the addition of NaCl. Solutions were prepared with CO₂-free distilled water and the titration was carried out in a N₂ atmosphere. Data from the pH-volume

titrations are given in tables 6.1 and 6.2. The data show one end point corresponding to the removal of one proton and the data were analysed in terms of the single concentration quotient

$$k = \frac{[\text{NH}_3^+\text{OCH}_3]}{[\text{NH}_2\text{OCH}_3][\text{H}^+]} \quad . \quad 6.1$$

The value of k was calculated independently for each data point throughout the titration in the range $\bar{n}_{\text{H}} = 0.2 - 0.9$ using the measured $p[\text{H}^+]$ and the stoichiometric concentrations of methoxyamine and titratable hydrogen ions as described in section 4.1.1. The mean value and standard deviation of $\log k$ were calculated for each titration (each of ca. 20 data points). The standard deviation for any titration was less than 0.02 $\log k$ units, indicating that equation 6.1 adequately described the equilibrium system. The mean value of $\log k$ (at $I = 0.10\text{M NaCl}$, 25.0°C) for 5 titrations (\pm standard deviation) was 4.62 ± 0.01 . For 1 titration at $I = 0.002\text{M}$ (25.0°C) the mean value observed for $\log k$ was 4.56 ± 0.02 .

6.1.2 Discussion

The protonation constant for methoxyamine has been reported as $\log k = 4.60 \pm 0.02$ at 25°C , $I = 0.025$ ¹⁸⁵ and 4.62 at 25°C (ionic strength not stated).¹⁹⁴ The $\log k$ values reported in this study compare favourably with these. For hydroxylamine $\log k$ has been reported as 6.0 ⁷⁹ and 5.97 at 25°C , $I = 0.0$.⁵⁶ The higher basicity for hydroxylamine is contrary to that expected on the basis of inductive effects. The Taft σ^* values for OH and OMe are approximately equal, being 0.55 and 0.52 respectively.¹⁹⁵ The observed trend in basicity may result from the contribution of a canonical form of the type $\text{NH}_2-\text{O}^-\text{H}^+$ to the electronic structure of hydroxylamine. This rationale is supported by the fact that the hydroxyl proton is weakly

TABLE 6.1

Representative Data for the Titration of NaOH into a

Solution of $\text{MeONH}_2, \text{HCl}$ at 25.0°C , $I = 0.10\text{M NaCl}$.

Initial Composition: $[\text{MeONH}_2, \text{HCl}] = 2.600 \times 10^{-3}\text{M}$

<u>Vol</u> ^a	<u>p[H⁺]</u> ^b	<u>Vol</u> ^a	<u>p[H⁺]</u> ^b
0.02	3.709	0.26	4.612
0.04	3.799	0.28	4.682
0.06	3.890	0.30	4.736
0.08	3.979	0.32	4.806
0.10	4.065	0.34	4.867
0.12	4.142	0.36	4.941
0.14	4.222	0.38	5.014
0.16	4.288	0.40	5.093
0.18	4.352	0.42	5.190
0.20	4.421	0.44	5.281
0.22	4.486	0.46	5.419
0.24	4.549	0.48	5.564

^aVolume (ml) of 0.242M NaOH added to 49.93 ml of solution

^bp[H⁺] derived from pH_m as detailed in section 3.1.3

TABLE 6.2

Representative Data for the Titration of NaOH into a
 Solution of $\text{MeONH}_2, \text{HCl}$ at 25.0°C , $I = 0.0025\text{M NaCl}$.
Initial Composition: $[\text{MeONH}_2, \text{HCl}] = 2.650 \times 10^{-3}\text{M}$.

<u>Vol</u> ^a	<u>p[H⁺]</u> ^b	<u>Vol</u> ^a	<u>p[H⁺]</u> ^b
0.02	3.667	0.24	4.473
0.04	3.753	0.26	4.535
0.06	3.838	0.28	4.597
0.08	3.922	0.30	4.662
0.10	4.003	0.32	4.731
0.12	4.079	0.34	4.799
0.14	4.155	0.36	4.867
0.16	4.222	0.38	4.943
0.18	4.286	0.40	5.030
0.20	4.348	0.42	5.124
0.22	4.411		

^aVolume (ml) of 0.242M NaOH added to 49.93 ml of
 solution

^bp[H⁺] derived from pH_m as detailed in section 3.1.3

acidic, $pK_a = 13.74$.⁵³ Alternatively the relative basicities may result from specific solvation effects e.g. the species $NH_3^+-O^-H^{\delta+}$ may be stabilized by solvation of the polar O-H bond. The observed trend, which is contrary to that expected on the basis of inductive effects, has been noted for other hydroxy and methoxy containing compounds.¹⁹⁶ For example CH_3OCH_2COOH (pK_a 3.48) is a stronger acid than $HOCH_2COOH$ (pK_a 3.82).¹⁸⁵ Similarly CH_3NHOH is a stronger base than CH_3NHOCH_3 ,¹⁸⁵ and $(CH_3)_2NOH$ a stronger base than $(CH_3)_2NOCH_3$ ¹⁸⁵ (see table 6.3).

6.2 PROTONATION OF THE TETRADENTATE DIAMINE DIOXIME LIGANDS

6.2.1 Results

p[H⁺] Data Protonation constants for the secondary amino groups in Hddmo and dddm were determined by titration of NaOH (0.163M) against solutions of the appropriate ligand dihydroperchlorate ($\sim 1 \times 10^{-3}M$) and NaCl (I = 0.10M) at 25.0°C. Solutions of the ligands were prepared with CO₂-free distilled water by the method outlined in section 3.1.4 (method (a)). Representative data from the pH-volume titrations for the ligands Hddmo and dddm are given in tables 6.4 and 6.5 respectively. The $\bar{n}_H(\text{obs}) - \text{pH}$ data for the ligands Hddmo and dddm are shown in fig 6.1.

Calorimetric Data Data from the calorimetric titrations of standard HCl ($\sim 1M$) against buffered solutions of the ligand dihydroperchlorate, alkali and NaCl (I = 0.10M) at 25°C (initial solution composition $T_L \sim 4 \times 10^{-3}M$, $\bar{n}_H \sim 0.15$), are given in tables 6.6 and 6.7 for Hddmo and dddm respectively. The tabulated heat change Q_m is the measured heat change corrected for the heat of dilution of HCl.¹⁶⁷

TABLE 6.3

Basicity of Some Hydroxy and Methoxy Substituted
Amines at 25°C.

<u>Amine</u>	<u>pK_a</u>
$\text{CH}_3\text{ONH}_3^+$ ^a	4.62
HONH_3^+ ^b	5.97
$\text{CH}_3\text{ONH}_2\text{CH}_3$ ^b	4.75
HONH_2CH_3 ^b	5.96
$\text{CH}_3\text{ONH}(\text{CH}_3)_2$ ^b	3.65
$\text{HONH}(\text{CH}_3)_2$ ^b	5.20

^aThis work; I = 0.10M NaCl

^bFrom ref. 185; I = 0.0M

TABLE 6.4

Representative Data for the Titration of NaOH into Solutions of

Hddmo, 2HClO_4 at 25.0°C , $I = 0.10\text{M}$ (NaCl)Initial Composition: $T_L = 9.804 \times 10^{-4}\text{M}$ $T_H = 1.961 \times 10^{-3}\text{M}$

<u>Vol</u> ^a	<u>pH</u> ^b	<u>Vol</u> ^a	<u>pH</u> ^b	<u>Vol</u> ^a	<u>pH</u> ^b
0.07	5.810	0.18	6.488	0.40	9.074
0.08	5.884	0.19	6.550	0.41	9.132
0.09	5.954	0.20	6.613	0.42	9.188
0.10	6.019	0.21	6.676	0.43	9.243
0.11	6.081	0.22	6.746	0.44	9.298
0.12	6.141	0.23	6.819	0.45	9.349
0.13	6.200	0.24	6.901	0.46	9.396
0.14	6.260	0.36	8.781	0.47	9.442
0.15	6.316	0.37	8.864	0.48	9.491
0.16	6.373	0.38	8.943	0.49	9.537
0.17	6.430	0.39	9.010	0.50	9.584

^aVolume (ml) of 0.1632M NaOH added to 49.93 ml of solution.^b $\text{pH} = 0.9951 \text{p}[\text{H}^+] + 0.086$; section 3.1.3

Fig. 6.1

\bar{n}_H vs pH for the Protonation of the Diamine Dioxime Ligands

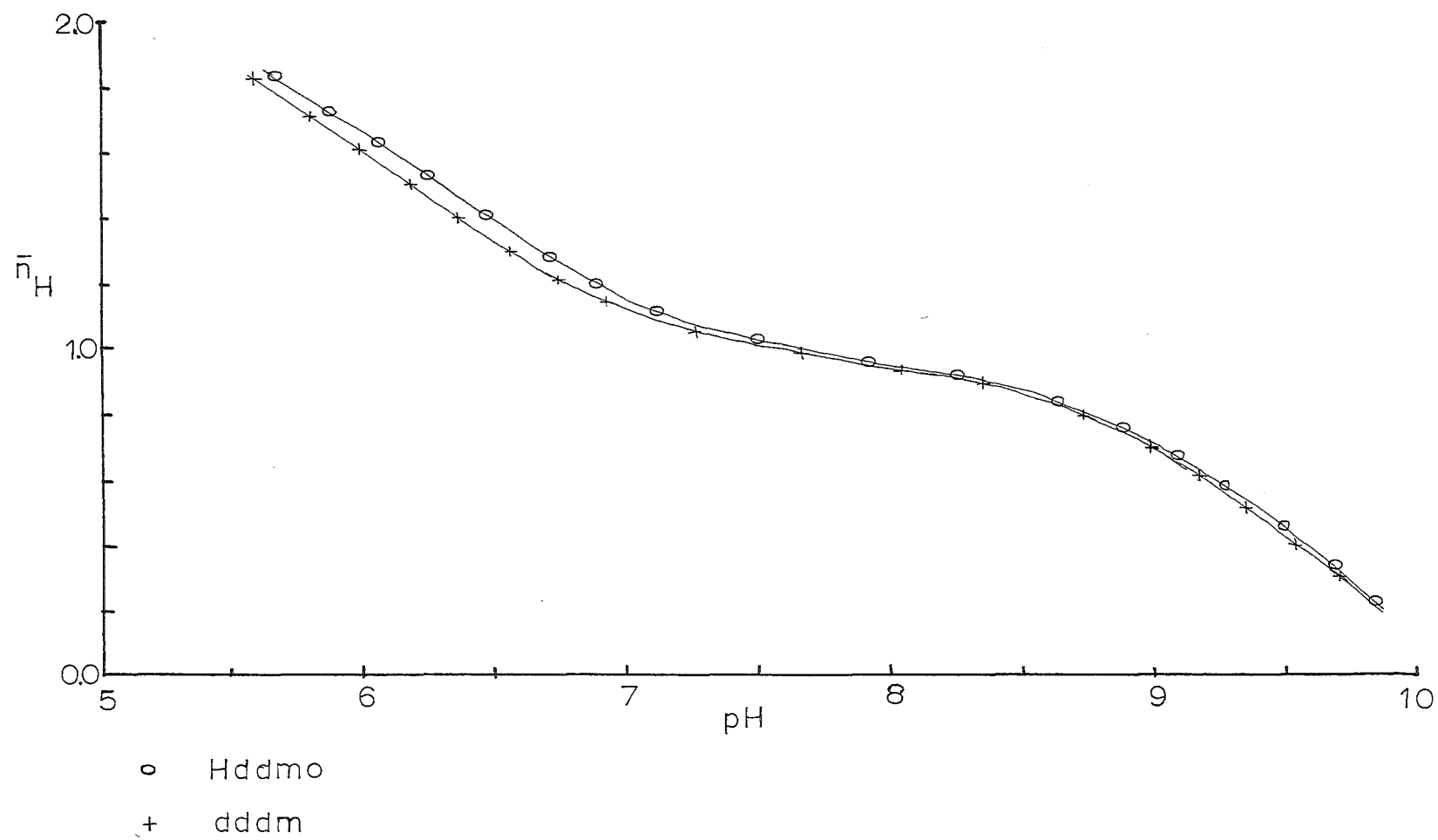


TABLE 6.5

Representative Data for the Titration of NaOH into Solutions of

dddm, 2HClO_4 at 25.0°C , $I = 0.10\text{M NaCl}$ Initial Composition: $T_L = 1.005 \times 10^{-3}\text{M}$ $T_H = 2.010 \times 10^{-3}\text{M}$

<u>Vol</u> ^a	<u>pH</u> ^b	<u>Vol</u> ^a	<u>pH</u> ^b	<u>Vol</u> ^a	<u>pH</u> ^b
0.05	5.564	0.17	6.334	0.38	8.841
0.06	5.652	0.18	6.392	0.39	8.912
0.07	5.730	0.19	6.450	0.40	8.978
0.08	5.790	0.20	6.512	0.42	9.096
0.09	5.870	0.21	6.574	0.44	9.204
0.10	5.932	0.22	6.642	0.46	9.306
0.11	5.994	0.23	6.713	0.48	9.402
0.12	6.048	0.24	6.790	0.50	9.498
0.13	6.108	0.25	6.879	0.52	9.592
0.14	6.164	0.26	6.976	0.54	9.689
0.15	6.222	0.36	8.674	0.56	9.785
0.16	6.278	0.37	8.762		

^aVolume (ml) of 0.1632M NaOH added to 49.93 ml of solution^b $\text{pH} = 0.9951 \text{p}[\text{H}^+] + 0.086$; section 3.1.3

TABLE 6.6

Representative Calorimetric Data from Titrations of HCl against buffered solutions of Hddmo, I = 0.10M NaCl

Vol^{a}	$\text{p}[\text{H}^+]$	$\frac{\bar{n}}{\text{H}}$	$10^4(\text{Hddmo})^{\text{b}}$	$10^4(\text{Hddmo}, \text{H}^+)$	$10^4(\text{Hddmo}, 2\text{H}^+)$	Q_{m}^{c}	$Q_{\text{corr}}^{\text{d}}$	$Q_{\text{calc}}^{\text{e}}$
(ml)			(mol)	(mol)	(mol)	(J)	(J)	(J)
0.180 ^f	9.361	0.551	1.803	1.882	0.002	-	-	-
0.320	8.549	0.877	0.472	3.197	0.017	5.463	5.289	5.099
0.460	6.755	1.249	0.007	2.757	0.923	5.335	5.304	5.278
0.600	6.063	1.622	0.001	1.392	2.294	5.328	5.328	5.340
0.020 ^g	10.177	0.138	3.174	0.507	0.000	-	-	-
0.160	9.453	0.458	1.994	1.685	0.001	5.375	4.284	4.471
0.300	8.724	0.823	0.664	3.006	0.011	5.250	5.043	5.076
0.440	6.889	1.194	0.010	2.946	0.725	5.300	5.253	5.250
0.580	6.159	1.569	0.001	1.586	2.094	5.209	5.208	5.340
0.720	5.079	1.941	0.000	0.218	3.463	5.436	5.436	5.313

TABLE 6.6 Continued

^aCumulative volume of HCl (0.984M) added at each titration point

^bValues for all ligand species are numbers of moles at each titration point

^cMeasured exothermic heat change between successive titration points, corrected for heat of dilution of HCl

^d Q_{corr} is Q_m corrected for the reaction $\text{H}^+ + \text{OH}^- \rightarrow \text{H}_2\text{O}$

^e $Q_{\text{calc}} = r\Delta H_1 + s\Delta H_2$ where ΔH_i are calculated from a least squares process, and r, s are the number of moles of Hddmo, H^+ and Hddmo, 2H^+ formed between successive titration points as outlined in section 4.2.1.

^fTitration 1. Initial volume (Vol = 0.0 ml) 98.84 ml. Initial composition; $T_L = 3.730 \times 10^{-3}\text{M}$, $T_H = 7.799 \times 10^{-5}\text{M}$

^gTitration 2. Initial volume (Vol = 0.0 ml) 98.84 ml. Initial composition; $T_L = 3.724 \times 10^{-3}\text{M}$, $T_H = 6.789 \times 10^{-5}\text{M}$

TABLE 6.7

Representative Calorimetric Data from Titrations of HCl against buffered solutions of dddm, I = 0.10M (NaCl)

<u>Vol</u> ^a	<u>p[H⁺]</u>	<u>\bar{n}_H</u>	<u>10⁴(dddm)^b</u>	<u>10⁴(dddm, H⁺)</u>	<u>10⁴(dddm, 2H⁺)</u>	<u>Q_m</u> ^c	<u>Q_{corr}</u> ^d	<u>Q_{calc}</u> ^e
(ml)			(mol)	(mol)	(mol)	(J)	(J)	(J)
0.320 ^f	8.912	0.733	1.355	3.678	0.007	-	-	-
0.480	7.433	1.042	0.058	4.711	0.272	5.491	5.420	5.623
0.640	6.452	1.355	0.004	3.244	1.792	5.448	5.446	5.743
0.800	5.892	1.667	0.001	1.677	3.362	5.525	5.525	5.745
0.160 ^g	9.480	0.424	2.899	2.127	0.001	-	-	-
0.430	8.196	0.944	0.330	4.651	0.046	9.401	9.144	9.390
0.590	6.652	1.256	0.008	3.724	1.296	5.847	5.833	5.719
0.750	6.072	1.569	0.001	2.163	2.863	5.595	5.595	5.746
0.910	5.322	1.882	0.000	0.595	4.432	5.445	5.445	5.734
0.000 ^h	10.227	0.116	4.352	0.572	0.000	-	-	-
0.160	9.537	0.392	2.995	1.926	0.001	5.855	4.652	4.837
0.320	8.974	0.703	1.467	3.451	0.006	5.923	5.698	5.508

TABLE 6.7 Continued

0.480	7.600	1.020	0.084	4.657	0.183	5.819	5.738	5.611
0.640	6.480	1.340	0.004	3.242	1.677	5.845	5.842	5.741
0.800	5.907	1.659	0.001	1.676	3.247	5.831	5.831	5.745

^aCumulative volume of HCl (0.984M) added at each titration point

^bValues for all ligand species are numbers of moles at each titration point

^cMeasured exothermic heat change between successive titration points, corrected for heat of dilution of HCl

^d Q_{corr} is Q_m corrected for the reaction $H^+ + OH^- \rightarrow H_2O$

^e $Q_{\text{calc}} = r\Delta H_1 + s\Delta H_2$ where ΔH_i are calculated from a least squares procedure and r, s are the number of moles of dddm, H^+ and dddm, $2H^+$ formed between titration points as outlined in section 4.2.1

^fTitration 1. Initial Volume (Vol = 0.0 ml) 98.84 ml. Initial Composition; $T_L = 5.099 \times 10^{-3}M$, $T_H = 5.366 \times 10^{-4}M$

^gTitration 2. Initial Volume (Vol = 0.0 ml) 98.84 ml. Initial Composition; $T_L = 5.086 \times 10^{-3}M$, $T_H = 5.117 \times 10^{-4}M$

^hTitration 3. Initial Volume (Vol = 0.0 ml) 98.84 ml. Initial Composition; $T_L = 4.981 \times 10^{-3}M$, $T_H = 3.019 \times 10^{-4}M$

Analysis of the Data The protonation of the ligands Hddmo

and dddm can be represented by the stepwise equilibria



where L represents the ligand Hddmo or dddm. The concentration quotients for these equilibria are given by

$$k_1 = \frac{[LH^+]}{[L][H^+]} \quad 6.2$$

and $k_2 = \frac{[LH_2^{2+}]}{[LH^+][H^+]} \quad 6.3$

The stepwise protonation constants were computed from derived $\bar{n}_H(\text{obs})$ - pH data as detailed in section 4.1.1. The protonation constants for Hddmo given in table 6.8 were determined for 6 titrations each of ca. 35 data points, and those for dddm from 14 titrations each of ca. 35 data points in the range \bar{n}_H 0.10 - 1.80. R factors (see section 4.6.1) of ca. 0.25% were achieved and there were no systematic trends in the residual terms ($\bar{n}_H(\text{obs}) - \bar{n}_H(\text{calc})$).

The calorimeter solution composition at each titration point was calculated from the derived values of k_1 and k_2 as outlined in section 4.1.1. The stepwise enthalpy changes for protonation (ΔH_1 and ΔH_2 for reactions I and II respectively) were calculated using a linear least squares procedure as outlined in section 4.2.1. The values of the heat change calculated from the least squares analysis $Q(\text{calc})$ are given in tables 6.6 and 6.7. A comparison of each $Q(\text{calc})$ value with $Q(\text{corr})$ (Q_m corrected for the heat of neutralization of hydroxide ion¹⁶⁸ produced in the reaction $H_2O + L \rightleftharpoons OH^- + LH^+$) indicates that the least squares refinement of the calorimetric data was satisfactory. The enthalpy changes (ΔH_1 and ΔH_2) for Hddmo

TABLE 6.8

Thermodynamic Data for the Protonation of Diamine Ligands, 25°C

<u>Diamine</u>	<u>log k₁</u>	<u>-ΔH₁</u> (kJ mol ⁻¹)	<u>ΔS₁</u> (J mol ⁻¹ K ⁻¹)	<u>log k₂</u>	<u>-ΔH₂</u> (kJ mol ⁻¹)	<u>ΔS₂</u> (J mol ⁻¹ K ⁻¹)
H ₂ dddo ^a	9.41 ± 0.02	39.6 ± 0.3	48 ± 1	6.35 ± 0.02	40.2 ± 0.3	-13 ± 1
Hddmo ^b	9.38 ± 0.01	37.9 ± 0.6	52 ± 2	6.28 ± 0.01	38.8 ± 0.5	-10 ± 2
dddm ^b	9.34 ± 0.01	35.9 ± 0.5	58 ± 2	6.19 ± 0.01	36.5 ± 0.4	-4 ± 2
N,N'-diethylethylenediamine ^c	10.44	45.5	46	7.51	44.0	-0.4
N,N'-di-n-butylethylenediamine ^d	10.19	-	-	7.46	-	-

^aData from ref. 184^bThis work; mean ± standard deviation, I = 0.10M NaCl^cData from ref. 199; I = 0.5M NaClO₄. Values calculated for I = 0.1 (section 2.2 and ref. 135) are -ΔH₁ = 45.5 and -ΔH₂ = 44.6 kJ mol⁻¹ respectively.^dData from ref. 198; I = 0.65M KNO₃

and dddm were determined from 10 data points (2 titrations) and 28 data points (6 titrations) respectively. The enthalpy changes for protonation of the ligands are given in table 6.8.

6.2.2 Discussion

Empirical Calculation of Thermodynamic Data

Empirical equations have been developed to predict the effect of substituents on ΔG , ΔH and ΔS for the amino protonation of amines and diamines.

Clark and Perrin reported¹⁹⁶ empirical equations of the form

$$pK_a = 13.23 - 3.14\Sigma\sigma^* \quad 6.4$$

$$pK_a = 12.13 - 3.23\Sigma\sigma^* \quad 6.5$$

$$pK_a = 9.61 - 3.30\Sigma\sigma^* \quad 6.6$$

to predict the pK_a of primary, secondary and tertiary aliphatic amines respectively ($\Sigma\sigma^*$ is the sum of the Taft σ^* values of the substituents attached to the amine nitrogen). These empirical equations assume no abnormal steric, solvation or resonance effects. Clark and Perrin also reported¹⁹⁶ an equation in terms of the observed base weakening effect of a substituent (ΔpK_a) and the typical pK_a values observed for a variety of primary (10.77), secondary (11.15) and tertiary (10.5) amines. When several substituents are present the base weakening effects are assumed to be additive and a transmission factor of 0.5 per carbon atom is assumed. As an example the pK_a for $^+NH_3(CH_2)_2NH_2$ is estimated as¹⁹⁶

$$\begin{aligned} pK_a &= \text{typical } pK_a \text{ (primary amine)} + \Delta pK_a \text{ (NH}_2\text{CH}_2\text{CH}_2\text{-)} \\ &= 10.77 - 0.80 \\ &= 9.97 \end{aligned}$$

where 0.80 is the base weakening effect of an NH_2 group two carbon atoms away from the site of deprotonation. The observed pK_a for ethylenediamine is 9.91.⁵⁶

Christensen and coworkers⁵⁶ have reported empirical formulae for the calculation of enthalpy and entropy changes for proton dissociation from protonated N-alkyl substituted primary and secondary amines. These equations are of the form

$$\Delta H^\circ = \Delta H_m^\circ + 1.59n_\alpha + 0.63n_\beta + 0.46n_\gamma \quad 6.7$$

and

$$\Delta S^\circ = \Delta S_m^\circ + S_\alpha n_\alpha + 3.14n_\beta + 0.63n_\gamma \quad 6.8$$

where ΔH° and ΔS° are expressed in kJ mol^{-1} and $\text{JK}^{-1} \text{mol}^{-1}$ respectively. In equations 6.7 and 6.8 ΔH_m° and ΔS_m° are the values of ΔH° and ΔS° observed for methylamine or dimethylamine (depending on whether a primary or secondary amine is being examined); n_α , n_β and n_γ are the number of carbon atoms 1, 2 and 3 carbon atoms from the carbon next to the site of protonation and S_α is the "entropy substituent effect" of an α carbon ($5.02 \text{ JK}^{-1} \text{mol}^{-1}$ for primary amines and $2.93 \text{ JK}^{-1} \text{mol}^{-1}$ for secondary amines).

Paoletti¹⁹⁷ also has reported a formula to predict enthalpy changes for the protonation of primary alkyl diamines. This formula is

$$-\Delta H = \Delta H(\text{NH}_2) + \sum \left(\frac{1}{2}\right)^{n-1} \delta(\text{C}) + \sum \left(\frac{1}{2}\right)^{n-1} \delta(\text{NH}_2) + \sum \left(\frac{1}{2}\right)^{n-1} \delta(\text{NH}_3^+)$$

where $\Delta H(\text{NH}_2)$ is an empirical value for the enthalpy change on protonation of an NH_2 group. The integer n is the numerical position of an atom or ionic centre with respect to the amino group being protonated and $\delta(\text{C})$, $\delta(\text{NH}_2)$ and $\delta(\text{NH}_3^+)$ measure the effect exerted by a carbon atom, NH_2 and NH_3^+ group respectively on the enthalpy of protonation.

Basicity of the Ligand Amino Groups

The log k data given in table 6.8 show that there is a considerable reduction in the basicity of the diamine dioxime ligands compared to that of N,N' -dimethylethylenediamine or N,N' -diethylethylenediamine. This observed reduction in basicity results from two factors:

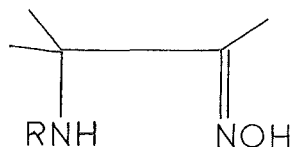
- (1) the effect of the N -alkyl substituents on the amine nitrogens, and
- (2) the electron withdrawing effect of the oxime substituents.

The Base Weakening Effect of Alkyl Substituents Increasing the chain length of the N -alkyl substituents in a diamine $RNHCH_2CH_2NHR$ causes a slight reduction in the basicity of the nitrogen atoms (e.g. for $R = Et, n\text{-}Pr, n\text{-}Bu$ $\log k_1 = 10.46, 10.27$ and 10.19 respectively at $25^\circ C, I = 0.65M$).¹⁹⁸ However with a large number of N -alkyl monoamines the basicity does not decrease uniformly with increasing chain length.¹⁹⁶ The basicities of the primary amines RNH_2 are $\log k (RNH_2 + H^+ \rightleftharpoons RNH_3^+) = 10.64, 10.63, 10.57$ and 10.64 for $R = Me, Et, n\text{-}Pr$ and $n\text{-}Bu$ respectively.⁵⁶ The enthalpy and entropy changes for these amines show that the approximately constant basicity arises from the compensation of the ΔH° and $T\Delta S^\circ$ terms. As the chain length increases $-\Delta H^\circ$ increases and ΔS° decreases. An explanation for this effect is in terms of "chain stiffening".^{141,197} Non-polarizable groups of low dielectric constant (the alkyl substituents) are repelled from the charged centre in preference to groups of high dielectric constant (e.g. solvent water). This results in a solvent constrained alkyl chain; a decrease in the number of degrees of freedom results in the decreased entropy change. However by reference to the protonation constants of N,N' -dialkyl substituted diamines it is expected

that only a small reduction in basicity would result from the alkyl chain in the diamine dioxime ligands.

The Base Weakening Effect of Oxime Substituents The markedly lower basicity of H_2dddo compared to N,N' -dimethylethylenediamine,¹⁹⁹ N,N' -diethylethylenediamine¹⁹⁹ and N,N' -di-*n*-butylethylenediamine¹⁹⁸ has been ascribed to the base weakening (electron withdrawing) effect of the oxime group¹⁸⁴ (see table 6.8). Examination of the data in table 6.8 shows that the base weakening effect of the *O*-methyloxime group is slightly (but significantly) greater (0.07 - 0.16 log *k* units) than that for an oxime group.

The base weakening effect of an oxime substituent can be estimated from the thermodynamic data for amine protonation of the amine α -oximes of the form



which were studied by Wang, Bauman and Murmann.⁹³ The thermodynamic data for amino protonation have been measured and a comparison with the ΔG and ΔH data calculated for the hypothetical ligand $RNHC(CH_3)_2CH_2CH_3$ from the empirical formulae of Christensen,⁵⁶ show that the base weakening effect of the oxime substituent is reflected by a decrease in log *k* by 1.7 and in $-\Delta H$ by 8 - 13 kJ mol⁻¹.¹²⁹ Assuming a transmission coefficient of 0.5 per carbon atom for substituent effects, then the base weakening effect of the oxime group in the ligands H_2dddo and $Hddmo$ would be 0.85 log *k* units. Considering N,N' -di-*n*-butylethylenediamine as a reference compound then the calculated protonation constants (log *k*) for H_2dddo are 9.34 and 6.61 which agree well with the measured values of 9.41 and 6.35 (see table 6.8). The calculations take no account of the possible amine-oxime hydrogen bonding in the α - and β -aminoketoximes.

Enthalpy Changes

Nitrogen- and carbon-substituted ethylenediamines generally show an enthalpy change for the first stepwise protonation (ΔH_1) which is more exothermic than that for the second stepwise protonation.^{79,199} This trend can be predicted from a consideration of the electrostatics of protonation; the electron withdrawing NH_2^+ group lowers the basicity of the second amino group and hence the exothermic contribution to ΔH_2 .

By use of the empirical formulae of Paoletti¹⁹⁷ the first and second enthalpy changes for the stepwise protonation of the amino groups in the diamine $(\text{CH}_3\text{CH}_2\text{CH}_2\text{C}(\text{CH}_3)_2\text{N}(\text{CH}_2-)_2)$ (the ligand H_2dddo without the oxime substituents) have been calculated as -51.6 and $-47.5 \text{ kJ mol}^{-1}$ respectively.¹⁸⁴ The difference of $7 - 16 \text{ kJ mol}^{-1}$ between these values and those for the protonation of the diamine H_2dddo give an estimate of the base weakening effect of the oxime groups.

Hedwig¹⁸⁴ has suggested the possibility of intramolecular hydrogen bonding between the oxime proton and the lone pair of electrons on the amino nitrogen as contributing to the lowered (exothermic) enthalpy of protonation. Breaking of the hydrogen bond in the protonation step would decrease $\log k_1$ and make an endothermic contribution to ΔH_1 . In the ligand dddm hydrogen bonding of this type could not occur. However the observed trend in $\log k_1$ and $-\Delta H_1$ values ($\text{dddm} < \text{Hddmo} < \text{H}_2\text{dddo}$) is opposite to that expected if $\text{N}:\text{---H-O-N=}$ hydrogen bonding were important. It is therefore deduced that this form of hydrogen bonding does not contribute to the observed basicity.

Entropy Changes

The factor which makes the greatest contribution to the observed entropy change for a reaction is the change in solvation of the reactants

and products; for the reaction $L + H^+ \rightleftharpoons LH^+$ the entropy change is dependent on the solvent ordering abilities of the species L , H^+ and LH^+ . For protonation of the diamine dioxime ligands H_2dddo , $Hddmo$ and $dddm$ the entropy change is contributed to by the liberation of solvent molecules from H^+ and by the solvent ordering ability of the protonated ligand. The protonated ligands each contain bulky hydrophobic groups which, to some extent, will shield the amino groups from the solvent and as a result the entropy change for protonation is expected to be positive. Configurational entropy changes are difficult to assess. Generally a "chain stiffening effect" (caused by the attraction of the high dielectric solvent molecules to protonated amine centre^{14,1}) can be expected on protonation. This would make a negative contribution to the entropy change. The ΔS_1 values observed for the ligands H_2dddo , $Hddmo$ and $dddm$ are all greater than those usually observed for the protonation of a secondary amino nitrogen (ca. $43 \text{ J mol}^{-1} \text{ K}^{-1}$)²⁰⁰ implying that there is less solvent ordering about these ammonium ions. The trend in the ΔS_1 values ($H_2dddo < Hddmo < dddm$) suggests that changing from an oxime to an O-methyloxime group further reduces the extent of solvent or intramolecular) ordering about the amino groups. The associated trend in the $-\Delta H_1$ values ($H_2dddo > Hddmo > dddm$) suggests that some specific solvation effect is operating. These data are consistent with a postulate of intramolecular hydrogen bonding of the form $\overset{+}{N}-H \cdots \overset{||}{N}-OR$ in the protonated ligands, with a six-membered ring being formed. By this means the group R could exert an effect on the solvent ordering about the ammonium ion. The trend in ΔH_1 and ΔH_2 values (most exothermic for H_2dddo) could imply that the intramolecular hydrogen bonding is strongest when $R=H$. This is consistent with the fact that hydroxylamine is more basic than methoxyamine.

The order $\Delta S_1 > \Delta S_2$ is consistent with that observed for other diamines (e.g. $\Delta S_1 - \Delta S_2 = 46 \text{ J mol}^{-1} \text{ K}^{-1}$ for N,N'-diethylethylenediamine). This difference in ΔS_i values can be rationalized in terms of electrostatic theory. For an ion with two charged centres sufficiently far apart ($> \text{ca. } 10 \text{ \AA}$) the solvent ordering ability of the ion is approximately twice that of each charged centre.¹⁴¹ When the two charged centres coincide then the volume of solvent influenced by the doubly charged centre will be 2.8 times as great as that for a singly charged centre.¹⁴¹ The solvent ordering about two charged centres less than 10 \AA apart will be greater than two times that for a singly charged centre. ΔS_2 is therefore expected to be less than ΔS_1 .

6.3 PROTONATION OF THE TRIDENTATE DIAMINE OXIME LIGANDS

6.3.1 Results

Protonation constants for the secondary and tertiary amino groups of the ligands Hdno and dnm were determined by titration of NaOH (ca. 0.3M) into solutions of the appropriate ligand dihydroperchlorate ($\sim 1 \times 10^{-3} \text{ M}$) and NaCl (I = 0.10M) at 25°C. In order to conserve ligand, the ligand salt was weighed just prior to the measurement of pH-volume data and dissolved in 50 ml of CO₂-free distilled water. The appropriate weight of NaCl was added to the solution. Data from the pH-volume titrations for the ligands Hdno and dnm are tabulated in tables 6.9 and 6.10 respectively. The protonation of the amino nitrogens could be represented by the stepwise equilibria I and II where L represents Hdno or dnm. The concentration quotients for these equilibria are given by equations 6.2 and 6.3 and k_1 and k_2 were computed from the derived $\bar{n}_H(\text{obs})$ - pH data as detailed in section 4.1.1. The $\bar{n}_H(\text{obs})$ - pH data are shown in fig 6.2 for Hdno and dnm. The derived amino protonation constants for both Hdno and dnm, as given in table 6.11, were determined for 3 titrations each

TABLE 6.9

Representative Data for the Titration of NaOH Against Solutions

of $\text{Hdno}, 2\text{HClO}_4$ at 25°C , $I = 0.10\text{M NaCl}$ Initial Composition: $T_L = 1.213 \times 10^{-3}\text{M}$ $T_H = 2.426 \times 10^{-3}\text{M}$

<u>Vol</u> ^a	<u>p[H⁺]</u> ^b	<u>Vol</u> ^a	<u>p[H⁺]</u> ^b	<u>Vol</u> ^a	<u>p[H⁺]</u> ^b	<u>Vol</u> ^a	<u>p[H⁺]</u> ^b
0.035	5.405	0.120	6.189	0.265	8.669	0.350	9.392
0.040	5.468	0.125	6.228	0.270	8.731	0.355	9.423
0.050	5.586	0.130	6.271	0.275	8.787	0.360	9.456
0.055	5.641	0.135	6.311	0.285	8.892	0.365	9.490
0.060	5.688	0.140	6.352	0.290	8.937	0.370	9.527
0.065	5.739	0.145	6.394	0.295	8.978	0.375	9.565
0.070	5.783	0.150	6.436	0.300	9.018	0.380	9.601
0.075	5.827	0.155	6.482	0.305	9.059	0.385	9.637
0.085	5.912	0.160	6.528	0.310	9.095	0.390	9.671
0.090	5.952	0.165	6.579	0.315	9.134	0.395	9.708
0.095	5.990	0.170	6.633	0.320	9.173	0.400	9.740
0.100	6.030	0.175	6.689	0.325	9.213		
0.105	6.069	0.180	6.752	0.330	9.251		
0.110	6.109	0.185	6.819	0.335	9.291		
0.115	6.150	0.190	6.889	0.345	9.357		

^aVolume (ml) of 0.2702M NaOH added to 49.93 ml of solution^bp[H⁺] derived from pH_m as detailed in section 3.1.3

TABLE 6.10

Representative Data for the Titration of NaOH Against Solutions

of $\text{dnm}, 2\text{HClO}_4$ at 25°C , $I = 0.10\text{M NaCl}$ Initial Composition: $T_L = 1.102 \times 10^{-3}\text{M}$ $T_H = 2.204 \times 10^{-3}\text{M}$

<u>Vol</u> ^a	<u>p[H⁺]</u> ^b	<u>Vol</u> ^a	<u>p[H⁺]</u> ^b	<u>Vol</u> ^a	<u>p[H⁺]</u>	<u>Vol</u> ^a	<u>p[H⁺]</u> ^b
0.020	5.054	0.085	5.857	0.160	6.667	0.295	9.260
0.025	5.152	0.090	5.907	0.170	6.850	0.300	9.300
0.030	5.237	0.095	5.950	0.230	8.606	0.305	9.342
0.035	5.313	0.100	5.994	0.240	8.733	0.310	9.383
0.040	5.380	0.110	6.086	0.245	8.793	0.315	9.424
0.045	5.446	0.115	6.133	0.250	8.846	0.320	9.467
0.050	5.504	0.120	6.183	0.255	8.897	0.325	9.510
0.055	5.560	0.125	6.231	0.265	8.993	0.330	9.555
0.060	5.613	0.130	6.286	0.270	9.039	0.335	9.595
0.065	5.665	0.135	6.339	0.275	9.085		
0.070	5.713	0.140	6.395	0.280	9.129		
0.075	5.762	0.145	6.456	0.285	9.173		
0.080	5.809	0.150	6.521	0.290	9.215		

^aVolume (ml) of 0.2857M NaOH added to 49.93 ml of solution^bp[H⁺] derived from pH_m as detailed in section 3.1.3

Fig. 6.2

\bar{n}_H vs pH for the Protonation of the Diamine Oxime Ligands

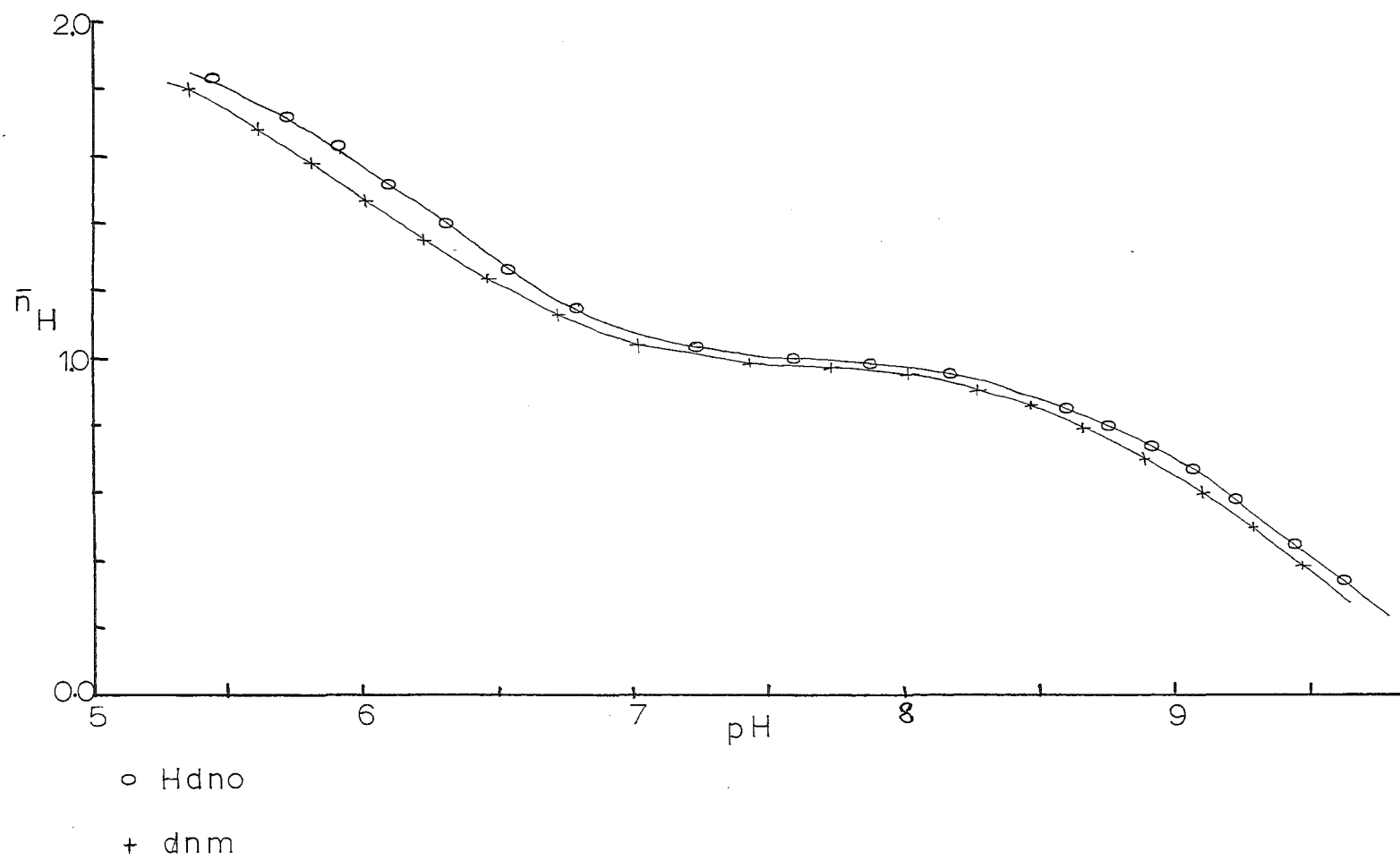


TABLE 6.11

Equilibrium Data for the Amino Protonation Reactions
of the Diamine Oxime Ligands, 25°C

<u>Diamine</u>	<u>log k₁</u>	<u>log k₂</u>
Hdno ^a	9.36 ± 0.02	6.13 ± 0.01
dnm ^a	9.23 ± 0.03	5.95 ± 0.01
N,N-dimethylethylenediamine ^b	9.69	6.69

^aThis work; mean ± standard deviation for 3 titrations, I = 0.10M NaCl

^bData from ref. 202

of ca. 40 data points in the range \bar{n}_H 0.30 - 1.80. R factors (see section 4.6.1) of ca. 0.35% were achieved and there were no systematic trends in the residual terms $\bar{n}_H(\text{obs}) - \bar{n}_H(\text{calc})$.

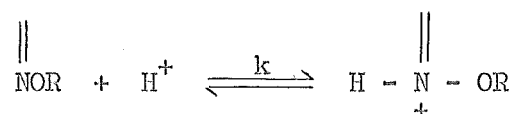
6.3.2 Discussion

In molecules containing two (or more) non-equivalent amino groups ΔH and ΔS values for the stepwise protonation reactions establish that each step involves partial protonation on each type of nitrogen centre.²⁰¹ Therefore it is not possible to directly compare $\log k_1$ and $\log k_2$ values for Hdno and dnm with related ligands such as N,N-dimethylethylenediamine (table 6.11) however values of $\Sigma \log k_i$ (the overall basicity of the ligand) may be directly compared. Comparison with a model compound N,N-dimethylethylenediamine shows there is a base weakening effect in Hdno and dnm associated with (1) the C-6 alkyl substituent attached to one of the amino nitrogens, and (2) the electron withdrawing properties of the oxime or O-methyloxime group. The effect of the C-6 alkyl substituent is hard to predict but by reference to the N,N'-dialkyl substituted ethylenediamines (see section 6.2.2) the alkyl group will have a base weakening effect of <0.3 in $\Sigma \log k_i$. The base weakening effect of the β -ketoxime group can be ascertained as ca. 0.9 and 1.2 log units for the β -ketoxime and β -ket-O-methyloxime substituents respectively by comparing the ligands Hdno and dnm with N,N-dimethylethylenediamine.²⁰² When the ligands H_2dddo , and $dddm$ are compared with ethylenediamine²⁰² the observed base weakening effects of a β -ketoxime and a β -ket-O-methyloxime group are 0.8 and 0.9 respectively. (Note that these values take no account of ionic strength effects. The ionic strength reported for the ethylenediamine and N,N-dimethylethylenediamine data is $I = 0.5M \text{ KNO}_3$. This work reports data at $I = 0.1M \text{ NaCl}$). Hdno is a stronger base than dnm ($\Delta(\Sigma \log k_i) = 0.31 \pm 0.07$). In the ligands H_2dddo , $Hddmo$ and $dddm$

a similar observation was interpreted, on the basis of ΔH and ΔS data, in terms of hydrogen bonding of the type $\overset{+}{N}-H \cdots \overset{+}{N}-OR$ (see section 6.2.2).

6.4 PROTONATION OF THE OXIME NITROGEN

An attempt to determine $\log k$ for protonation of the oxime nitrogen, i.e.



by p.m.r. spectroscopy was unsuccessful because of the acid catalysed E-Z isomerization of the oxime group which occurs when the oxime nitrogen is protonated (see section 5.2.2). Determination of this constant by ultraviolet spectroscopy is hampered by the acid catalysed hydrolysis of the oxime group,⁴ and of the β -aminoketoxime group¹⁸⁴ forming as products the parent ketone and mesityl oxide respectively; the latter product absorbs strongly in the ultraviolet.²⁰³ An indication of the relative basicities of the oxime and O-methyloxime groups can however be obtained from the reaction of the ligands Hdno and dnm with copper(II) ions (see Chapter 7).

CHAPTER 7

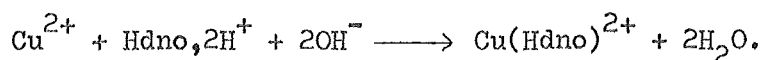
COPPER(II) COMPLEXES OF THE DIAMINE-OXIME LIGANDS

To assess the different co-ordinating powers of the oxime and O-methyloxime functional groups, the stability constants for the formation of copper(II) complexes with the tridentate ligands Hdno and dnm have been determined at 25.0°C and I = 0.10M NaCl. The complexes $[\text{Cu}(\text{Hdno})]^{2+}$, $[\text{Cu}(\text{dno})]^+$, $[\text{Cu}(\text{dnm})]^{2+}$ and $[\text{Cu}(\text{dnm})(\text{OH})]^+$ have been characterized in solution and their visible and ultraviolet absorption spectra are reported.

7.1 RESULTS

The copper(II) complexes of Hdno and dnm were studied by titration of NaOH (ca. 0.3M) into solutions of ligand dihydroperchlorate ($\sim 1 \times 10^{-3}\text{M}$), CuCl_2 ($7 - 9 \times 10^{-4}\text{M}$) and NaCl (I = 0.10M) at 25.0°C. Typical pH-volume data from the titrations are given in tables 7.1 and 7.2 for the ligands Hdno and dnm respectively. Only one set of reproducible data is tabulated. The data given in tables 7.1 and 7.2 are shown graphically in fig 7.1.

Titration of NaOH against solutions containing copper(II) ion and $\text{Hdno}, 2\text{HClO}_4$ gave two buffer regions, at pH 3.4 - 4.3 and pH 5.3 - 6.3, followed by marked inflexions (end points) at pH 4.4 - 5.2 and at pH 6.5 - 9.1 respectively (see fig 7.1). The first end point titre corresponded to the completion of the reaction



The second end point corresponded to the removal of one proton from the complex to give $\text{Cu}(\text{dno})^+$ (plus the reaction $\text{Hdno}, 2\text{H}^+ + \text{OH}^- \rightarrow \text{Hdno}, \text{H}^+ + \text{H}_2\text{O}$ for excess ligand present). Electronic absorption

TABLE 7.1

Representative Data for the Titration of NaOH Against Solutions
of H₂NO₂, 2HClO₄ and Copper Dichloride at 25°C, I = 0.10M NaCl

Initial Composition: $T_L = 1.101 \times 10^{-3} M$

$T_M = 8.987 \times 10^{-4} M$

<u>Vol</u> ^a	<u>p[H⁺]</u> ^b	<u>Vol</u> ^a	<u>p[H⁺]</u> ^b	<u>Vol</u> ^a	<u>p[H⁺]</u> ^b	<u>Vol</u> ^a	<u>p[H⁺]</u> ^b
0.010	3.371	0.130	3.688	0.250	4.132	0.420	5.767
0.020	3.398	0.140	3.717	0.260	4.174	0.430	5.854
0.030	3.423	0.150	3.746	0.270	4.233	0.440	5.940
0.040	3.449	0.160	3.774	0.280	4.301	0.450	6.027
0.050	3.474	0.170	3.806	0.290	4.380	0.460	6.121
0.060	3.497	0.180	3.840	0.300	4.461	0.470	6.229
0.070	3.525	0.190	3.874	0.360	5.221	0.480	6.358
0.080	3.552	0.200	3.908	0.370	5.330	0.490	6.514
0.090	3.581	0.210	3.944	0.380	5.432	0.500	6.703
0.100	3.605	0.220	3.984	0.390	5.524	0.510	6.973
0.110	3.630	0.230	4.028	0.400	5.606		
0.120	3.660	0.240	4.075	0.410	5.685		

^aVolume (ml) of 0.2702M NaOH added to 49.93 ml of solution

^bp[H⁺] derived from pH_m as outlined in section 3.1.3

TABLE 7.2

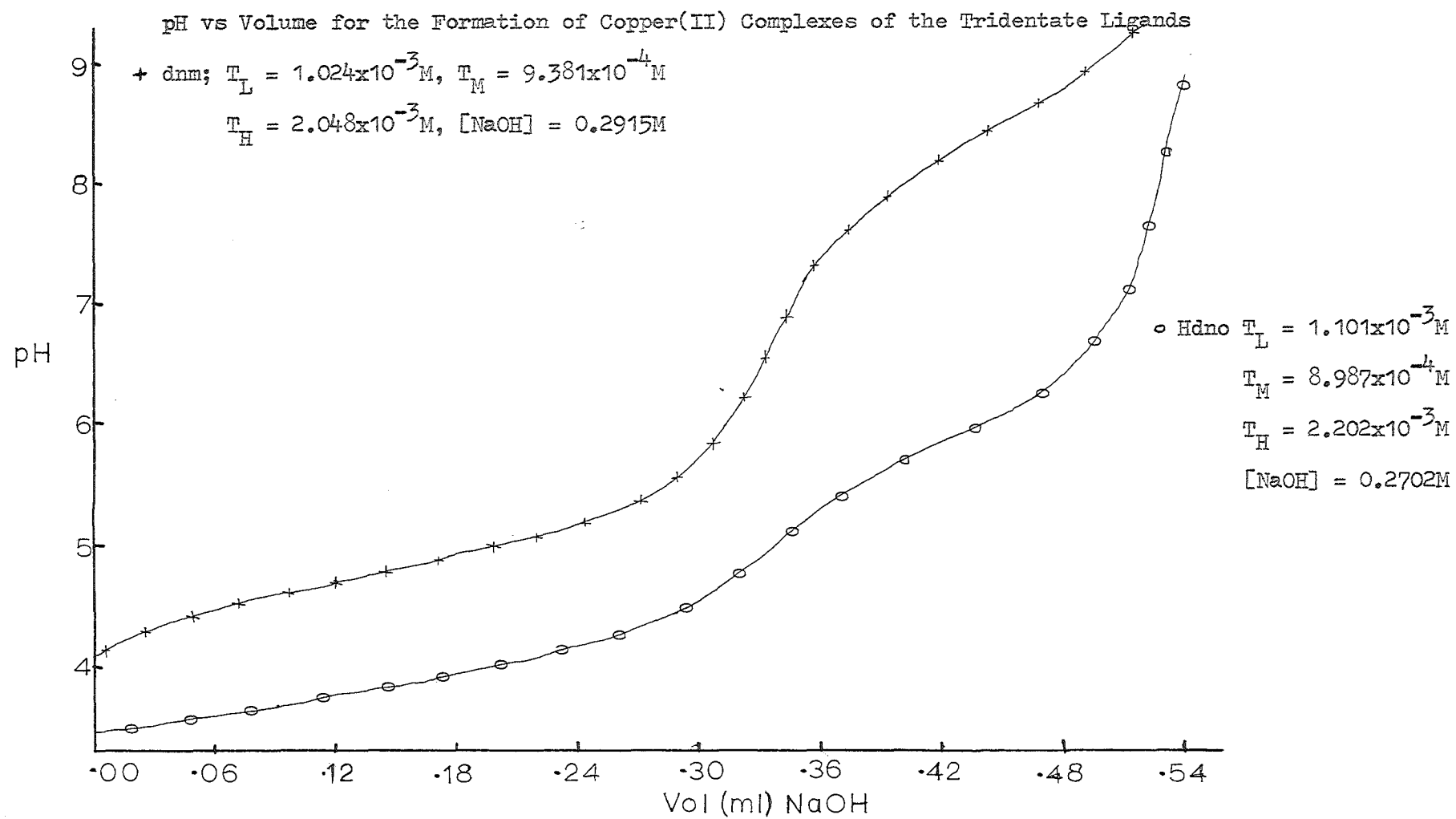
Representative Data for the Titration of NaOH Against Solutions of

dm, 2HClO_4 and Copper Dichloride at 25°C , $I = 0.10\text{M NaCl}$.Initial Composition: $T_L = 1.024 \times 10^{-3}\text{M}$ $T_M = 9.381 \times 10^{-4}\text{M}$

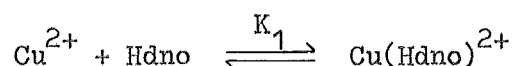
<u>Vol</u> ^a	<u>p[H⁺]</u> ^b	<u>Vol</u> ^a	<u>p[H⁺]</u> ^b	<u>Vol</u> ^a	<u>p[H⁺]</u> ^b
0.050	4.324	0.170	4.805	0.290	5.491
0.060	4.365	0.180	4.844	0.370	7.483
0.070	4.416	0.190	4.885	0.380	7.651
0.080	4.458	0.200	4.927	0.390	7.797
0.090	4.500	0.210	4.970	0.400	7.920
0.100	4.539	0.200	5.018	0.410	8.033
0.110	4.577	0.230	5.068	0.420	8.138
0.120	4.615	0.240	5.122	0.430	8.245
0.130	4.652	0.250	5.179	0.440	8.339
0.140	4.690	0.260	5.245	0.450	8.435
0.150	4.727	0.270	5.312	0.460	8.533
0.160	4.765	0.280	5.394	0.470	8.633

^aVolume (ml) of 0.2915M NaOH added to 49.93 ml of solution^b $p[H^+]$ derived from pH_m as outlined in section 3.1.3

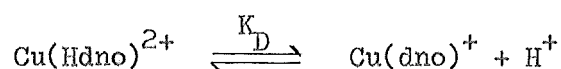
Fig. 7.1



spectra run on test samples throughout a titration confirmed that only one complex species was formed in each of the two buffer regions. The appearance of a third absorption band at 416 nm (ϵ 205 l mol⁻¹ cm⁻¹) during the second buffer region suggested that oxime deprotonation was occurring, although this band is of comparatively low intensity. $(\text{Cu}(\text{Hdddo}))^+$ shows absorptions at 583, 330 (ϵ 2800 l mol⁻¹ cm⁻¹) and 272 nm;¹⁶⁵ the absorption at 330 nm is diagnostic of an oximato group). Spectrophotometric data for the complexes $\text{Cu}(\text{Hdno})^{2+}$ and $\text{Cu}(\text{dno})^+$ are given in table 7.3. On the basis of the titration and spectrophotometric data the system could best be represented by the following equilibria:



and



and the equilibrium constants:

$$K_1 = \frac{[\text{Cu}(\text{Hdno})]}{[\text{Cu}][\text{Hdno}]} \quad 7.1$$

$$K_D = \frac{[\text{Cu}(\text{dno})][\text{H}]}{[\text{Cu}(\text{Hdno})]} \quad 7.2$$

where charges have been omitted for clarity. Values of K_1 and K_D were calculated for each data point in the first and second buffer regions respectively by the method outlined in section 4.1.2. The derived equilibrium constant values showed no systematic trends. The values of $\log K_1$ and $\log K_D$ (\pm standard deviation) given in table 7.4 were calculated from three titrations each of ca. 25 data points.

TABLE 7.3

Spectrophotometric Data for the Copper(II) Complexes of
Hdno and dnm in Aqueous Solution (I = 0.10M NaCl)

<u>Complex</u>	λ_{max} (ε)	
	(nm)	(l mol ⁻¹ cm ⁻¹)
Cu(Hdno) ²⁺	612(121)	274(5620)
Cu(dno) ⁺	568(129)	416(~205) ^a 247(5360)
Cu(dnm) ²⁺	619(144)	286(5180)
Cu(dnm)(OH) ⁺	606(90)	271(6020)

^aShoulder

TABLE 7.4

Equilibrium Data for the Complexing of the Ligands Hdno, dnm and
N,N-dimethylethylenediamine with copper(II) ions at 25°C

<u>Ligand</u>	<u>Hdno</u>	<u>dnm</u>	<u>N,N-dimethylethylenediamine</u>
log K ₁	11.29 ± 0.05	8.85 ± 0.05	9.27
log K _{OH}	-	5.57 ± 0.11	-
log K _D	-5.93 ± 0.11	-	-

^aThis work; mean ± standard deviation for 3 titrations, I = 0.10M NaCl

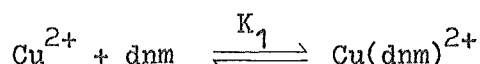
^bData from ref. 204; I = 0.5M KNO₃

Titration of NaOH against solutions containing CuCl_2 and $\text{dnm}, 2\text{HClO}_4$ gave buffer regions at pH 4.3 - 5.5 (with an end point at pH 5.9 - 6.9) and at pH 7.6 - 9.2 (followed by a second, less well-defined, inflexion at pH 9.2). The titre for the first end point corresponded to the completion of the reaction

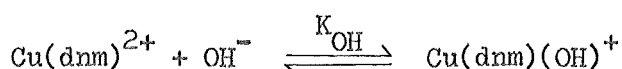


(plus $\text{dnm}, 2\text{H}^+ + \text{OH}^- \rightarrow \text{dnm}, \text{H}^+ + \text{H}_2\text{O}$ for excess ligand present).

The second buffer region was interpreted in terms of the formation of an hydroxy species $\text{Cu}(\text{dnm})(\text{OH})^+$ and the data for the two buffer regions were analysed in terms of the equilibria



and



and the equilibrium constants

$$K_1 = \frac{[\text{Cu}(\text{dnm})]}{[\text{Cu}][\text{dnm}]} \quad 7.3$$

and

$$K_{\text{OH}} = \frac{[\text{Cu}(\text{dnm})(\text{OH})]}{[\text{Cu}(\text{dnm})][\text{OH}]} \quad 7.4$$

where charges have been omitted for clarity. Values of K_1 and K_{OH} were calculated independently for each data point in the first and second buffer regions respectively by the method outlined in section 4.1.2. The derived equilibrium constants ($\log K$) had a standard deviation of less than 0.05 and thus equations 7.3 and 7.4 adequately explained the experimental data. $\log K_1$ and $\log K_{\text{OH}}$ values (\pm standard deviation) derived from data for 3 titrations are given in table 7.4.

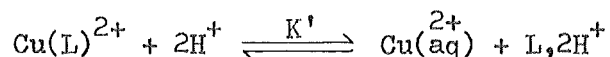
Electronic absorption spectra recorded throughout a titration confirmed the formation of a single complex in each buffer region. Spectrophotometric data for the complexes $\text{Cu}(\text{dnm})^{2+}$ and $\text{Cu}(\text{dnm})(\text{OH})^+$ are recorded in table 7.3.

7.2 DISCUSSION

7.2.1 The Complexes $\text{Cu}(\text{Hdno})^{2+}$ and $\text{Cu}(\text{dnm})^{2+}$

Stability Constants The results show that the complex $\text{Cu}(\text{Hdno})^{2+}$ is significantly more stable than the complex $\text{Cu}(\text{dnm})^{2+}$, $\Delta(\log K_1) = 2.4 \pm 0.1$, indicating that the $\text{C}=\text{NOH}$ group is a better donor than $\text{C}=\text{NOMe}$. In section 6.1.2 the greater basicity of hydroxylamine, compared to methoxyamine, was attributed to the importance of structures such as $\text{NH}_2-\text{O}^-\text{H}^+$ contributing to the basicity of the amine group. Assuming a linear relationship between $\log K_1$ and the overall basicity of the donor atoms in the complex $(\sum \log k_i)^{98}$ then the results show that the group $\text{C}=\text{NOH}$ is more basic than the $\text{C}=\text{NOCH}_3$ group. This suggests the importance of structures such as $\text{C}=\text{NO}^-\text{H}^+$ contributing to the basicity of the oxime group. This postulate is supported by the fact that the oxime hydroxyl proton is weakly acidic (pK_a for $\text{H}_2\text{dddo} = 12.3$).¹⁶⁵

A method for comparing the donor properties of the oxime and the O-methyloxime groups is by consideration of the equilibrium



and equilibrium constant

$$K' = \frac{[\text{Cu}^{2+}][\text{L}, 2\text{H}^+]}{[\text{Cu}(\text{L})^{2+}][\text{H}^+]^2} \quad 7.5$$

which takes into account the different (amino) basicities of the two ligands. The $\log K'$ values for the copper(II) complexes of dnm and

Hdno are 6.3 ± 0.1 and 4.20 ± 0.07 respectively, the latter giving the more stable copper complex. The difference in the $\log K'$ values (2.1 ± 0.2) suggests that the C=NOH group is a better donor to copper(II) than the C=NOCH₃ group.

By comparing the $\log K'$ values for the copper(II) complexes of Hdno and dnm with that for $[\text{Cu}(\text{N,N-dimethylethylenediamine})]^{2+}$ (table 7.4) the effect of an added β -ketoxime chelate ring on the stability of a 1,2-diamine can be assessed. The $\log K'$ value for $[\text{Cu}(\text{N,N-dimethylethylenediamine})]^{2+}$ is 7.1^{204} and it is therefore inferred that the β -ketoxime substituent contributes 2.9 log units to the stability of the $\text{Cu}(\text{Hdno})^{2+}$ complex while the contribution by the β -ket-O-methyloxime substituent in $\text{Cu}(\text{dnm})^{2+}$ is only 0.8 log units. These contributions arise from (1) the extra bonding associated with the oxime donor, and (2) the formation of a second chelate ring. The use of $\log K'$ values takes into account the reduced basicity of the amino groups on changing from a primary amine in N,N-dimethylethylenediamine to a secondary amino group in the ligands Hdno and dnm.

Absorption Spectra The visible absorption spectra of the complexes $\text{Cu}(\text{Hdno})^{2+}$ and $\text{Cu}(\text{dnm})^{2+}$ show that the oxime group produces a slightly stronger ligand field than does the O-methyloxime group. This is consistent with the stability constant data. Spectrophotometric data have been reported²⁰⁵ for the complexes NiL_6Cl_2 where $\text{L} = \text{NH}_2\text{OH}$ and NH_2OCH_3 . These data show NH_2OCH_3 to be a slightly weaker donor than NH_2OH .

The triamine complexes $[\text{Cu}(\text{3-azaheptan-1,7-diamine})]^{2+}$ and $[\text{Cu}(\text{4-azaheptan-1,7-diamine})]^{2+}$ have d-d transitions at 613 nm^{206} and 611 nm^{207} respectively. The stability constants for these two complexes are $\log K_1 = 13.4^{206}$ and 14.2^{208} respectively. The oxime and O-methyloxime groups both generate a ligand field strength similar to that of an amino group. The addition of an alkyl-oxime,

alkyl-O-methyloxime or alkyl-amine group to a diamine ligand co-ordinated to copper(II) increases the ligand field strength substantially (c.f. $[\text{Cu}(\text{N,N-dimethylethylenediamine})]^{2+}$ λ_{max} 700 nm²⁰⁴) although the oxime ligands both form complexes which are much less stable than the triamine complexes. Thermodynamic data for the co-ordination of the diamine dioxime H_2dddo ¹⁸⁴ (and for Hddmo (see chapter 8)) to copper(II) ions shows that the entropy change on co-ordination is similar to that for the analogous tetramine²⁰⁹ ($\sim 80 \text{ J mol}^{-1} \text{ K}^{-1}$) but that the enthalpy change is markedly less exothermic ($-\Delta H = 55 \text{ kJ mol}^{-1}$ for the formation of $\text{Cu}(\text{H}_2\text{dddo})^{2+}$ c.f. 104 kJ mol^{-1} for the analogous tetramine complex). It is inferred that the lower stability of the oxime complexes relates mainly to the strength of the metal-ligand bond. The approximately equal ligand field strengths for Hdno , dnm and the triamines may indicate that the weaker bonding in the oxime complexes involves π back co-ordination from the metal to the ligand, thus increasing the ligand field splitting parameter Δ . This increase in Δ with π -back bonding is clearly illustrated by the diagrams of Cotton and Wilkinson.²¹⁰

The ultraviolet absorptions at 274 and 286 nm for $\text{Cu}(\text{Hdno})^{2+}$ and $\text{Cu}(\text{dnm})^{2+}$ respectively are assigned to $\text{L}_\text{O} \rightarrow \text{M}$ charge transfer transitions. A similar charge transfer transition is observed in many copper(II) polyamine and poly-(amine-imine) complexes.²¹¹

7.2.2 The Complex $\text{Cu}(\text{dno})^+$

Metal ion co-ordination to an oxime group increases the acidity of that group, just as co-ordination enhances proton dissociation from water,¹⁰⁴ amines,⁸⁸ and hydroxylamine.¹⁰⁶ For deprotonation of the oxime H_2dddo a value of $\log k_\text{D} = -12.3$ has been determined.¹⁶⁵ For deprotonation of the co-ordinated oxime group in $\text{Cu}(\text{Hdno})^{2+}$ $\log K_\text{D} = -5.93$; an increase in acidity of ca. 6.4 log units. For the complex

$\text{Cu}(\text{H}_2\text{dddo})^{2+}$ deprotonation may be accompanied by intramolecular oxime-oximato hydrogen bonding, and $\log K_D$ is increased further to -3.24.¹⁶⁵

The formation constant for $\text{Cu}(\text{dno})^+$ can be determined by assuming a value of $\log k_D = -12.3$ for the reaction $\text{Hdno} \rightleftharpoons \text{dno}^- + \text{H}^+$. The formation constant $\log K^* (\text{Cu}^{2+} + \text{dno}^- \rightleftharpoons \text{Cu}(\text{dno})^+) = -\log k_D + \log K_D + \log K_1 (\text{Cu}(\text{Hdno})^{2+}) = 12.3 - 5.9 + 11.3 = 17.7$. The sequence of donor strengths inferred from the stability constant values ($\log K$) for $\text{Cu}(\text{dno})^+$, $\text{Cu}(\text{Hdno})^{2+}$ and $\text{Cu}(\text{dnm})^{2+}$ is oximato (17.7) >> oxime (11.3) > O-methyloxime (8.8). Deprotonation of the oxime enhances the stability of its copper(II) complex by ca. 6.4 log units.

The absorption spectrum of $\text{Cu}(\text{dno})^+$ reflects the increased donor strength of the oximato group compared with that of the oxime group. The d-d absorption band is shifted from 612 nm for $\text{Cu}(\text{Hdno})^{2+}$ to 568 nm for $\text{Cu}(\text{dno})^+$ (see table 7.3). The band in the ultraviolet at 247 nm is assigned to a $L_O \rightarrow M$ charge transfer transition. A third absorption band occurs in the visible at 416 nm for $\text{Cu}(\text{dno})^+$. A similar band for the complex $\text{Cu}(\text{Hdddo})^+$ ($\lambda_{\text{max}} = 330$ nm, $\epsilon = 2800 \text{ l mol}^{-1} \text{ cm}^{-1}$)¹⁶⁵ has been assigned to a charge transfer transition between the oximato group and the metal ion. The band occurring in $\text{Cu}(\text{dno})^+$ has a much lower intensity ($\epsilon = 205 \text{ l mol}^{-1} \text{ cm}^{-1}$) but it also is considered to be diagnostic of an oximato group.

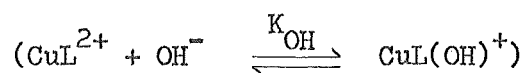
7.2.3 Hydroxy Complex Species

The $\log K_{\text{OH}}$ value observed for the formation of $\text{Cu}(\text{dnm})(\text{OH})^+$ is in the range observed for aqua deprotonation from a variety of copper(II) triamine complexes with combinations of 5,6 and 7-membered chelate rings^{206,207,212,213} (see table 7.5). The hydroxy complex is assumed to be of the form

TABLE 7.5

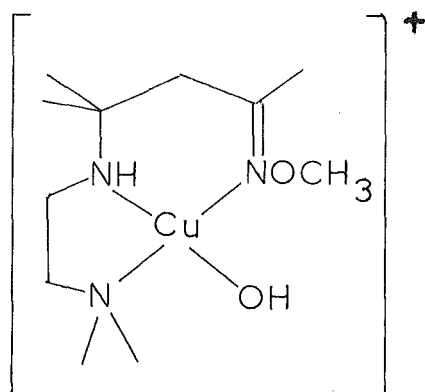
Equilibrium Constants for the Formation of some triamine Copper(II)

Hydroxo Complexes at 25°C



<u>Triamine (L)</u>	<u>Chelate Ring Sizes</u>	<u>log K_{OH}</u>
3-azapentane-1,5-diamine ^a	5,5	4.50
3-azahexane-1,6-diamine ^b	5,6	4.72
3-azaheptane-1,7-diamine ^c	5,7	4.42
4-azaheptane-1,7-diamine ^d	6,6	4.1
4-azaoctane-1,8-diamine ^a	6,7	4.48

^aData from ref. 212; I = 0.1M KCl^bData from ref. 213; I = 0.5M KNO₃^cData from ref. 206; I = 0.1M NaCl^dData from ref. 204; I = 0.1M KCl



In contrast to $\text{Cu}(\text{dnm})^{2+}$, the oximato complex $\text{Cu}(\text{dno})^+$ does not undergo (aqua) proton dissociation up to $\text{pH} = 10.4$, as determined from spectrophotometric and potentiometric measurements. This may reflect the strong donor properties of the oximato group which would reduce the positive charge on the metal centre and hence decrease its polarizing power on co-ordinated water molecules.

CHAPTER 8

METAL COMPLEXES OF THE DIAMINE DIOXIME LIGANDS

The ligands H_2dddo , $Hddmo$ and $dddm$ were studied in their reactions with the divalent metal ions of Fe, Co, Ni, Cu and Zn. Log K (potentiometric), ΔH (calorimetric) and ΔS for the formation of the copper(II) complexes of these ligands, and for the deprotonation reactions of these complexes were determined at 25°C and $I = 0.10M$ NaCl (section 8.1). The objective was to assess the contributions of hydrogen bonding and oxime deprotonation to the stability of oxime complexes.

Log K values were obtained for the complexes of H_2dddo with iron(II), nickel(II) and zinc(II), and they are compared with that for the cobalt(II) complex (as determined by Kee and Powell²¹⁴) and with the results which Hedwig and Powell¹⁸⁴ obtained for the copper(II) complexes (section 8.2). The formation constants for the cobalt(II), nickel(II) and zinc(II) complexes of $Hddmo$ were determined (section 8.3), and the formation of complexes of $dddm$ with nickel(II) and zinc(II) was studied (section 8.4).

Spectrophotometric (visible and ultraviolet) data are reported for the copper(II) and nickel(II) complexes of the tetradentate ligands and infrared data are reported for the complexes $Ni(Hdddo)(ClO_4)$ and $Zn(Hdddo)(ClO_4)$.

8.1 COPPER(II) COMPLEXES OF THE TETRADENTATE LIGANDS

8.1.1 Results

p[H⁺] Data The copper(II) complexes of $Hddmo$ were studied by titration of NaOH (0.178M) into solutions of copper dichloride and ligand dihydroperchlorate, at 25°C and $I = 0.10M$, with metal to ligand ratios of 1 : 1 and 1 : 1.5. For the 1 : 1 metal to ligand titrations, solution composi-

tions were CuCl_2 ($\sim 1 \times 10^{-3}\text{M}$), $\text{Hddmo}, 2\text{HClO}_4$ ($\sim 1 \times 10^{-3}\text{M}$), HCl ($\sim 6 \times 10^{-4}\text{M}$) and NaCl ($I = 0.10\text{M}$). For the 1 : 1.5 metal to ligand titrations typical conditions were CuCl_2 ($\sim 5 \times 10^{-4}\text{M}$), $\text{Hddmo}, 2\text{HClO}_4$ ($\sim 7.5 \times 10^{-4}\text{M}$), HCl ($\sim 5 \times 10^{-4}\text{M}$) and NaCl ($I = 0.10\text{M}$). pH-volume data from representative titrations at metal to ligand ratios of 1 : 1 and 1 : 1.5 are given in tables 8.1 and 8.2 respectively. The data for one titration are shown graphically in fig. 8.1.

The formation of the copper(II) complex of dddm was studied by titration of NaOH (0.163M) against solutions of copper dichloride ($0.97 \times 10^{-3}\text{M}$), $\text{dddm}, 2\text{HClO}_4$ ($1.0 \times 10^{-3}\text{M}$), HCl ($1 \times 10^{-3}\text{M}$) and NaCl ($I = 0.10\text{M}$) at 25°C . Typical pH-volume data are given in table 8.3 and fig. 8.1. In the alkaline ($\text{pH} > 8$) region of the titration curve the solution pH was unstable. At a pH of 9.6 the solution pH decreased at a rate of ca. 0.01 pH/minute. This appeared to result from decomposition of the complex to give $\text{Cu}(\text{OH})_2$. Data obtained above pH 8 were not used in subsequent analyses.

Calorimetric Measurements Calorimetric titrations on the copper(II)-Hddmo system were performed by titration of HCl ($\sim 1\text{M}$) against buffer solutions containing CuCl_2 ($1.4 \times 10^{-3}\text{M}$), $\text{Hddmo}, 2\text{HClO}_4$ ($1.9 \times 10^{-3}\text{M}$), NaCl ($I = 0.10\text{M}$) and NaOH (such that the initial pH was ca. 7.9). As a check on ligand purity each titration involved ligand derived from a different synthesis. Q_m -volume data from the calorimetric titrations are given in table 8.4 where Q_m is the measured heat change corrected for the heat of dilution of HCl .

For the copper(II)-dddm system calorimetric data were obtained from the titration of HCl ($\sim 1\text{M}$) against solutions of $\text{dddm}, 2\text{HClO}_4$ ($3.1 \times 10^{-3}\text{M}$), CuCl_2 ($3.0 \times 10^{-3}\text{M}$), NaCl ($I = 0.10\text{M}$) and NaOH (such that the initial pH was ca. 6). Q_m -volume data from the calorimetric titrations are presented in table 8.5.

TABLE 8.1

Representative Data from the Titration of NaOH Against Solutions of
Hddmo, 2HClO_4 and Copper Dichloride at 25°C , $I = 0.10\text{M NaCl}$

(Metal:Ligand = 1:1)

Initial Composition: $T_L = 1.049 \times 10^{-3}\text{M}$

$T_M = 9.694 \times 10^{-4}\text{M}$

$T_H = 3.777 \times 10^{-3}\text{M}$

<u>Vol</u> ^a	<u>p[H⁺]</u> ^b	<u>Vol</u> ^a	<u>p[H⁺]</u> ^b	<u>Vol</u> ^a	<u>p[H⁺]</u> ^b
0.030	3.035	0.280	3.399	0.560	4.091
0.040	3.047	0.300	3.433	0.580	4.191
0.060	3.073	0.320	3.469	0.600	4.315
0.080	3.099	0.340	3.507	0.820	6.529
0.100	3.125	0.360	3.544	0.840	6.790
0.120	3.153	0.380	3.584	0.860	7.009
0.140	3.180	0.400	3.625	0.880	7.115
0.160	3.208	0.420	3.668	0.900	7.322
0.180	3.239	0.440	3.713	0.920	7.541
0.200	3.269	0.480	3.814	0.940	7.793
0.220	3.302	0.500	3.871	0.960	8.130
0.240	3.334	0.520	3.935		
0.260	3.364	0.540	4.008		

^aVolume (ml) of 0.1779M NaOH added to 49.93 ml of solution

^bp[H⁺] derived from pH_m as outlined in section 3.1.3

TABLE 8.2

Representative Data from the Titration of NaOH Against Solutions of
Hddmo, 2HClO_4 and Copper Dichloride at 25°C , $I = 0.10\text{M NaCl}$

(Metal:Ligand = 1:1.5)

Initial Composition: $T_L = 7.521 \times 10^{-4}\text{M}$
 $T_M = 4.877 \times 10^{-4}\text{M}$
 $T_H = 2.758 \times 10^{-3}\text{M}$

<u>Vol</u> ^a	<u>p[H⁺]</u> ^b	<u>Vol</u> ^a	<u>p[H⁺]</u> ^b	<u>Vol</u> ^a	<u>p[H⁺]</u> ^b
0.03	3.162	0.18	3.470	0.35	4.034
0.04	3.178	0.19	3.496	0.51	6.474
0.05	3.196	0.20	3.523	0.52	6.619
0.06	3.214	0.22	3.577	0.53	6.754
0.08	3.251	0.24	3.632	0.54	6.886
0.10	3.281	0.25	3.662	0.55	7.016
0.11	3.303	0.26	3.692	0.56	7.145
0.12	3.332	0.27	3.724	0.57	7.278
0.13	3.354	0.28	3.755	0.58	7.415
0.14	3.376	0.30	3.823	0.59	7.566
0.15	3.399	0.31	3.861	0.60	7.743
0.16	3.420	0.33	3.943		
0.17	3.444	0.34	3.987		

^aVolume (ml) of 0.1779M NaOH added to 49.93 ml of solution

^bp[H⁺] derived from pH_m as in section 3.1.3

TABLE 8.3

Representative Data from the Titration of NaOH Against Solutions of
 dddm, 2HClO_4 and Copper Dichloride at 25°C , $I = 0.10\text{M NaCl}$

Initial Composition: $T_L = 1.034 \times 10^{-3}\text{M}$

$T_M = 9.694 \times 10^{-4}\text{M}$

$T_H = 2.541 \times 10^{-3}\text{M}$

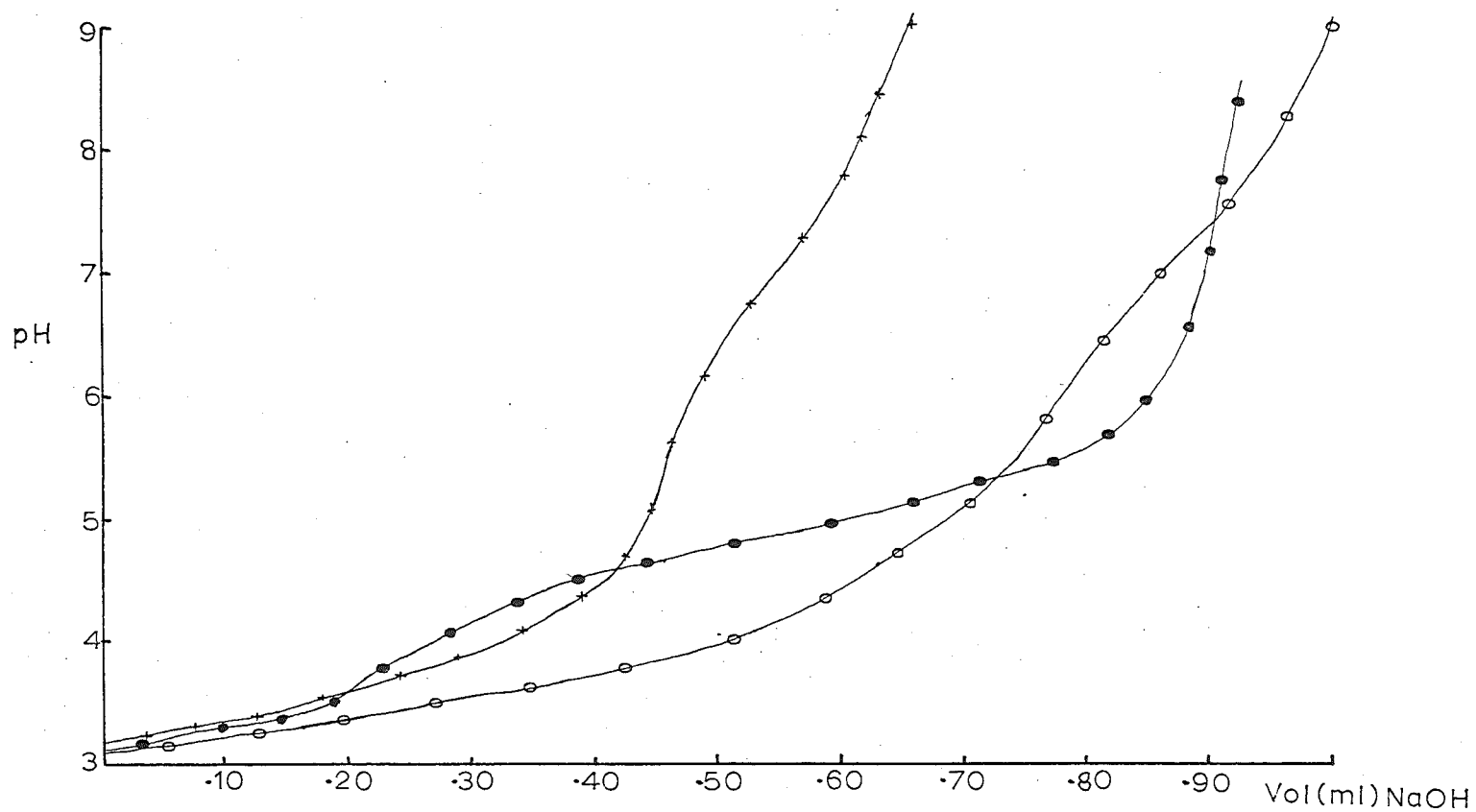
<u>Vol</u> ^a	<u>p[H⁺]</u> ^b	<u>Vol</u> ^a	<u>p[H⁺]</u> ^b	<u>Vol</u> ^a	<u>p[H⁺]</u> ^b
0.22	4.344	0.37	4.694	0.55	5.110
0.23	4.373	0.38	4.714	0.56	5.139
0.24	4.401	0.39	4.736	0.57	5.169
0.25	4.427	0.40	4.756	0.58	5.201
0.26	4.451	0.42	4.799	0.59	5.236
0.27	4.475	0.43	4.819	0.60	5.212
0.28	4.499	0.45	4.863	0.61	5.309
0.30	4.544	0.46	4.885	0.63	5.391
0.31	4.566	0.47	4.908	0.64	5.438
0.32	4.588	0.48	4.931	0.65	5.488
0.33	4.610	0.49	4.955	0.66	5.544
0.34	4.631	0.50	4.979	0.67	5.604
0.35	4.653	0.52	5.028		
0.36	4.673	0.53	5.054		

^aVolume (ml) of 0.1632M NaOH added to 49.93 ml of solution

^bp[H⁺] derived from pH_m as in section 3.1.3

Fig. 8.1

pH vs Volume for the Formation of Copper(II) Complexes of the Tetradentate Ligands



o 1:1 Hddmo; $T_L = 1.049 \times 10^{-3} M$, $T_M = 9.694 \times 10^{-4} M$, $T_H = 3.778 \times 10^{-3} M$, $[NaOH] = 0.1779 M$
 + 1:1.5 Hddmo; $T_L = 7.317 \times 10^{-4} M$, $T_M = 4.877 \times 10^{-4} M$, $T_H = 2.758 \times 10^{-3} M$, $[NaOH] = 0.1779 M$
 • dddm; $T_L = 1.002 \times 10^{-3} M$, $T_M = 9.694 \times 10^{-4} M$, $T_H = 3.011 \times 10^{-3} M$, $[NaOH] = 0.1632 M$

TABLE 8.4

Representative Calorimetric Data for the Titrations of HCl Against Buffered Solutions of Hddmo,
Copper Dichloride and NaOH, I = 0.10M NaCl

<u>Vol</u> ^a	<u>p[H⁺]</u>	<u>10⁴Δ(Hddmo)</u> ^b	<u>10⁴Δ(Hddmo,H⁺)</u> ^b	<u>10⁴Δ(Hddmo,2H⁺)</u> ^b	<u>10⁴Δ(Cu(Hddmo)²⁺)</u> ^b	<u>10⁴Δ(Cu(ddmo)⁺)</u> ^b	<u>Q_{corr}</u> ^c
(ml)		(mol)	(mol)	(mol)	(mol)	(mol)	(J)
0.02 ^d	7.830	-	-	-	-	-	-
0.18	6.762	-0.0321	-0.2242	0.2544	1.2890	-1.2890	3.8615
0.34	6.080	-0.0022	-0.4602	0.4624	1.1050	-1.1050	4.3490
0.59	3.492	-0.0002	-0.4705	1.0220	0.0006	-0.5517	4.9466
0.84	3.080	0.0000	-0.0012	0.9650	-0.9627	-0.0011	3.4821
1.09	2.786	0.0000	-0.0006	0.8162	-0.8153	-0.0003	2.5113
0.00 ^e	8.080	-	-	-	-	-	-
0.16	5.808	-0.0204	-0.2976	0.3180	1.2310	-1.2310	4.0745
0.19	4.460	-	-	-	-	-	-
0.44	3.126	0.0000	-0.0058	0.8610	-0.8483	-0.0070	3.0350

TABLE 8.4 Continued

0.00 ^f	8.170	-	-	-	-	-	-
0.16	5.816	-0.0237	-0.2787	0.3023	1.2400	-1.2410	3.9054
0.19	4.461	-	-	-	-	-	-
0.44	3.127	0.0000	-0.0055	0.8635	-0.8510	-0.0070	2.7675

^aCumulative volume (ml) of 0.984M HCl added at each titration point

^bIncrease in the number of moles of the ligand and metal-ligand species between successive titration points

^cMeasured exothermic heat change between successive titration points, corrected for heat of dilution of HCl

^dTitration 1. Initial Volume (Vol = 0.0) 99.41 ml, $T_L = 4.447 \times 10^{-3} M$, $T_M = 3.216 \times 10^{-3} M$, $T_H = 2.533 \times 10^{-3} M$

^eTitration 2. Initial Volume (Vol = 0.0) 99.10 ml, $T_L = 1.893 \times 10^{-3} M$, $T_M = 1.455 \times 10^{-3} M$, $T_H = 9.324 \times 10^{-4} M$

^fTitration 3. Initial Volume (Vol = 0.0) 99.10 ml, $T_L = 1.872 \times 10^{-3} M$, $T_M = 1.455 \times 10^{-3} M$, $T_H = 8.703 \times 10^{-4} M$

TABLE 8.5

Representative Calorimetric Data from the Titrations of HCl against Buffered Solutions of
dddm, Copper Dichloride and NaOH, I = 0.10M NaCl

<u>Vol</u> ^a	<u>p[H⁺]</u>	<u>10⁴Δ(dddm, H⁺)</u> ^b	<u>10⁴Δ(dddm, 2H⁺)</u> ^b	<u>10⁴Δ(Cu(dddm)²⁺)</u> ^b	<u>Q_{corr}</u> ^c
(ml)		(mol)	(mol)	(mol)	(J)
0.00 ^d	8.801	-	-	-	-
0.18	4.949	-0.0509	0.8950	-0.8202	4.8981
0.36	4.532	-0.0125	0.8766	-0.8698	4.7730
0.00 ^e	8.779	-	-	-	-
0.18	4.949	-0.0519	0.8978	-0.8230	4.8673
0.36	4.533	-0.0125	0.8760	-0.8690	4.9011
0.04 ^f	5.645	-	-	-	-
0.20	4.881	-0.0231	0.7867	-0.7686	4.3585
0.36	4.520	-0.0121	0.7932	-0.7862	4.2697
0.52	5.645	-0.0148	0.7782	-0.7686	4.1782

TABLE 8.5 Continued

0.00 ^g	5.645	-	-	-	-
0.16	4.881	-0.2310	0.7885	-0.7704	4.2432
0.32	4.522	-0.0120	0.7917	-0.7845	4.2647
0.48	4.166	-0.0148	0.7762	-0.7664	4.1642

^aCumulative volume (ml) of 0.984M HCl added at each titration point

^bIncrease in the number of moles of the ligand and metal-ligand species between successive titration points

^cMeasured exothermic heat change between successive titration points, corrected for heat of dilution of HCl

^dTitration 1. Initial volume (Vol = 0.0) 99.34 ml, $T_L = 3.128 \times 10^{-3} M$, $T_M = 2.995 \times 10^{-3} M$, $T_H = 9.280 \times 10^{-5} M$

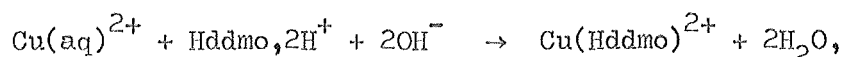
^eTitration 2. Initial volume (Vol = 0.0) 100.09 ml, $T_L = 3.104 \times 10^{-3} M$, $T_M = 2.972 \times 10^{-3} M$, $T_H = 9.360 \times 10^{-5} M$

^fTitration 3. Initial volume (Vol = 0.0) 99.34 ml, $T_L = 3.182 \times 10^{-3} M$, $T_M = 2.995 \times 10^{-3} M$, $T_H = 1.968 \times 10^{-4} M$

^gTitration 4. Initial volume (Vol = 0.0) 100.38 ml, $T_L = 3.150 \times 10^{-3} M$, $T_M = 2.964 \times 10^{-3} M$, $T_H = 5.956 \times 10^{-4} M$

Analysis of $p[H^+]$ and Calorimetric Titration Data The titration

curves for the copper(II)-Hddmo systems (figs. 8.1 and 8.2) show a buffer region at pH 3.2 - 4.7 followed by an inflexion (end point) at pH 4.9 - 6.0. The end point titre corresponds to the addition of two moles of OH^- per mole of copper(II) ions (i.e. the reaction

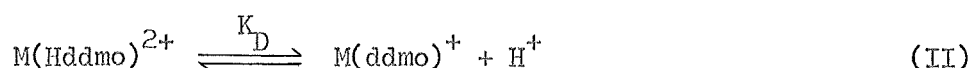
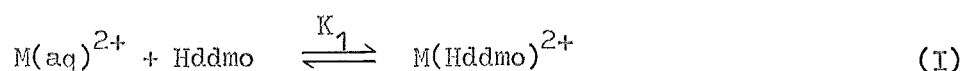


plus one mole of OH^- per mole of excess acid (HCl) present). A second buffer region at pH 6.3 - 8.0 was followed by an end point at pH 8.0 - 9.2. This end point corresponds to the further addition of one mole of OH^- per mole of copper(II) ion (i.e. the reaction



plus one mole of OH^- per mole of excess ligand ($Hddmo, 2H^+ + OH^- \rightarrow Hddmo, H^+ + H_2O$)).

Equilibrium constants were calculated for reactions (I) and (II) for the respective buffer regions.



Values of K_1 and K_D were calculated independently for each point throughout the titration by the method outlined in section 4.1.2.

For the 1 : 1 metal to ligand titration data, the derived values of K_1 and K_D showed a systematic trend in their values with extent of reaction. For example $\log K_1$ decreased from 12.02 ($\bar{n}_L = 0.2$) to 11.49 ($\bar{n}_L = 0.7$) and $\log K_D$ decreased from -7.01 (at 30% formation of the deprotonated species $Cu(ddmo)^+$) to -7.27 (at 70% formation of $Cu(ddmo)^+$).

The $\log K_1$ and $\log K_D$ values obtained from the titrations using a 1 : 1.5 ratio of metal to ligand are given in table 8.6. These $\log K$ values did not vary with the extent of reaction. The results given in table 8.6 are for 3 titrations each of ca. 30 data points for

TABLE 8.6

Thermodynamic Data for the Formation of Copper(II) Complexes of the Diamine Dioxime Ligands

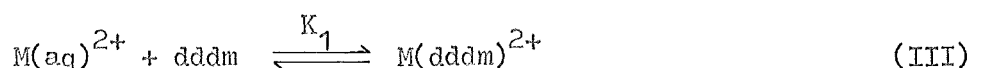
at 25°C, I = 0.10M NaCl

<u>Reaction</u>	<u>log K</u>	<u>ΔG</u> (kJ mol ⁻¹)	<u>-ΔH</u> (kJ mol ⁻¹)	<u>ΔS</u> (kJ mol ⁻¹)
$\text{Cu}^{2+} + \text{H}_2\text{dddo} \rightleftharpoons \text{Cu}(\text{H}_2\text{dddo})^{2+}$ ^a	13.24 ± 0.05	-75.6 ± 0.3	54.8 ± 0.3	70 ± 2
$\text{Cu}(\text{H}_2\text{dddo})^{2+} \rightleftharpoons \text{Cu}(\text{Hdddo})^+ + \text{H}^+$ ^a	-3.24 ± 0.08	18.5 ± 0.5	-23.7 ± 0.3	18 ± 3
$\text{Cu}^{2+} + \text{Hddmo} \rightleftharpoons \text{Cu}(\text{Hddmo})^{2+}$ ^b	12.11 ± 0.04	-69.1 ± 0.2	43.3 ± 2.0	87 ± 8
$\text{Cu}(\text{Hddmo})^{2+} \rightleftharpoons \text{Cu}(\text{ddmo})^+ + \text{H}^+$ ^b	-6.76 ± 0.09	38.6 ± 0.5	-21.9 ± 0.9	-56 ± 5
$\text{Cu}^{2+} + \text{dddm} \rightleftharpoons \text{Cu}(\text{dddm})^{2+}$ ^b	9.10 ± 0.01	-51.9 ± 0.1	17.9 ± 0.4	114 ± 2

^aData from ref. 184^bThis work

\bar{n}_L 0.25 - 0.88 (K_1) and $[Cu(ddmo)^+]/T_M$ 0.4 - 0.9 (K_D). The error values are the standard deviation for all data from 3 titrations. Hedwig¹²⁹ observed that for the formation of oximato complexes satisfactory refinement of the data was obtained only with metal to ligand ratios greater than 1 : 1.5. The effect observed at low ligand to metal ratios was attributed to the possible formation of polynuclear complexes involving a bidentate oximato group.

The titration curve for the copper(II)-dddm system (fig. 8.1) showed a single buffer region at pH 4.5 - 5.7, followed by a well-defined end point at pH 6.5 - 8.8 after the addition of two moles of OH^- per mole of copper(II) ion (plus one mole of OH^- per mole of HCl). The data from the buffer region were interpreted in terms of the single equilibrium



The value of $\log K_1$ (\pm standard deviation) for 9 titrations (each of ca. 30 data points) is given in table 8.6.

ΔH data for the formation and deprotonation of $Cu(Hddmo)^{2+}$ were obtained from 3 titrations each of between 4 and 10 data points. The $p[H^+]$ of the solution was calculated by the iterative process described in section 4.2.2; an initial estimate of the pH at each data point was obtained from a subsequent titration of the calorimeter solution with standard alkali. The solution composition was derived from the calculated $p[H^+]$ and the known values of K_1 and K_D . The values of ΔH_1 (for reaction (I)) and ΔH_D (for reaction (II)) are given in table 8.6 (mean \pm standard deviation).

For the enthalpimetric titration of $Cu(dddm)^{2+}$ the solution composition was determined by two different methods.

(1) The pH of the calorimeter solution, at each data point, was determined after completion of the calorimetric titration by back titration with

standard alkali. These pH values were used to calculate the equilibrium hydrogen ion concentrations $[H^+]$ (using the correlation curve described in section 3.1.3) and these were used to calculate the solution composition. Discrepancies (up to 20%) between the observed and calculated total metal concentrations were detected. These were attributed to the accumulation of errors associated with the additional titration against standard alkali and to slight errors in the measured pH.

(2) The $p[H^+]$ of the calorimeter solution was determined by the iterative procedure outlined in section 4.2.2, commencing from an initial estimate of the solution pH. The changes in the composition of the calorimeter solution (between successive data points) are reported in table 8.5. This method gave no significant difference between the observed and calculated total metal concentrations. The derived value for ΔH_1 , obtained from the results of these iterative calculations, is reported in table 8.6.

Ultraviolet and visible absorption spectra were recorded throughout a potentiometric titration to determine the nature and number of species present in solution. Spectrophotometric data confirmed the presence of only two copper-ligand species in the titration of copper(II) ions with $Hddmo, 2HClO_4$ and only one metal-ligand species in the $dddm, 2HClO_4$ -copper(II) ion titrations. Spectrophotometric parameters for the complexes $Cu(Hddmo)^{2+}$, $Cu(ddmo)^+$ and $Cu(dddm)^{2+}$ are shown in table 8.7 along with those determined for $Cu(H_2dddo)^{2+}$ and $Cu(Hdddo)^+$,¹⁶⁵ and that for $Cu(dddm)(ClO_4)_2$ (reflectance).

8.1.2 The Molecular Structure of $Cu(dddm)(ClO_4)_2$

The single crystal X-ray molecular structure of $Cu(dddm)(ClO_4)_2$ has been determined.¹⁸⁶ The structure consists of square pyramidal

TABLE 8.7

Spectrophotometric Data for the Copper(II) Complexes of the
Diamine Dioxime Ligands in Aqueous Solution. I = 0.10M NaCl

<u>Complex</u>	λ_{\max} (ε)	
	(nm)	(l mol ⁻¹ cm ⁻¹)
$\text{Cu}(\text{H}_2\text{dddo})^{2+}$ ^a	592(176)	277(5210)
$\text{Cu}(\text{Hdddo})^+$ ^a	583(214)	330(2800) 272(4500)
$\text{Cu}(\text{Hddmo})^{2+}$	597(188)	276(5380)
$\text{Cu}(\text{ddmo})^+$	580(223)	346(2240) -
$\text{Cu}(\text{dddm})^{2+}$	615(140)	303(3700)
$[\text{Cu}(\text{dddm})(\text{ClO}_4)]\text{ClO}_4$ ^b	552	

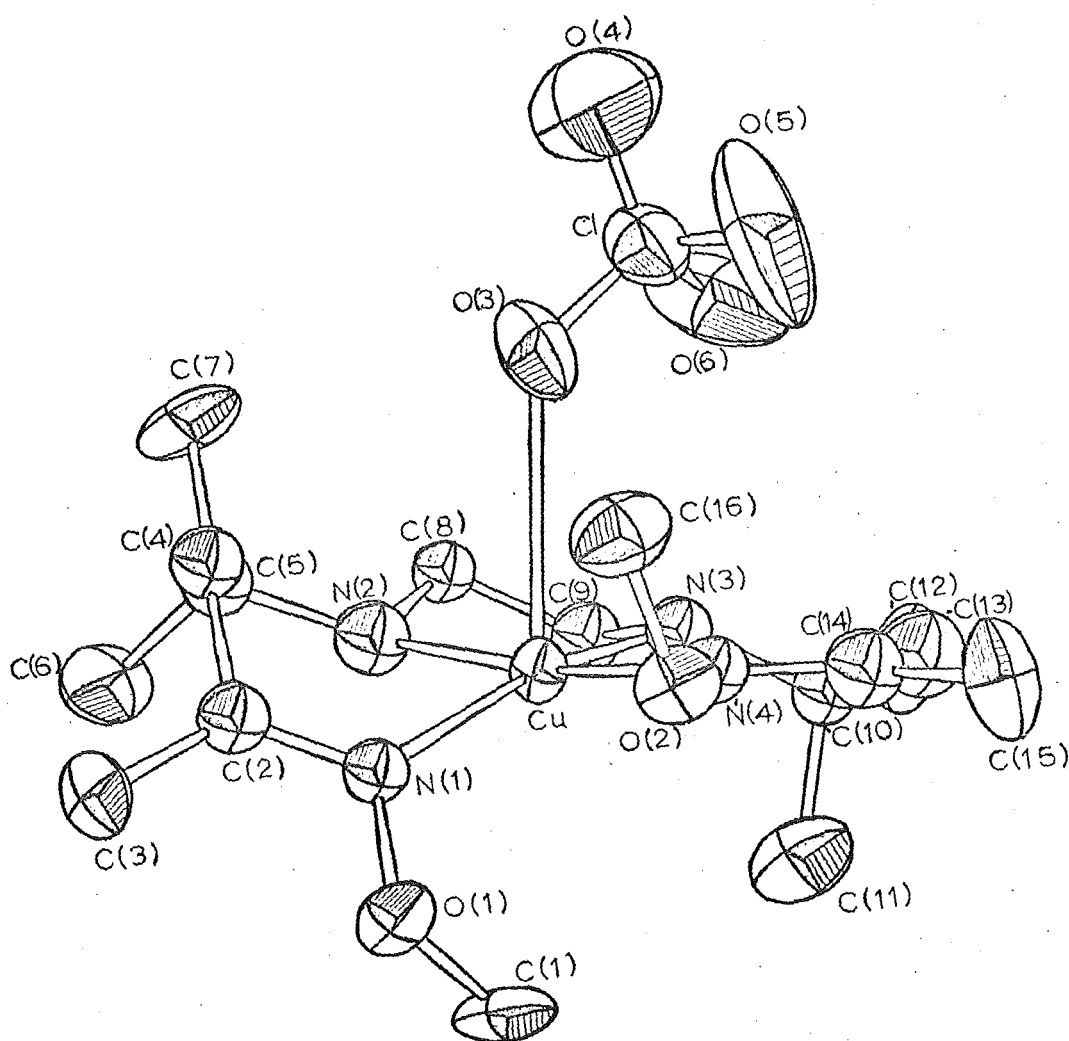
^aData from ref. 165

^bReflectance spectrum

$[\text{Cu}(\text{dddm})(\text{ClO}_4)]^+$ units (see fig. 8.2) and perchlorate anions. The ligand dddm occupies the basal plane of the square pyramid with a perchlorate group semi-coordinated^{215,216} in the apical position. Possible sources of steric interaction in this complex are between the O-methyl oxime groups, and between these and the gem-dimethyl and terminal methyl groups. The non-bonded distance C(1)-C(11) (OCH_3 -gem-dimethyl) is 4.01 Å and the distance C(15)-C(16) (OCH_3 -terminal methyl) is 3.46 Å. However these distances are approximately the same as the shortest C-C distances between adjacent cations (3.58 Å) in the structure. This suggests that the dddm ligand can adopt a configuration which does not involve significant steric interaction between the CH_3 groups of the O-methyl substituents and other CH_3 groups in the cation. Other short non-bonded distances in the cation are C(9)-C(12) (2.87 Å) and C(7)-C(8) (2.97 Å).

The structure determination also shows that the >C=N-O units are planar and that N(2) and N(4) are displaced towards the semi-coordinated perchlorate group, and N(1) and N(3) are moved away from it. This results in the angle between the planes containing the atoms C(3), C(4), C(2), N(1) and O(1) and C(13), C(15), C(14), N(4) and O(2) being 55.6°. The O(1)-O(2) distance is 3.12 Å which exceeds the sum of the van der Waals radii of two oxygen atoms (2.8 Å).²¹⁷ It is possible that the large dihedral angle between the "oxime planes" arises from a minimization of steric interaction between the atoms O(1) and O(2). In oxime complexes containing only 5-membered chelate rings the oxime groups are more readily accommodated in cis-planar positions e.g. for many glyoximates, dimethyl-, ethylmethyl- and diphenyl-glyoximates dihedral angles close to zero have been observed.^{121,218,219} The geometry about the copper atoms in $[\text{Cu}(\text{Hdddo})]_2\text{Br}_2$ is slightly distorted trigonal bipyramidal,¹⁶⁵ but the chelate rings in both diamine dioxime complexes have similar conformations despite the presence of O-methyloxime groups in $[\text{Cu}(\text{dddm})](\text{ClO}_4)_2$.

Fig. 8.2

Structure of $\text{Cu}(\text{dddm})(\text{ClO}_4)^+$ 

8.1.3 Formation of the Complexes $\text{Cu}(\text{H}_2\text{dddo})^{2+}$, $\text{Cu}(\text{Hddmo})^{2+}$ and $\text{Cu}(\text{dddm})^{2+}$

log K The conductivity of the complex $\text{Cu}(\text{dddm})(\text{ClO}_4)_2$ was measured in aqueous solution. The molar conductivity, Λ_m , is $229 \text{ cm}^2 \text{ mol}^{-1} \Omega^{-1}$ at 25°C , which corresponds to a 1 : 2 electrolyte.²²⁰ It is inferred that the complex exists as $\text{Cu}(\text{dddm})^{2+}$ ions and ClO_4^- ions in aqueous solution.

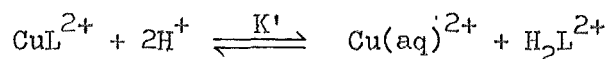
The $\log K_1$ values for the complexes $\text{Cu}(\text{H}_2\text{dddo})^{2+}$, $\text{Cu}(\text{Hddmo})^{2+}$ and $\text{Cu}(\text{dddm})^{2+}$ allow assessment of:

- (1) the effect of changing an oxime group to an O-methyloxime group, and
- (2) the effect of adding a second β -ketoxime chelate ring to the tridentate ligands Hdno and dnm (Chapter 7).

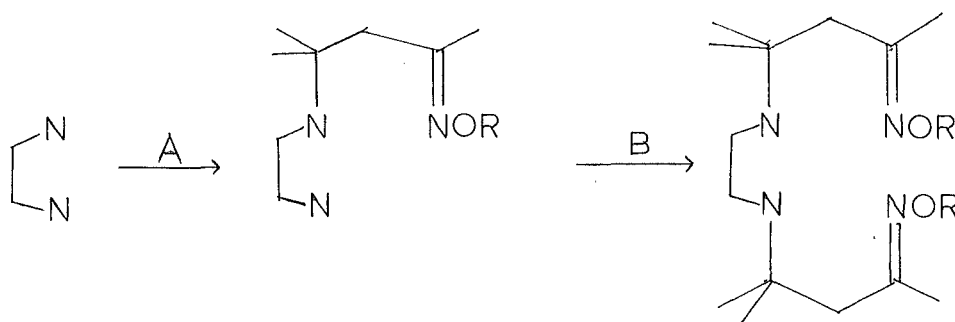
By comparing the stabilities of $\text{Cu}(\text{H}_2\text{dddo})^{2+}$ and $\text{Cu}(\text{dddm})^{2+}$, it is seen that the effect of changing two $=\text{NOH}$ groups to two $=\text{NOCH}_3$ groups is to reduce $\log K(\text{CuL})$ by 4.14. As determined in section 7.2.1 the effect of changing one $=\text{NOH}$ group to an $=\text{NOCH}_3$ group was to reduce the stability of the copper(II) complex by 2.4 log units. The effect observed for the tetradentate ligands is approximately twice that for the tridentate ligands. The conclusion drawn is that no significant steric strain is introduced by changing $=\text{NOH}$ to $=\text{NOCH}_3$ in an oxime complex.

In Chapter 7 it was established, by comparing $\text{Cu}(\text{N,N-dimethylethylenediamine})^{2+}$ and $\text{Cu}(\text{Hdno})^{2+}$, that the addition of a β -ketoxime chelate ring to a diamine co-ordinated to copper(II) increased $\log K(\text{CuL})$ by 2.9. The increase in $\log K(\text{CuL})$ on adding a β -keto-methyloxime was only 0.8 log units. By comparing the stabilities of the copper(II) complexes with the tridentate and tetradentate ligands the effect of a second additional chelate ring can be assessed. However, because the ligands have different basicities it is desirable to compare the relative stabilities of their copper(II) complexes in terms of the

equilibrium



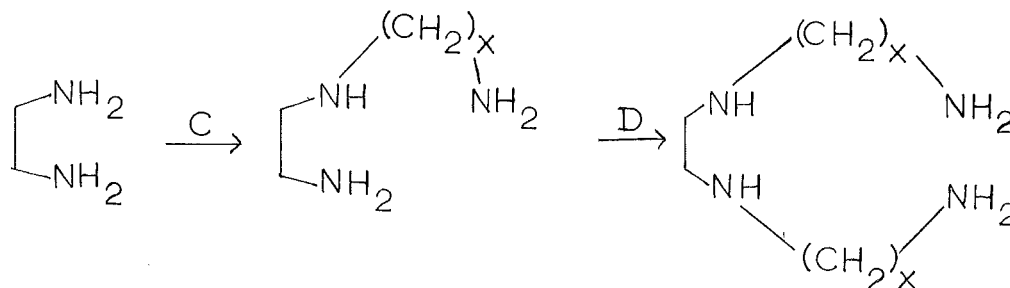
which takes this different basicity into account by considering the competition of H^+ and M^{2+} for the ligand L ^{133,206} (assuming $\log k \sim 0$ for oxime protonation). The $\log K'$ values for $\text{Cu}(\text{H}_2\text{dddo})^{2+}$, $\text{Cu}(\text{Hddmo})^{2+}$ and $\text{Cu}(\text{dddm})^{2+}$ are 2.5 ± 0.1 , 3.55 ± 0.06 and 6.43 ± 0.03 respectively, and those for $\text{Cu}(\text{Hdno})^{2+}$ and $\text{Cu}(\text{dnm})^{2+}$ are 4.20 ± 0.07 and 6.3 ± 0.1 respectively. The smallest value of $\log K'$ corresponds to the most stable chelate ring system. Comparison of the data for $\text{Cu}(\text{Hdno})^{2+}$ and $\text{Cu}(\text{H}_2\text{dddo})^{2+}$ show that a second β -ketoxime chelate ring (change B) increases the stability of the copper(II) complex ($\Delta \log K'$) by 1.7, whereas the addition of a second β -ket-O-methyloxime substituent decreases the stability ($\log K' (\text{Cu}(\text{dddm})^{2+}) - \log K' (\text{Cu}(\text{dnm})^{2+})$) by 0.1.



SCHEMATIC REPRESENTATION OF THE ADDITION OF CHELATE RINGS

In contrast, for the addition of a first β -ketoxime substituent to a diamine (change A), the stability of the copper(II) complex increases by 2.9 ($\Delta \log K'$), and, for addition of a β -ket-O-methyloxime substituent, by 0.8. In summary, the addition of a first oxime chelate ring to a co-ordinated diamine (change A) contributes a larger increase to the stability than does a second chelate ring (change B). In contrast,

for the copper(II) complexes of a variety of linear polyamines^{204,206} a second chelate ring (change D) increases the stability of the complex by approximately the same amount as the first chelate ring (change C).



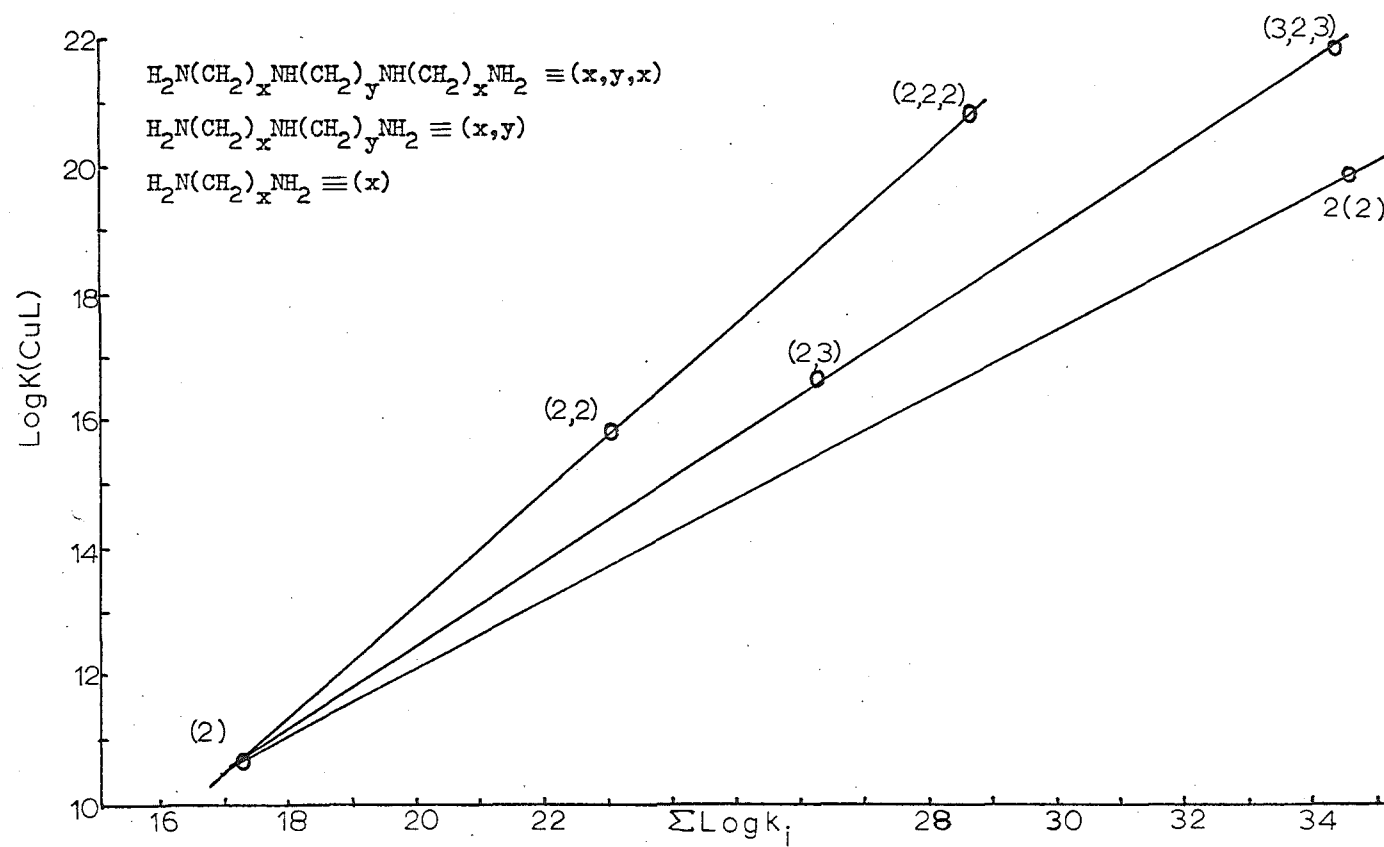
The log K(CuL) data for some polyamine chelate complexes are shown in fig. 8.3. There is a uniform increase in the stability with addition of successive chelate rings. The increase in stability will be contributed to by (1) the increase in the basicity of the ligands, and (2) the chelate effect, but will be offset by the cumulative ring strain. [Here one must consider logK(CuL) values rather than log K' values because the number of strongly basic donors is being increased.] In the complexes Cu(H₂dddo)²⁺, Cu(Hddmo)²⁺ and Cu(dddm)²⁺ the decreased contribution to the stability by the second β-ketoxime chelate rings may result from accumulated ring strain and/or the possible steric interaction between the adjacent NOR (R = H or CH₃) groups.

Interpretation of the ΔH and ΔS values. Typical values of ΔS for the co-ordination of tetra-amines to copper(II) ions are 66 - 80 J mol⁻¹ K⁻¹.^{209,221} The data for the complexes Cu(H₂dddo)²⁺ (ΔS = 70 J mol⁻¹ K⁻¹) and Cu(Hddmo)²⁺ (ΔS = 87 J mol⁻¹ K⁻¹) suggest that here also four sites in the copper co-ordination sphere are occupied by ligand donor atoms.

It is inferred from the enthalpy changes for the formation of Cu(H₂dddo)²⁺ (ΔH = -54.8 kJ mol⁻¹) and Cu(Hddmo)²⁺ (ΔH = -43.3 kJ mol⁻¹)

Fig. 8.3

Complex Stability ($\log K(\text{CuL})$) vs Ligand Basicity ($\sum \log k_i$) for the Copper(II) Complexes of Some Polyamines



that (1) the copper-oxime co-ordinate bond strength is weaker than the copper-O-methyloxime bond strength, and (2) the oxime- and O-methyloxime-copper bonds are much weaker than a copper-amine bond. For the structurally related tetra-amine 2,11-diamino-4,4,9,9-tetramethyl-5,8-diazadodecane ΔH is -104 kJ mol^{-1} .²⁰⁹ The formation of this tetra-amine copper(II) complex has an entropy change ($\Delta S = 80 \text{ J mol}^{-1} \text{ K}^{-1}$) similar to those observed for the formation of $\text{Cu}(\text{H}_2\text{dddo})^{2+}$ and $\text{Cu}(\text{Hddmo})^{2+}$, but a much higher exothermic heat of formation.

The molecular structure of $\text{Cu}(\text{dddm})(\text{ClO}_4)_2$ shows the orientations of the $-\text{OCH}_3$ groups and the gem-dimethyl groups to be such that one of the axial octahedral co-ordination sites of copper(II) is significantly shielded, and it is inferred that the higher ΔS value for the formation of $\text{Cu}(\text{dddm})^{2+}$ ($\Delta S = 114 \text{ J mol}^{-1} \text{ K}^{-1}$) relates to the desolvation of one of these co-ordination sites. This increased desolvation is also reflected in the very low value of ΔH ($-17.9 \text{ kJ mol}^{-1}$); desolvation makes an endothermic contribution to ΔH .

Spectrophotometric Data. Data from the ultraviolet and visible absorption spectra for the complexes $\text{Cu}(\text{H}_2\text{dddo})^{2+}$, $\text{Cu}(\text{Hddmo})^{2+}$ and $\text{Cu}(\text{dddm})^{2+}$ in aqueous solution are reported in table 8.7 along with the data for the reflectance spectrum of $[\text{Cu}(\text{dddm})(\text{ClO}_4)](\text{ClO}_4)$.

From the λ_{max} values for the d-d transitions it is inferred that in solution the copper(II) ion is co-ordinated by two amino nitrogen donors and two oxime nitrogen donors in each complex. The λ_{max} value for $\text{Cu}(\text{en})(\text{H}_2\text{O})_2^{2+}$ (2 amino donors, 2 oxygen donors) is 660 nm^{222} while that for $\text{Cu}(\text{en})_2$ is 550 nm^{99} . λ_{max} for $\text{Cu}(\text{dien})(\text{H}_2\text{O})^{2+}$ (3 amino donors, 1 oxygen donor) is 611 nm^{207} . Allowing for the different donor strengths of the oxime and amino functional groups it is inferred that the diamine dioxime ligands are co-ordinated to the copper atom through the 2 amino nitrogens and 2 oxime nitrogens. This deduction is supported by the molecular structure determination of $\text{Cu}(\text{dddm})(\text{ClO}_4)_2$.

From the values of λ_{\max} for the d-d transition in the diamine dioxime complexes it follows that the contribution to the ligand field splitting term by an =NOH group is greater than that for an =NOCH₃ group. For the complexes Cu(Hdno)²⁺ and Cu(dnm)²⁺ a similar observation was made; further, the oxime and O-methyloxime groups in these tridentate diamine oxime ligands each make a contribution to the ligand field splitting similar to that of a primary amino group. In contrast, in the tetradentate ligands two terminal oxime groups are seen to make a much smaller contribution to the ligand field splitting than do two primary amino groups, c.f. λ_{\max} (Cu(H₂dddo)²⁺) = 592 nm and λ_{\max} (Cu(2,11-diamino-4,4,9,9-tetramethyl-5,8-diazadodecane)) = 534 nm.²⁰⁹ [This effect is also seen by noting that addition of one oxime donor to a diamine copper(II) complex decreases λ_{\max} by ca. 90 nm (Cu(Hdno)²⁺), and adding an O-methyloxime donor decreases λ_{\max} by ca. 80 nm (Cu(dnm)²⁺) (see section 7.2.1). However, introduction of a second oxime donor group decreases λ_{\max} by a further 20 nm (Cu(H₂dddo)²⁺) while a second O-methyloxime group decreases λ_{\max} by only 4 nm (Cu(ddd_m)²⁺).

From the molecular structure determination of Cu(ddd_m)(ClO₄)⁺ it was inferred that a possible steric interaction between the oxime oxygens may have been offset by a distortion from square planar symmetry. Such a distortion would also decrease the overlap of the copper and ligand orbitals. The ligand field strength per oxime group is therefore expected to be less in the diamine dioxime complexes than that observed in the tridentate diamine oxime complexes where no steric interaction of this type occurs.

Cu(H₂dddo)²⁺, Cu(Hddmo)²⁺ and Cu(ddd_m)²⁺ show strong absorptions at 277, 276 and 303 nm respectively and these are assigned to L_O → M charge transfer transitions. Similar charge transfer transitions are observed in many copper(II) amine and amine-imine complexes.²¹¹

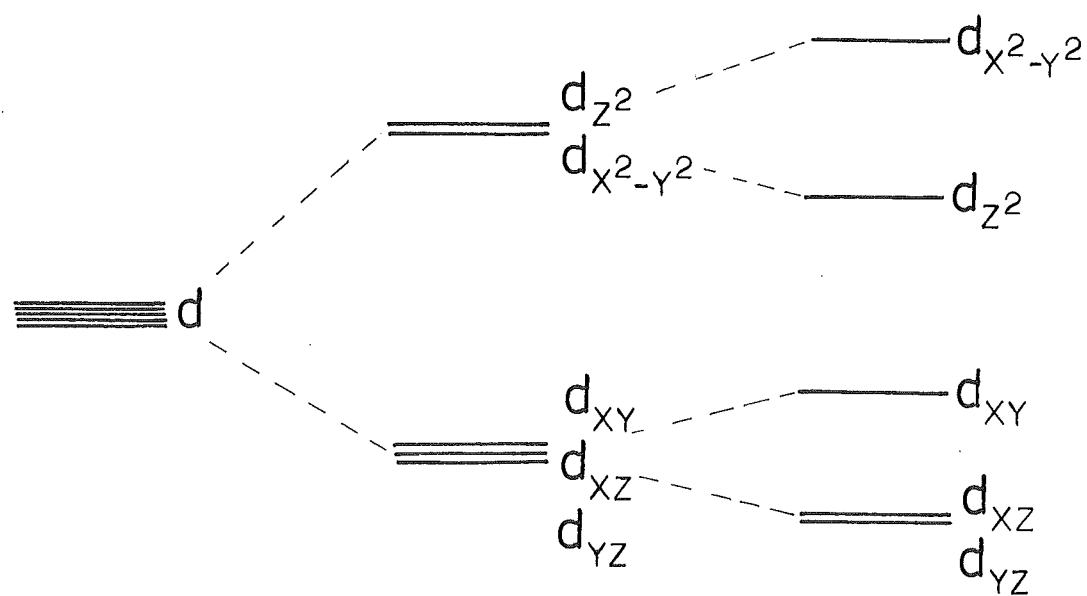
The reflectance spectrum of $[\text{Cu}(\text{dddm})(\text{ClO}_4)]\text{ClO}_4$ shows a shift of the d-d transition to higher energy (λ_{max} 552 nm) compared to the same complex in aqueous solution (λ_{max} 615 nm). The molecular structure of the cation $[\text{Cu}(\text{dddm})(\text{ClO}_4)]^+$ in the solid state shows the copper atom to be five co-ordinate, and in solution the copper atom is probably 5 co-ordinate in the cation $\text{Cu}(\text{dddm})(\text{H}_2\text{O})^{2+}$. A square pyramidal co-ordination sphere produces the metal ion energy level scheme shown in fig. 8.4. The greater ligand field splitting observed in the solid state suggests that the degree of axial distortion is greater in the solid, and therefore a water molecule in the 5th co-ordination site acts more strongly than does a perchlorate ion.

8.1.4 The Complexes $\text{Cu}(\text{Hdddo})^+$ and $\text{Cu}(\text{ddmo})^+$

The pK_a for proton dissociation from the =NOH group in H_2dddo has been determined as 12.3 ± 0.3 .¹⁶⁵ On co-ordination of this ligand to copper(II) ions the acidity of the hydroxyl proton increases, with pK_a 3.24.¹⁶⁵ It can be assumed that the pK_a of Hddmo is also 12.3. On co-ordination of Hddmo to copper(II) ions the acidity of the oxime proton again increases, with pK_a 6.76. This observation is consistent with that observed for many ligands which contain acidic protons on or near the donor atom (e.g. amines,⁸⁸ water¹⁰⁴ and hydroxylamine¹⁰⁶). On co-ordination of pyridine-2-aldoxime (HL) to copper(II) ions to give $\text{Cu}(\text{HL})_2^{2+}$, the pK_a for the oxime group decreases from 10.0 to 2.8 (for the first acid dissociation to give $\text{Cu}(\text{HL})(\text{L})^+$), and to 6.7 (for the second acid dissociation).⁸⁷ This increase in acidity was interpreted in terms of stabilization of the co-ordinated anionic oximate ligand by means of conjugation involving the metal ion. For the complexes $\text{Cu}(\text{H}_2\text{dddo})^{2+}$ and $\text{Cu}(\text{Hddmo})^{2+}$ the increased acidity results from the inductive effect of the metal ion on the oxime O-H bond. The complex $\text{Cu}(\text{Hdddo})^+$ is further stabilized by formation of an intramolecular hydrogen bond. $\text{Cu}(\text{Hdddo})^+$ did not undergo proton dissociation at

Fig. 8.4

d Orbital Energies for a Metal Ion in an Octahedral
and Square Pyramidal Field



Spherically
Symmetrical
Field

Octahedral
Field

Square
Pyramidal
Field

pH < 10,^{129,165} indicating the stabilizing effect of hydrogen bond formation.

Assuming a value of $\log k_D = -12.3$ for the reaction $\text{Hddmo} \xrightleftharpoons{k_D} \text{ddmo}^- + \text{H}^+$, the formation constant for $\text{Cu}(\text{ddmo})^+$ can be derived as $\log K^*(\text{Cu}(\text{aq})^{2+} + \text{ddmo}^- \rightleftharpoons \text{Cu}(\text{ddmo})^+) = (\log K_1 + \log K_D - \log k_D) = 17.7$. The corresponding value of $\log K^*$ derived for the formation of $\text{Cu}(\text{Hdddo})^+$ is 22.3. By comparing these values with $\log K_1$ for the complexes $\text{Cu}(\text{H}_2\text{dddo})^{2+}$ and $\text{Cu}(\text{Hddmo})^{2+}$ the contribution to the stability of the copper(II) complexes arising from deprotonation and hydrogen bond formation is assessed as 9.1 ($\log K^*(\text{Cu}(\text{Hdddo})^+) - \log K_1(\text{Cu}(\text{H}_2\text{dddo})^{2+})$) and for deprotonation in the absence of intramolecular hydrogen bonding as 5.6 ($\log K^*(\text{Cu}(\text{ddmo})^+) - \log K_1(\text{Cu}(\text{Hddmo})^{2+})$). Intramolecular hydrogen bond formation is therefore assessed as adding $10^{3.5}$ to the stability of these oxime complexes.

The stability constant data for bis-(dioxime) complexes (e.g. dimethylglyoxime) illustrate the effects of oxime deprotonation and hydrogen bond formation. These ligands do not co-ordinate to metal ions without oxime deprotonation,^{81,82} reflecting the greater donor strength of the oximate group. Secondly, the contribution of intramolecular hydrogen bonding ($10^{3.5}$ in the diamine dioxime complexes where one hydrogen bond is formed) enhances the stability of the bis-dioxime complex (where two hydrogen bonds are formed) relative to the mono-complex.

The data in table 8.6 show that the enthalpy change for deprotonation from a co-ordinated oxime group is endothermic and of similar magnitude for both $\text{Cu}(\text{H}_2\text{dddo})^{2+}$ and $\text{Cu}(\text{Hddmo})^{2+}$. These enthalpy changes are contributed to by (1) an endothermic term associated with breaking the oxime O-H bond, (2) an exothermic term associated with the formation of intra or intermolecular hydrogen bonds and with the

increased strength of the copper-ligand co-ordinate bonds, and (3) solvation terms associated with changes in secondary sphere solvation of the complex and solvation of the released proton.

The entropy change for oxime deprotonation from $\text{Cu}(\text{H}_2\text{dddo})^{2+}$ is positive (favourable) but negative for the deprotonation from $\text{Cu}(\text{Hddmo})^{2+}$. For the deprotonation from $\text{Cu}(\text{Hddmo})^{2+}$ the unfavourable entropy change may be interpreted in terms of solvent ordering effected by the oximato group hydrogen bonding to the solvent. This entropy change ($-56 \text{ J mol}^{-1} \text{ K}^{-1}$) can be compared with that for the deprotonation of a water molecule ($\Delta S = -80 \text{ J mol}^{-1} \text{ K}^{-1}$)²²³ (i.e. comparing $\text{HOH} \rightleftharpoons \text{OH}^- + \text{H}^+$ with $\text{C=NOH} \rightleftharpoons \text{C=NO}^- + \text{H}^+$). In contrast, the favourable entropy change for proton dissociation from $\text{Cu}(\text{H}_2\text{dddo})^{2+}$ results from rotation of the O-H bond about the N-O bond to give an intramolecular hydrogen bond. Hydrogen bonding to the solvent is thereby reduced. In the complex $\text{Cu}(\text{Hdddo})^+$ intramolecular hydrogen bonding is favoured over hydrogen bonding to the solvent by a positive entropy change.

Spectrophotometric Data. The ultraviolet and visible absorption spectral data for the complexes $\text{Cu}(\text{Hdddo})^+$ and $\text{Cu}(\text{ddmo})^+$ in solvent H_2O are reported in table 8.7. Deprotonation of the complexes $\text{Cu}(\text{H}_2\text{dddo})^{2+}$ and $\text{Cu}(\text{Hddmo})^{2+}$ decreases λ_{max} by 9 nm and 17 nm respectively, reflecting the greater donor strength of the oximato group. However the shift in λ_{max} is not as great as that observed upon deprotonation of $\text{Cu}(\text{Hdno})^{2+}$ (44 nm, see section 7.2.2). This may reflect the influence of steric strain between the oxime oxygen atoms in the tetradentate ligand complexes (which would reduce the overlap of the ligand and metal orbitals). This steric interaction is absent in the tridentate ligand complexes.

$\text{Cu}(\text{Hdddo})^+$ and $\text{Cu}(\text{ddmo})^+$ also show charge transfer transitions at 330 nm and 272 nm, and at 346 nm respectively. In $\text{Cu}(\text{Hdddo})^+$ the band at 272 nm has been assigned to a ligand to metal charge transfer

transition and the band at 330 nm (ϵ 2800 l mol⁻¹ cm⁻¹) to a charge transfer transition associated with the oximato group.¹⁶⁵ This band is observed to be solvent dependent. The band at 346 nm (ϵ 2240 l mol⁻¹ cm⁻¹) in the spectrum of Cu(ddmo)⁺ is assigned to a similar transition. No charge transfer transition was observed for Cu(ddmo)⁺ at ~270 nm, although these complexes absorb very strongly below 200 nm and this very strong absorption tails into the region around 270 nm.

8.2 THE METAL COMPLEXES OF H₂dddo

8.2.1 Results

The log K values for the equilibria between the ligand H₂dddo and copper(II) ions^{165,184} and cobalt(II) ions²¹⁴ have been reported. The nickel(II) and zinc(II) complexes of H₂dddo were studied by titration of NaOH (~0.2M) into solutions containing H₂dddo, 2HClO₄ (1 x 10⁻³M), the appropriate metal chloride (6.7 - 9.5 x 10⁻⁴M), HCl (5 x 10⁻⁴M) and NaCl (I = 0.10M) at 25°C. Typical pH-volume data from the nickel(II) and zinc(II) titrations are given in tables 8.8 and 8.9 respectively. The data from the titrations are shown graphically in fig. 8.5. For the nickel(II) system the pH reached a stable reading only slowly (20 - 30 minutes) following each titrant addition. A complete titration thus took 4 - 5 hours to complete (~12 data points).

The iron(II)-H₂dddo system was studied in the closed titration cell, in an oxygen free atmosphere (section 3.3), by titration of NaOH (ca. 0.3M) into solutions containing FeSO₄ (3 x 10⁻⁴M), H₂dddo, 2HClO₄ (1 x 10⁻³M), HCl (1 x 10⁻³M) and NaCl (I = 0.10M) at 25°C. Typical pH-volume data are given in table 8.10 and in fig. 8.6.

The pH-volume data for the iron(II), nickel(II) and zinc(II) systems show buffer regions at pH 5.4 - 8.4, pH 5.0 - 7.0 and pH 5.9 - 7.5 respectively, followed by end-points at pH 8.6, pH 7.5 - 9.0 and pH 7.5 - 9.0 respectively. The end point titres correspond to the completion of the reaction



(where H₂L refers to the ligand H₂dddo) plus the reaction H₂L, 2H⁺ + OH⁻ → H₂L, H⁺ + H₂O for excess ligand present.

As observed for the cobalt(II) system,²¹⁴ the experimental data could not be analysed in terms of the equilibria

TABLE 8.8

Representative Data from the Titration of NaOH Against Solutions
Containing $\text{H}_2\text{dddo}, 2\text{HClO}_4$, Nickel Dichloride and Hydrochloric Acid

at 25.0°C , $I = 0.10\text{M NaCl}$

Initial Composition: $T_L = 1.009 \times 10^{-3}\text{M}$
 $T_M = 6.667 \times 10^{-4}\text{M}$
 $T_H = 4.430 \times 10^{-3}\text{M}$

<u>Vol</u> ^a	<u>p[H⁺]</u> ^b	<u>Vol</u> ^a	<u>p[H⁺]</u> ^b
0.125	4.993	0.300	5.367
0.150	5.067	0.325	5.419
0.200	5.162	0.350	5.454
0.225	5.232	0.375	5.520
0.250	5.260	0.400	5.576
0.275	5.316	0.450	5.762

^aVolume (ml) of 0.2415M NaOH added to 49.93 ml of solution

^b $p[\text{H}^+]$ derived from pH_m as outlined in section 3.1.3

TABLE 8.9

Representative Data from the Titration of NaOH into Solutions
Containing $\text{H}_2\text{dddo}, 2\text{HClO}_4$, Zinc Dichloride, and HCl at 25.0°C ,

$I = 0.10\text{M NaCl}$

Initial Composition: $T_L = 1.024 \times 10^{-3}\text{M}$

$T_M = 6.762 \times 10^{-4}\text{M}$

$T_H = 4.488 \times 10^{-3}\text{M}$

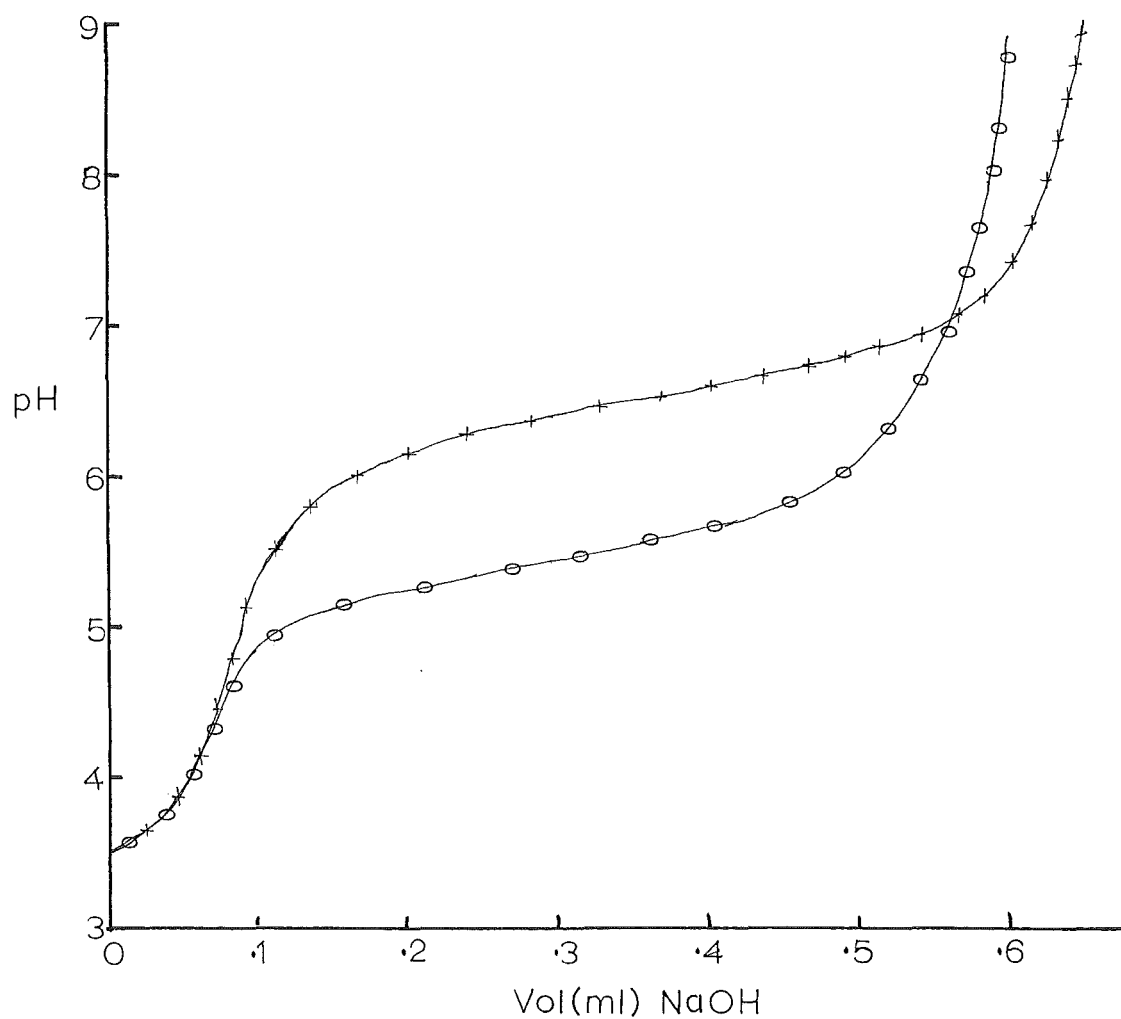
<u>Vol</u> ^a	<u>p[H⁺]</u> ^b	<u>Vol</u> ^a	<u>p[H⁺]</u> ^b
0.250	6.230	0.700	9.390
0.275	6.288	0.750	9.729
0.300	6.338	0.800	9.983
0.350	6.438	0.850	10.218
0.375	6.486	0.900	10.404
0.400	6.536	0.950	10.564
0.425	6.585	1.000	10.690
0.450	6.639		
0.475	6.701		

^aVolume (ml) of 0.2248M NaOH added to 49.93 ml of solution

^b $p[\text{H}^+]$ derived from pH_m as outlined in section 3.1.3

Fig. 8.5

pH vs Volume for the Titration of NaOH into
Solutions containing MCl_2 ($M = Zn$ or Ni) and
 $H_2C_2O_4 \cdot 2HClO_4$ at $25^\circ C$ and $I = 0.10M$ NaCl



○ Ni^{2+} ; $T_L = 1.009 \times 10^{-3}M$, $T_M = 6.667 \times 10^{-4}M$, $T_H = 4.430 \times 10^{-3}M$,

$[NaOH] = 0.2415M$

+ Zn^{2+} ; $T_L = 1.024 \times 10^{-3}M$, $T_M = 6.762 \times 10^{-4}M$, $T_H = 4.488 \times 10^{-3}M$,

$[NaOH] = 0.2248M$

TABLE 8.10

Representative Data from the Titration of NaOH into Solutions of
Iron(II) sulphate, H_2SO_4 , 2HClO_4 and HCl at 25.0°C and $I = 0.10\text{M NaCl}$

Initial Composition: $T_L = 8.446 \times 10^{-4}\text{M}$

$T_M = 2.940 \times 10^{-4}\text{M}$

$T_H = 4.329 \times 10^{-3}\text{M}$

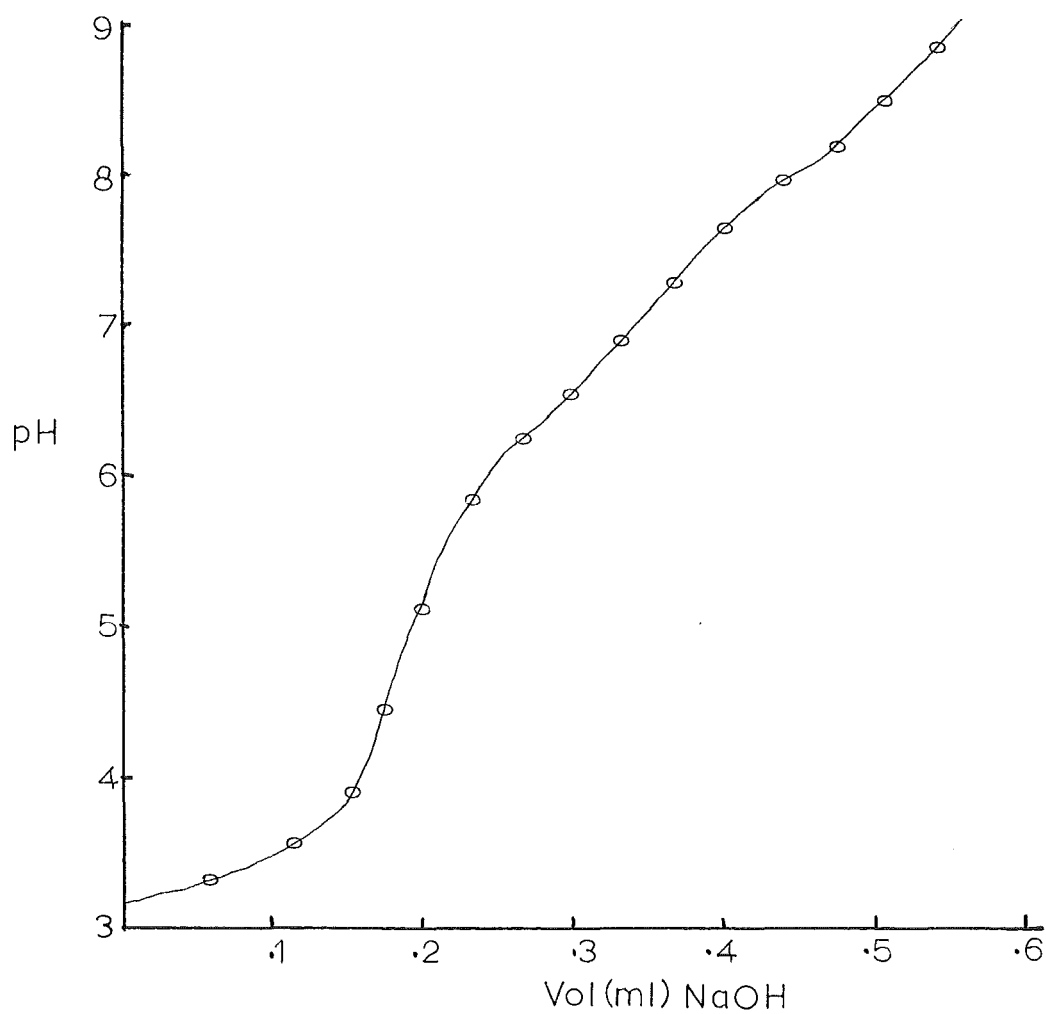
<u>Vol</u> ^a	<u>p[H⁺]</u> ^b
0.410	7.689
0.430	7.839
0.450	8.034
0.470	8.109
0.490	8.260
0.510	8.452
0.530	8.688

^aVolume (ml) of 0.2829M NaOH added to 64.0 ml. of solution

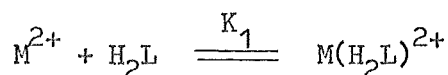
^bp[H⁺] derived from pH_m as outlined in section 3.1.3

Fig. 8.6

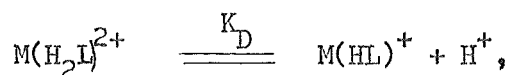
pH vs Volume for the Titration of NaOH into a
 Solution Containing FeSO_4 and $\text{H}_2\text{C}_2\text{O}_4 \cdot 2\text{HClO}_4$ at
 25°C and $I = 0.10\text{M NaCl}$



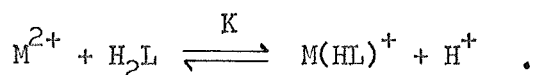
$$T_L = 8.446 \times 10^{-4} \text{M}, T_M = 2.940 \times 10^{-4} \text{M}, T_H = 4.329 \times 10^{-3} \text{M}, [\text{NaOH}] = 0.2829 \text{M}$$



and

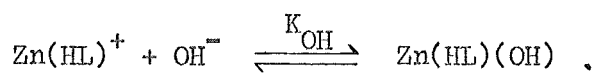


but was best analysed in terms of the concerted reaction



The results given in table 8.11 for the complexes of iron(II), nickel(II) and zinc(II) are the mean values of $\log K$ (\pm standard deviation) for 2 titrations (each of ca. 8 data points), 7 titrations (each of ca. 8 data points) and 8 titrations (each of ca. 20 data points) respectively.

The zinc(II) complex was observed to lose a proton in a buffer region at $pH > 9.2$. The data in this region were analysed in terms of the equilibrium reaction



The value of $\log K_{OH}$ was derived from the experimental data by the method outlined in section 4.1.2 and is given in table 8.11 (mean \pm standard deviation) for 4 titrations.

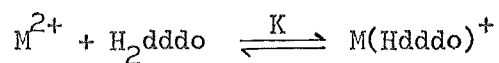
Spectrophotometric data recorded throughout a nickel(II)- H_2dddo titration confirmed the formation of only one metal-ligand species in the buffer region $pH\ 5.0 - 7.0$. (Spectrophotometric data for $Ni(Hdddo)^+$: λ_{max} 478 nm, ϵ 258 $l\ mol^{-1}\ cm^{-1}$; λ_{max} 298 nm, ϵ 3000 $l\ mol^{-1}\ cm^{-1}$). The complex $Ni(Hdddo)(ClO_4)(H_2O)$ prepared under slightly alkaline conditions (see section 3.7.2) showed the same spectrophotometric properties on dissolution in water.

8.2.2 Discussion

The ligand H_2dddo co-ordinates to the metal ions iron(II), cobalt(II), nickel(II) and zinc(II) in the oxime-oximato form; the species $M(H_2dddo)^{2+}$ was not detected in solution. This contrasts with the

TABLE 8.11

Thermodynamic Data for the Equilibrium



for the Metal Ions Iron(II), Cobalt(II), Nickel(II),
Copper(II) and Zinc(II) at 25°C and I = 0.10M NaCl

<u>Metal Ion</u>	<u>log K</u>
Fe ²⁺ a	-3.51 ± 0.07
Co ²⁺ b	-0.58 ± 0.06
Ni ²⁺ a	2.85 ± 0.12
Cu ²⁺ c	10.00 ± 0.13
Zn ²⁺ a	-0.31 ± 0.03

^aThis work

^bDatum from ref. 214

^cDatum from ref. 165

co-ordination of H_2dddo to copper(II) ions where two metal-ligand species are formed in the pH range 2.0 - 5.0,¹⁶⁵ viz. $Cu(H_2dddo)^{2+}$ followed by $Cu(Hdddo)^+$. The complex $Cu(H_2dddo)^{2+}$ represents more than 20% of the total metal concentration between pH 2.6 and 3.8 with a maximum concentration of 46% of the total metal at pH 3.1. Co-ordination of H_2dddo to copper(II) ions lowers the pK_a for the oxime group from 12.3 to 3.24.¹⁶⁵ Co-ordination to the metal ions iron(II), cobalt(II), nickel(II) and zinc(II) occurs only at a pH > 5 (i.e. above the pH for proton dissociation in the case of $Cu(H_2dddo)^{2+}$) and it is observed that ligand co-ordination and oxime deprotonation occur in one step.

Using the value -12.3 for $\log k_D$ ($H_2dddo \rightleftharpoons Hdddo^- + H^+$)¹⁶⁵ the formation constants for the complexes can be derived as

$$\log K^*(M^{2+} + Hdddo^- \rightleftharpoons M(Hdddo)^+) = \log K - \log k_D.$$

Values of $\log K^*$ are given for the divalent metal ions Fe, Co, Ni, Cu and Zn in table 8.12. The stability order $Fe < Co < Ni < Cu > Zn$ is observed, viz. the Irving-Williams stability order.²²⁴ Data for the same metal ions forming mono(glycinato) complexes⁷⁹ and mono- and bis-(ethylenediamine) complexes⁷⁹ are shown in fig. 8.7. These data show that zinc(II) complexes are generally of similar stability to the cobalt(II) complexes. The $\log K^*$ data for the dioxime complexes also show this.

The cobalt(II)²¹⁴ and zinc(II) complexes of $Hdddo^-$ form hydroxy species, $M(Hdddo)(OH)$. The value of $\log K_{OH}$ observed for the cobalt(II) complex (3.32) is similar to those observed for other cobalt(II) hydroxy complexes,²¹⁴ while $\log K_{OH}$ for the formation of $Zn(Hdddo)(OH)^+$ (3.87) is similar to those observed for other zinc(II) complexes (e.g. for $ZnL(OH)$, $L = N,N$ -bis(2-aminoethyl)glycinate, $\log K_{OH} = 4.1$ ²²⁵ and $L = 3$ -azahexane-1,6-diamine, $\log K_{OH} = 4.4$ ²¹³).

The slow rate with which nickel(II) ions and H_2dddo achieve equilibrium is related to the mechanism by which the ligand replaces

TABLE 8.12

Log K^* data^a ($M^{2+} + L^- \rightleftharpoons ML^+$; $L^- = Hdddo^-$ or $dddm^-$)

<u>M^{2+}</u>	<u>$\log K^* (M(Hdddo)^+)$</u>	<u>$\log K^* (M(ddmo)^+)$</u>
Fe	8.8 ± 0.1	-
Co	11.7 ± 0.1^b	9.3 ± 0.3
Ni	15.2 ± 0.1	10.7 ± 0.2
Cu	23.3 ± 0.1^c	17.7 ± 0.1
Zn	12.0 ± 0.1	-

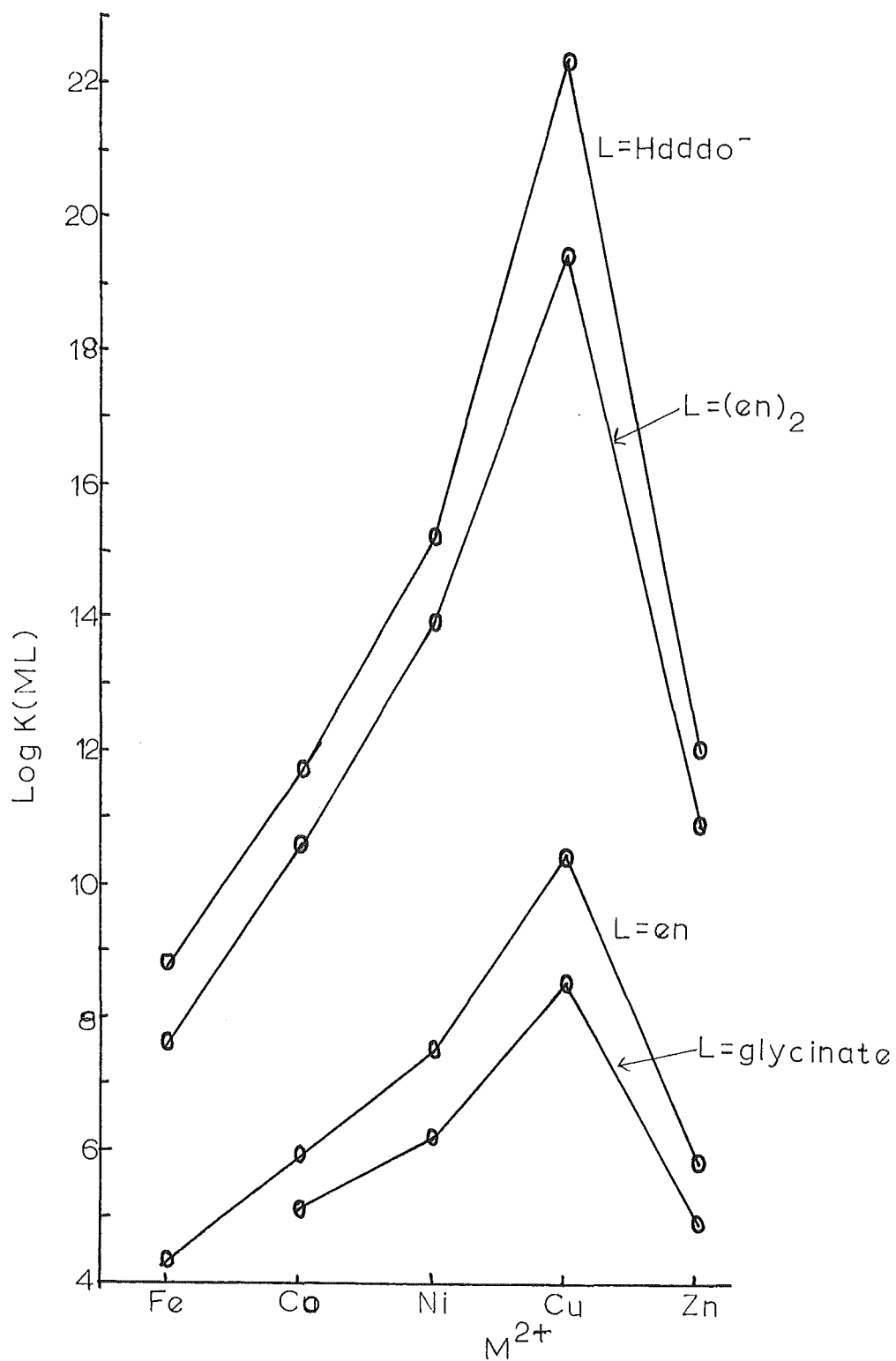
^aSee text

^bData derived from ref. 214

^cData derived from ref. 165

Fig. 8.7

Stability Constants for the Fe^{2+} , Co^{2+} , Ni^{2+} , Cu^{2+} and Zn^{2+} Complexes of Selected Ligands



the co-ordinated water molecules. The mechanism of ligand replacement is thought to be a dissociative one.^{226,227} The rate controlling step is the breaking of the $\text{Ni}^{2+} - \text{OH}_2$ bond and the accompanying formation of the 5-coordinate transition state. In nickel(II) systems the formation of this transition state is accompanied by a greater loss in ligand field stabilization energy than for other divalent metal ions (Mn-Zn).

8.2.3 The Complexes $\text{Ni}(\text{Hdddo})(\text{ClO}_4)_4 \cdot \text{H}_2\text{O}$ and $\text{Zn}(\text{Hdddo})\text{ClO}_4$

The complexes $\text{Ni}(\text{H}_2\text{dddo})(\text{ClO}_4)_2$ (red) and $\text{Ni}(\text{Hdddo})\text{ClO}_4$ (green) have been prepared by Fraser.²²⁸ Both these complexes were isolated from non-aqueous solution. In this work the hydrated complex $\text{Ni}(\text{Hdddo})(\text{ClO}_4)_4 \cdot \text{H}_2\text{O}$ (orange) has been isolated from aqueous solution at $\text{pH} > 7$. In aqueous solution λ_{max} for this complex is at 478 nm indicating a diamagnetic square planar structure. Infrared absorptions are reported in table 8.13. In contrast to green $\text{Ni}(\text{Hdddo})\text{ClO}_4$, the orange hydrate of this complex shows infrared absorptions at 3580 (sharp) and 3350 cm^{-1} . These are assigned to $\nu(\text{O-H})$ of an oxime group and $\nu(\text{O-H})$ of lattice water respectively. Absorptions at $2800 - 2300 \text{ cm}^{-1}$ and at $1700 - 1500 \text{ cm}^{-1}$, which occur for many oxime and dioxime complexes, have been assigned to $\nu(\text{O}---\text{H-O})$ and $\delta(\text{O}---\text{H-O})$ vibrations respectively.^{114,165} These absorptions are absent in the hydrated $\text{Ni}(\text{Hdddo})\text{ClO}_4 \cdot \text{H}_2\text{O}$ complex. It is inferred that no oxime-oximato hydrogen bonding exists in the solid state and that the water is perhaps associated with the oximato group rather than co-ordinated to the metal ion in an axial octahedral position. This result suggests that for hydrogen bonding to occur in an oxime-oximato complex in the solid state the oximato group must be present in a hydrophobic environment. The single crystal X-ray structure analysis of $\text{Ni}(\text{Hdmg})_2$ ⁷⁸ shows that adjacent square planar units in the solid state are staggered at 90° to each other; each oxime-oximato hydrogen bridge has two hydro-

TABLE 8.13

Infrared Absorptions (cm^{-1}) for the Complexes
 $\text{Ni}(\text{Hdddo})\text{ClO}_4$, $\text{Ni}(\text{Hdddo})\text{ClO}_4 \cdot \text{H}_2\text{O}$ and $\text{Zn}(\text{Hdddo})\text{ClO}_4$

	<u>$\text{Ni}(\text{Hdddo})\text{ClO}_4^{\text{a}}$</u>	<u>$\text{Ni}(\text{Hdddo})\text{ClO}_4 \cdot \text{H}_2\text{O}$</u>	<u>$\text{Zn}(\text{Hdddo})\text{ClO}_4$</u>
$\nu(\text{O-H})$	-	3580^{b} , 3350^{c}	-
$\nu(\text{N-H})$	3255	3200, 3140	3275, 3250
$\nu(\text{O-H} \cdots \text{O})$	2755 - 2600	-	2800 - 2600
$\nu(\text{C=N})$	1670	1630	1680, 1630
$\delta(\text{O-H} \cdots \text{O})$	1520	-	1530

^aData from ref. 228

^bSharp; $\nu(\text{NO-H})$

^cBroad; $\nu(\text{HO-H})$

phobic methyl substituents above and below it.

$[\text{Zn}(\text{Hdddo})](\text{ClO}_4)_4$ shows absorptions in the infrared at $2600 - 2800 \text{ cm}^{-1}$ and at 1530 cm^{-1} indicating the presence of hydrogen bonding in the solid state.

The visible and ultraviolet spectral data for the complex $\text{Ni}(\text{Hdddo})^+$ in aqueous solution yields some information on the nature of the charge transfer transitions in these dioxime complexes. The relative energy order of the d orbitals in a series of divalent transition metal ions can be ascertained from the values of the third ionization potentials, which establish the d orbital energy order to be $\text{Mn} > \text{Fe} > \text{Co} > \text{Ni} > \text{Cu}$. If the observed charge transfer transition in oximato complexes is from a low-lying ligand orbital to the higher energy metal orbitals ($\text{L} \rightarrow \text{M}$) then the $\text{L} \rightarrow \text{Cu}$ transition will occur at lower energy than the $\text{L} \rightarrow \text{Ni}$ transition. If the charge transfer involves a transition from a metal orbital to a higher energy ligand orbital ($\text{M} \rightarrow \text{L}(\pi^*)$) then the $\text{Cu} \rightarrow \text{L}$ transition will be at higher energy than the $\text{Ni} \rightarrow \text{L}$ transition. The charge transfer transition observed in $\text{Cu}(\text{Hdddo})^+$ at 272 nm ($\epsilon 4500 \text{ l mol}^{-1} \text{ cm}^{-1}$) ($\text{L}_\sigma(\text{amino}) \rightarrow \text{M}$) is shifted to below 200 nm in the nickel(II) complex. This confirms that the band arises from a $\text{L} \rightarrow \text{M}$ transition. The oximato charge transfer absorption occurs at 330 nm ($\epsilon 2800 \text{ l mol}^{-1} \text{ cm}^{-1}$) and at 298 nm ($\epsilon 3000 \text{ l mol}^{-1} \text{ cm}^{-1}$) in $\text{Cu}(\text{Hdddo})^+$ and $\text{Ni}(\text{Hdddo})^+$ respectively. The absorption for the nickel(II) complex is at higher energy and the transition is therefore assigned to a $\text{L}(\text{oximato}) \rightarrow \text{M}$ transition. This assignment is supported by the spectrophotometric data for $\text{Cu}(\text{Hdddo})^+$ obtained in a variety of solvents, as reported by Fraser et al.¹⁶⁵ The absorption is at highest energy in strongly hydrogen bonding solvents (e.g. H_2O). This observation is interpreted in terms of a stabilization of the oximato group by hydrogen bonding; the charge transfer $\text{L} \rightarrow \text{M}$ increases in energy with stabilization of the oximato orbitals.

8.3 THE METAL COMPLEXES OF Hddmo

8.3.1 Results

The log K data have been determined for the complexes with cobalt(II), nickel(II), copper(II) and zinc(II) ions. The cobalt(II) system was studied by titration of NaOH (0.29M) into solutions containing Hddmo, 2HClO_4 ($6.6 \times 10^{-4}\text{M}$), CoCl_2 ($5 \times 10^{-4}\text{M}$) and NaCl ($I = 0.10\text{M}$) at 25.0°C in the air-tight cell described in section 3.3.1. Before the commencement of a titration the solutions of CoCl_2 and Hddmo, 2HClO_4 were flushed with oxygen-free nitrogen gas until the concentration of dissolved oxygen was <0.05 ppm. A stream of oxygen-free nitrogen was blown across the top of the test solution throughout the titration. The solution oxygen concentration, as determined by the polarographic oxygen sensor, did not differ significantly from 0.0 ppm throughout a titration. Typical pH-volume data are reported in table 8.14. These pH-volume data are shown graphically in fig. 8.8. Titrated solutions ($\text{pH} > 9$) rapidly change colour from near colourless to deep amber (typical of oxygenated cobalt(II) complexes²¹⁴) on exposure to the atmosphere.

Oxygenation of the cobalt complex was studied by titration of CoCl_2 (0.3M) into air-saturated solutions of Hdddo ($6.9 \times 10^{-4}\text{M}$), NaOH (such that the pH was ~ 6.2 and ~ 8.1 , corresponding to the start of the first and second buffer regions respectively) and NaCl ($I = 0.10\text{M}$) at 25°C . These results showed a partial uptake of oxygen at each pH (see table 8.15); however the oxygen adduct formed was non-labile. On addition of edta to a solution ($\text{pH} \sim 9$) of the oxygen adduct no colour change was detected. Edta forms a stable cobalt(II) complex which is not oxygen sensitive up to pH 11.6.²¹⁴ On addition of HCl to pH ~ 1 only 50% of the oxygen taken up during the titration at pH 6.2 was released after 30 minutes, while, after acidification, no increase in oxygen concentration was detected after 30 minutes for the oxygenation

TABLE 8.14

Representative Data from Titrations of NaOH into Solutions Containing
Hddmo, 2HClO_4 , cobalt dichloride and HCl at 25.0°C and $I = 0.10\text{M NaCl}$

Initial Composition: $T_L = 6.098 \times 10^{-4}\text{M}$

$T_M = 4.983 \times 10^{-4}\text{M}$

$T_H = 1.829 \times 10^{-3}\text{M}$

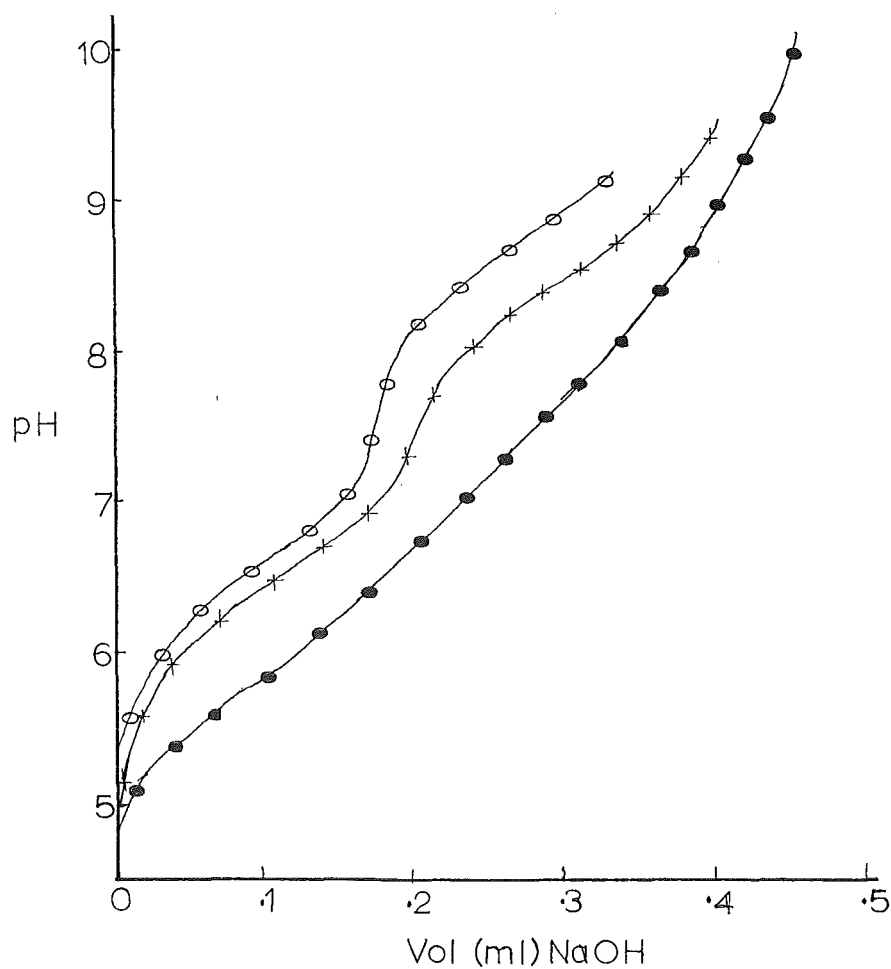
<u>Vol</u> ^a	<u>p[H⁺]</u> ^b	<u>Vol</u> ^a	<u>p[H⁺]</u> ^b
0.08	6.399	0.20	8.107
0.09	6.460	0.21	8.221
0.10	6.534	0.22	8.310
0.11	6.595	0.23	8.382
0.12	6.660	0.24	8.450
0.13	6.729	0.25	8.519
0.14	6.807	0.26	8.587
0.15	6.911	0.27	8.651
0.16	7.050	0.28	8.718
0.17	7.262	0.29	8.790
0.18	7.600	0.30	8.865
0.19	7.920	0.31	8.951

^aVolume (ml) of 0.2857M NaOH added to 60.0 ml of solution

^bp[H⁺] derived from pH_m as in section 3.1.3

Fig. 8.8

pH vs Volume for the Titration of NaOH into Solutions
Containing a 1:1.5 ratio of MCl_2 ($M = Co, Ni$ and Zn)
and Hddmo, $2HClO_4$ at $25^\circ C$ and $I = 0.10M$ NaCl



○ Co^{2+} ; $T_L = 6.098 \times 10^{-4} M$, $T_M = 4.983 \times 10^{-4} M$, $T_H = 1.829 \times 10^{-3} M$, $[NaOH] = 0.2857 M$

● Ni^{2+} ; $T_L = 9.181 \times 10^{-4} M$, $T_M = 6.637 \times 10^{-4} M$, $T_H = 2.754 \times 10^{-3} M$, $[NaOH] = 0.2829 M$

+ Zn^{2+} ; $T_L = 8.443 \times 10^{-4} M$, $T_M = 5.002 \times 10^{-4} M$, $T_H = 2.533 \times 10^{-3} M$, $[NaOH] = 0.2829 M$

TABLE 8.15

Representative Data from the Titrations of Cobalt Dichloride into
Air-Saturated Solutions of Hddmo, 2HClO_4 at 25°C and $I = 0.10\text{M NaCl}$

<u>Vol</u> ^a	<u>Initial pH_m</u> ^b	<u>Final pH_m</u> ^c	<u>$\Delta[\text{O}_2]$</u> ^d
0.015 ^e	8.170	7.405	0.20
0.030	7.842	7.170	0.95
0.030	8.000	7.801	0.50
0.025	7.801	7.654	0.15
0.30 ^f	6.629	6.566	0.08
0.30	6.636	6.562	0.14
0.30	6.613	6.550	0.16

^aVolume increment (ml) of CoCl_2 (0.299M) added to 63.0 ml of
solution

^bpH (measured) before volume increment

^cpH (measured) after volume increment

^dDecrease in solution oxygen concentration (p.p.m.) on adding
 CoCl_2 titrant increment

^eTitration 1; $T_L = 6.682 \times 10^{-4}\text{M}$

^fTitration 2; $T_L = 6.577 \times 10^{-4}\text{M}$

titration performed at pH 8.1. The cobalt(II) concentration of a solution that had been oxygenated at pH ~ 10 and acidified to pH ~ 1 was determined (as $\text{Co}(\text{NCS})_4^{2-}$ in 50% acetone) after 24 hours at pH ~ 1 . This determination showed a 98% recovery of the initial concentration of cobalt(II) ions. Spectrophotometric measurements performed immediately prior to the determination of the cobalt(II) concentration indicated that only 50% of the oxygen adduct had decomposed. These two results do not agree but may indicate that the thiocyanate or acetone aids the decomposition of the oxygen adduct.

The nickel(II) system was studied by titration of NaOH (0.28M) into solutions containing Hddmo, 2HClO_4 ($1 \times 10^{-3}\text{M}$), NiCl_2 ($6.6 \times 10^{-4}\text{M}$) and NaCl ($I = 0.10\text{M}$) at 25.0°C . Typical pH-volume data from a titration are shown in table 8.16 and graphically in fig. 8.8. As observed for the formation of $\text{Ni}(\text{Hdddo})^+$ (section 8.2.1) the system reached equilibrium only slowly after each titrant addition (20 - 30 minutes).

The zinc(II) system was studied at metal to ligand ratios of 1 : 1.5 and 1 : 4. The 1 : 1.5 (M:L) titration data were obtained from the titration of NaOH ($\sim 0.29\text{M}$) into solutions containing Hddmo, 2HClO_4 ($\sim 7.5 \times 10^{-4}\text{M}$), ZnCl_2 ($5.0 \times 10^{-4}\text{M}$) and NaCl ($I = 0.10\text{M}$) at 25°C . Typical pH-volume data are tabulated in table 8.17 and are shown graphically in fig. 8.8. At the completion of a titration (pH ~ 9) there was some $\text{Zn}(\text{OH})_2$ precipitate. The zinc(II)-Hddmo system was therefore studied with a metal to ligand ratio of 1 : 4. Typical pH-volume data are given in table 8.18 and graphically in fig. 8.9.

The pH-volume data from the cobalt(II), nickel(II) and zinc(II) (M:L = 1 : 1.5) systems show buffer regions at pH 6.1 - 7.1, pH 5.7 - 7.3 and pH 6.2 - 7.4 respectively, followed by end points at pH 7.2 - 7.9, pH ~ 9.4 and pH 7.4 - 7.9 respectively. There was a second buffer region in the cobalt and zinc systems at pH > 8.3 and pH > 8.0 respectively. In these two systems the end point corresponded to the completion of the reaction

TABLE 8.16

Representative data from the Titrations of NaOH into Solutions of
Nickel Dichloride, Hddmo, 2HClO_4 and HCl at 25.0°C and $I = 0.10\text{M NaCl}$

Initial Composition: $T_L = 9.181 \times 10^{-4}\text{M}$

$T_M = 6.637 \times 10^{-4}\text{M}$

$T_H = 2.754 \times 10^{-3}\text{M}$

<u>Vol</u> ^a	<u>p[H⁺]</u> ^b	<u>Vol</u> ^a	<u>p[H⁺]</u> ^b
0.09	5.687	0.29	7.578
0.11	5.773	0.31	7.783
0.13	5.972	0.33	7.992
0.15	6.179	0.35	8.213
0.17	6.360	0.37	8.455
0.19	6.549		
0.21	6.740		
0.23	6.939		
0.25	7.153		
0.27	7.383		

^aVolume (ml) of 0.2829M NaOH added to 49.93 ml of solution

^bp[H⁺] derived from pH_m as outlined in section 3.1.3

TABLE 8.17

Representative Data from the Titration of NaOH into Solutions Containing
Zinc Dichloride, Hddmo, 2HClO_4 and HCl at 25.0°C and $I = 0.10\text{M NaCl}$

Initial Composition: $T_L = 8.443 \times 10^{-4}\text{M}$

$T_M = 5.002 \times 10^{-4}\text{M}$

$T_H = 2.533 \times 10^{-3}\text{M}$

<u>Vol</u> ^a	<u>p[H⁺]</u> ^b	<u>Vol</u> ^a	<u>p[H⁺]</u> ^b	<u>Vol</u> ^a	<u>p[H⁺]</u> ^b
0.08	6.251	0.18	6.993	0.28	8.253
0.09	6.325	0.19	7.148	0.29	8.317
0.10	6.396	0.20	7.365	0.30	8.384
0.11	6.458	0.21	7.572	0.31	8.458
0.12	6.523	0.22	7.752	0.32	8.532
0.13	6.585	0.23	7.887	0.33	8.627
0.14	6.651	0.24	8.008		
0.15	6.725	0.25	8.074		
0.16	6.800	0.26	8.133		
0.17	6.882	0.27	8.191		

^aVolume (ml) of 0.2829M NaOH added to 49.93 ml of solution

^bp[H⁺] derived from pH_m as outlined in section 3.1.3

TABLE 8.18

Representative Data from the Titration of NaOH into Solutions Containing
Zinc Dichloride, Hddmo, 2HClO_4 and HCl at 25.0°C and $I = 0.10\text{M NaCl}$

(Ligand to metal ratio 4:1)

Initial Composition: $T_L = 2.216 \times 10^{-3}\text{M}$

$T_M = 5.001 \times 10^{-4}\text{M}$

$T_H = 6.647 \times 10^{-3}\text{M}$

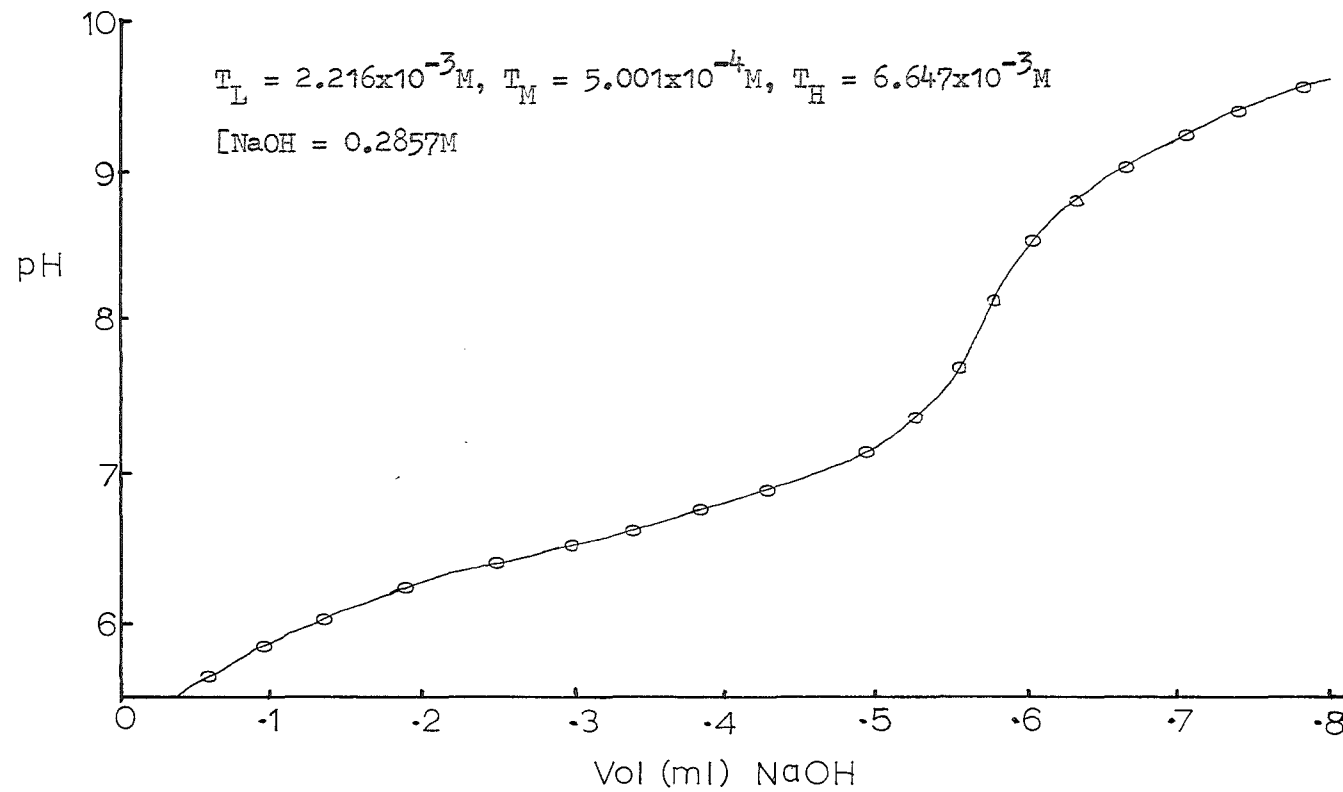
<u>Vol</u> ^a	<u>p[H⁺]</u> ^b	<u>Vol</u> ^a	<u>p[H⁺]</u> ^b	<u>Vol</u> ^a	<u>p[H⁺]</u> ^b
0.22	6.243	0.44	6.851	0.62	8.639
0.25	6.323	0.45	6.886	0.63	8.728
0.27	6.376	0.46	6.924	0.64	8.805
0.30	6.452	0.47	6.971	0.65	8.871
0.32	6.503	0.48	7.019	0.66	8.932
0.34	6.554	0.49	7.070	0.67	8.993
0.36	6.604	0.50	7.126	0.68	9.051
0.38	6.662	0.51	7.185	0.69	9.104
0.40	6.717	0.52	7.263	0.70	9.153
0.41	6.747	0.53	7.353	0.72	9.249
0.42	6.780	0.60	8.420	0.74	9.342
0.43	6.815	0.61	8.532		

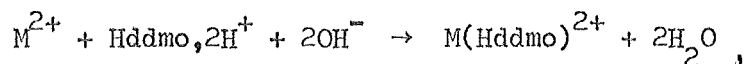
^aVolume (ml) of 0.2857M NaOH added to 49.93 ml of solution

^bp[H⁺] derived from pH_m as outlined in section 3.1.3

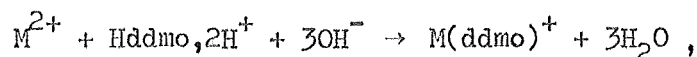
Fig. 8.9

pH vs Volume for the Titration of NaOH into a Solution Containing a 1:4 ratio of ZnCl_4
and $\text{Hddmo}, 2\text{HClO}_4$ at 25°C and $I = 0.10\text{M NaCl}$



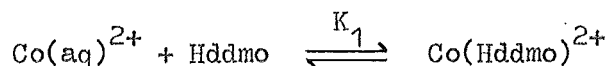


plus the reaction $\text{Hddmo}, 2\text{H}^+ + \text{OH}^- \rightarrow \text{Hddmo}, \text{H}^+ + \text{H}_2\text{O}$ for excess ligand present. In the nickel system the end point corresponded to the completion of the reaction

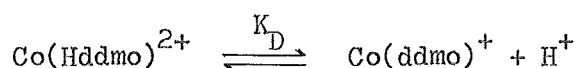


plus the reaction $\text{Hddmo}, 2\text{H}^+ + 2\text{OH}^- \rightarrow \text{Hddmo} + 2\text{H}_2\text{O}$ for excess ligand present.

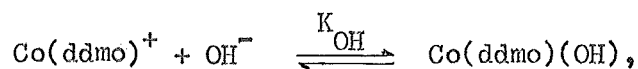
The cobalt(II)-Hddmo data corresponding to the two buffer regions were initially analysed in terms of the respective equilibria



and

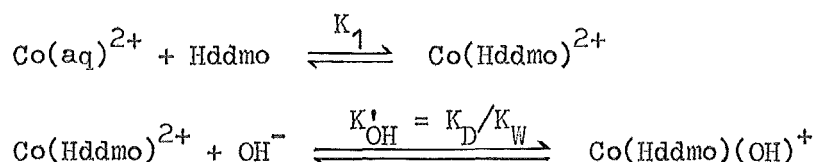


by the least squares method outlined in section 4.1.2. The data from two titrations gave $\log K_1 = 5.56 \pm 0.12$ and $\log K_D = -8.92 \pm 0.09$ with R factors of ca. 3.1%, when the function $\sum((T_H - [\text{H}^+])_{\text{obs}} - (T_H - [\text{H}^+])_{\text{calc}})^2$ was minimised over all data points. When the third equilibrium,

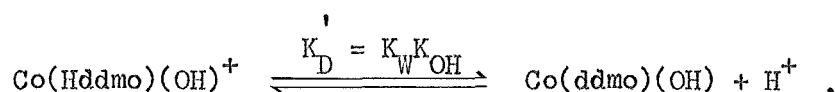


was considered as a contributor to the second buffer region the data gave results $\log K_1 = 5.73 \pm 0.12$, $\log K_D = -9.33 \pm 0.18$ and $\log K_{\text{OH}} = 5.09 \pm 0.23$ with R factors of ca. 2.5% and a better fit of the experimental data to the calculated results in the second buffer region. It was inferred from the Hamilton test¹⁷⁷ that at a level of significance 0.01 the reduction in the value of R was significant and consequently the 3 equilibrium model system was accepted. Complexes with weak donors form hydroxy species at lower pH than those with strong donors (c.f. $\text{Co(H}_2\text{O)}_6^{2+}$, $\log K_{\text{OH}} = 4.2$ ²²⁹ and $\text{Co(Hdddo)(H}_2\text{O)}_2$, $\log K_{\text{OH}} = 3.32$ ²¹⁴).

It is therefore likely that Co(Hddmo)^{2+} will form an hydroxy species at lower pH than Co(ddmo)^+ . The computer analysis cannot however distinguish between the species Co(Hddmo)(OH)^+ and Co(ddmo)^+ as both complexes contain the same number of ionizable protons. The complexes formed in aqueous solution may therefore correspond to the equilibria



and



The values tabulated in table 8.19 are the mean values (\pm standard deviation) derived for $\log K_1$, $\log K'_{\text{OH}}$ and $\log K'_D$.

The nickel(II)-Hddmo system was analysed in terms of equilibria (I) and (II) (p.182) for the single buffer region, $\text{pH} < 9.3$. The values of $\log K_1$ and $\log K_D$ given in table 8.19 are the mean values (\pm standard deviation) from 2 titrations. R values of ca. 4.5% were achieved.

Visible and ultraviolet absorption spectra were recorded throughout a titration. These showed maxima for Ni(ddmo)^+ at 476 nm (ϵ 237 $\text{l mol}^{-1} \text{cm}^{-1}$) and 309 nm (ϵ 2530 $\text{l mol}^{-1} \text{cm}^{-1}$). The species Ni(Hddmo)^{2+} did not contribute measurably to the observed spectrum, suggesting that the co-ordination about the nickel atom is pseudo-octahedral with two water molecules co-ordinated in the axial sites. Such high spin complexes have low molar extinction coefficients (generally $< 10 \text{ l mol}^{-1} \text{cm}^{-1}$).²³⁰

The zinc(II)-Hddmo data determined at a metal to ligand ratio of 1 : 1.5 were analysed in terms of equilibria (I) and (II) for the respective buffer regions. The results obtained from 3 titrations gave $\log K_1 = 5.54 \pm 0.12$ and $\log K_D = -8.22 \pm 0.08$. However at $\text{pH} > 8$ the calculated $[\text{Zn}^{2+}]$ (using the derived values of K_1 and K_D) is such

TABLE 8.19

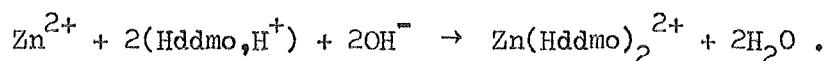
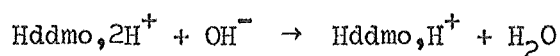
Equilibrium Constants for the Reactions of Hddmo with the Divalent
Metal Ions of Cobalt, Nickel, Copper and Zinc

<u>Metal Ion</u>	<u>log K₁</u>	<u>log K₂</u>	<u>log K_D</u>	<u>log K_{OH}</u>
Co ²⁺	5.73 ± 0.12	-	-8.73 ± 0.23	4.41 ± 0.18
Ni ²⁺	6.64 ± 0.10	-	-8.16 ± 0.10	-
Cu ²⁺	12.11 ± 0.04	-	-6.76 ± 0.09	-
Zn ²⁺	5.34 ± 0.03	5.89 ± 0.07	-9.19 ± 0.06 ^a	-

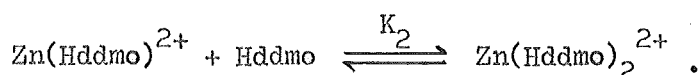
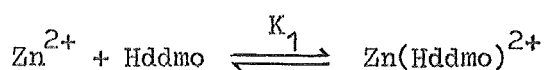
^aRefers to reaction of the bis complex.

that the solubility product for $\text{Zn}(\text{OH})_2$ ($2 \times 10^{-16} \text{ M}^3$)²³¹ is exceeded. The value of $\log K_D$ is therefore in error.

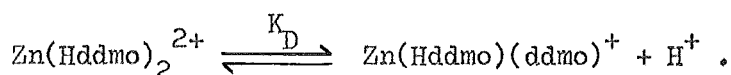
The titrations performed at a metal to ligand ratio of 1 : 4 showed a buffer region at pH 5.8 - 7.5 followed by an end point at pH 7.6 - 8.1. A second buffer region was observed at pH > 8.3. The first end point corresponded to the addition of one mole of OH^- per mole of ligand plus two moles of OH^- per mole of metal ion. This may correspond to the formation of a bis complex i.e.



Analysis of the titration data from the first buffer region was therefore made in terms of the equilibria



The values of $\log K_1$ and $\log K_2$ (\pm standard deviation) for two titrations are reported in table 8.19. The same results were obtained irrespective of whether the function $\Sigma(T_H - [\text{H}^+])_{\text{obs}} - (T_H - [\text{H}^+])_{\text{calc}})^2$ or $\Sigma(\bar{n}_{L,\text{obs}} - \bar{n}_{L,\text{calc}})^2$ was minimised, but the R factors obtained for the $T_H - [\text{H}^+]$ and \bar{n}_L functions were ca. 0.049% and 0.45% respectively. The pH-volume data obtained from pH > 8.4 were analysed in terms of the equilibrium



The value of $\log K_D$ (\pm standard deviation) is given in table 8.19.

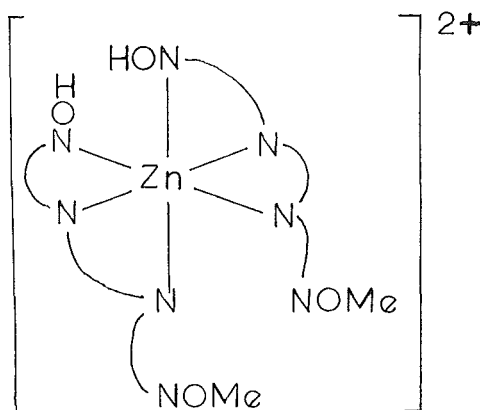
8.3.2 Discussion

Hddmo forms 1 : 1 complexes with the divalent metal ions of cobalt, nickel and copper. The d-d transition for $\text{Ni}(\text{ddmo})^+$ (λ_{max} 476 nm;

ϵ 237 l mol⁻¹ cm⁻¹) suggests that this complex is square planar and of low spin. It is inferred that in solution the complexes $M(\text{ddmo})^+$ ($M = \text{Co}, \text{Ni}$ and Cu) are square planar. The data from the zinc system having a metal to ligand ratio of 1 : 4, were best interpreted in terms of a complex of the form $\text{Zn}(\text{Hddmo})_2^{2+}$. However, the formation of a bis complex did not adequately explain the titration curve at a metal to ligand ratio of 1 : 1.5.

For the zinc(II)-Hddmo system the value of K_2 is greater than K_1 . This is contrary to that observed for the formation of many other bis complexes. However the stereochemistry of many d^{10} complexes is observed to change with increasing ligand substitution. This often leads to "anomalous" stability orders. The results observed in this study suggest that a change in stereochemistry has occurred from tetrahedral ($\text{Zn}(\text{Hddmo})^{2+}$) to octahedral ($\text{Zn}(\text{Hddmo})_2^{2+}$).

Proton dissociation was observed to occur from the complex $\text{Zn}(\text{Hddmo})_2^{2+}$. This suggests (assuming the deprotonation occurs from an oxime group) that the oxime groups are co-ordinated to the zinc(II) ion. The most likely structure of the complex is with the ligands co-ordinated through two amino nitrogens and one oxime nitrogen:



Deprotonation could then give rise to a complex with intramolecular hydrogen bonding.

The stability constants for the formation of the 1 : 1 complexes of the metal ions cobalt(II), nickel(II), copper(II) and zinc(II) are observed to follow that predicted from crystal-field stabilization energies and ionic radii viz. the Irving-Williams series ($\text{Mn} < \text{Fe} < \text{Co} < \text{Ni} < \text{Cu} > \text{Zn}$).

Comparison of the $\log K_D$ values shows that the acidity of the oxime proton is enhanced by divalent transition metal ions in the order $\text{Cu} > \text{Ni} > \text{Co} (> \text{Zn})$. (Note, however, that deprotonation from $\text{Zn}(\text{Hddmo})_2^{2+}$ may involve intramolecular hydrogen bonding). This trend is similar to that observed for deprotonation from co-ordinated water molecules in aqua ions (see table 8.20). However the values of pK_a given in table 8.20 must be treated with caution as (1) the hydroxy ions have a tendency to form polynuclear species,^{229,232} and (2) in the study of these equilibria the degree of formation of the hydroxy complex was small (e.g. in the determination of the equilibrium constant for $2\text{Cu}^{2+} + 2\text{H}_2\text{O} \rightleftharpoons \text{Cu}_2(\text{OH})_2^{2+} + 2\text{H}^+$, \bar{n}_{OH} (the average number of OH^- ions per metal ion) was only 0.03 - 0.24).²³³

The stability constants for the oximate complexes, $\log K^*$ ($\text{M}(\text{ddmo})^+$) can be derived by assuming $\log k_D (\text{Hddmo} \rightleftharpoons \text{ddmo}^- + \text{H}^+) = -12.3$.¹⁶⁵ $\log K^*$ values are given in table 8.12. These results show the order of stabilities to be $\text{Cu} > \text{Ni} > \text{Co}$. On comparison of the $\log K^*$ ($\text{M}(\text{ddmo})^+$) values with those obtained for the formation of $\text{M}(\text{Hdddo})^+$ it is seen that the ligand Hdddo^- forms more stable complexes than does ddmo^- . The observed difference between $\log K^* (\text{M}(\text{Hdddo})^+)$ and $\log K^* (\text{M}(\text{ddmo})^+)$ for any metal ion can be attributed to the weaker donor strength of the $=\text{NOCH}_3$ group compared to the $=\text{NOH}$ group and to the loss of intramolecular hydrogen bonding in the $\text{M}(\text{ddmo})^+$ complexes.

The contribution that deprotonation of the oxime group makes to the stability of the metal complexes can be assessed by comparing the stabilities of $\text{M}(\text{Hddmo})^{2+}$ ($\log K_1$) and $\text{M}(\text{ddmo})^+$ ($\log K^*$). This contribu-

TABLE 8.20

$\log K_D(M(H_2O)_n^{2+} \rightleftharpoons M(H_2O)_{n-1}(OH)^+ + H^+)$ Data for the Metal Ions
Iron, Cobalt, Nickel, Copper and Zinc(II).^a

<u>M²⁺</u>	<u>log K_D</u>
Fe ²⁺	-6.74
Co ²⁺	-9.85
Ni ²⁺	-9.86
Cu ²⁺	-8.0
Zn ²⁺	-8.96

^aData from ref. 229

tion is 3.6, 4.1 and 5.6 for the cobalt, nickel and copper complexes respectively. This compares with a value of 6.4 obtained for the copper(II) complexes of Hdno.

Oxygenation of the Cobalt Complex. The data in table 8.15 show that at pH 6.6 and pH 8.1 the uptake of oxygen was incomplete, but at pH 10.0 the oxygen uptake was quantitative with the formation of a complex of stoichiometry $(\text{CoL})_2(\text{O}_2)$. The addition of hydrochloric acid to the test solutions only slowly released the co-ordinated oxygen. The complex was therefore non-labile and a detailed study of the oxygenation reaction was not carried out. The incomplete oxygenation of the cobalt complex at pH 8.5, but complete oxygenation at pH 10, suggests that the complex undergoing oxygenation is $\text{Co}(\text{ddmo})(\text{OH})$ or that the adduct is hydroxy bridged. The absorption spectrum of oxygenated solutions showed an absorption maximum at 510 nm (ϵ 390 $\text{l mol}^{-1} \text{cm}^{-1}$) and this is in the range reported for stable peroxo complexes of the type $[\text{X}(\text{cyclam})\text{CoO}_2\text{Co}(\text{cyclam})\text{X}]$ where X and O_2 are trans and cyclam is 1,4,8,11-tetraazacyclotetradecane.²³⁴

The absorption spectrum also shows a shoulder at 340 nm. This band is very weak ($\epsilon \sim 40 \text{ l mol}^{-1} \text{cm}^{-1}$). It has been reported^{235,236,237} that labile mono-bridged dioxygen complexes show two intense (ϵ 6 - 10,000 $\text{l mol}^{-1} \text{cm}^{-1}$)²³⁸ charge transfer bands, one at ~ 300 nm and the other at ~ 330 nm. Dibridged complexes (μ -dioxygen, μ -hydroxo) show a single absorption at ~ 350 nm. Absorptions of this intensity are not observed in the oxygen adduct reported here.

Cobalt(II) ions form many complexes which react with oxygen to form 1 : 1 and 1 : 2 oxygen adducts. E.s.r. studies have established that on co-ordination of the oxygen molecule there is an electron transfer from the cobalt atom to the oxygen molecule. Because of this electron transfer co-ordination of strong electron donors enhances oxygenation. It has been suggested that a minimum of three nitrogen

donors co-ordinated to the cobalt is required before oxygenation takes place.²³⁸ Ligands such as OH^- co-ordinated in the fifth co-ordination site are well known to enhance oxygenation.^{239,240} The results obtained for the oxygenation of $\text{Co}(\text{ddmo})(\text{OH})$ differ from those reported for the complex $\text{Co}(\text{Hdmg})_2$ ²⁴¹ and many amine and amino acid complexes.^{236,238} The latter complexes are labile and often the oxygenation step can be reversed several times. For the complex with H_2dddo , Kee and Powell²¹⁴ report similar results to those obtained in this study. The complex $\text{Co}(\text{Hdddo})(\text{OH})$ forms an adduct $\text{Co}(\text{LH})-\text{O}_2-\text{Co}(\text{LH})$. In the cobalt(II) complexes of Hdddo^- and ddmo^- oxygenation does not appear to occur unless an hydroxyl group is co-ordinated to the cobalt ion.

8.4 THE METAL COMPLEXES OF dddm

8.4.1 Results

The stability constant for the formation of $\text{Cu}(\text{dddm})^{2+}$ is reported in section 8.1. Titrations of NaOH into solutions of dddm, 2HClO_4 and nickel dichloride (with metal to ligand ratio 1 : 10) gave a precipitate of $\text{Ni}(\text{OH})_2$ at $\text{pH} > 8.5$. [The solubility product of $\text{Ni}(\text{OH})_2$ is reported as $1 \times 10^{-16} \text{M}^3$ ⁷⁹ and it is exceeded at $\text{pH} 8.8$ with a $[\text{Ni}^{2+}] = 5 \times 10^{-4} \text{M}$]. Titration of NaOH into solutions containing ZnCl_2 and dddm, 2HClO_4 produced a precipitate of $\text{Zn}(\text{OH})_2$ at $\text{pH} > 7.7$. The solubility product of $\text{Zn}(\text{OH})_2$ ($\text{pK}_{\text{sp}} = 15.7 - 16.9$)^{231,242} is exceeded at approximately this pH with a $[\text{Zn}^{2+}] = 5 \times 10^{-4} \text{M}$.

8.4.2 Discussion

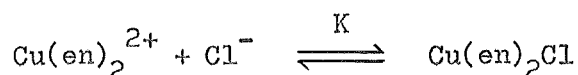
For both nickel(II) and zinc(II) no complex formation with dddm was detected. Higher concentrations of ligand could not be used because of the low solubility of dddm, 2HClO_4 . A maximum value for $\log K_1$ ($\text{M}^{2+} + \text{dddm} \xrightleftharpoons{K_1} \text{M}(\text{dddm})^{2+}$) can be assessed if the degree of complex formation is assumed to be 10% at the pH where precipitation of $\text{M}(\text{OH})_2$

occurs. These maximum values are determined as $\log K_1 (\text{Ni}(\text{dddm})^{2+}) = 2.5$ and $\log K_1 (\text{Zn}(\text{dddm})^{2+}) = 3$. These results reflect the low donor strength of the $=\text{NOCH}_3$ group.

A nickel complex of stoichiometry $\text{Ni}(\text{dddm})\cdot\text{Ni}(\text{OH})_2(\text{ClO}_4)_2$ was isolated from dry ethanol (see section 3.7.4). This complex decomposed in water. This observation supports those made above concerning the stability of the nickel(II) complex.

8.5 THE INFLUENCE OF 0.1M NaCl ON THE METAL-LIGAND EQUILIBRIA

The measured equilibrium constants in this study will be influenced by the formation of weak complexes with the anion of the "inert" electrolyte. Values of K_1 and K_2 for the formation of $\text{CuCl}(\text{aq})^+$ and $\text{CuCl}_2(\text{aq})^{2+}$ have been reported as 2.3 and 0.72 respectively in 1M HClO_4 solution.²⁴³ Assuming that these values also hold in 0.1M NaCl solution, then the copper(II) chloro species do not exceed 20% of the total metal ion concentration at the start of a titration. Data have recently been reported for the formation of halide complexes with $\text{Cu}(\text{en})_2^{2+}$.²⁴⁴ For the equilibrium



K has been reported as ca. 0.5.

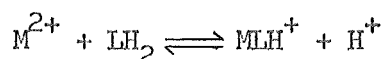
Values for the formation of zinc(II) chloro species have also been reported.²⁴⁵ The formation constants of ZnCl^+ , ZnCl_2 and ZnCl_3^- in 3M NaClO_4 are 0.65, 0.38 and 5.6 respectively. It is assessed that the total concentration of zinc chloro species does not exceed 6% of the total metal concentration in the titrations performed with $I = 0.10\text{M NaCl}$.

The effect of these constants on the equilibria studied here has not been taken into account in the calculations. This approach is valid so long as comparisons for a given metal ion involve measurements for the same ionic medium. However, for comparisons involving ligand systems with different metal ions a small variable contribution will result from the formation of metal chloro species.

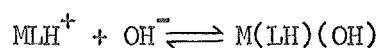
APPENDIX

COMPUTER PROGRAMS USED IN THIS STUDY.

- A. Subroutines PRELIM and CALC used to calculate protonation constants for the ligands.
- B. Subroutines PRELIM and CALC used in the least squares program to determine the equilibrium constants for the formation of mono and bis ligand complexes (\bar{n}_L method).
- C. Subroutines PRELIM and CALC used in the least squares program for the calculation of the equilibrium constants for the formation of the species $M(LH_2)$, $M(LH)$ and $M(LH)(OH)$.
- D. Program to calculate equilibrium constants for the formation of $M(LH_2)$ and $M(LH)$ in well-separated buffer regions.
- E. Program to calculate equilibrium constants for the equilibria



and



in well separated buffer regions.

- F. Subroutines PRELIM (to calculate changes in solution composition) and CALC (to calculate Q_{calc}) used in the least squares calculation of the enthalpy changes for ligand protonation.
- G. Program to calculate changes in the calorimeter solution composition from an estimate of the pH for titration of acid into a solution containing the species $M(LH)^+$ and $M(LH_2)^{2+}$.

55
56
57
58
59
60

A

```

7
8      SUBROUTINE PRELIM(YO,X,NO)
9      DIMENSION YO(60),X(2,60)
10     READ(5,40) ANADH,VOL,TLI
11     WRITE(6,42)
12     DO 2 I=1,NO
13     X(1,I)=(X(1,I)-0.086)/0.9953
14     H=10.0**(-X(1,I))
15     TL=TLI*VOL/(VOL+YO(I))
16     ACID=2.0*TL-ANADH*YO(I)/(VOL+YO(I))
17     HYDROL=1.637E-14/H
18     TH=ACID+HYDROL-H
19     WRITE(6,41)ACID,HYDROL
20     Y0(I)=TH/TL
21     40 FORMAT(F10.4,F10.2,E10.4)
22     41 FORMAT(E10.4,5X,E10.4)
23     42 FORMAT('0 ACID          HYDROL')
24     RETURN
25     END

```

```

1
2
3      SUBROUTINE CALC(X,P,I,Y)
4      DIMENSION X(2,60),P(2)
5      H=10.0**(-X(1,I))
6      Y=(P(1)*H+2.0*P(2)*P(1)*H**2)/(1.0+P(1)*H+P(2)*P(1)*H**2)
7      RETURN
8      END
9
10
11
12
13
14
15
16
17
18
19
20
21
22
23
24
25
26
27
28
29
30
31
32
33
34
35
36
37
38
39
40
41
42
43
44
45
46
47
48

```


B

31
32
33
34
35
36
6
7
8
9
10
11
12
13
14
15
16
17
18
19
20
21
22
23
24
25

1
2
3
4
5
6
7
8
9
10
11
12
13
14
15
16
17
18
19
20
21
22
23
24
25
26
27
28
29
30
31
32
33
34
35
36
37
38
39
40
41
42
43
44

```

SUBROUTINE PRELIM(YO,X,NO,TL,TM)
  NBAR METHOD B
  DIMENSION YO(100),X(2,100),TL(100),TM(100)
  DIMENSION ACID(100)
  REAL K1,K2
  REAL NAOH
  K1=2.399E+9
  K2=1.905E+6
  READ(5,10)TMI,TLI,ACIDI,NAOH
  DO 20 I=1,NO
    Q=49.93/(49.93+YO(I))
    ACID(I)=ACIDI*Q
    TM(I)=TMI*Q
    TL(I)=TLI*Q
    X(1,I)=(X(1,I)-0.086)/0.9953
    X(1,I)=10.**(-X(1,I))
    ALK=YO(I)*NAOH/(49.93+YO(I))
    TOTA=2.0*TL(I)+1.63436E-14/X(1,I)-ALK-X(1,I)
    ALIG=TOTA/(K1*X(1,I)+2.0*K1*K2*X(1,I)**2)
    YO(I)=(TL(I)-ALIG*(1.0+K1*X(1,I)+K1*K2*X(1,I)**2))/TM(I)
  20 CONTINUE
  10 FORMAT(3(E10.3),F10.4)
  RETURN
END

SUBROUTINE CALC(I,X,Y,P,TL,TM,ROOT,Z3,Z4,CM,CMLHH,CMLH)
  NBAR METHOD B
  DIMENSION CM(100),CMLHH(100),CMLH(100)
  DIMENSION X(2,100),P(20),TL(100),TM(100),ROOT(100)
  REAL LSAVE,NEWL,M
  ESTIMATE LH2 AT NBAR EQUALS ZERO
  LSAVE=TL(I)/(1.0+Z3*X(1,I)+Z3*Z4*X(1,I)**2)
  SOLVE FOR BRITER LH2 BY NEWTON RAPHSON
  A=P(1)*P(2)+Z3*P(1)*P(2)*X(1,I)+Z3*Z4*P(1)*P(2)*X(1,I)**2
  B=P(1)+Z3*P(1)*X(1,I)+Z3*Z4*P(1)*X(1,I)**2+2.*P(1)*P(2)*TM(I)-P(1)
  1 *P(2)*TL(I)
  C=1.0+Z3*X(1,I)+Z3*Z4*X(1,I)**2+P(1)*TM(I)-P(1)*TL(I)
  D=-TL(I)
  N=1
  30 FX=A*LSAVE**3+B*LSAVE**2+C*LSAVE+D
  FDX=3.*A*LSAVE**2+2.*B*LSAVE+C
  NEWL=LSAVE-FX/FDX
  IF(ABS(NEWL-LSAVE).LE.0.005*NEWL)GO TO 10
  N=N+1
  IF(N.GT.15)GO TO 20
  LSAVE=NEWL
  GO TO 30
  20 WRITE(6,40)NEWL,N
  10 ROOT(I)=NEWL
  M=TM(I)/(1.0+P(1)*ROOT(I)+P(1)*P(2)*ROOT(I)**2)
  Y=(P(1)*M*ROOT(I)+2.*P(1)*P(2)*M*ROOT(I)**2)/TM(I)
  CM(I)=M*100.0/TM(I)
  CMLHH(I)=P(1)*M*ROOT(I)*100.0/TM(I)
  CMLH(I)=(P(1)*P(2)*M*100.0*ROOT(I)**2)/TM(I)
  40 FORMAT(1X,' UNREFINED LH2IS ',E10.3,' NO OF CYCLES IS ',I2)
  RETURN
END

```

C

```

6
7 SUBROUTINE PRELIM(YO,X,NO,TL,TM)
8 DIMENSION YO(100),X(2,100),TL(100),TM(100)
9 DIMENSION ACID(100)
10 REAL NAOH
11 READ(5,10)TMI,TLI,ACIDI,NAOH
12 DO 20 I=1,NO
13 Q=60.00/(60.00+YO(I))
14 ACID(I)=ACIDI*Q
15 TM(I)=TMI*Q
16 TL(I)=TLI*Q
17 X(1,I)=(X(1,I)-0.086)/0.9953
18 X(1,I)=10.**(-X(1,I))
19 ALK=YO(I)*NAOH/(60.00+YO(I))
20 YO(I)=4.*TL(I)+ACID(I)+1.63436E-14/X(1,I)-ALK-X(1,I)
21 CONTINUE
22 FORMAT(3(E10.3),F10.4)
23 RETURN
24 END

```

```

1
2 SUBROUTINE CALC(I,X,Y,P,TL,TM,ROOT,Z3,Z4,CM,CMLHH,CMLH)
3 REAL M
4 DIMENSION CM(100),CMLHH(100),CMLH(100)
5 DIMENSION X(2,100),P(20),TL(100),TM(100),ROUT(100)
6 D=1.0+Z3*X(1,I)+Z3*Z4*X(1,I)**2
7 E=4.0*Z3*Z4*X(1,I)**2+3.0*Z3*X(1,I)+2.0
8 OH=1.6374E-14/X(1,I)
9 A=D*(P(1)+P(1)*P(2)/X(1,I)+P(1)*P(2)*P(3)*OH/X(1,I))
10 B=D*(TM(I)-TL(I))*(P(1)+P(1)*P(2)/X(1,I)+P(1)*P(2)*P(3)*OH/X(1,I))
11 ROOT(I)=(-B+SQRT(B**2+4.0*A*TL(I)))/(2.0*A)
12 M=TM(I)/(1.0+P(1)*ROOT(I)+P(1)*P(2)*ROOT(I)/X(1,I)+P(1)*P(2)*P(3)*
13 ROOT(I)*OH/X(1,I))
14 Y=ROOT(I)*(E+2.0*P(1)*M+P(1)*P(2)*M/X(1,I))
15 CM(I)=M
16 CMLHH(I)=P(1)*CM(I)*ROOT(I)
17 CMLH(I)=P(1)*P(2)*CM(I)*ROOT(I)/X(1,I)
18 CM(I)=CM(I)*100.0/TM(I)
19 CMLHH(I)=CMLHH(I)*100.0/TM(I)
20 CMLH(I)=CMLH(I)*100.0/TM(I)
21 RETURN
22 END

```

D

```

34
35
36
37
38
39
5
6   DIMENSION VOL(80),PH(80),PK(80)
7   REAL M,L,NBAR,K1,K2,K3,K4
8   READ(5,69) KODE
9
10  INTE=1
11  READ(5,78) K1,K2,K3,K4
12  8 READ(5,70) TM,TH,TL,ALK,AISTR,TN
13  J=0
14  SIG=0.0
15  AK=1.0
16  NN=0
17  2 J=J+1
18  READ(5,71) ISENT,VOL(J),PH(J)
19  IF(ISENT) 2,2,3
20  3 NO=J-1
21  WRITE(6,72) AISTR,TN
22
23  WRITE(6,73) TL,ALK
24  WRITE(6,79) TM
25  WRITE(6,74) K1,K2,K3,K4
26  WRITE(6,75)
27  DO 6 I=1,NO
28  PH(I)=(PH(I)-0.086)/0.9953
29  H=10.**(-PH(I))
30  Q=49.93/(49.93+VOL(I))
31  ACID=TH*Q
32  TLIG=TL*Q
33  ALKA=VOL(I)*ALK/(49.93+VOL(I))
34  TMET=TM*Q
35  B=1.+K1*H+K2*K1*H**2+K3*K2*K1*H**3+K4*K3*K2*K1*H**4
36  A=K1*H+2.*K2*K1*H**2+3.*K3*K2*K1*H**3+4.*K4*K3*K2*K1*H**4
37  L=(ACID-H-ALKA+1.6374E-14/H)/A
38  M=L*B+TMET-TLIG
39  STABK=(TLIG-L*B)/(M*L)
40  NBAR=(TLIG-L*B)/TMET
41  IF(PH(I).GT.6.0)GO TO 12
42  IF(L) 12,12,13
43  12 STABK=1.0
44  L=(TLIG-TMET)/(1.0+K1*H+K1*K2*H**2)
45  AMLD=(ACID-ALKA-H+1.6374E-14/H-L*(K1*H+2*K1*K2*H**2))
46  AK=AMLD*H/(TMET-AMLD)
47  NBAR=AMLD/TMET
48  IF(AK) 14,14,15
49  14 AK=1.0
50  15 AK=ALOG10(AK)
51  GO TO 6
52  13 IF(STABK) 4,4,5
53  4 WRITE(6,76)
54  PK(I)=1.
55  GO TO 6
56  5 PK(I)=ALOG10(STABK)
57  SIG=SIG+PK(I)
58  NN=NN+1
59  6 WRITE(6,77) VOL(I),PH(I),NBAR,L,M,PK(I),AK
60  ANO=NN
61  AVPK=SIG/ANO
62  SUM=0.0
63  DO 10 I=1,NN
64  10 SUM=SUM+(AVPK-PK(I))**2
65  D=SUM/ANO
66  STDEV=SQRT(D)
67  WRITE(6,80) AVPK,STDEV
68  INTE=INTE+1
69  IF(INTE=KODE) 8,8,9
70  9 STOP
71  69 FORMAT(I2)
72  70 FORMAT(3(E10.3),F10.4,F10.2,8X,I2)
73  71 FORMAT(I1,F8.3,9X,F10.3)
74  72 FORMAT('0 SOLUTION IONIC STRENGTH IS ',F5.2,'TITRATION NUMBER IS ',I2)
75  73 FORMAT('0 TOTAL LIGAND CONCENTRATION IS ',E11.4,'0 ALKALI CONCEN
76  TITRATION IS ',F7.4)

```

```
1
2 74 FORMAT(//,'0 LIGAND PROTONATION CONSTANTS ARE',4(E10.4,3X))
3 75 FORMAT(//,'0 VOLUME PH NBAR FREE LIGAND FREE METAL
4 1LOG K LOG KD ')
5 76 FORMAT('0 STABILITY CONSTANT IS NEGATIVE')
6 77 FORMAT('0',F7.3,3X,F6.3,3X,F5.3,3X,2(E11.4,3X),F6.3,3X,F6.3)
7 78 FORMAT(4(E12.4))
8 79 FORMAT('0 TOTAL METAL CONCENTRATION IS ',E10.4)
9 80 FORMAT('0 AVERAGE PK IS ',F6.3,' STANDARD DEVIATION IS ',F6.3)
10 END
11
12
13
14
15
16
17
18
19
20
21
22
23
24
25
26
27
28
29
30
31
32
33
34
35
36
37
38
39
40
41
42
43
44
45
46
47
48
49
50
51
52
53
54
55
56
57
58
59
60
```

E

```

38
39
40
41
42
5   DIMENSION PK(50)
6   DIMENSION V(50),X(50),H(50),TH(50),TL(50)
7   REAL NBAR,LH2,LH3,LH4
8   AK3=2.570E+9
9   AK4=2.239E+6
10  READ (5,47)KODE
11
12  L=0
13  6 J=0
14  SUMSQ=0.0
15  PKTOT=0.0
16  2 J=J+1
17  READ(5,40)ISENT,V(J),X(J)
18  IF(ISENT)2,2,3
19  3 NO=J-1
20  READ(5,41)TLIG,TMET,ACID,ANAOH
21  ACID=ACID
22  GAMMA=1.623
23  WRITE(6,45)
24
25  WRITE(6,46)TLIG,TMET
26  DO 10 I=1,NO
27  Q=60.0/(V(I)+60.0)
28  ACID=ACID*Q
29  TL(I)=TLIG*Q
30  ALK=V(I)*ANAOH/(V(I)+60.0)
31  X(I)=(X(I)-0.086)/0.9953
32  H(I)=10.0**(-X(I))
33  TH(I)=1.007E-14*GAMMA/H(I)+2.0*TL(I)+ACID-ALK
34  TM=TMET*Q
35  P=1.0+2.0*AK3*H(I)+3.0*AK3*AK4*H(I)**2
36  B=1.0+AK3*H(I)+AK3*AK4*H(I)**2
37  IF(X(I)-10.0)20,21,21
38  21 LH2=(TL(I)-TM)/B
39  COHL=TH(I)-H(I)-2.0*LH2-3.0*AK3*LH2*H(I)
40  HYDR=1.007E-14*GAMMA/H(I)
41  STABK2=(TM-COHL)/(HYDR*COHL)
42  IF(STABK2)11,11,12
43  11 STABK2=1.0
44  12 PK2=ALOG10(STABK2)
45  PCENT=(TM-COHL)*100.0/TM
46  GO TO 10
47  20 CONTINUE
48  LH2=(TH(I)-TL(I)-H(I))/P
49  LH3=AK3*LH2*H(I)
50  LH4=AK4*LH3*H(I)
51  CO=TM-TL(I)+LH2+LH3+LH4
52  COHL=TM-CO
53  STABK=P*(TM-CO)*H(I)/((TH(I)-TL(I)-H(I))*(TM-TL(I)+LH2+LH3+LH4))
54  NBAR=COHL/TM
55  IF(STABK)4,4,5
56  4 STABK=1.0
57  5 PK(I)=ALOG10(STABK)
58  PKTOT=PKTOT+PK(I)
59  10 WRITE(6,42)V(I),X(I),NBAR,CO,COHL,LH2,LH3,LH4,PK(I),PK2,PCENT
60  AVPK=PKTOT/NO
61  DO 60 I=1,NO
62  DEV=(AVPK-PK(I))**2
63  SUMSQ=SUMSQ+DEV
64  60 CONTINUE
65  STDEV=SQRT(SUMSQ/(NO-1))
66  WRITE(6,58)AVPK
67  WRITE(6,59)STDEV
68  59 FORMAT(1X,'STANDARD DEVIATION IS ',F8.4//)
69  58 FORMAT(1X,'AVERAGE PK IS ',F8.4)
70  47 FORMAT(11)
71  40 FORMAT(I1,F8.3,9X,F9.3)
72  41 FORMAT(3(E10.4),F10.4)
73  42 FORMAT('0' 3(F6.3,3X),5(E9.3,3X),2(F7.4,3X),F5.2)
74  45 FORMAT('0 STABILITY CONSTANT FOR NICKEL DIOXIME COMPLEX')
75  46 FORMAT('0 LIGAND CONC N IS',E9.3,'METAL CONC N IS',E9.3)
76  L=L+1
77  IF(KODE=L)7,7,6
78
79
80

```

1	7 CONTINUE
2	STOP
3	END
4	
5	
6	
7	
8	
9	
10	
11	
12	
13	
14	
15	
16	
17	
18	
19	
20	
21	
22	
23	
24	
25	
26	
27	
28	
29	
30	
31	
32	
33	
34	
35	
36	
37	
38	
39	
40	
41	
42	
43	
44	
45	
46	
47	
48	
49	
50	
51	
52	
53	
54	
55	
56	
57	
58	
59	
60	

57
58
59
60

E

```

C      SUBROUTINE PRELIM(YO,R,S,T,U)
      TO CALCULATE THE CHANGES IN THE SOLUTION COMPOSITION
      REAL K1,K2,K3,K4,KW,NBAR,L
      REAL LH(50),LH2(50),LH3(50),LH4(50),FL(50)
      DIMENSION PH(50),VOL(50)
      DIMENSION R(50),S(50),T(50),U(50),OH(50),YO(50)
      READ(5,41) K1,K2,K3,K4,KW,DELHH
      WRITE(6,51)
      WRITE(6,52) K1,K2,K3,K4
      WRITE(6,46)
      INTE=1
      NM=0
      READ(5,37) KODE
      2  READ(5,38) NO
      READ(5,40) ACID,TL,THI
      WRITE(6,50) ACID,TL
      READ(5,36) (VOL(J),PH(J),J=1,NO)
      BETA1=K1
      BETA2=K2*K1
      BETA3=K3*K2*K1
      BETA4=K4*K3*K2*K1
      DO 11 I=1,NO
      PH(I)=(PH(I)-0.086)/0.995
      H=10.**(-PH(I))
      N=1
      Q=98.84/(98.84+VOL(I))
      ACIDA=THI*Q
      TH=ACID*VOL(I)/(98.84+VOL(I))+ACIDA
      TVOL=98.84+VOL(I)
      YH=H
      B=BETA3+4.*TL*Q*BETA4-TH*BETA4
      C=3.*TL*Q*BETA3-KW*BETA4+BETA2-TH*BETA3
      D=2.*TL*Q*BETA2-KW*BETA3+BETA1-TH*BETA2
      E=BETA1*TL*Q-KW*BETA2+1.-TH*BETA1
      F=-KW*BETA1-TH
      C      CALCULATE AN IMPROVED VALUE FOR H
      7  FX=BETA4*YH**6+B*YH**5+C*YH**4+D*YH**3+E*YH**2+F*YH-KW
      FXP=6.*BETA4*YH**5+5.*B*YH**4+4.*C*YH**3+3.*D*YH**2+2.*E*YH+F
      XH=YH-FX/FXP
      IF(XH) 8,8,9
      9  PYH=ALOG10(YH)
      PXH=ALOG10(XH)
      G=PXH-PYH
      IF(ABS(G)-0.0005) 5,5,6
      6  N=N+1
      IF(N,GE,15) GO TO 4
      YH=XH
      GO TO 7
      4  WRITE(6,45) N,PYH,PXH
      GO TO 11
      8  WRITE(6,42) N,I
      GO TO 11
      C      CALCULATE THE SOLUTION COMPOSITION(IN MMOLES) FROM THE REFINED PH
      5  H=XH
      OH(I)=TVOL*KW/H
      NBAR=(TH-H+KW/H)/(TL*Q)
      L=TL*Q/(1.+BETA1*H+BETA2*H**2+BETA3*H**3+BETA4*H**4)
      FL(I)=TVOL*L
      LH(I)=TVOL*BETA1*L*H
      LH2(I)=TVOL*BETA2*L*H**2
      LH3(I)=TVOL*BETA3*L*H**3
      LH4(I)=TVOL*BETA4*L*H**4
      WRITE(6,47) VOL(I),PXH,NBAR,FL(I),LH(I),LH2(I),LH3(I),LH4(I),N
      11 CONTINUE
      C      CALCULATION OF THE CHANGE IN COMPOSITION( IN MMOLES)
      C      AND APPLY HYDROLYSIS CORRECTION TO YO
      WRITE(6,55)
      NN=NO-1
      DO 12 J=1,NN
      L=NM+J

```

```

CORR=(OH(J+1)-OH(J))*DELHH
YD(L)=YD(L)+CORR
R(L)=FL(J)-FL(J+1)
S(L)=LH(J)+R(L)-LH(J+1)
T(L)=S(L)+LH2(J)-LH2(J+1)
WRITE(6,56) R(L),S(L),T(L)
12 U(L)=LH4(J+1)-LH4(J)
NM=NM+NM
INTE=INTE+1
IF(INTE.LE.KODE) GO TO 2
CONTINUE
36 FORMAT(F10.4,F10.3)
38 FORMAT(I2)
37 FORMAT(I2)
40 FORMAT(F10.4,2(E10.3))
41 FORMAT(5(E10.3),F10.2)
42 FORMAT('0 THE SOLUTION IS NEGATIVE OR ZERO FOR CYCLE NUMBER',I2 '
1 FOR DATA POINT NUMBER',I2)
45 FORMAT('0 NO CONVERGENCE WITHIN',I2,' CYCLES. VALUE OF PH ON PENUL
1 TIMATE CYCLE=',F7.3,' VALUE ON LAST CYCLE=',F7.3)
46 FORMAT('0 COMPOSITION (IN MMOL) OF CALORIMETER SOLUTION AS A FUN
1 CTION OF VOLUME AND PH'// '0 VOL HCL CAL PH CAL NBAR L
2 LH LH2 LH3 LH4 NO OF CYCLES')
47 FORMAT('0' F6.3,3X,F7.3,3X,F6.3,2X,5(F7.5,3X),3X,I2)
50 FORMAT('0 CONCENTRATION OF TITRANT ACID =',F6.4/'0' 'TOTAL LIGAND
1 CONCENTRATION =',E10.4)
51 FORMAT('0' K1 K2 K3 K4')
52 FORMAT('0' 4(E10.4,3X))
55 FORMAT('0 CALCULATION OF THE CHANGES IN CONCENTRATION BETWEEN
1 SUCCESSIVE TITRATION POINTS'// '0 R S T')
56 FORMAT('0' 3(F7.5,3X))
RETURN
END

```

```

SUBROUTINE CALC(I,R,S,T,U,P,Y)
DIMENSION P(20),R(50),S(50),T(50),U(50)
Y=R(I)*P(1)+S(I)*P(2)+T(I)*P(3)+U(I)*P(4)
RETURN
END

```



```

46
47
48
49
50
51 G
52
53
54
55
56
57
58
59
60
61
62
63
64
65
66
67
68
69
70
71
72
73
74
75
76
77
78
79
80
81
82
83
84
85
86
87
88
89
90
91
92
93
94
95
96
97
98
99
100
101
102
103
104
105
106
107
108
109
110
111
112
113
114
115
116
117
118
119
120
121
122
123
124
125
126
127
128
129
130
131
132
133
134
135
136
137
138
139
140
141
142
143
144
145
146
147
148
149
150
151
152
153
154
155
156
157
158
159
160
161
162
163
164
165
166
167
168
169
170
171
172
173
174
175
176
177
178
179
180
181
182
183
184
185
186
187
188
189
190
191
192
193
194
195
196
197
198
199
200
201
202
203
204
205
206
207
208
209
210
211
212
213
214
215
216
217
218
219
220
221
222
223
224
225
226
227
228
229
230
231
232
233
234
235
236
237
238
239
240
241
242
243
244
245
246
247
248
249
250
251
252
253
254
255
256
257
258
259
260
261
262
263
264
265
266
267
268
269
270
271
272
273
274
275
276
277
278
279
280
281
282
283
284
285
286
287
288
289
290
291
292
293
294
295
296
297
298
299
300
301
302
303
304
305
306
307
308
309
310
311
312
313
314
315
316
317
318
319
320
321
322
323
324
325
326
327
328
329
330
331
332
333
334
335
336
337
338
339
340
341
342
343
344
345
346
347
348
349
350
351
352
353
354
355
356
357
358
359
360
361
362
363
364
365
366
367
368
369
370
371
372
373
374
375
376
377
378
379
380
381
382
383
384
385
386
387
388
389
390
391
392
393
394
395
396
397
398
399
400
401
402
403
404
405
406
407
408
409
410
411
412
413
414
415
416
417
418
419
420
421
422
423
424
425
426
427
428
429
430
431
432
433
434
435
436
437
438
439
440
441
442
443
444
445
446
447
448
449
450
451
452
453
454
455
456
457
458
459
460
461
462
463
464
465
466
467
468
469
470
471
472
473
474
475
476
477
478
479
480
481
482
483
484
485
486
487
488
489
490
491
492
493
494
495
496
497
498
499
500
501
502
503
504
505
506
507
508
509
510
511
512
513
514
515
516
517
518
519
520
521
522
523
524
525
526
527
528
529
530
531
532
533
534
535
536
537
538
539
540
541
542
543
544
545
546
547
548
549
550
551
552
553
554
555
556
557
558
559
560
561
562
563
564
565
566
567
568
569
570
571
572
573
574
575
576
577
578
579
580
581
582
583
584
585
586
587
588
589
590
591
592
593
594
595
596
597
598
599
600
601
602
603
604
605
606
607
608
609
610
611
612
613
614
615
616
617
618
619
620
621
622
623
624
625
626
627
628
629
630
631
632
633
634
635
636
637
638
639
640
641
642
643
644
645
646
647
648
649
650
651
652
653
654
655
656
657
658
659
660
661
662
663
664
665
666
667
668
669
670
671
672
673
674
675
676
677
678
679
680
681
682
683
684
685
686
687
688
689
690
691
692
693
694
695
696
697
698
699
700
701
702
703
704
705
706
707
708
709
710
711
712
713
714
715
716
717
718
719
720
721
722
723
724
725
726
727
728
729
730
731
732
733
734
735
736
737
738
739
740
741
742
743
744
745
746
747
748
749
750
751
752
753
754
755
756
757
758
759
760
761
762
763
764
765
766
767
768
769
770
771
772
773
774
775
776
777
778
779
780
781
782
783
784
785
786
787
788
789
790
791
792
793
794
795
796
797
798
799
800
801
802
803
804
805
806
807
808
809
810
811
812
813
814
815
816
817
818
819
820
821
822
823
824
825
826
827
828
829
830
831
832
833
834
835
836
837
838
839
840
841
842
843
844
845
846
847
848
849
850
851
852
853
854
855
856
857
858
859
860
861
862
863
864
865
866
867
868
869
870
871
872
873
874
875
876
877
878
879
880
881
882
883
884
885
886
887
888
889
890
891
892
893
894
895
896
897
898
899
900
901
902
903
904
905
906
907
908
909
910
911
912
913
914
915
916
917
918
919
920
921
922
923
924
925
926
927
928
929
930
931
932
933
934
935
936
937
938
939
940
941
942
943
944
945
946
947
948
949
950
951
952
953
954
955
956
957
958
959
960
961
962
963
964
965
966
967
968
969
970
971
972
973
974
975
976
977
978
979
980
981
982
983
984
985
986
987
988
989
990
991
992
993
994
995
996
997
998
999
1000

```

REAL LL
 REAL L,LSAVE,K,KD,K1,K2,KW
 REAL LH2(20),LH3(20),LH4(20)
 DIMENSION PH(20),CULH2(20),CULH(20)
 DIMENSION TVOL(20)
 INTEGER TITN
 READ DATA
 READ(5,140)K1,K2,KD,K,KW
 READ(5,400)CNAOH,CHCL,CHCLCU
 READ(5,100)NGPS
 I=1
 130 READ(5,200)TITN
 READ(5,300)TLL,TMM
 READ(5,500)NPTS
 N=1
 WRITE(6,150)TITN
 WRITE(6,950)
 80 READ(5,600)VNAOH,VHCL,VHCLCU,TVOL(N)
 READ(5,700)PH(N)
 TL=TLL*1000.0/TVOL(N)
 TM=TMM*1000.0/TVOL(N)
 TTH=4.0*TL-CNAOH*VNAOH/TVOL(N)+CHCL*VHCL/TVOL(N)+CHCLCU*VHCLCU/TVOL(N)
 1 L(N)
 H=10.0*(-PH(N))
 LL=(TL-TM)/(1.0+K1*H+K1*K2*H**2)
 NN=0
 LSAVE=0.0
 29 C CALCULATE VALUE FOR FREE LIGAND CONCENTRATION
 40 A=K+K*K1*H+K*K1*K2*H*H+K*KD/H+K*KD*K1+K*KD*K1*K2*H
 B=TM*K*KD/H+TM*K+1.0+K1*H+K1*K2*H*H-K*TL=K*KD*TL/H
 C=-TL
 L=(-B+SQRT(B**2-4.0*A*C))/(2.0*A)
 IF(ABS(L-LSAVE).LE.0.005*L)GO TO 10
 NN=NN+1
 IF(NN.GT.60)GO TO 20
 LSAVE=L
 GO TO 30
 20 WRITE(6,650)N
 GO TO 10
 38 C START NEWTON RAPHSON TO FIND IMPROVED PH
 30 MM=0
 60 TH=TTH+KW/H
 D=4.0*K1*K2*L+4.0*K1*K2*K*L**2
 E=1.0+K*L+3.0*K1*L+3.0*K1*K*L+4.0*K1*K2*K*KD*L*L
 F=K*KD*L+2.0*L+2.0*K*L+3.0*K1*K*KD*L*L+2.0*K*L*TM-TH=K*TH*L
 G=2.0*K*KD*L*L+K*KD*L*TM-K*KD*L*TH
 FX=D*H**3+E*H**2+F*H+G
 FDX=3.0*D*H**2+2.0*E*H+F
 ANH=H-FX/FDX
 PH(N)=ALOG10(H)
 PNH=ALOG10(ANH)
 H=ANH
 IF(ABS(PH(N)-PNH).LE.0.005)GO TO 40
 MM=MM+1
 IF(MM.GE.15)GO TO 50
 GO TO 60
 50 WRITE(6,750)N
 GO TO 10
 52 C CALCULATE MOLES OF EACH SPECIES AT EACH POINT
 10 LH2(N)=L*TVOL(N)/1000.0
 LH3(N)=K1*H*L*TVOL(N)/1000.0
 LH4(N)=K1*K2*H*H*TVOL(N)/1000.0*L
 CU=TM/(1.0+K*L+K*KD*L/H)
 CULH2(N)=K*CU*L*TVOL(N)/1000.0
 CULH(N)=K0*K*CU*L*TVOL(N)/(1000.0*H)
 PH(N)=ALOG10(H)
 WRITE(6,900)L,LL,LH4(N),CULH(N),CU
 N=N+1

```

1      IF(N.GT.NPTS)GO TO 70
2      GO TO 80
3      C  CALCULATE CHANGE IN COMPOSITION BETWEEN POINTS
4      70  M=2
5      110 DCULH=CULH(M)-CULH(M-1)
6          DCULH2=CULH2(M)-CULH2(M-1)
7          DLH2=LH2(M)-LH2(M-1)
8          DLH3=LH3(M)-LH3(M-1)
9          DLH4=LH4(M)-LH4(M-1)
10         WRITE(6,800)PH(M-1)
11         WRITE(6,900)DCULH,DCULH2,DLH2,DLH3,DLH4
12         M=M+1
13         IF(M.GT.NPTS)GO TO 90
14         GO TO 110
15         90 WRITE(6,800)PH(M-1)
16         I=I+1
17         IF(I.GT.NGPS)GO TO 120
18         GO TO 130
19         140 FORMAT(5E10.4)
20         400 FORMAT(1X,F6.4,2X,F6.4,2X,F6.4)
21         100 FORMAT(I1)
22         200 FORMAT(I1)
23         300 FORMAT(2E10.3)
24         500 FORMAT(I1)
25         600 FORMAT(3(F5.3,1X),F7.3)
26         700 FORMAT(F6.3)
27         650 FORMAT(1X,'NO REFINEMENT OF L AFTER 60 CYCLES ON POINT',2X,I1,/)
28         750 FORMAT(1X,'NO REFINEMENT OF PH AFTER 15 CYCLES ON POINT',2X,I1,/)
29         800 FORMAT(1X,F7.4,/)
30         900 FORMAT(12X,4(E11.4,5X),E11.4)
31         950 FORMAT(5X,'PH',9X,'DCULH',10X,'DCULH2',8X,'DLH2',15X,'DLH3',11X,'D
32             1LH4')
33         150 FORMAT(1X,'TITRATION ON IS',2X,I1)
34         120 STOP
35         END
36
37
38
39
40
41
42
43
44
45
46
47
48
49
50
51
52
53
54
55
56
57
58
59
60

```

REFERENCES

1. A. I. Vogel, "A Textbook of Quantitative Inorganic Analysis", Longman, London, 3rd Ed., 1962, p124-129.
2. K. Burger, "Organic Reagents in Metal Analysis", Pergamon Press, Oxford, 1973, p23.
3. A. Chakravorty, Coord. Chem. Rev., 1974, 13, 1.
4. B. Egneus, Talanta, 1972, 19, 1387.
5. J. March, "Advanced Organic Chemistry: Reactions, Mechanisms and Structure", McGraw-Hill Kogakusha, Tokyo, International Students Ed., 1968, p675.
6. W. Theilheimer, "Synthetic Methods of Organic Chemistry", S. Karger, New York, Vol. 14, 1960, Reaction 430.
7. L. G. Donaruma, J. Org. Chem., 1957, 22, 1024.
8. Ref. 5, p327.
9. O. L. Brady and H. M. Perry, J. Chem. Soc., 1925, 2874.
10. S. Patai, "The Chemistry of the Carbon Nitrogen Double Bond", Interscience, London, 1970, p6.
11. G. St. Nickolov and N. Tyutyulkov, Inorg. Nucl. Chem. Lett., 1970, 6, 697.
12. I. N. Levine, J. Chem. Phys., 1963, 38, 2326.
13. S. Califano and W. Luttbe, Z. Phys. Chem., 1955, 5, 240.
14. D. Hadzi and L. Permr, Spectrochim. Acta (A), 1967, 23, 35.
15. A. Palm and H. Werbin, Canad. J. Chem., 1953, 31, 1004.

16. B. Jerslev, Nature, 1950, 166, 741.
17. B. Jerslev, Nature, 1957, 180, 1410.
18. L. L. Merritt and E. Lanterman, Acta Cryst., 1952, 5, 811.
19. W. C. Hamilton, Acta Cryst., 1961, 14, 95.
20. F. K. Winkler, P. Seiler, J. P. Chesnick and J. D. Dunitz, Helvetica Chim. Acta, 1976, 59, 1417.
21. "Rules for the Nomenclature of Organic Chemistry, Section E: Stereochemistry (Recommendations 1974), Pure and Appl. Chem., 45, 17.
22. G. B. Kauffman, J. Chem. Ed., 1966, 43, 155.
23. A. Hantzsch and A. Werner, J. Chem. Ed., 1966, 43, 156.
24. A. D. McLaren and R. E. Schachat, J. Org. Chem., 1949, 14, 254.
25. G. J. Karabatsos and N. Hsi, Tetrahedron, 1967, 23, 1079.
26. R. A. Krause, N. B. Colthup and D. H. Busch, J. Phys. Chem., 1961, 65, 2216.
27. B. Roos, Acta Chem. Scand., 1965, 19, 1715.
28. M. Raban, Chem. Comm., 1970, 1415.
29. H. Kessler, Angew. Chemie (Int. Ed.), 1970, 9, 219.
30. D. Curtin, E. Grubbs and C. G. McCarty, J. Am. Chem. Soc., 1966, 88, 2775.
31. N. P. Marullo and E. H. Wagener, Tet. Lett., 1969, 2555.

32. W. B. Jennings, D. R. Boyd and L. C. Waring, J. Chem. Soc.
(Perkin II), 1976, 610.
33. T.W.J. Taylor and E.M.W. Lavington, J. Chem. Soc., 1934, 980.
34. R. K. Norris and S. Sternhill, Aust. J. Chem., 1969, 22, 935.
35. T. S. Patterson and H. H. Montgomerie, J. Chem. Soc., 1912, 2100.
36. P.A.S. Smith in "Molecular Rearrangements", Ed. P. De Mays,
Interscience, New York, 1963, p486.
37. E. Jordon and C. R. Hauser, J. Am. Chem. Soc., 1936, 58, 1304,
1419.
38. E. G. Vassian and R. K. Murmann, J. Org. Chem., 1962, 27, 4309.
39. P.A.S. Smith, "Open Chain Nitrogen Compounds", Benjamin, New York,
Vol. 2, 1965, p29.
40. J. W. Fraser, G. R. Hedwig, M. M. Morgan and H.K.J. Powell,
Aust. J. Chem., 1970, 23, 1847.
41. O. L. Brady and L. Klein, J. Chem. Soc., 1927, 874.
42. G. W. Wheland, "Advanced Organic Chemistry", J. Wiley, New York,
2nd Ed., 1949, p344.
43. Ref. 5, p821.
44. P. T. Lansbury and N. R. Mancuso, Tet. Lett., 1965, 2445.
45. L. E. Sutton and T.W.J. Taylor, J. Chem. Soc., 1931, 2190.
46. T.W.J. Taylor and L. E. Sutton, J. Chem. Soc., 1933, 63.
47. J. V. Hatton and R. E. Richards, Mol. Phys., 1962, 5, 153.
48. J. R. Jennings and K. Wade, J. Chem. Soc. (A), 1967, 1333.

49. G. B. Karabatsos and R. A. Taller, Tetrahedron, 1968, 24, 3347.
50. H. Saito and K. Nukada, J. Mol. Spec., 1965, 18, 1.
51. M. Cocivera, A. Effio, H. E. Chen and S. Vaish, J. Am. Chem. Soc., 1976, 98, 7362.
52. A. C. Huitric, D. B. Roll and J. R. De Boer, J. Org. Chem., 1967, 32, 1661.
53. M. N. Hughes, H. G. Nicklin and K. Shrimanker, J. Chem. Soc. (A), 1971, 3485.
54. Ref. 5, p219.
55. N. V. Sidgwick, "The Organic Chemistry of Nitrogen", rewritten by T.W.J. Taylor and W. Baker, Clarendon Press, Oxford, 1937, p20.
56. J. J. Christensen, R. M. Izatt, D. P. Wrathall and L. D. Hansen, J. Chem. Soc. (A), 1969, 1212.
57. P. R. Ellefsen and L. Gordon, Talanta, 1967, 14, 409.
58. N. F. Hall, J. Am. Chem. Soc., 1930, 52, 5115.
59. J. B. Conant and P. D. Bartlett, J. Am. Chem. Soc., 1932, 54, 2881.
60. H. Saito, K. Nukada and M. Ohno, Tet. Lett., 1964, 2124.
61. H. Saito, J. Terasawa, M. Ohno and K. Nukada, J. Am. Chem. Soc.,
62. B. L. Fox and J. E. Reboulet, J. Org. Chem., 1970, 35, 4234.
63. B. Sen and M. E. Pickerell, J. Inorg. Nucl. Chem., 1973, 35, 2573.
64. K. Burger and E. Papp-Molnar, Acta Chim. Academica Scientiarum Hung. Tomm., 1967, 53, 111.

65. A. A. Grinberg, A. I. Stetsenko and S. G. Strelin, Russ. J. Inorg. Chem., 1968, 13, 569.
66. A. I. Stetsenko, S. G. Strelin and M. I. Gel'fman, Russ. J. Inorg. Chem., 1970, 15, 68.
67. M. M. Dhingra, R. N. Mukherjee, M. S. Venkateshan and M. D. Zingde, J. Inorg. Nucl. Chem., 1976, 38, 1259.
68. E. G. Cox, E. Sharratt, W. Wardlaw and K. C. Webster, J. Chem. Soc., 1936, 129.
69. H. A. Svedung, Acta. Chem. Scand., 1969, 23, 2865.
70. A. Singh, A. K. Rai and R. C. Mehrotra, Inorg. Chim. Acta, 1973, 7, 450.
71. E. Frasson, R. Bardi and S. Bezzi, Acta Cryst., 1959, 12, 201.
72. N. S. Biradar, V. B. Mahale and V. H. Kulkarni, J. Inorg. Nucl. Chem., 1973, 35, 2565.
73. A. E. Martell and M. Calvin, "The Chemistry of Metal Chelate Compounds", Prentice-Hall, New York, 1952, p328.
74. S. Bruckner, M. Calligaris, G. Nardin and L. Randaccio, Inorg. Chim. Acta, 1969, 3, 278.
75. R. K. Murmann and E. O. Schlemper, Inorg. Chem., 1973, 12, 2625.
76. E. O. Schlemper and R. K. Murmann, Inorg. Chem., 1974, 13, 2424.
77. F. A. Cotton and J. G. Norman, J. Am. Chem. Soc., 1971, 93, 80.
78. L. E. Godycki and R. E. Rundle, Acta Cryst., 1953, 6, 487.

79. L. G. Sillen and A. E. Martell, "Stability Constants", Special Publications Nos 17 and 25, 1964 and 1971, The Chemical Society, London.
80. S. J. Ashcroft and C. T. Mortimer, "Thermochemistry of Transition Metal Complexes", Academic Press, London, 1971, p71.
81. V. M. Bochkova and V. M. Peshkova, Russ. J. Inorg. Chem., 1958, 3, 1131.
82. R. G. Charles and H. Freiser, Analyt. Chim. Acta, 1954, 11, 101.
83. C. V. Banks and S. Anderson, Inorg. Chem., 1963, 2, 112.
84. K. Burger and I. Ruff, Talanta, 1963, 10, 329.
85. K. Burger and I. Egyed, J. Inorg. Nucl. Chem., 1965, 27, 2361.
86. K.M.J. Al-Komser and B. Sen, Inorg. Chem., 1963, 2, 1219.
87. C. H. Lui and C. F. Lui, J. Am. Chem. Soc., 1961, 83, 4167, 4169.
88. G.I.H. Hanania and D. H. Irvine, J. Chem. Soc., 1962, 2745, 2750.
89. R. K. Murmann, J. Am. Chem. Soc., 1958, 80, 4174.
90. B. Sen, Anal. Chim. Acta, 1962, 27, 515.
91. J. A. Partridge, J. J. Christensen and R. M. Izatt, J. Am. Chem. Soc., 1966, 88, 1649.
92. D. D. Perrin, "Dissociation Constants of Organic Bases in Aqueous Solution", Butterworths, London, 1965.
93. J. C. Wang, J. E. Bauman and R. K. Murmann, J. Phys. Chem., 1964, 68, 2296.

94. D. C. Shuman and B. Sen, Analyt. Chim. Acta, 1965, 38, 487.
95. C. V. Banks and D. W. Barnum, J. Am. Chem. Soc., 1958, 80, 3579.
96. D. Fleischer and H. Freiser, J. Phys. Chem., 1962, 66, 389.
97. C. V. Banks and S. Anderson, J. Am. Chem. Soc., 1962, 84, 1486.
98. F.J.C. Rossotti in "Modern Co-ordination Chemistry", Editors J. Lewis and R. G. Wilkins, Interscience, New York, 1970, p1-77.
99. Chr. K. Jorgensen, Acta Chem. Scand., 1956, 10, 887.
100. C. K. Jorgensen, "Absorption Spectra and Chemical Bonding in Complexes", Pergamon Press, Oxford, 1962, p109.
101. F. A. Cotton and G. Wilkinson, "Advanced Inorganic Chemistry", Interscience, New York, 2nd Edition, 1966, p680.
102. Y. Ohashi, I. Hanazaki and S. Nagakura, Inorg. Chem., 1970, 9, 2551.
103. T. R. Harkins and H. Freiser, J. Am. Chem. Soc., 1956, 78, 1143.
104. A. J. Cunningham, D. A. House and H.K.J. Powell, Aust. J. Chem., 1970, 23, 2375.
105. A. A. Grinberg and A. I. Stetsenko, Russ. J. Inorg. Chem., 1962, 7, 1396.
106. A. A. Grinberg and A. I. Stetsenko, Russ. J. Inorg. Chem., 1961, 6, 55.
107. A. Vaciago and L. Zambonelli, J. Chem. Soc. (A), 1970, 218.
108. E. Frasson and C. Panattoni, Acta Cryst., 1960, 13, 893.
109. A. Gleizes, T. J. Marks and J. A. Ibers, J. Am. Chem. Soc., 1975, 97, 3545.

110. E. Frasson, C. Panattoni and R. Zannetti, Acta Cryst., 1959, 12, 1027.
111. M. Calleri, G. Ferraris and D. Viterbo, Acta Cryst., 1967, 22, 468.
112. D. E. Williams, G. Wohlauser and R. E. Rundle, J. Am. Chem. Soc., 1959, 81, 755.
113. J. E. Caton and C. V. Banks, Inorg. Chem., 1967, 6, 1670.
114. K. Burger, I. Ruff and F. Ruff, J. Inorg. Nucl. Chem., 1965, 27, 179.
115. B. A. Jillot and R.J.P. Williams, J. Chem. Soc., 1958, 462.
116. I. Adato and A.H.I. Ben-Bassat, J. Phys. Chem., 1971, 75, 3828.
117. J. E. Fergusson, W. T. Robinson and G. A. Rodley, Aust. J. Biol. Sci., 1972, 25, 1365.
118. B. G. Anex and F. K. Krist, J. Am. Chem. Soc., 1967, 89, 6114.
119. R. E. Rundle, J. Phys. Chem., 1957, 61, 45.
120. K. Krogmann, Angew. Chemie (Int. Ed.), 1969, 8, 35.
121. T. W. Thomas and A. E. Underhill, Chem. Soc. Rev., 1972, 1, 99.
122. R. E. Rundle, J. Am. Chem. Soc., 1954, 76, 3101.
123. L. L. Ingraham, Acta Chem. Scand., 1966, 20, 283.
124. R. D. Cadavieco, M.P.C. De Dias, D. Dyrssen and B. Egneus,
"Contributions to Coordination Chemistry in Solution", Ed.
E. Hogfeldt, Swedish Natural Science Research Council, Stockholm,
1972, p351.
125. G. Basu, G. M. Cook and R. L. Belford, Inorg. Chem., 1964, 3, 1361.

126. T. W. Thomas and A. E. Underhill, Chem. Comm., 1969, 725.
127. Ref. 1, p890.
128. D. S. Flett, D. N. Okuhara and D. R. Spink, J. Inorg. Nucl. Chem., 1973, 35, 2471.
129. G. R. Hedwig, Ph.D. Thesis, University of Canterbury, 1972.
130. W. J. Moore, "Physical Chemistry", Longman, London, 5th Ed., 1972, p441.
131. J. J. Christensen, R. M. Izatt, L. D. Hansen and J. A. Partridge, J. Phys. Chem., 1966, 70, 2003.
132. H.K.J. Powell, J. Chem. Soc. (Dalton), 1973, 1947.
133. H.K.J. Powell, Chemistry in New Zealand, 1976, 40, 9.
134. R. M. Izatt, D. Eatough, J. J. Christensen, C. H. Bartholomew, J. Chem. Soc. (A), 1969, 47.
135. H.K.J. Powell and N. F. Curtis, J. Chem. Soc. (B), 1966, 1205.
136. F. Basolo and R. G. Pearson, "Mechanisms of Inorganic Reactions A Study of Metal Complexes in Solution", Wiley, New York, 2nd Ed., 1967, p63.
137. W. M. Latimer and W. L. Jolly, J. Am. Chem. Soc., 1953, 75, 1548.
138. M. T. Beck, "Chemistry of Complex Equilibria", Von Nostrand Reinhold, London, 1970, p262.
139. A. E. Martell in "Werner Centennial", Advances in Chemistry", Series 62, Am. Chem. Soc. Pub., 1967, p275.
140. P. George and D. S. McClure in "Progress in Inorganic Chemistry", Interscience, New York, Volume 1, 1959, p381.
141. D. H. Everett and B. R. W. Pinsent, Proc. Roy. Soc. London (A), 1952, 215, 416.

142. R. G. Bates, "Determination of pH Theory and Practice", J. Wiley, New York, 1964, p75.
143. H. S. Harned and F. C. Hickey , J. Am. Chem. Soc., 1937, 59, 1284.
144. M. C. Taylor, private communication.
145. G. R. Hedwig and H.K.J. Powell, Analyt. Chem., 1971, 43, 1206.
146. I. Grenthe, H. Ots and O. Ginstруп, Acta Chem. Scand., 1970, 24, 1067.
147. G. Ojelund and I. Wadso, Acta Chem. Scand., 1968, 22, 2691.
148. T. S. Kee, M.Sc. Thesis, University of Canterbury, 1975.
149. R. Battins and H. L. Clever, Chem. Revs., 1966, 395.
150. H. Hjeds, Acta Chem. Scand., 1965, 19, 1764.
151. O. Scherer, G. Hoerkin, R. Huebner and G. Schneider, C.A., 56, 8561c.
152. J. L. Love and H.K.J. Powell, Chem. Comm., 1968, 39.
153. N. F. Curtis, private communication to H.K.J. Powell.
154. N. F. Curtis, to be published.
155. K. Nakamoto, "Infrared Spectra of Inorganic and Coordination Compounds", J. Wiley, New York, 1963, p107.
156. Ref. 1, p531.
157. Ref. 1, p527.
158. Ref. 1, p433.
159. Ref. 1, p498.
160. G. Schwarzenbach and H. Flaschka, "Complexometric Titrations", translated by H.N.M.H. Irving, Methuen, 2nd English Ed., p256.
161. Ref. 1, p468.

162. Ref. 1, p786.
163. H. S. Harned and B. B. Owen, "The Physical Chemistry of Electrolytic Solutions", Reinhold, New York, 1958, pp638, 752.
164. F.J.C. Rossotti and H. Rossotti, "The Determination of Stability Constants and other Equilibrium Constants in Solution", McGraw-Hill, New York, 1961, p40.
165. J. W. Fraser, G. R. Hedwig, H.K.J. Powell and W. T. Robinson, Aust. J. Chem., 1972, 25, 747.
166. W. S. Dorn and D. D. McCracken, "Numerical Methods with Fortran IV Case Studies", Wiley, New York, 1972, p25.
167. D. D. Wagman, W. H. Evans, V. B. Parker, I. Halow, S. M. Bailey, and R. H. Schumm, N.B.S. Technical Note 270-3, 1968.
168. P. Gerding, I. Leden and S. Sunner, Acta Chem. Scand., 1963, 17, 2190.
169. W.A.E. McBryde, private communication to H.K.J. Powell.
170. K. H. Schroder, Acta Chem. Scand., 1966, 20, 1401.
171. Ref. 164, p1.
172. F.J.C. Rossotti and H. S. Rossotti, Acta Chem. Scand., 1955, 9, 1166.
173. A. Sabatini, A. Vacca and P. Gans, Talanta, 1975, 21, 53.
174. A. Vacca, A. Sabatini and M. A. Cristina, Coord. Chem. Rev., 1972, 8, 45.
175. G. H. Stout and L. H. Jensen, "X-ray Structure Determination A Practical Guide", Collier-Macmillan, London, 1968, p407.
176. P. G. Hoel, "Elementary Statistics", Wiley, New York, 2nd Ed., 1966, p209.

177. Ref. 175, p407.
178. M. J. Moroney, "Facts from Figures", Penguin, England, 1965, p249.
179. W. C. Hamilton, Acta Cryst., 1965, 18, 502.
180. N. F. Curtis, Coord. Chem. Rev., 1968, 3, 3.
181. Ref. 5, p667.
182. Ref. 5, p568.
183. H. O. House, "Modern Synthetic Reactions" Benjamin, New York, 2nd Ed., 1972, p204.
184. G. R. Hedwig and H.K.J. Powell, J. Chem. Soc. (Dalton), 1974, 47.
185. T. C. Bissot, R. W. Parry and D. H. Campbell, J. Am. Chem. Soc., 1957, 79, 796.
186. E. A. Daniel, B.Sc.(Hons) Project Report, University of Canterbury.
187. G. J. Karabatsos, R. A. Taller and F. M. Vane, J. Am. Chem. Soc., 1963, 85, 2326, 2327.
188. A. K. Covington, J. G. Freeman and T. H. Lilley, J. Phys. Chem., 1970, 74, 3773.
189. W. Dannhauser and R. H. Cole, J. Am. Chem. Soc., 1952, 74, 6105.
190. F. E. Harris and C. T. O'Konski, J. Am. Chem. Soc., 1954, 76, 4317.
191. S. F. Dyke, A. J. Floyd, M. Sainsbury and R. S. Theobald, "Organic Spectroscopy: An Introduction", Penguin Books Ltd, England, 1971, p74.
192. Von J. Goubeau and I. Fromme, Z. Anorg. Chem., 1949, 258, 18.

193. H. M. Randall, R. G. Fowler, N. Fuson and J. R. Dangle,
"Infrared Determination of Organic Structures", Von Nostrand,
Princeton, New Jersey, 1949, p61.
194. E. Borek and H. T. Clarke, J. Biol. Chem., 1938, 125, 483.
195. K. B. Wiberg, "Physical Organic Chemistry", Wiley, New York,
1964, p410.
196. J. Clark and D. D. Perrin, Quart. Rev., 1964, 18, 295.
197. R. Barbucci, P. Paoletti and A. Vacca, J. Chem. Soc. (A),
1970, 2202.
198. F. Basolo, R. K. Murmann and Y. T. Chen, J. Am. Chem. Soc.,
1953, 75, 1478.
199. C. Bianchi, L. Fabbrizzi and P. Paoletti, J. Chem. Soc. (Dalton),
1975, 1036.
200. A. G. Evans and S. D. Hamann, Transact. Faraday Soc., 1951, 47,
34.
201. G. R. Hedwig and H.K.J. Powell, J. Chem. Soc. (Dalton), 1973,
793.
202. P. Paoletti, R. Barbucci, A. Vacca and A. Dei, J. Chem. Soc. (A),
1971, 310.
203. R. M. Silverstein and G. C. Bassler, "Spectrometric Identifica-
tion of Organic Compounds", J. Wiley, New York, 2nd Ed., 1967,
p159.
204. R. Barbucci, L. Fabbrizzi, P. Paoletti and A. Vacca, J. Chem.
Soc. (Dalton), 1972, 740.
205. M. N. Hughes and K. Shrimanker, Inorg. Chim. Acta, 1976, 18, 69.
206. B. N. Palmer and H.K.J. Powell, J. Chem. Soc. (Dalton), 1974,
2089.

207. Chr. K. Jorgensen, Acta Chem. Scand., 1955, 9, 1362.
208. A. Vacca, D. Arenare, P. Paoletti, Inorg. Chem., 1966, 5, 1384.
209. G. R. Hedwig and H.K.J. Powell, J. Chem. Soc. (Dalton), 1973, 1942.
210. Ref. 101, p706.
211. G. R. Hedwig, J. L. Love and H.K.J. Powell, Aust. J. Chem., 1970, 23, 981.
212. M. Campolini, P. Paoletti and L. Sacconi, J. Chem. Soc., 1961, 2994.
213. R. Barbucci, L. Fabbriizzi and P. Paoletti, Inorg. Chim. Acta, 1973, 7, 157.
214. T. S. Kee and H.K.J. Powell, Aust. J. Chem., 1976, 29, 921.
215. D. S. Brown, J. D. Lee, B.G.A. Melson, B. G. Hathaway, I. M., Procter and A. A. G. Tomlinson, Chem. Comm., 1967, 369.
216. D. L. Lewis and D. J. Hodgson, Inorg. Chem., 1974, 13, 143.
217. L. Pauling, "The Nature of the Chemical Bond", Cornell University Press, New York, 3rd Ed., 1960, p260.
218. K. Bowman, A. P. Gaughan and Z. Dori, J. Am. Chem. Soc., 1972, 94, 727.
219. K. G. Coulton and F. A. Cotton, J. Am. Chem. Soc., 1969, 91, 6517.
220. F. Daniels and R. A. Alberty, "Physical Chemistry", J. Wiley, New York, 3rd Ed., 1966, p388.
221. L. Sacconi, P. Paoletti and M. Ciampolini, J. Chem. Soc., 1961, 5115.
222. J. Bjerrum and E. J. Nielsen, Acta Chem. Scand., 1948, 2, 297.

223. C. E. Vanderzee and J. A. Swanson, J. Phys. Chem., 1963, 67, 2608.
224. Ref. 138, p250.
225. G. McLendon, D. T. MacMillan, M. Hariharan and A. E. Martell, Inorg. Chem., 1975, 14, 2322.
226. Ref. 136, p146.
227. R. G. Wilkins, Acc. Chem. Res., 1970, 3, 408.
228. J. W. Fraser, M.Sc. Thesis, University of Canterbury, 1970.
229. D. D. Perrin, Pure Appl. Chem., 1969, 20, 133.
230. Ref. 101, p882.
231. T. Sekine, Acta Chem. Scand., 1965, 19, 1526.
232. R. Arnek, Arkiv. for Kemi, 32, 55.
233. D. D. Perrin, J. Chem. Soc., 1960, 3189.
234. B. Bosnich, C. K. Poon and M. L. Tobe, Inorg. Chem., 1966, 5, 1514.
235. G. McLendon and A. E. Martell, Coord. Chem. Rev., 1976, 19, 1.
236. M. S. Michailidis and R. B. Martin, J. Am. Chem. Soc., 1969, 91, 4683.
237. L. G. Stadtherr, R. Prados and R. B. Martin, Inorg. Chem., 1973, 12, 1814.
238. T. S. Kee and H.K.J. Powell, J. Chem. Soc. (Dalton), 1975, 2023.
239. D. V. Stynes, H. C. Stynes, B. R. James and J. A. Ibers, J. Am. Chem. Soc., 1973, 95, 1796.
240. B. S. Tovrog, D. J. Kitko and R. S. Drago, J. Am. Chem. Soc., 1976, 98, 5144.

241. G. N. Schrauzer and L. P. Lee, J. Am. Chem. Soc., 1970, 92, 1551.
242. A. O. Gubeli and J. Ste-Marie, Canad. J. Chem., 1967, 45, 827.
243. B. Carlson and G. Wettermark, J. Inorg. Nucl. Chem., 1976, 38, 1525.
244. V. Romano, T. Pizzino, A. Gianguzza and F. Maggio, Inorg. Nucl. Chem. Lett., 1975, 11, 177.
245. S. Ahrland and N.-O. Bjork, Coord. Chem. Rev., 1975, 16, 115.